A NOVEL APPLICATION OF NON-INVASIVE MICROELECTRODE ION FLUX MEASURING TECHNIQUE IN FOOD MICROBIOLOGY

by

Svetlana (Lana) Shabala

B.Sc. (Hons)

Submitted in fulfilment of the requirements

for the degree of

Doctor of Philosophy

University of Tasmania

Hobart

April, 2002

Declaration

I hereby declare that this thesis contains no material which has been accepted for the award of any other degree or Diploma in any University, and to the best of my knowledge contains no copy or paraphrase of material previously published or written by any other person, except where due reference is made in the text of this thesis.

Svetlana (Lana) Shabala
University of Tasmania
Hobart
April, 2002

This thesis may be made available for loan and limited copying in accordance with the *Copyright Act 1968*.

Svetlana (Lana) Shabala

ABSTRACT

At present, both the control of bacterial growth to ensure food safety, and the balancing of nutritional requirements and optimization of culture growth conditions for beneficial food microorganisms, are essentially empirically based. An alternative time- and money-saving approach to this implies a better understanding of the physiological processes underlying the cellular response to the applied treatment. In the present work, the non-invasive microelectrode ion flux measuring technique (MIFE®) was first introduced in food microbiology, to address some of the above issues and to shed some light on adaptive responses of bacterial and fungal cells to environmental change.

Several "case studies" were undertaken to explore the utility of the MIFE technique to study of adaptive responses in a variety of microorganisms.

First, various methodological aspects of ion-flux measurements in microorganisms were addressed. These included the issue of cell immobilisation, specific details of culture growth and preparation, and potentially confounding effects of environmental "hurdles" on measuring electrodes such as ionic strength of solution, pH etc.

Second, a marine protist thraustochytrid ACEM C, proposed as a valuable single source of polyunsaturated fatty acids, was used to demonstrate the applicability of the MIFE technique to understanding the physiology of growth and adaptive responses at the single cell level. Various aspects of membrane-transport processes, associated with thraustochytrid cell growth and development, as well as its adaptive responses to osmoticum, temperature, and nutritional status, were studied.

Third, in a pioneering application of the MIFE technique to bacterial cells, adaptive responses of immobilised bacteria of different genera were studied at the population level. The major emphasis was on *Listeria monocytogenes* and *Escherichia coli*, two physiologically contrasting organisms of great economic importance to food microbiology. The adaptive responses were studied in relation to acid stress, bacteriocin (nisin) action, and substrate availability.

Finally, an investigation was made into the feasibility and utility of combining the MIFE technique with another method and study of bacterial adaptive responses, specifically, Fluorescence Ratio Imaging Microscopy (FRIM), *L. monocytogenes* responses to acid stress were used as a case study.

Overall, this study showed, for the first time, that the application of the MIFE technique to study membrane-transport processes in food-related microorganisms might lead to significant conceptual advances in the understanding of the mechanisms underlying growth and adaptive responses of bacterial and fungal cells and could contribute to reducing food-borne infections or towards improved productions of nutritionally important compounds.

ACKNOWLEDGMENTS

The funding for the project was provided by the School of Agricultural Science. During this time I was supported by a School of Agricultural Science Research Scholarship, an ASM Foundation Scholarship, and the DISR Target Research Alliances program. All this help is greatly acknowledged.

More specifically, I would like to thank my academic supervisors Professor Tom McMeekin and Dr. Tom Ross for their guidance, providing me with valuable scientific inspiration and criticism. I am also very grateful to my research supervisor Dr. Ian Newman of the Physics Department for introduction to the field of biophysical research. To Dr. Birgitte Budde and Dr. Henrik Siegumfeldt at the Royal Veterinary and Agricultural University (Denmark), I am thankful for introducing me to the Fluorescence Ratio Imaging Microscopy. Professor Morgens Jacobsen was a gracious host during my work in Denmark.

I have been fortunate enough to carry out this work in a productive and friendly environment. All my colleagues and staff members at the School of Agricultural Science have made this work extremely enjoyable. Specifically I would like to thank Bill Peterson, Sally Jones, Jane Bailey, as well as the Food Microbiology Group. Tom Lewis is thanked for providing me with thraustochytrid culture and valuable information on its handling. I'm grateful to Dr. June Olley for constructive criticism, particularly during the thesis preparation stage. My colleagues at the Membrane Transport Laboratory from the School of Agricultural Science are thanked for participating in many fruitful discussions on difficult subjects such as transport processes and life.

Last but not least, I am indebted to my friends and parents for being a constant source of support, humour and friendship. Many thanks to my wonderful sons, Stas and Alex, for the constant inspiration, help with thesis preparation and for just being there and keeping my feet firmly on the ground. And the biggest thank you of all to Sergey for sharing his knowledge and technical expertise that was indispensable during the MIFE work, for endless support and encouragement during my work, and for providing me with fun outside of work.

Table of Contents

Publications Produced from this Thesis

ARTICLES IN SCHOLARLY REFEREED JOURNALS

- Shabala L, Shabala S, Ross T and McMeekin T (2001). Membrane transport activity and ultradian ion flux oscillations associated with cell cycle of *Thraustochytrium* sp. *Aust. J. Plant Physiol.* **28:** 87-99.

- Shabala L, Ross T, Newman I, McMeekin T and Shabala S (2001). Measurements of net fluxes and extracellular changes of H^+, Ca^{2+}, K^+, and NH_4^+ in *Escherichia coli* using ion-selective microelectrodes. *Journal of Microbiological methods* **46:** 119-129.

- Shabala L, Budde B, Ross T, Siegumfeldt H and McMeekin T (2002). Responses of *Listeria monocytogenes* to acid stress and glucose availability monitored by measurements of intracellular pH and viable counts. *International Journal of Food Microbiology* **75:** 89-97.

- Shabala L, Budde B, Ross T, Siegumfeldt H, Jakobsen M and McMeekin T (2002). Responses of *Listeria monocytogenes* to acid stress and glucose availability revealed by a novel combination of fluorescence microscopy and microelectrode ion-selective techniques. *Applied and Environmental Microbiology* **68:** 1794-1802.

ARTICLES IN NONREFEREED JOURNALS

- Shabala L (2001). Towards understanding *Listeria* survival: a novel approach. *Microbiology Australia* **22(3):** 38-39.

CONFERENCE PUBLICATIONS

- Shabala S, Newman I, Ross T, McMeekin T (1999). Ion selective microelectrode flux measurements in microbiological research. *Proceedings of the IXth International Congress of Bacteriology and Applied Microbiology.* Sydney, 16-20 Aug (Poster).

- Shabala L, Shabala S, Ross T, Newman I, McMeekin T (2000). A novel non-invasive microelectrode technique and its application to membrane transport activity measurements of *Thraustochytrium* sp. *Proceedings of the 2000 Joint Scientific Meeting of ASM.* Cairns, 8-13 July (Oral presentation).

- Shabala L, Shabala S, Ross T, McMeekin T (20000). Oscillatory activity and ion flux profiles associated with growth and nutritional status of the marine eukaryote *Thraustochytrium* sp. *Proceedings of the 2000 Scientific Meeting of ASM.* Cairns, 8-13 July (Poster).

- Shabala L, Ross T, Newman I, McMeekin T (2000). Measurements of net fluxes and extracellular concentration changes of H^+ and Ca^{2+} of *Escherichia coli* in batch and film cultures using non-invasive ion selective microelectrodes. *Proceedings of the 2000 Scientific Meeting of ASM.* Cairns, 8-13 July (Poster).

- Shabala L, Shabala S, Ross T, McMeekin T (2000). Ion flux profiles and ultradian oscillatory activity associated with cell cycle of *Thraustochytrium* sp. *Proceedings of the 2000 Combined Meeting of ASBMB-ASPP-NZSBMB-NZSPP.* New Zealand, Wellington, 11-14 Dec (Poster).

- Shabala L, Budde B, Ross, T, Siegumfeldt H, Jakobsen M and McMeekin T (2001). Responses of *Listeria monocytogenes* to acid stress and glucose availability as revealed by a combined study using the microelectrodes and fluorescence imaging microscopy. *Proceedings of the 2001Annual Scientific Meeting of ASM.* Perth, 30 Sept – 5 Oct (Oral presentation).

- Shabala L, Newman I, McMeekin T, Ross T, Shabala S (2001). Physiological responses of Thraustochytrium sp. to hypoosmotic shift and chilling revealed by non-invasive microelectrode technique. *Proceedings of the 2001 Combined Meeting of ASBMB-ASPP-ANZSCDB-IPC.* Australia, Canberra, 30 Sept – 5 Oct. (Poster).

LIST OF FIGURES

LIST OF TABLES

LIST OF ABBREVIATIONS

$\Delta\psi$	membrane potential
Ψ	turgor pressure
ΔpH	pH gradient (pH_i-pH_o)
ΔpIon	chemical gradient
AAS	atomic absorption spectroscopy
ACT	apparent critical temperature
AM	acetoxymethyl
ATR	acid tolerance response
a_w	water activity
BHI	Brain Heart Infusion Broth
CCA	cross-correlation analysis
CCC	cross-correlation coefficient
CCCP	carbonyl cyanide-*m*-chlorophenyl hydrazone
cF	5-(and 6-)-carboxyfluorescein
cFSE	5(6)-carboxyfluorescein diacetate, succinimidyl ester
CPFA	cyclopropane fatty acid
CSP	cold shock protein
DCCD	N,N'-dicyclohexylcarbodiimide
DFT	Discrete Fourier Transform
DHA	docosahexaenoic acid
DMSO	dimethylsulfoxide
dV	voltage gradient
EDTA	Ethylenediaminetetraacetic Acid
EGTA	Ethylene Glycol-bis (β-aminoethyl Ether) N,N,N',N'-Tetraacetic Acid
FB	fermentative bacteria
FAB	facultative anaerobe (bacteria)
FA	fatty acid

FRIM	Fluorescent Ratio Image Microscopy
GN	Gram-negative bacteria
GP	Gram-positive bacteria
LAB	lactic acid bacteria
LIX	liquid exchanger (ion-selective resin used in microelectrode fabrication)
LSC	liquid scintillation counting
MIFE®	Microelectrode Ion Flux measurement system
MUFA	monounsaturated fatty acid
MM	Minimal Broth
MP	membrane potential
MRS	de Man, Rogosa, Sharpe Broth
MSC	mechanosensitive channel
NB	Nutrient Broth
NMR	nuclear magnetic resonance
OD	optical density
pH_i	internal (cytosolic) pH
pH_o	external pH
PM	plasma membrane
PMF	proton motive force
PTS	phosphotransferase system
PUFA	polyunsaturated fatty acid
RCT	real critical temperature
RP	resting potential
rRNA	ribosomal ribonucleic acid
RVD	regulatory volume decrease
SAS	School of Agricultural Science, University of Tasmania
SEM	standard error mean
SFA	saturated fatty acid

Chapter 1

GENERAL INTRODUCTION

1.1 Research aims, significance, and project layout

One of the most remarkable properties of bacteria is their ability to survive extreme environmental stresses. Bacteria "break the rules" that biologists take for granted and, by doing that, give researchers unique insights into the limits of life. These remarkable attributes of bacteria inevitably pose several important questions. How do bacteria cope with such extremes? What are the physiological mechanisms behind this? How can we exploit this knowledge to efficiently control bacterial growth?

Central to food microbiology is food safety. According to recent USDA estimates, food-borne disease costs USA $6.9 billion per year (www.meatingplace.com). The Australia New Zealand Food Authority (ANZFA) stated the incidence of foodborne disease in Australia in 1999 as 4.2 million cases per annum, similar to most industrialised nations (Sumner et al., 2000). Almost half of that amount is attributed to two food-borne pathogens, namely *Escherichia coli* and *Listeria monocytogenes*. Recent increase in incidence, magnitude and severity of food-borne disease outbreaks in industrialised nations (Altekruse et al., 1997; Miller et al., 1998; ANZFA, 1999) has highlighted the importance of thorough studies into mechanisms underlying bacterial growth and survival.

E. coli is a Gram-negative, mesophilic bacterium, that is an important component of the facultatively anaerobic biota in the intestine of warm-blooded animals (Orskov, 1984). During the last two decades, several strains of *E. coli*, specifically O157:H7 and non-O157:H7 shiga-toxic *E. coli* emerged as a major cause of food-borne disease outbreaks. In the USA the cost due to each of these strains was estimated at $659.1 and $329.7 million annually, with over 90,000 registered cases in 2000 (USDA estimates on 12-06-01, see www.meatingplace.com/ meatingplace/DailyNews/). A recent outbreak of *E. coli* in Canada in 2000 involved more than 1346 cases and claimed lives of 6 people (BGOSHU report,

www.plant.uoguelph.ca/safefood/). The highest likelihood of pathogenic *E. coli* contamination was found to be in meat products, unpasteurised milk, cheese, mayonnaise and apple cider (Wells et al., 1991; Besser et al., 1993; Willshaw et al., 1994; Hathcox et al., 1995).

L. monocytogenes is a food-borne Gram-positive bacterial pathogen that causes severe illnesses including meningitis, septicemia, and abortion. The reported mortality rates are as high as 40% (Farber and Peterkin, 1991). In 1998, it caused higher rates of hospitalization than any other food-borne pathogen in the USA and caused nearly half the reported deaths (DHHS/FDA/CFSAN, 2001). The estimated cost of food-borne listeriosis is $2.33 billion a year (USDA estimates on 12-06-01, see www.meatingplace.com/ meatingplace/DailyNews/). *L. monocytogenes* can 'colonise' food processing factories making it difficult to eliminate (Smoot and Pierson, 1998 a, b) and frequently leads to post-processing contamination. *L. monocytogenes*' ability to grow at refrigeration temperatures and in the presence of high salt levels, and its ubiquity in nature (Gray and Killinger, 1996) make it a threat to susceptible consumers of long shelflife foods that are eaten without further cooking, e.g. pasteurized milk, soft cheeses, cold smoked fish, delicatessen meats, 'fresh-cut' vegetables and salads, etc. The risk to public health of *L. monocytogenes* in foods has recently been the subject of several large national and international scientific reviews (DHHS/FDA/CFSAN, 2001; WHO/FAO, 2001).

Current consumer trends favour foods which are perceived to be "natural", i.e. that have few added preservatives, and have received minimal processing. At the same time, consumers expect all foods to be safe, creating a paradox for the food industry, i.e. how to achieve affordable, minimally-processed foods that are stable enough to reach increasingly distant markets, and are safe from pathogens. The traditional approach has been to use a number of inhibitory factors (low pH; salt; temperature), each at an average level, which are believed to act synergistically to *prevent* growth. This approach has been termed "Hurdle Technology" (Leistner, 1987). Conventional ways to screen for the most optimal combinations involve lengthy and costly empirical processes. Many inhibitors are routinely used for food processing (preservation with different chemicals including acid preservatives and

high salt levels; extreme temperatures; bacteriocins; UV treatment, etc.). Not only should each of these be tested in a wide range of concentrations/values, specific for each organism, but also the sequence of stress factors might significantly affect bacterial growth and survival patterns (Shadbolt et al., 2001).

Improving the application of "Hurdle Technology" implies a better understanding of the physiological processes underlying cellular response to the applied treatments. Insights into early events, associated with environmental perception and signalling in microorganisms, might offer efficient measures to control their growth with minimal doses of treatments used.

Although microbial growth is a problem when it results in food spoilage, microorganisms are also used beneficially in the food industry for food production. Controlled growth of microorganisms on or in foods is used to produce numerous foods and beverages that are considered gastronomic delights. For the most part, the fermentative metabolism of microorganisms is exploited in food production. For example, the growth of microorganisms in or on milk produces a variety of dairy products such as sour cream, yogurt, kefir, and cheese; fermentation of fruits and grains results in wine and beer production, respectively. Furthermore, fermentative bacteria and yeast are used in production of fermented meat (eg., salamis) and vegetables, as well as leavening of bread. Another example is vinegar production, where microbial oxidative metabolism is used. In all these cases optimisation of microbial growth and accumulation of their metabolic products is desirable.

Microorganisms can also be used as a source of single-cell protein (SCP) (Atlas, 1984). Various bacteria, fungi and algae are potential sources of large amounts of SCP. There is also growing interest towards using microorganisms as a source for edible oil production. Thraustochytrids have attracted special interest as a rich source of polyunsaturated fatty acids (PUFA) with high level of docosahexaenoic acid (DHA) in particular. The current and potential market for PUFA products spans animal feeds, human food additives (for bread, spreads, soft drinks, infant formula enrichment), nutraceuticals, and pharmaceutical industries (Takahata et al., 1998; Lewis et al., 1999). Fish oils, commonly used at present, cannot satisfy growing demand for PUFA (Lewis et al., 1999). Furthermore, the

amount of DHA in thraustochytrids reaches as high as 40% as compared with 7-14% in fish oil (Singh and Ward, 1996; Iida et al., 1996). In the United Kingdom, fish oils account for approximately 29% (US $140 million) of the total annual market for nutraceuticals (Mukherjee, 1999). The western European market for infant formula increased from 81,500 tonnes in 1988 to 103,933 tonnes in 1994 (Lewis et al., 1999). Efficiency of PUFA production can be optimised by varying the culture and growth conditions. For such microorganisms, understanding of cell adaptive responses might be used to optimise growth conditions, ultimately enhancing efficiency of technological processes in the food industry. Microorganisms are potentially an important inexpensive source of SCP and PUFA rich products.

Cellular membranes are traditionally considered to act as a semi-permeable barrier allowing the preferential uptake of some nutrients, and preventing or restricting accumulation of undesirable chemicals (Maloney and Wilson, 1996). Recent progress in electrophysiology and molecular genetics has revealed the crucial role of plasma membrane transporters in perception and signalling in response to literally every known environmental factor (Zimmermann et al., 1999). Changes in plasma membrane potential and/or ion flux modulations are amongst the earliest cellular events ever measured in response to light (Grishanin et al., 1996; Hegemann, 1997; Spudich, 1998; Shabala and Newman, 1999), temperature (Ilan et al., 1995), hormonal stimuli (Blatt and Thiel, 1994), elicitors (Nurnberger et al., 1994), osmotic stress (Shabala, 2000) and mechanical stimulation (Gustin et al., 1986) in many organisms. However, little is known of early events in the adaptive response of bacterial cells occurring at the cell membrane that enable their survival in hostile environments or their growth in ready-to-eat foods.

In this work, a new approach to understanding the mechanisms of inactivation or inhibition of growth, required to advance minimal preservation technology, is undertaken based on the novel application of the Microelectrode Ion Flux Estimation (MIFE®) technique in food microbiology. The MIFE technique was developed at the University of Tasmania and since the late 1990's has been successfully applied to the study of various aspects of membrane-transport processes in plants (Shabala et al., 1997; Shabala and Newman, 1997 a, b, 1998; Pharmawati et al., 1999; Babourina et

al., 2000; Shabala, 2000; Newman, 2001). In the present work, a comprehensive study on the feasibility of MIFE application in food microbiology was undertaken, aimed to shed light on adaptive responses of bacterial and fungal cells.

Proper cell immobilisation is one of the key factors in successful MIFE measurements of bacterial cells. Therefore, an efficient experimental protocol for cell immobilisation was developed.

Considering the large number of microorganisms of particular significance to the food industry, it might take years, if not decades, to provide the explicit coverage of all aspects of cell adaptive responses to all known "hurdles". That is clearly beyond the scope of a PhD project. A few "case studies" to explore the feasibility of application of non-invasive ion-flux measurements were undertaken to study adaptive responses in food-related microorganisms. The experimental part consists of three major blocks: methodological aspects, single-cell level, and population studies (Fig. 1-1).

The first block deals with methodological aspects of ion-flux measurements in food microbiology. The pioneering nature of this study meant that many important methodological issues had to be addressed to ensure absence of unwanted side-effects on measurements. That included the issue of cell immobilisation, and potentially confounding effects of environmental "hurdles" such as ionic strength of solution, pH, etc. on measuring electrodes. All those were addressed prior to commencement of physiological studies into adaptive responses of the studied organisms and are presented in Chapter 3.

The second block is related to MIFE application at the single cell level. As a "case study", the marine protist thrausochytrid ACEM C, which is used in food biotechnology as a valuable single source of poly-unsaturated fatty acids, was used. Chapter 4 covers application of the MIFE technique to study various aspects of thrausochytrid ACEM C cell growth and development, as well as its adaptive responses to osmoticum, temperature, and nutritional status. Specific emphasis was placed on the role of ion flux oscillations associated with the cell life cycle and on adaptive responses to hypoosmotic stress and low temperature effects (Fig.1-1).

In the third block of the study, the MIFE technique was applied to study adaptive responses of immobilised bacteria at the population level. First, the application of MIFE to study transport processes at bacterial membranes using different bacterial genera was demonstrated. The studies included screening a variety of bacteria to ensure MIFE applicability. The major emphasis was on *Listeria monocytogenes* and *Escherichia coli*, two physiologically contrasting (Gram-positive and Gram-negative, respectively) organisms of great economic significance to food microbiology (see above). Adaptive responses were studied in relation to acid stress, bacteriocin action (nisin), and substrate availability. Finally, the feasibility and utility of combining the MIFE technique with Fluorescence Ratio Imaging Microscopy (FRIM) to study bacterial adaptive responses was investigated (using *L. monocytogenes* responses to acid stress as a case study).

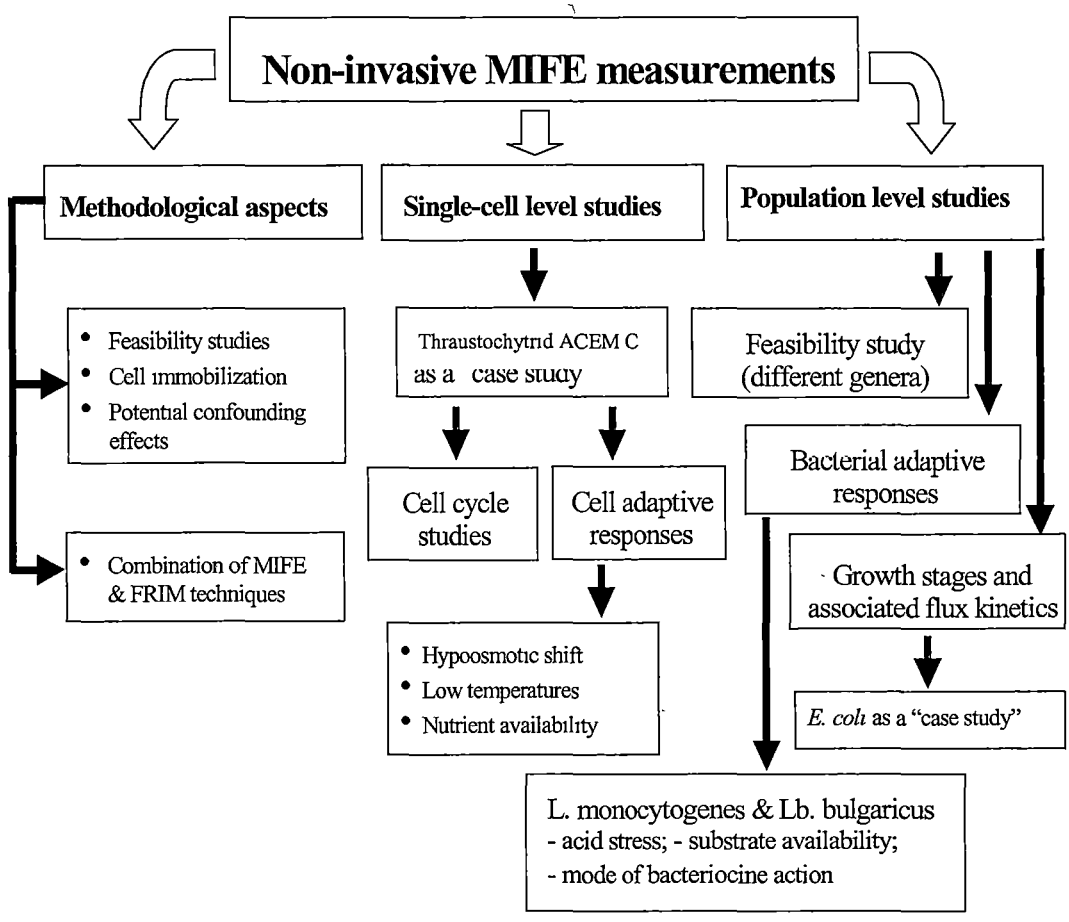

Fig. 1-1. General layout of the study.

Consequently, the **major objectives** of this study were:

(i) Developing an efficient experimental protocol for cell immobilisation, thus providing a bacterial monolayer for MIFE measurements;

(ii) Assessing the feasibility of the non-invasive ion flux measuring (the MIFE) technique in food microbiology for a variety of microbial and fungal organisms;

(iii) Developing experimental protocols enabling ion flux measurements from the surface of immobilised bacteria, thus providing an opportunity to study their adaptive response mechanisms;

(iv) Showing the practicability of using bacterial (*E. coli*) and fungal (thrausochytrid ACEM C) organisms as model subjects for studying the role of membrane-transport processes and associated ion flux kinetics in cell growth and development;

(v) Demonstrating feasibility of application and providing new insights into membrane-transport processes associated with bacterial response to some major "hurdles" used in food preservation, such as low pH, salt, or bacteriocins;

(vi) Exploring the feasibility and utility of combining the MIFE technique with FRIM.

1.2. Role of membrane-transport processes in growth and adaptive responses of microbial organisms

The cytoplasmic membrane is a selective barrier that restricts entry and exit of solutes thus being regarded as a "natural' barrier of an organism. When integrity of the membrane is lost, the cells are freely permeable to all solutes, finally leading to their death (Yeagle, 1989). Membranes play a central role in both the structural organization and function of all cells. Membranes control the movement of essential solutes (inorganic ions and nutrients) in and out of the cell. Whereas the primary role of membrane lipids is the formation of a stable bilayer, membrane proteins provide the active components for biological membranes. These proteins are responsible for the trans-membrane communication and functional interactions within the plane of the membrane.

The processes at and in the plasma membrane largely determine why, for instance, a specific environment results in a specific growth rate or in the overproduction of a specific metabolite (Maloney and Wilson, 1996; Burgstaller, 1997). Membrane transport and the metabolism are thus 'two sides of the same fence', which cannot be separated.

Membrane transporters are involved in a response to any environmental or endogenous stimuli (Zimmermann et al., 1999). Changes in membrane-transport activity have been demonstrated in a large number of bacteria in response to virtually every known environmental constraint such as temperature extremes, osmolarity, high and low pH and other factors. Membrane transport underpins a wide range of essential processes, the most important of which are:

(1) Nutrient acquisition and waste product excretion;

(2) Cell energetics;

(3) Cytosolic pH homeostasis;

(4) Osmotic regulation;

(5) Signal transduction.

Details of these important functions of the membrane are given below.

1.2.1 Transport of nutrients and extrusion of wastes

Transport of nutrients into the cell and extrusion of wastes is a fundamental requirement for any organism. Both fungi and bacteria survive in environments that are poor in nutrients. As a consequence, they have developed a variety of mechanisms for the transport of metabolites from the external medium, where such molecules may occur at very low concentrations, to the cytoplasm where the concentrations must be considerably higher to sustain metabolism. Apart from the nutrients, some inorganic ions (eg. potassium and ammonium) must also be taken up against a concentration gradient. Potassium is the most abundant cytoplasmic cation in growing bacterial cells, playing a crucial role in the activation of cytoplasmic enzymes, maintenance of turgor pressure, and regulation of cytoplasmic pH (Bakker et al., 1987; Silver, 1996; Booth, 1985, 1999). The concentration of K^+ in the bacterial cytoplasm is generally much higher than in the surrounding medium, approximately 200 mM in Gram-negatives and up to 400 mM in Gram-positives (Nicholls and Ferguson, 1992; Silver, 1996). Consequently, energy is usually required to take K^+ up against the concentration gradient. The same is true for ammonium uptake. *E. coli* was shown to have an energy-dependent NH_4^+ uptake system (Stevenson and Silver, 1977; Barnes and Jayakumar, 1993).

For the uptake of anions, energy is necessary (active transport) even if the extracellular concentration of the nutrient is higher than the intracellular concentration. The reason for this is that the membrane potential is negative inside (e.g. steep uphill electrical gradient for anions). The uptake of orthophosphate is an example (Jennings, 1995). These uptakes are therefore entirely dependent on metabolic energy.

Regardless of an organisms structure (eukaryotic or prokaryotic), very rigid physiological constraints are imposed on intracellular Na^+ and Ca^{2+} concentrations. High sodium levels in the cytosol are believed to impair significantly the activity of key cellular enzymes and, therefore, must be kept at some reasonably low level (Padan and Schuldiner, 1996; Silver, 1996). As for Ca^{2+}, due to its unique role as a second messenger in all living organisms (Norris et al., 1996; Sanders and Bethke, 2000), its cytosolic concentrations are maintained at constant levels of the order of

100 nM (Sanders and Bethke, 2000). Both intracellular Ca^{2+} and Na^{+} homeostasis is regulated by the active extrusion of these ions via either corresponding pumps (in some organisms), or using hydrogen-coupled secondary active transport mechanisms (Silver, 1996; Smith et al., 1999; Sanders and Bethke, 2000).

Furthermore, metabolism inevitably generates waste products that must be removed from the cytosol. The examples of the latter include lactate and acetate, products of metabolism of most bacteria (Huisman et al., 1996). In biotechnology, membrane transport exerts an important influence on useful product formation via the excretion mechanism(s). This enables an easier separation of the desired product from the cell mass (Burgstaller, 1997).

1.2.2 Role in cell energetics

The bacterial membrane plays a crucial role in cell energetics. In the living cell two major forms of energy are ATP and ion gradients across the cell membrane. ATP represents a pool of free chemical energy that is released upon hydrolysis of the molecule. The ion gradients represent free energy stored in an electrochemical gradient of either H^{+} or (in some organisms) Na^{+}, and is a result of membrane semi-permeability (reviewed by Nicholls and Ferguson, 1992; Lolkema et al., 1996). The gradients exert a force on the ions (the ion motive force) that consists of two components, the chemical potential difference ΔpIon and the electrical potential difference $\Delta\psi$. A proton electrochemical potential difference is known as the proton motive force (PMF). The PMF is a measure of the free energy stored in a trans-membrane electrochemical potential difference for H^{+} and may be expressed in volts. Consequently, the PMF consists of two components: the chemical potential difference ΔpH and the electrical potential difference $\Delta\psi$, according to the following equation:

$$PMF=\Delta\psi - 2.3\ RT/F\ \Delta pH \qquad (1)$$

where R is the gas constant, T is the absolute temperature, F is the Faraday constant. The equation is also applicable if the ion and electrochemical gradients represents Na^{+}.

The PMF can be generated by different mechanisms depending on the energy conversion pathways in the organism (Mitchell, 1973). In anaerobic organisms, which lack the respiratory chain, the ATP produced during fermentation is hydrolyzed by the proton-translocating ATPase. The ATPase system utilises the free energy of ATP hydrolysis to carry out the extrusion of protons with concomitant generation of PMF (Harold, 1986). Conversely, in aerobes, the translocation of protons down the electrochemical gradient during respiration can be efficiently coupled with ATP synthesis, generating PMF (Maloney, 1990). The respiratory chain is a metabolic pathway consisting of alternating carriers for hydrogen and electrons. These carriers couple the oxidation of a substrate (using oxygen as the final electron acceptor) with the net extrusion of protons from the cytoplasm. Therefore, a major function of the respiratory chain is to pump protons across the cytoplasmic membrane with the consequent establishment of a PMF. The ATPase utilises the PMF to power the phosphorylation of ADP for ATP synthesis (Harold, 1986).

The PMF is the driving force for a number of energy-demanding processes in the cell (Fig. 1-2). The different pools of free energy are inter-convertible through the action of reversible ATPases/synthases that couple transport of either H^+ or Na^+ to the hydrolysis/synthesis of ATP. The total free energy in the pools increases as a result of ATP synthesis by substrate level phosphorylation and the translocation of proton and sodium ions across the cell membrane (Lolkema et al., 1996). The PMF is generated as a result of both metabolic and transport steps.

Biological processes directly linked to the PMF include ATP synthesis, protein phosphorylation, flagellar synthesis and rotation, reversed electron transfer, transmembrane transport of proteins, accumulation of ions and metabolites with the help of specific carriers etc (Fig. 1-2).

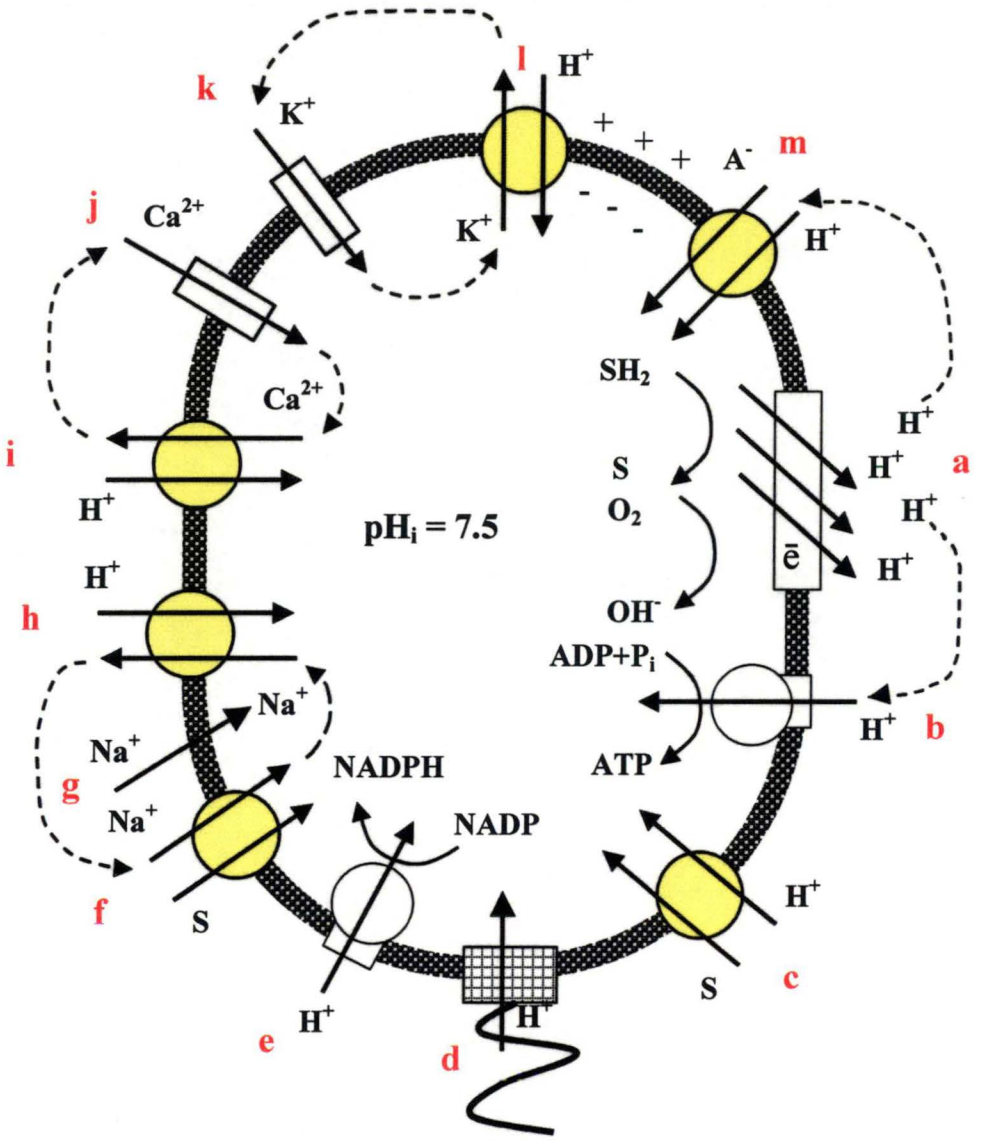

Fig. 1-2. Energy transduction by the H^+ circulation and the coupled transport in *E. coli*. Respiration drives H^+ extrusion from the cell (a) that generates a proton potential. H^+ re-enter the cell via a number of routes and perform useful work: (b) H^+-ATPase, (c) by symport with a substrate (S), (d) the flagellar motor, (e) pyridine nucleotide transhydrogenase; several kinds of H^+-linked transport systems: (h) the Na^+/H^+ antiport, (i) Ca^{2+}/H^+ antiport, (l) K^+/H^+ antiport, (m) symport with anions. In (g), (j), and (k) the presence of Na^+ and Ca^{2+} leak and active uptake systems for K^+, respectively, together with their respective antiports, constitute the Na^+, Ca^{2+}, and K^+ cycles of the cell. Also shown an example of Na^+-linked substrate (S) transport (f). (Based on Booth, 1985; Harold, 1986; Harold and Maloney, 1996).

Since the activity of these processes will cause the dissipation of the PMF, a continuous extrusion of protons is necessary for the maintenance of a fairly constant PMF. It is accepted that for a normal bacterial cell to function, the PMF values should be maintained at about –100 mV to –200 mV (Hellingwerf and Konings, 1985). Another important feature of PMF is maintaining a relatively high membrane potential, typically of about – 120 to –150 mV (negative inside), which is used as a driving force for passive uptake of many ions (Kashket, 1981). In addition, there are also active transport processes that are powered by a Na^+ electrochemical gradient or by the direct hydrolysis of ATP (Nicholls and Ferguson, 1992). The sodium electrochemical gradient was demonstrated to be used in some organisms where Na^+ circuits are generally important, e.g. *Vibrio* species (Nicholls and Ferguson, 1992).

1.2.3 Maintenance of cytosolic pH homeostasis

The structure and function of most macromolecules is influenced by pH. Among the most pH-sensitive are enzymes. Changes in pH are known to alter the charges of the 3D active site and the substrate such that the binding capacity is affected (Raven et al., 1999). Therefore, the intracellular "metabolic kitchen" is efficient only within a certain narrow range of internal pH (pH_i). This is achieved by a complex network of mechanisms aimed at maintaining pH_i at an almost constant level despite variations in the pH of the environment, termed "pH homeostasis" (Guern et al., 1991; Hall et al., 1995).

Based on the actual pH_i values, three major groups of bacterial organisms are distinguished: acidophiles, neutrophiles and alkaliphiles (Booth, 1985; Hall et al., 1995). When the difference between pH_i and pH_o is high, the pH homeostasis might collapse resulting in the organism's death.

Maintaining the pH homeostasis is achieved via numerous mechanisms (Datta and Benjamin, 1997; Dilworth and Glenn, 1999) including:

i) decrease in membrane permeability;

ii) increase in cytoplasmic buffering capacity;

iii) amelioration of pH_o;

iv) proton extrusion/uptake.

Membrane permeability. The first line of defence is to minimize membrane permeability, to prevent either the uptake or loss of H^+, depending on the pH_o. The permeability barrier to protons, and no other ions, is therefore an important component of the homeostatic system. It was shown that H^+ permeability may be regulated by changes in membrane lipid composition (Booth, 1999). Growth at low pH was shown to have altered the lipid composition of bacterial membranes, leading to a decreased ratio between unsaturated and saturated fatty acids, and to an increase in cyclopropane fatty acids (CPFAs) (Lepage et al., 1987; Brown et al., 1997). Other adaptive responses include increase in phospholipids with amino head groups (Koostra and Smith, 1969; Gould and Lennarz, 1970; Kocun, 1970, Haest et al., 1972). Such lipid changes have been proposed as a barrier to proton entry (Haest et al., 1972) and could directly affect the proton permeability leading to a higher pH homeostatic capacity.

Although there is evidence that this option is implemented (Booth, 1985), and that membrane composition can vary with pH (Arneborg et al., 1993), it clearly has its limits. Reducing membrane permeability for H^+ or OH^- will inevitably result in the dramatic reduction in permeability for other ions required to maintain the cell metabolism (Dilworth and Glenn, 1999). Therefore, some other avenues to maintain pH_i homeostasis should be explored.

Buffering capacity. Another strategy for pH_i homeostasis involves cytoplasmic buffering to counteract potential upward or downward shifts in pH_i. Buffering due to synthesis of intracellular metabolites involves continuous production of buffering materials and consequently a steadily increasing concentration of them. In the neutral to slightly acidic pH_0 range the buffering capacity of the cytoplasm has been estimated to be of the order of 50-100 nmol H^+/pH unit per mg cell protein (Booth, 1985). Data of Krulwich et al. (1985) support these findings. For most cells that maintain pH_i in the neutral range the buffering capacity derives from the titration of the phosphate groups and carboxylates of physiologically abundant metabolic species. Although the buffering of cytoplasm might avert a temporary crisis, later reports consider that it is difficult to envisage it as a long-term strategy (Ingraham

and Marr, 1996; Dilworth and Glenn, 1999) and conclude that cytoplasmic buffering capacity plays a limited role in cellular pH homeostasis.

Amelioration of pH_o. Bacteria commonly modify pH_o through metabolic activities. Catabolism of sugars or sugar alcohols generally results in acidification, whereas catabolism of organic acids or amino acids leads to rises in pH_o (Gale and Epps, 1942; Meng and Bennett, 1992; Watson et al., 1992; Stim and Bennett, 1993). A major disadvantage of the amelioration strategy is the requirement for continuous access to suitable substrates in sufficient quantities. For enteric or other bacteria in nutrient-rich environments, such as the gut or elsewhere inside animals, amelioration may be practical. For many bacteria in natural pH-stressed environments, appropriate substrates are unavailable and amelioration is not achievable. Dilworth and Glenn (1999) also suggest that amelioration of the external environment is unlikely to be a major factor in resistance to change in pH_o.

Ion extrusion/uptake. Another extremely important option involves energy-requiring systems to pump ions actively in such a way that pH_i can be maintained. Booth (1985) proposed to consider a bacterial homeostatic system as being composed of two major components: "passive" and "active". The former includes membrane permeability and buffering capacity, the latter is achieved through the controlled movement of cations across the membrane. Active homeostasis implies the ability to sense, and respond to, perturbations of pH_i (Booth, 1999). To maintain specific pH_i the cell needs to be able to either acidify or alkalinise the cytoplasm beyond the desired set point depending upon the direction of the initial perturbation. Cation transport, specifically Na^+ and K^+, is essential to these processes. The movement of sodium ions has a major role in regulation of the cytoplasmic pH of alkaliphiles (Padan and Schuldiner, 1994; Krulwich et al., 1997). Potassium transport plays a major role in pH homeostasis in *E. coli* and other bacteria living at neutral pH (Kroll and Booth, 1981; Kroll and Booth, 1983; Booth, 1999).

1.2.4 Osmotic regulation

Unlike animal cells, plant, fungal, and bacterial cells (with the exception of the mollicutes) are all surrounded by a cell wall that resists deformation. The presence of a wall permits them to generate turgor (positive pressure). Consequently these organisms maintain an intracellular osmotic pressure greater than that of the surrounding medium. Maintenance of turgor pressure is essential for growth and division of the cell (reviewed by Ingraham and Marr, 1996). For example, *E. coli* maintains a turgor pressure of approximately 0.3 MPa over a wide range of osmolality of external medium. It follows that the concentration of solutes in the cytoplasm must increase linearly with external osmolarity in order to maintain turgor pressure. Transport processes play a crucial role in this homeostasis. K^+ is particularly important in this respect (Epstein and Schultz, 1966; Ingraham and Marr, 1996). Species of microorganisms differ significantly with respect to the lower limits of water activity (a_w), or upper limits of osmolality, permitting growth; the lower limit tolerated by any microorganism is about 0.62, equivalent to about 30 osM (Ingraham and Marr, 1996). For example, *E. coli* is in the mid range of osmotic tolerance exhibited by nonhalophilic bacteria, and is more tolerant than *B. subtilis* and *Pseudomonas aeroginosa* but less so than many lactobacilli and particularly *Staphylococcus aureus* (Ingraham and Marr, 1996).

Transport of ions helps maintain osmotic potential of an organism. Thus, for *E. coli* growing in minimal medium at high external osmolality, the osmolality of the cytoplasm is increased by the accumulation of K^+, glutamate, and trehalose, and ionic strength is reduced by the exchange of K^+ for putrescine. These adjustments permit growth up to an external osmolality of at least 2 osM (McLaggan et al., 1994). *L. monocytogenes* and many other non-halophiles were also shown to transport compatible solutes (e.g. glycine betaine, carnitine) from the external media (Galinski, 1995; Verheul et al.,1997a). Other bacteria exhibit similar strategies (reviewed by Galinski, 1995).

Conversely, transport of solutes from the cell during hypoosmotic shock enables cells to survive in dilute media without bursting (reviewed by Lang et al., 1998; Wood, 1999). Bakker (1992) found that if a culture of *E. coli* growing in 0.4 M

NaCl is abruptly diluted 1:1 with water, 90% of the K^+ and glutamate and 60% of the trehalose are lost from the cells while ATP and alanine are retained. These examples illustrate the importance of transport processes in osmoregulation.

1.2.5 Signal transduction

Membrane transport involvement in signal transduction is best documented for plant and animal systems. Many biotic and abiotic signals for plant growth and development trigger their respective responses by transiently increasing the concentration of cytosolic free calcium, which is accomplished through the activities of two kinds of transport systems. First, Ca^{2+}-translocating ATPase removes Ca^{2+} from the cytosol by pumping it across the plasma membrane, thereby maintaining the cytosolic concentration of free Ca^{2+} at about 0.1-0.2 μM. This low concentration of free Ca^{2+} is essential in all cells to prevent precipitation of phosphates, but in eukaryotes it has become a base on which stimulus-response coupling pathways are built. Second, Ca^{2+}-permeable channels open in response to particular stimuli and allow the passive entry of Ca^{2+} into the cytosol, thereby propagating the signal (Sanders and Bethke, 2000).

Recent evidence suggests that a similar calcium signalling system exists in bacteria (reviewed by Norris et al., 1996). More than 30 receptors are known in *E. coli*, including 15 chemoreceptors, as well as pH, temperature, and proton-motive force sensors. The latter are outstanding among these receptors because changes in the PMF can activate or deactivate a transport system (Stein, 1986). This regulation includes voltage-gated calcium channels responsible for influx and efflux, and calmodulin-like proteins responsible for mediating responses to calcium, thus implicating signal transduction across the cellular membrane. Calcium is increasingly implicated in a number of bacterial functions, including heat shock, pathogenicity, chemotaxis, differentiation, and the cell cycle (reviewed by Norris et al., 1996). Signal transduction mechanisms in yeast are also well studied (Rep et al., 1999; Holyoak et al., 2000; de Groot et al., 2001). In contrast, less details are known about signal transduction in fungi (Burgstaller, 1997).

1.3. Membrane transport systems in microorganisms

Membrane transport plays a fundamental role in many biological processes in cells. The complete sequence of the yeast genome reveals that about 2000 of the 6000 genes encode proteins associated with membranes, of which a large portion are transport system components (Sanders and Bethke, 2000).

For an ion bearing a net charge, two factors determine the energy requirements of its movements across the membrane: the concentration difference across the membrane, and the membrane electrical potential difference (membrane potential).

Transport processes occur via primary active transporters (pumps), secondary transporters (carriers), and channels.

1.3.1 Pumps

Only a few systems directly couple ion transport to the scalar events of intermediary metabolism. These are associated with electron transport, Na^+-translocated decarboxylases and ATPases that are linked to the hydrolysis or synthesis of ATP (Harold and Maloney, 1996). Pumps catalyse transport of ions or complex organic molecules against their electrochemical gradients. H^+ pumps are generally driven by ATP hydrolysis (in plants, fungi, and fermenting bacteria), removing H^+ from the cytosol and generating a PMF across each membrane. In respiring bacteria, the electron transport chain is arranged across the cellular membrane in such a way that protons are translocated outside the membrane, and ATP is synthesised when protons enter the cell.

Two major classes of ATP-linked ion motive force are recognized in bacteria:

(i) the P-type ATPases, named so because they are phosphorylated during their reaction cycle, and

(ii) F0F1-ATPases, of which there are two distinct subgroups, F and V types. As a general rule, F-type ATPases are found in the eubacteria and their descendants, while V-type ATPases populate archaebacterial and eukaryotic domains (Harold and Maloney, 1996).

P-type ATPases hydrolyse ATP to move one or more cations inward or outward, or in exchange (H^+, Na^+, K^+, Ca^{2+}, Mg^{2+}, Cu^{2+}, Cd^{2+} are known substrates) (Stokes

UNIVERSITY OF [illegible] LIBRARY

and Nakamoto, 1994). Examples include the Mg^{2+} ATPase of *Salmonella typhimurium*, Kdp (K^+)-ATPase of *E. coli* (reviewed by Harold and Maloney, 1996), Cu^{2+}-ATPase of *L. monocytogenes* (Agranoff and Krishna, 1998). All P-type ATPases share extensive amino acid sequence homology. Four large clusters can be distinguished. These are composed of Ca^{2+}- and Mg^{2+}-motive ATPases (cluster 1); K^+/H^+- and K^+/Na^+-exchange pumps (cluster 2); electrogenic H^+-ATPases of fungi and plants (cluster 3); and H^+-, Cd^{2+}-, K^+, and Cu^{2+}-ATPases (cluster 4) (Fagan and Saier, 1994).

The main bacterial ion pump is the H^+-translocating F0F1-ATPase. Barring a few exceptions, it is found in all bacterial membranes. In obligate or facultative aerobes, it functions to synthesize ATP during oxidative phosphorylations, while under anaerobic conditions it itself initiates the H^+ circulation by pumping out H^+ (Harold and Maloney, 1996).

The proton pumps at plasma membranes are electrogenic. They create electrical current because the ions they remove from the cytosol carry charge. Therefore, these H^+-pumping ATPases not only contribute directly to the chemical component of the PMF, the ΔpH, but also tend to make the electrical component more negative (see equation 1).

The PMF generated by the plasma membrane (PM) H^+-pumping ATPase powers the transport through a variety of carriers; it also influences ion channel activity through its impact on membrane potential. The enzyme therefore constitutes a foundation for other transport processes at the plasma membrane (secondary active transporters).

1.3.2 Carriers

Carriers represent transport systems that couple the electrochemically "downhill" flow of ions such as H^+ or Na^+ with the electrochemically "uphill" flow of inorganic ions and solutes. Carriers translocate a wide range of simple solutes, including ions, sugars, and amino acids. The transport process does not involve chemical modification of any of the compounds bound to the carrier. Solute transport through carriers is generally energized through coupling of PMF-driven H^+-transport

to the flow of the solute against the electrochemical gradient. Carriers translocate a wide variety of inorganic ions and small organic solutes with high specificity. The principal inorganic nutrients translocated by carriers include NH_4^+, NO_3^-, phosphate, and K^+. Among organic solutes translocated into cells by carriers are sugars, amino acids, and purine and pyrimidine bases (reviewed by Harold and Maloney, 1996). Many carriers are symporters or antiporters of H^+ or Na^+. In some marine algae, uptake of NO_3^- and some amino acids is Na^+-dependent.

The carriers can be classified into three groups (Lolkema et al., 1996).:

(i) uniporters that catalyse the translocation of a single solute across the cytolasmic membrane,

(ii) symporters that couple the movement of solutes in the same direction, and

(iii) antiporters that couple the movement of solutes in opposite direction

Uniporters transport a substrate down its electrochemical gradient (Harold and Maloney, 1996). Electrogenic uniporters have been noted for malate and citrate uptake in the lactic acid bacterium *Leuconostoc oenos* (Salema et al., 1994; Ramos et al., 1994); and the glycerol, nitrate, and formate uniporters of *E. coli* (Maloney and Wilson, 1996).

Carriers that catalyse solute flux in the same direction as H^+ or Na^+ flux are known as ***symporters***. Because protons flow passively across most membranes in the direction of the cytosol, symporters typically energize uptake of solute into the cytosol. Examples of symporters include:

- citrate/Na^+ in *K. pneumoniae* (Lolkema et al., 1996)
- accumulation of K^+ in symport with H+ in *E. coli* (Maloney and Wilson, 1996)
- β-galactoside/H^+ symport in *E. coli* (Maloney and Wilson, 1996).

Protons were once thought to be the only cations to move in symport with sugars and amino acids into *E. coli*. It is now known that melibiose and proline transport both occur in symport with Na^+, driven by the Na^+ electrochemical gradient (reviewed by Nicholls and Ferguson, 1992; Maloney and Wilson, 1996). The Na^+ role of the circuit has been established for many species of bacteria (Nicholls and Ferguson, 1992; Maloney and Wilson, 1996). Regarding alkaliphilic

bacteria this can be explaned on the basis that electrochemical proton gradient is too small to drive the transport process.

Exchange of solutes for protons or sodium ions occurs via ***antiporters.*** Examples for bacteria include:

- citrate/H^+, malate/H^+, lactate/H^+ in *Lc. mesenteroides*;
- malate/H^+ and lactate/H^+ in *L. lactis* (Lolkema et al., 1996);
- Na^+/H^+ antiport that plays a role in regulation of cytosolic pH (Orlowski et al., 1992; Fliegel and Frohlich, 1993; Padan and Schuldiner, 1996; Maloney and Wilson, 1996).

Both symporters and antiporters tend to dissipate the PMF, and this energy is conserved in the form of an electrochemical potential for particular solutes.

1.3.3 Channels

Channels facilitate the movement of specific ions down their electrochemical gradients. Thus ion flow through channels is passive. Channels gate between open and closed states. Channel gating might be controlled by a large number of signal molecules, as well as by membrane voltage or ligands, depending on channel type. In a broad sense, two major type of channels may be distinguished: (a) specific and (b) non-specific.

(a) ***Specific channels*** exhibit ionic selectivity. Several classes of ion channels have been described in a variety of organisms, including those specific for K^+, Ca^{2+}, and anions (including Cl^-, NO_3^-, and organic acids) that are highly selective (reviewed by Stumpe et al., 1996).

(b) ***Non-specific channels*** are also present in membranes. These are mechano-sensitive (or stretch-activated) channels (MSC) that are opened in response to application of some stretch to the membrane (eg. in response to swelling after a hypoosmotic shock) and are not ion specific. The direction of net ion flux through a channel is determined solely by the sign of the electrochemical driving force acting on that ion. These channels are found in both prokaryotes and eukaryotes (Letellier and Bonhivers, 1996; Lang et al., 1998).

Both channels and transporters mediate solute movement across the membrane. A major distinction that can be drawn between them is that while there is a relatively fixed stoichiometry of solute movements per conformational cycle of the transporter, there is no strict linkage between the cycle of opening and closing of a channel and the number of ions moving. Transporters can create solute gradients using energy, provided by either H^+ or Na^+ motive force of the hydrolysis of ATP, which may modify the conformational cycle (Booth et al., 1996). The membrane potential is an integral part of the electrochemical driving force on ions, and any membrane potential generated by the action of electrogenic pumps will contribute to the overall force that drives ions through channels. Plasma membrane anion channels were shown to facilitate salt release during turgor adjustment (particularly in response to hypoosmotic shock) as well as elicit membrane depolarisation after stimulus perception (Bisson et al., 1995; Wood, 1999; Stento et al., 2000).

1.3.4 Membrane transport systems in model organisms employed in this study

Recent progress in electrophysiology and molecular genetics has revealed the crucial role of membrane transporters in perception and signalling in response to environmental factors (Zimmerman et al., 1999). Changes in membrane potential and/or ion flux modulations are amongst the earliest cellular events measured in response to a variety of treatments (high and low temperature, osmotica, low pH, etc.) used in food preservation. However, transport processes are not equally well studied in different microorganisms that are of interest in food microbiology.

E. coli is the model organism used to study transport processes in bacteria since the establishment of chemiosmotic theory by Mitchell (1961) with a concomitant intensity of study. As a result, its electrophysiology is well characterised. In their 1996 review, Maloney and Wilson listed more than 70 different transporters known to be present at the inner plasma membrane of *E. coli*; that number has increased significantly since that time.

In contrast, membrane-transport systems in *L. monocytogenes* are understood less well. Only a score of publications are available. These include the evidence of

transport systems for carnitine and glycine betaine transporters (Verheul et al., 1995a, 1997a; Sleator et al., 1999; Ko and Smith, 1999; Fraser et al., 2000; Gerhardt et al., 2000), glucose (Parker and Hutkins, 1997), peptides (Verheul et al., 1995b, 1998), extrusion of heavy metals (Lebrun et al., 1994; Francis and Thomas, 1997; Agranoff and Krishna, 1998; Dalet et al., 1999), and multidrug efflux transporter (Mata et al., 2000). Despite known salt tolerance of *L. monocytogenes*, there is no information about either the Na^+ or K^+ transport system in this bacterium. It is assumed that transport systems for different bacteria might be similar. However, it is not always the case. For example, it is well established that melibiose is transported in *E. coli* in symport with either H^+, Na^+, or Li^+ as coupling ions (Maloney and Wilson, 1996), while in a closely related bacterium, *K. pneumoniae*, the sugar is transported in symport with H^+ but not Na^+ (Hama and Wilson, 1992).

Information on transport systems in thrausochytrids is even more scarce. Goldstein and coworkers demonstrated that Na^+ is required in the cotransport of solutes into the organism (Siegenthaler et al., 1967 a, b; Belsky et al., 1970). Wethered and Jennings (1985) demonstrated that inorganic solutes are the major contributors to osmotic potential of thrausochytrid grown at different salinity. Garrill and co-workers (1992) presented evidence for the presence of an H^+-ATPase and absence of a Na^+ pump in *Thraustochytrium* spp. As sodium is considered to be an essential element in thrausochytrids, a better understanding of transport processes of this ion and its interaction with others (eg. H^+, Ca^{2+}) might contribute to the improvement of biotechnological processes facilitating thrausochytrid growth.

1.4. Modern methods of studying membrane transport processes

Historically, the transport of ions into and out of the cell has been studied using various methods of chemical analysis and tracer techniques. More recently, attention has been focussed on the transporters themselves, located in the plasma membrane of cells. To understand the mechanisms involved in membrane transport processes, a number of modern methods have been employed including destructive sampling and depleting methods (atomic absorption spectroscopy or flame photometry), radioactive labeling (Soupene et al., 1998; Giraldez-Ruiz et al., 1999; Onoda and Oshima, 1988; Kashket, 1982), nuclear magnetic resonance (NMR) technique (Salhany et al., 1975, Nicholls and Ferguson, 1992; Gillies, 1994; Kim et al., 1996), fluorescent dyes (Gangola and Rosen, 1987; Knight et al., 1991), patch-clamp technique (Cui and Adler, 1996; Berrier et al., 1992), and different types of ion-selective electrodes (Busa and Nuccitelli, 1984; Russell and Rosenberg, 1979). Each of the techniques described in this section has some particular advantages that make it best suited for a particular application, explaining its popularity among researches in a given field. At the same time, each of them also imposes certain limitations that makes their use problematic, if not unfeasible, in some circumstances. This section discusses both the advantages and limitations of the different methodologies in order to assess the necessity for application of MIFE in microbiological research.

1.4.1 Destructive sampling and depletion experiments

In the recent past, destructive sampling and depletion experiments were the most widely used analytical methods to determine the elemental content of organisms. These methods are based on cell or tissue sampling followed by determination of ions using atomic absorption spectroscopy (AAS) or flame photometry (White and Gadd, 1995; Standard Methods, 1985). The rate at which a specific ion will be depleted or extruded into solution is the characteristic of the nutritional demands of bacterial cells for that element. Samples for analysis must be liquid, and biological samples are solubilised using different methods, such as wet combustion, leading to destruction of the organism under study. The response of AAS or flame photometry is not reliably linear over wide concentration ranges so

that the most essential calibration tool is a multi-point standard curve covering the concentration range used. The quality assurance of the data is quite low. The matrix may affect the response of AAS in some cases. For example, both Co^{2+} and Cu^{2+} give reduced absorption in the presence of certain other metals (Phillips Scientific, 1988). It is therefore important to make up standards in a matrix similar to the samples. Such interactions present potential problems if there are multiple unknowns.

The advantages of the method include simplicity of handling and a relatively low cost per assay. The major problems associated with this approach include: limitations on the rate of sampling, which impose severe restrictions on the time resolution of this method, and that sample taking over some prolonged period of time will result in progressive (and sometimes very significant) decrease of the solution volume, additionally complicating calculations, and changing substrate availability for bacteria. Also, the destructive nature of the methods makes impossible any kinetic studies performed on the same organisms. Finally, it is an extremely time-consuming method. This severely limits applications of these methods in bacterial physiology.

1.4.2 Radioactive tracers

Radioisotope tracers are widely used to study transport processes (Kashket, 1982; Onoda and Oshima, 1988;White and Gadd, 1995; Soupene et al., 1998; Giraldez-Ruiz et al., 1999). This method is based on monitoring transport of radioactive tracer fluxes using liquid scintillation counting (LSC). Recovery of radiotracers can be readily determined by carrying out a mass-balance of radioactivity in the various components such as cells and supernatants and comparing this with the total activity. Tracers are especially applicable to transport experiments involving unidirectional fluxes. They can also be used to monitor assimilation or intracellular distribution of low amounts of cations (White and Gadd, 1995). In recent times, the most frequently used method to measure pH_i in bacteria was determination of the distribution of radiolabeled weak acids or bases in combination with silicon oil centrifugation (Bakker, 1990; Booth, 1985; Bruno et al., 1992; Cook

et al., 1994; Kashket, 1985). The potential negative effects of weak acids on cell metabolism can not be ruled out (Breeuwer et al., 1996).

The advantage of the method is the small sample size required. The method is relatively straightforward and simple. However, kinetics of only one ion may be monitored in the same experiment. Finally, the main disadvantage of this technique is the limited time resolution of this method which severely limits its application to study kinetics of fast adaptive responses in bacteria (Kim et al., 1996; Breeuwer et al., 1996).

1.4.3 Nuclear magnetic resonance technique

Nuclear magnetic resonance is increasingly used for direct measurement of pH inside and outside a cell or organelle (Salhany et al., 1975; Nicholls and Ferguson, 1992; Gillies, 1994; Kim et al., 1996). NMR measures the resonance frequency of nuclei which are magnetically 'visible', i.e. which have a non-zero spin value, by exposing the sample to an alternating electromagnetic field (see Gillies, 1994 for a general review on NMR). Each nucleus has a characteristic frequency, which can be resolved on the NMR spectrum. The magnetic field imposed on the nucleus is locally affected by the electronic structure of the atom, thus enabling some nuclei to 'sense' their chemical environment. Consequently, an ion that alters its electronic structure in a pH-dependent manner will have a resonance frequency that shifts on the NMR spectrum. The observed small changes (typically a few Hz on the MHz scale of the NMR) are compared with a reference compound that does not alter its electronic structure as a function of pH. ^{31}P-NMR is generally used to measure intracellular pH (Salhany et al., 1975; Szwergold, 1992). The theory of the technique is based on the fact that the resonance energy of the phosphorus nucleus (^{31}P) in P_i varies according to the protonation state of the latter. As the pK_a for $H_2PO_4^-/HPO_4^{2-}$ is 6.8, the technique can report values in the range 6 to 7.5 (Nicholls and Ferguson, 1992). The NMR signal is the average for the two ionisation states of phosphate, since proton exchange is fast on the NMR timescale. If phosphate is present in both the external and internal phases, ΔpH can be calculated. Shifts in the NMR spectrum of inorganic phosphate are often compared to the creatine phosphate signal, that is invariant with

pH. Some organic phosphate-containing compounds can also be used for pH measurements. These include 2-deoxy-D-glucose, which is phosphorylated into 2-deoxy-D-glucose-6-phosphate, a species that is pH-sensitive in the physiological range (Kim et al., 1996).

The advantages of NMR include its non-invasive nature. It may measure not only intracellular pH, but also other physiologically relevant metabolites.

A drawback is that NMR has a low sensitivity with the absolute precision being limited by the lack of accurate calibration. Finally, NMR requires expensive equipment and dedicated operators (Kim et al., 1996). Nonetheless, the technology is becoming increasingly available for biological research.

1.4.4 Fluorescence microscopy

Fluorescent staining techniques have been successfully applied during the last decade for measurements of

(i) membrane potential and

(ii) pH_i,and cytosolic concentrations of a number of ions (Ca^{2+}, K^+, Cl^-).

ΔΨ measurements. In microorganisms a membrane potential ($\Delta\Psi$) is generally generated by the extrusion of H^+ by the H^+-ATPase or the electron transport chain. Theoretically, this potential can be determined by the distribution of lipophilic ionic molecules between the cells and the suspending medium according to the Nernst equation (Ehrenberg et al., 1988; Gross and Loew, 1989; Shapiro, 1990; Mason et al., 1993; Breeuwer and Abee, 2000). Fluorescent probes, used in microbiology for membrane potential determination include: rhodamine 123, carbocyanines such as 3,3-dihexylocarbocyanine iodide ($DiOC_6(3)$), 3,3-diethyloxacarbocyanine iodide ($DiOC_2(3)$), and 3,3-dipropylthiadicarbocyanine iodide ($DiSC_3(5)$), and bis-(1,3-dibutylbarbituric acid)-trimethine oxonol ($DiBAC_4(3)$). Rhodamine 123 has been successfully used in *S. cerevisiae* (Dinsdale et al., 1995), *Micrococcus luteus* (Kaprelyants and Kell, 1992), and some bacterial biofilms (Yu and McFeters, 1994; McFeters et al., 1995). The oxonol DiBAC4 was used to determine the plasma membrane potential in *S. cerevisiae* (Dinsdale et al., 1995), and in some bacteria

such as *Staphylococcus aureus*, *Pseudomonas aeroginosa*, *E. coli* and *Salmonella typhimurium* (Deere et al., 1995; Jepras et al., 1997; Suller and Lloyd, 1999). The choice of staining reagent depends on the microorganism to be studied and their physiological conditions. The reagents are not universal due to variation in cell permeability and differences in the interaction between fluorochromes and their biological target for different bacteria and at different physiological conditions (Comas and Vives-Rego, 1998).

Cytosolic pH and other ion concentrations measurements. Fluorescent probes that have been exploited to measure pH_i in food-related microorganisms include fluorescein 5- (and 6-)-carboxyfluorescein (cF), BCECF, pyranine, and cSNARF-1 (Breeuwer et al., 1997; Guldfeldt and Arneborg, 1998; Siegumfeldt et al., 1999; Budde and Jakobsen, 2000; Bunthof et al., 2000). The cells are loaded with fluorescent dyes, and changes in cytosolic ion concentrations may be monitored. The acetoxymethyl (AM) ester derivatives of fluorescent indicators make up one of the most useful group of compounds to study pH_i kinetics in live cells. Modification of carboxylic acids with AM ester groups results in an uncharged molecule that can permeate cell membranes. Inside the cell, the lipophilic blocking groups are cleaved by nonspecific esterases, resulting in a charged form that leaks out of cells far more slowly than its parent compound.

The advantage of such methods is that they are non-invasive, very sensitive, have high time resolution, are relatively simple in use and allow analysis of individual cells (Tsien, 1989; Kim et al., 1996). Applications include the analysis of stress resistance of cells to antimicrobial compounds and investigation of complex microbial communities, such as biofilms; and enabling kinetic studies of transport processes.

Unfortunately, the application of this method is severely limited by the number of dyes used (only dyes for cytosolic H^+, K^+, Cl^-, and Ca^{2+} have been intensively measured although a range of dyes suitable for other ions is also available). Furthermore, some dyes (eg., carboxycyanine) may be toxic to the cells, especially when strong illumination is used (phototoxicity) (Shapiro, 1990; Kim et al., 1996).

Moreover, in Gram negative bacteria the addition of EDTA or EGTA (to assist the substrate to penetrate the outer membrane) is necessary to allow proper distribution of probes (Matsuyama, 1984). Obviously, such treatments may influence cell viability (Breeuwer and Abee, 2000). Finally, special optical configurations are required to take advantage of the spectral properties of the dyes and high resolution fluorescent microscopes remains expensive.

1.4.5 Patch clamp technique

The patch-clamp technique is the most advanced method of studying ion-transport processes at the molecular level (Petersen, 1992; Garrill and Davies, 1994; Hamill and Martinac, 2001). It can provide comprehensive information about the kinetics and properties of specific transport proteins at bacterial plasma membrane. The method is based on a tight attachment of a plasma membrane patch to a microelectrode glass pipette, thus establishing a so-called "giga seal" (with up to 10^9 Ohm resistance), enabling measurements of very low (pA range) currents through the prepared isolated plasma membrane patch. In one configuration, known as the "whole-cell patch", the membrane is then ruptured, and a protoplast is attached to the electrode tip like a balloon. As the electrode volume is much more than the volume of the clamped cell, the cytosol content is quickly replaced by the electrode-filling solution. As a result, ionic concentrations both inside and outside the plasma membrane are known, and can be easily controlled. Because of that, by applying a sequence of voltage clamps, and measuring the resultant current, it becomes possible to estimate quantitatively the contribution of each transporter for each specific ion to the resultant cell response. In another configuration, called the "excised patch", a piece of membrane remains stuck to the electrode tip, while the remaining protoplast is removed. Current traces measured in this configuration may provide valuable information about single-channel activity. Ultimately, channels may be characterised with respect to the ion they conduct (and their specificity for that ion), the conductance value of their open state, their gating properties, and their sensitivity to pharmacological agents (Garrill and Davies, 1994).

However, the patch-clamp method is not easily applicable to every bacterial organism. To start with, the cell wall must be removed to get access to the plasma membrane and form a "giga seal". Small cell size is another problem. Almost all successful patch-clamp studies from bacterial membranes were obtained from the use of spheroplasts or giant cells (Martinac et al., 1987; Saimi et al., 1992; Kubalski, 1995; Levina et al., 1995; Cui and Adler, 1996;) which are themselves highly artificial systems. For large organisms (e.g., fungi), protoplasts derived from the tissue can be used. The procedure of protoplast, spheroplast, or giant cell preparation involves digestion of the cell wall by enzymes, a step that may damage the PM and thus alter the organism's response (Jennings, 1995). Patch clamp is a sophisticated method that requires high level technical and data interpretation skills.

1.4.6 Ion selective microelectrode technique

Finally, membrane-transport processes, associated with bacterial adaptive responses may be measured with microelectrodes whose tip is selectively permeable to an ion of interest (reviewed by Ammann, 1986; Kim et al., 1996). This approach provides an immediate estimate of the ion concentration with high precision (eg., ±0.01 pH units for pH measurements) as ion electrodes have an almost Nernstian voltage response. The electrochemical potential across the ion-selective membrane is measured by connecting the electrode inside the pipette (which is filled with a solution of known pH or ion concentration) to an external (bath) electrode via a high-impedance voltmeter. When the electrode is used to measure extracellular ion concentration, the voltage output can be directly converted into a measure of concentration or pH values, provided that the electrode is calibrated in a proper range of standards (solutions with a known concentration). When an electrode is used to measure intracellular ion concentration, however, the electrochemical potential across the electrode tip is in series with the membrane potential of the cell, which has to be subtracted from the voltage output. Hence, membrane potential has to be measured independently, either with a separate microelectrode or by using a special double-barrelled electrode, with one barrel dedicated to ion concentration measurements and the other to voltage determination. Regardless of the electrode

type, the approach is restricted to preparations that can withstand invasive procedures.

The use of traditional (standard-size) commercially available ion-selective electrodes (Ammann 1986) is severely limited by several factors. The large size of the probe restricts the method to quite large objects (comparable with the size of an electrode tip). Due to this and in order to minimize damage to the object, there is a tendency to use instead a liquid-type ion-selective microelectrode (the so-called LIX microelectrodes), with the tip diameter in μm range. Such electrodes may be prepared on a routine basis and impaled in an organism or a biofilm to study concentration of a specific ion (reviewed by White and Gadd, 1995; Kim et al., 1996). The latter examples include reports for pH (Masson et al., 1994; Lens et al., 1995), Cl^- (DeBeer et al., 1994; Xu et al., 1996), O_2 (Horn 1994; Xu et al., 1998; Rasmussen and Lewandowski, 1998), and NO_3^- (DeBeer et al., 1997) profiles in various types of artificial and natural biofilms. An unreliable electrode can be replaced by another one within minutes if necessary (the cost of microelectrodes is much less than the cost of the standard-size commercial electrodes). Obtaining a good microelectrode is the critical step. The LIX microelectrodes are faster than glass microelectrodes with response times usually in the range of seconds (Kim et al., 1996).

Microelecrodes were used to monitor ion changes in the external medium as a function of bacterial metabolic activity and to measure ion concentrations of lysed bacterial cells (Russell and Rosenberg, 1979; Busa and Nuccitelli, 1984). Although concentration measurements by means of ion-selective microelectrodes have become widely used in microbiology, interpretation of the results is difficult at times. The major pitfall is the origin of observed concentration changes. As many different processes may contribute to these changes, unambiguous interpretation of the underlying mechanisms is impossible.

A major advantage is that the measurement itself is quite simple. Furthermore, ion selective electrodes may be used for continuous recordings of ion concentration changes thus enabling kinetic studies. Despite the advantages of using the invasive microelectrode technique to study membrane transport processes, its application is

restricted to plant physiology and study of fungi. Invasive microelectrodes can not be inserted into bacteria due to their small size, thus restricting the area of their application in microbiology.

Taken together, these led to the requirement for some other techniques to be used in conjunction with ion-selective measurements and/or improvement of the existing microelectrode technique.

1.4.7 Non-invasive ion flux measurements

To make an unambiguous interpretation on the underlying mechanisms, it was suggested that ***fluxes*** of ions (not just their concentrations), may be measured with LIX-filled microelectrodes. This idea was put forward by Prof Bill Lucas at the NATO Advanced Studies Institute in Italy in 1984 (Lucas and Kochian, 1986). The microelectrodes were proposed to measure ion concentration ***gradients*** (strictly, electrochemical potential differences), between two positions outside the organism tissues, and use those gradients to calculate the ***net fluxes*** of ions in question crossing the membrane tissue. The first rigorous test of the theory was performed on corn roots to measure the stoichiometry of H^+ and K^+ fluxes (Newman et al., 1987). The idea of non-invasive ion flux measurements was further developed by Dr Ian Newman (School of Mathematics and Physics, University of Tasmania) and resulted in the construction of the MIFE^R system, which is now commercially available. Another system, sharing the basic idea for non-invasive flux measurements, was developed at the National Vibrating Probe Facility at Woods Hole MA in the USA (Kuhtreiber and Jaffe, 1990; Smith, 1995; Smith et al., 1999). That system has been used by numerous visiting researchers to the centre (Miller, 1989; Felle and Hepler, 1997; Lew, 1998, 1999), and some of the reported data are relevant to yeast and fungi (Lew, 1998, 1999). Only a few laboratories around the world possess similar facilities (Kochian *et al.* 1992; Cardenas et al., 1999). The leaders in non-invasive ion flux measurements (on plants) are the Hobart group that pioneered the application of the MIFE technique in stress physiology (Shabala et al. 1997; Shabala and Newman, 1997ab; Shabala, 2000; Shabala et al., 2000; Newman, 2001). No attempts, however, were made to apply this technique to bacterial cells.

The non-invasive ion selective microelectrode technique has a number of advantages. Being non-invasive, microelecrodes not interfere with cell integrity. Furthermore, the MIFE technique allows measurements of several ions simultaneously and essentially from the same site which enables stoichiometry between ions to be established. Together with high spatial (a few microns) and temporal (5 s) resolution, the MIFE has become a unique tool for kinetic studies of transport processes.

1.4.8 Evaluation of the methods

Although all the sophisticated techniques discussed above have already provided valuable information on ion distribution and movement, and thus on transporter properties and ionic mechanisms of transport, the causal link between membrane-transport processes and other metabolic or physiological processes in the cell is not always clear. For this link to be established, kinetics of the transport processes must be monitored, followed by thorough comparison of the revealed time constants for transport processes with those known for other cellular metabolic processes. As both bacterial and fungal life cycle and adaptive responses are fast, time resolution becomes a critical issue. From this point of view, the most suitable methods for kinetic studies are FRIM, MIFE and, to some extent, patch-clamp techniques.

FRIM is a highly sensitive method. However, it lacks the ability to monitor the long-term kinetic process due to possible photobleaching. This happens if a large number of images are taken. In addition, the experimental pH range for the indicator used for pH_i measurements is restricted, and determined by the pK value of the titratable group, as fluorescence changes linearly with pH only over a ~0.5 pH range around the pK (Kim et al., 1996). This creates problems if the desired experimental pH range significantly exceeds that of the indicator pK (as in experiments with pH shifts). Finally, the high capital cost of the FRIM is another barrier for many laboratories.

The patch clamp technique, being on the frontier of transport studies, enables stoichiometry establishment as well as providing a better understanding of the

mechanisms of transport processes in general. However, this technique is not easily applicable to the practical needs of Food Microbiology. Only a handful of bacterial cells were patched; most of these are in artificial (e.g. spheroplasts) conditions (Saimi et al., 1992; Cui and Adler, 1996).

As mentioned before, the non-invasive ion selective microelectrode technique has been successfully used to study various aspects of membrane transport processes in higher plants, protoplasts derived from plant tissue, and fungi. However, apart from fungi and yeasts (that are relatively large microorganisms), food microbiology deals mainly with bacterial cells, the size of which is comparable with the microelectrode tip diameter. Because of that, the general view was that the application of non-invasive microelectrode measurements to bacteria is unfeasible and, no successful attempts to measure ion fluxes from bacterial cells have been reported. In this project this view is challenged, and the issue tackled by measuring net ion fluxes from the surface of immobilised bacterial "monolayers". The feasibility of such an approach is demonstrated. The results of this work show that application of the MIFE technique could lead to a significant progress in our understanding of membrane transport processes in microorganisms, ultimately contributing to addressing a large number of important issues which food microbiology faces.

Chapter 2

MATERIALS AND METHODS

2.1.Bacterial and fungal cultures and growth conditions

2.1.1 Thraustochytrid ACEM C

Thraustochytrid strain ACEM C, an isolate from coastal marine sediments in south-eastern Tasmania (Australia), provided by Dr T. Lewis (School of Agricultural Science, University of Tasmania), was used throughout this study. The culture was maintained in a medium adapted by Lewis (2001) from Iida et al. (1996) and Singh and Ward (1996). It contained (per liter) bacteriological peptone - 5 g, glucose - 5 g, sodium glutamate - 5 g, yeast extract - 2 g, KH_2PO_4 - 100 mg, $NaHCO_3$ - 100 mg, $MnCl_3.4H_2O$ - 8.6 mg, $FeCl_3.6H_2O$ - 3.0 mg, $ZnCl_2.7H_2O$ - 1.3 mg, $CoCl_2.6H_2O$ - 0.3 mg, $CuSO_4.5H_2O$ - 0.2 mg, sea salts - 30 g, vitamin solution - 1.0 ml. The composition of vitamin solution per 1L was: pyridoxine hydrochloride - 20.0 mg, thiamin hydrochloride - 10.0 mg, calcium pantothenate - 10.0 mg, *p*-aminobenzoic acid - 10.0 mg, riboflavin - 10.0 mg, nicotinamide - 10.0 mg, biotin - 4.0 mg, folic acid - 4.0 mg, vitamin B_{12} - 0.2 mg. Media were prepared without addition of vitamins and sterilised by autoclaving at 10 psi for 15 min. Vitamins were added to the medium at a temperature below 50 ^{0}C. The same nutrient composition with addition of 1% agar was used to maintain a slope stock culture of thraustochytrid ACEM C that was kept at 4 ^{0}C.

Inoculum preparation

An inoculum was prepared by inoculating a 250 ml Erlenmeyer flask containing 50 ml of the above medium with thraustochytrid ACEM C from a slope

stock followed by incubation at 20 °C on a rotary-shaking table (GIO Gyrotary Shaker, New Brunswick, USA) at 200 rpm for 7 days.

Culture preparation

The inoculum was used for preparation of working cultures. The growth medium used was the same as for inoculum preparation. An Erlenmeyer flask of 250 ml containing 50 ml of the growth medium was inoculated with 1mL of 7-d old inoculum and grown at similar conditions for 4 days (when not indicated otherwise). Apart from the growth study, cells of the same stage of growth were used in an individual study to avoid variations.

2.1.2 Food-borne bacteria

Bacterial strains used in this study, their characteristics and growth conditions are shown in Table 2-1.

Experiments with bacteria were performed at different stages of growth. For experiments at the exponential phase of growth, bacteria were grown using side-arm flasks immersed in a shaking water bath (Ratek Instruments Pty Ltd, Australia) to ensure constant growth temperature throughout the experiment. The growth stage was determined by measuring optical density (OD) value at 540 nm with a spectrophotometer (Spectronic 20D, Milton Roy Co., USA). The observed OD value was compared with that from previously determined standard growth curve. An aliquot of the culture was removed aseptically from the flask at the desired OD value (see Fig. 2-1) and the flask was returned to the water bath for further incubation. Bacteria used for the experiments were at the OD values indicated in Figure 2-1.

Table 2-1. List of bacterial strains and growth conditions

Bacterial strain	Character.	Growth conditions	Origin
E. coli SB1	FAB	MM broth + 0.1% glucose; 37°C; shaking @ 60 rpm	Clinical isolate provided by Ms. S. Bettiol, School of Pathology, Univ. of Tasmania
E. coli M23	FAB	NB; 37°C; @ 60 rpm	School of Ag. Sci. (SAS), Univ. of Tasmania
L. monocytogenes 4140	FAB	BHI broth; 37°C; without agitation	Bacon isolate provided by the Danish Meat Research Institute, Roskilde, DenmarkSAS
L. monocytogenes Scott A	FAB	BHI broth; 25 °C; @ 60 rpm	SAS
Salmonella typhimurium	FAB	NB; 37°C; @ 60 rpm	SAS
Enterobacter	FAB	NB; 37°C; @ 60 rpm	SAS
Klebsiela oxytoca	FAB	NB; 37°C; @ 60 rpm	SAS
Staphylococcus aureus	FAB	NB; 25 °C; @ 60 rpm	SAS
Bacillus cereus	FAB	NB; 25 °C; @ 60 rpm	SAS
Lactobacillus delbrueckii, subsp. *bulgaricus*	FB	MRS broth; 42 °C; without agitation	Provided by Dr H. Siegumfeldt, Dept Dairy & Food Sci., KVL, Copenhage Denmark

FAB – facultative anaerobe; FB- fermentative bacteria

Broth details: MM – Minimal Medium Broth, Difco, Davis, 0756-1-7

BHI – Brain Heart Infusion Broth, Difco, Detroit, Michigan

NB – Nutrient Broth, Oxoid, Hampshire, England

MRS –Oxoid, Hampshire, England

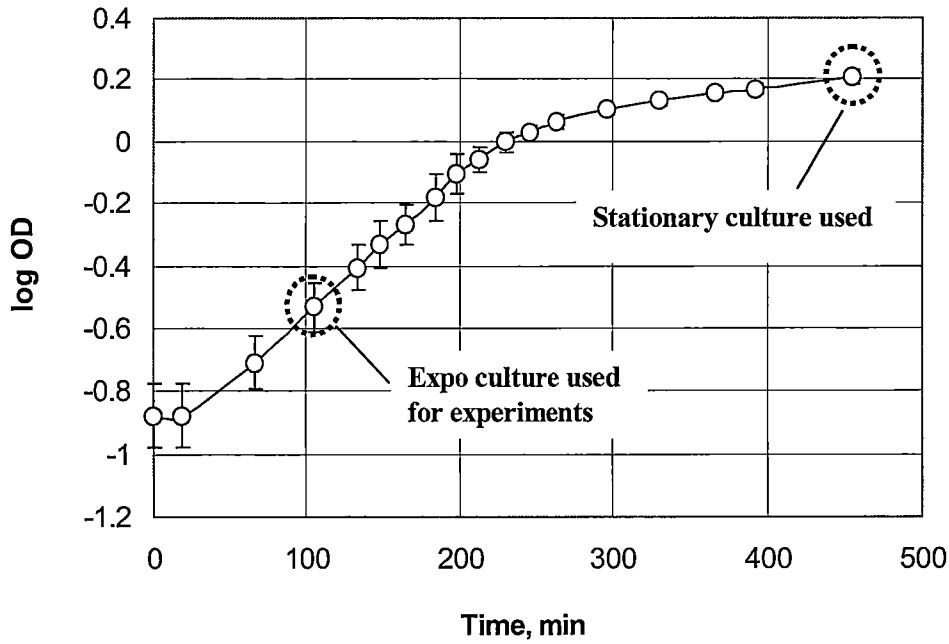

Fig. 2-1. Growth phases of bacteria used in experiments. Growth was monitored using a spectrophotometer at λ=540 nm. The data are the average of two individual experiments performed in duplicate. Data for *L. monocytogenes*; growth conditions as per Table 2-1.

Basic protocol for inoculum preparation. The inoculum was usually prepared by inoculating a 125 mL conical flask containing 25 mL of the appropriate medium (see Table 2-1) from a slope stock followed by incubation for 15-16 h under conditions indicated in Table 2-1.

Basic protocol for culture preparation. A 125 mL sidearm flask containing 25 mL of the appropriate inoculum (see above), to give a starting OD_{540}=0.05 A followed by outgrowth as descussed in Table 2-1. Cultures were harvested in the exponential (OD_{540}=0.3 A), or stationary (culture grown for 16 h, OD_{540}=1.4 A) phases of growth ,washed and resuspended in the desired experimental solution (Appendix A), and used immediately or kept on ice for up to 0.5 h, if not indicated

otherwise. All the bacterial cultures were prepared in a similar way, unless stated otherwise.

Preparation of L. monocytogenes 4140 culture

Inoculum preparation. Inocula of *L. monocytogenes* were prepared in a standardised manner to reduce variations in culture physiological state. A 100 ml bottle containing 50 ml of BHI with pH adjusted to 6.0 using 5 M HCl was inoculated with 1 full loop of *L. monocytogenes* 4140 and vortexed. The culture was incubated for 18 hours at 37 °C without agitation. A 10 ml aliquot of stationary phase culture was harvested by centrifugation at 5000xg for 10 min, the pellet resuspended with 2.75 mL of the same broth and 1.75 ml of 50% glycerol (Merck, Darmstadt, Germany). Aliquots of 0.25 ml suspension were placed into Eppendorff tubes aseptically and kept at the temperature of -40°C until use (up to 3 months).

Culture preparation. A tube with 15 ml of BHI adjusted to pH 6 was inoculated with 0.25 mL stock of *L. monocytogenes* 4140 inoculum and grown at 37 °C for 18 h without agitation.

2.2. Culture preparation and immobilisation

2.2.1 Importance of immobilisation

The theory of ion flux measurements using MIFE assumes unstirred layer conditions. Also, in most cases, accurate electrode positioning is crucial for flux measurements. Therefore, it was of particular importance to design an efficient protocol for cell immobilisation. Not only might position changes affect the accuracy of ion flux calculations, but moving cells might also block the fine electrode tip. Last, but not least, without proper cell immobilisation, any change of experimental solution in a chamber would result in cell movement making kinetic studies impossible.

Different approaches have been utilised by others to ensure the object is positioned steadily in the measuring chamber. Larger objects, such as plant roots or coleoptiles, are usually attached to plastic partitions using a fine cotton thread (Shabala et al. 1997; Shabala and Newman 1998; Babourina et al. 1998). For macerated or cultured cells, semi-solidified agar is usually used (Babourina et al. 2000). However, all these approaches can only be applied to an object that is large enough, and are not likely to be suitable for bacterial cells.

In most patch-clamp protocols, protoplasts are attached to a properly cleaned glass surface by electrostatic forces (Tyerman et al., 2001). Combined with mechanical support provided by the sealing electrode, it is adequate to immobilise the protoplast in the chamber. This is not the case for MIFE measurements, where ion-selective microelectrodes are not in contact with the measured cell.

Bacterial cell immobilisation for fluorescence microscopy is usually based on placing a filter with bacterial cells on the glass bottom of the measuring chamber up-side-down thus exposing cells to observations through the bottom of the glass chamber using an inverted microscope (Siegumfieldt et al., 1999; Budde and Jakobsen, 2000). However, in this protocol, immobilised cells are not accessible for microelectrodes. Moreover, the filter might cause some unknown delay in bacterial response to the change of experimental solution and consequently affect the measurements (Budde and Jakobsen, 2000).

Finally, poly-L-lysine was reported to be used for cell adhesion to solid surfaces (Mazia et al., 1975). Polycationic poly-L-lysine molecules are known to absorb strongly to various solid surfaces, leaving cationic sites. The interaction between polyanionic cell surfaces and a charged cationic surface results in cell adhesion.

The immobilisation procedure for the MIFE measurements has some specific requirements that include:

(i) accessibility of the object to microelectrodes without being damaged

(ii) stable positioning of cells to allow experimental solution to be changed quickly enough without the cells re-positioning, and

(iii) neutral nature of the chemical used for attachment to eliminate possible chemical interference with cells or the flux measurements.

Poly-L-lysine was used for cell immobilisation in the present work, as follows:

- a glass cover-slip was cleaned with ethanol, thoroughly rinsed with running distilled water, and then dried;
- poly-L-lysine (0.1% w/v aqueous solution, P 8920, Sigma diagnostics, St. Louis, USA) was used to attach cells to the glass surface. One drop (≈ 30 μL) of the poly-L-lysine solution was applied to the glass surface and left for approximately 3 min;
- the cover-slip was then well rinsed again with running distilled water and an appropriate experimental solution (Appendix A) to ensure a complete elimination of the chemical after charging the surface.

Effect of poly-L-lysine on cell activity/viability was assessed indirectly through monitoring the ability of bacterial cells to acidify the medium (H^+ flux measurements using MIFE technique) as well as pH_i measurements (using FRIM). Long-term experiments using the developed protocol for cell immobilisation showed no change in bacterial or fungal ability to extrude protons (Figs.5-10-5-14; 4-6, 4-14, 4-26), as well as to maintain constant pH_i (Fig.5-21) thus validating the use of poly-L-lysine.

Additional tests were performed to ensure absence of any influence of poly-L-lysine used on the flux measurements (Chapter 3.1).

2.2.2 Immobilisation of thraustochytid cells.

Culture preparation for immobilisation. Cells were harvested by centrifugation of 1 ml of culture at 3000xg for 10 min. The pellet was washed twice with 2 ml of experimental solution with desired concentration of glucose (Appendix A) by centrifugation at parameters similar to those indicated above. Cells were subsequently suspended in 1 ml of the same experimental solution, and kept at ambient temperature for at least 2 h before measurements to allow adaptation to the new conditions. Ambient temperature was ~23 °C in all experiments, unless indicated otherwise.

Immobilisation procedure. In contrast to bacterial cells, thraustochytium cells are large enough to be measured individually (typically 20 to 40 μm in diameter compared to 2-3 μm for the microelectrode tip). The immobilization procedure was to separate cells to avoid the influence of neighboring cells on flux measurements (Fig. 2-2).

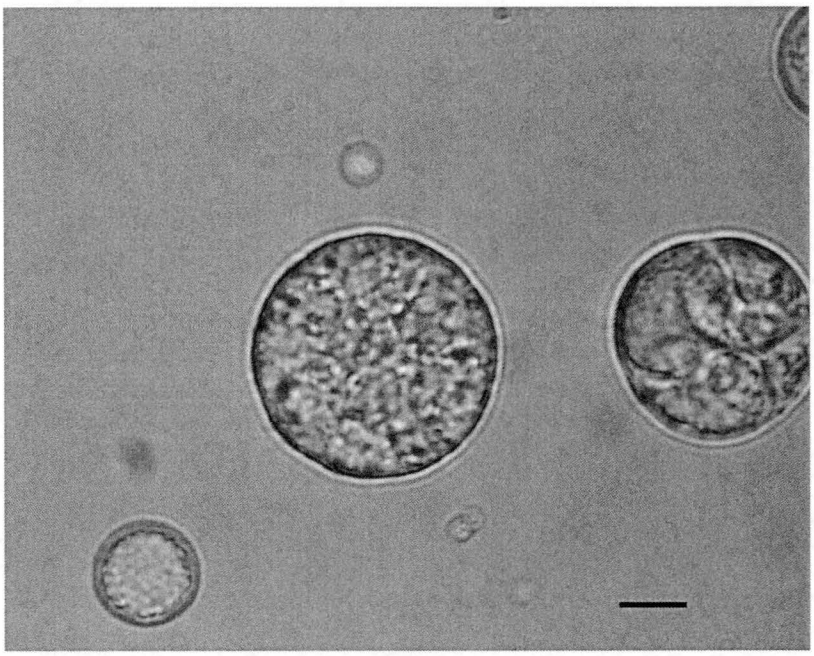

Fig. 2-2. Immobilised thraustochytium cells in the measuring chamber. A scale bar indicates 10 μm.

The prepared cover-slip coated with poly-L-lysine was placed in the measuring

chamber. The chamber was fixed on the hydraulic manipulator stage in the Faraday cage and filled with an appropriate experimental solution (Appendix A) having the desired concentration of glucose. The ACEM C culture was diluted with an appropriate experimental solution (see Appendix A) with a ratio 1:5 and an aliquot of 50 μL was spread along the measuring chamber to ensure a loose cell distribution. Cells were allowed to settle down on the coverslip. The process was monitored using the microscope (IX50, Olympus Optical Co., Ltd, Tokyo, Japan) with long working distance 40x objectives (W.D. 2.6 mm), providing total magnification of 500x. After most of the cells were settled, about 30 mL (>6 chamber volumes) of the experimental solution were perfused through the chamber to remove unattached cells. Measurements started 30 min after all solution changes were over.

2.2.3 Immobilisation of bacterial cells.

Two different types of measuring chambers were used in this study and consistent results were achieved. The procedure for cell immobilization described below was similar for both chamber types.

Bacterial culture preparation. A sample of 1 mL from the batch culture was harvested by centrifugation at 4,200x*g* for 10 min (Biofuge A, Heraeus Sepatech GmbH, Germany), unless stated otherwise. The pellet was washed with equal volumes of cold experimental solution (experimental solution N1 or N2, Appendix A), centrifuged again at parameters similar to the above and suspended in 20 μL of the same experimental solution.

Bacterial culture immobilisation. The culture was immediately applied to the prepared cover-slip, left for approximately 3 min, and unattached cells eliminated by washing the cover-slip with ~10 ml of experimental solution. The cover-slip with immobilised bacteria was placed at the bottom of a perfusion chamber (Fig. 2-3).

The measuring chamber was filled with the desired experimental solution. Another cover-glass was placed at the top of the chamber resting on two supports at opposite sides of the chamber perimeter thus creating water-tension. The free space between the glass-covers on two other sides of the chamber perimeter was used for

electrode insertion (Fig. 2-3). The photograph of the experimental chamber is shown in Figure 2-4.

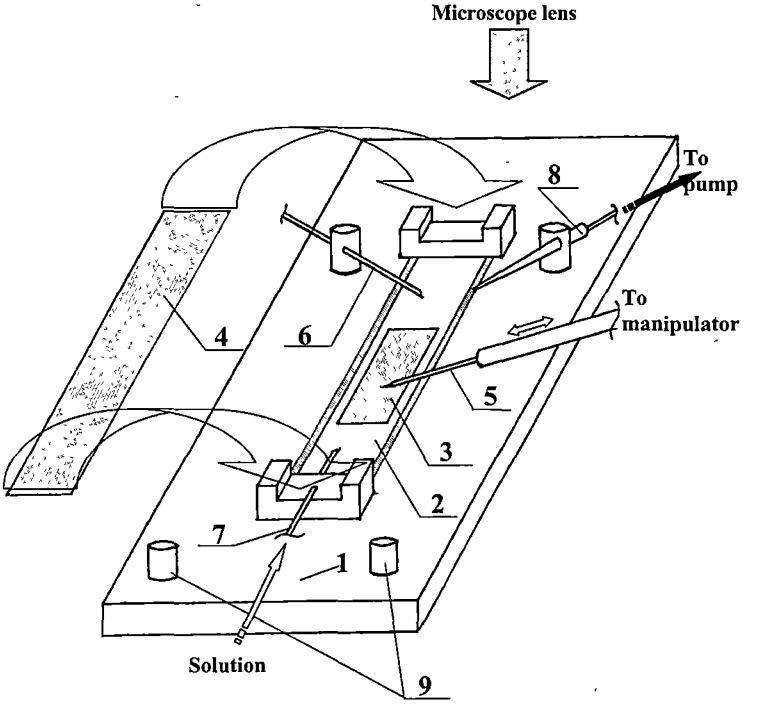

Fig. 2-3. A schematic view of an open type perfusion chamber used in this study. Solution is held by surface tension created between a glass cover slide (4) and the glass base of the chamber (2) allowing safe insertion of microelectrodes (5) and a reference electrode (6) through the lateral meniscus. Solution enters the chamber through a needle (7) and is pumped out via a tube (8) by a peristaltic pump. A glass slide with adherent bacteria (3) is put on the glass base (2). The perfusion chamber base (1) is fixed to a microscope stage by screws (9).

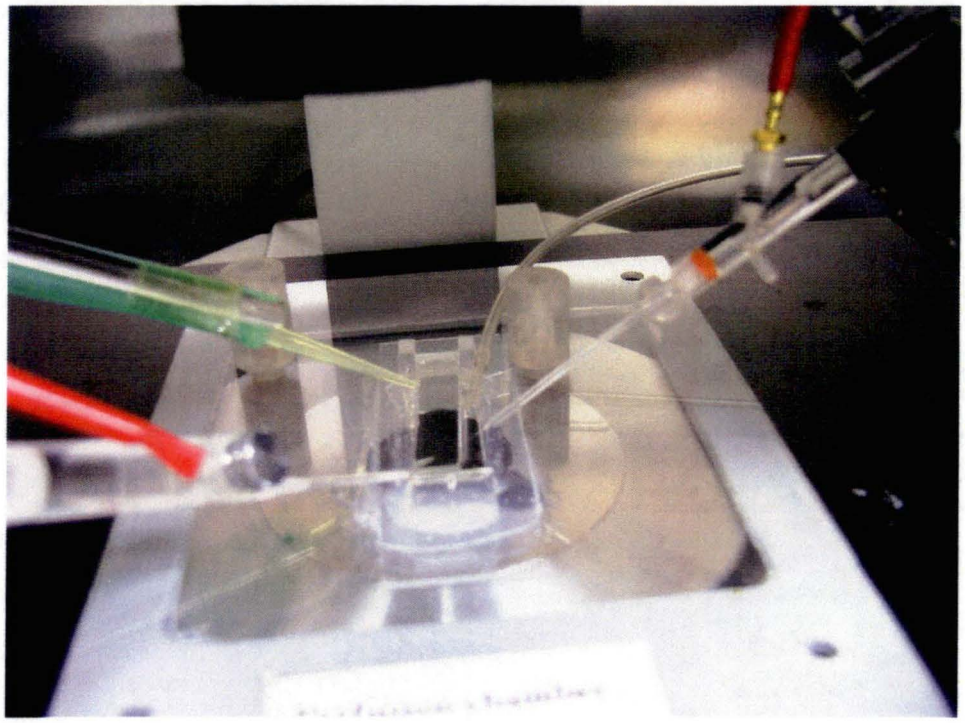

Fig. 2-4. A photograph of an experimental chamber shown in Fig. 2-3.

For FRIM experiments bacterial cells were immobilised in a similar way to that presented above with some modifications:

(i) bacterial cells were stained with cFSE (see Chapter 2.4.2) prior to the immobilisation procedure, followed by washing with experimental solution;

(ii) culture was diluted in ratio 1:5 with the same medium;

(iii) an aliquot of 0.1 mL was applied to the prepared cover-slip, left for about 3 min and excess bacteria washed out as described above.

All the preparations were performed under reduced illumination in the room due to the instability of fluorescent preparations.

A similar approach was used for immobilisation of bacterial cells on the bottom of another type of measuring chamber used (Fig. 2-5).

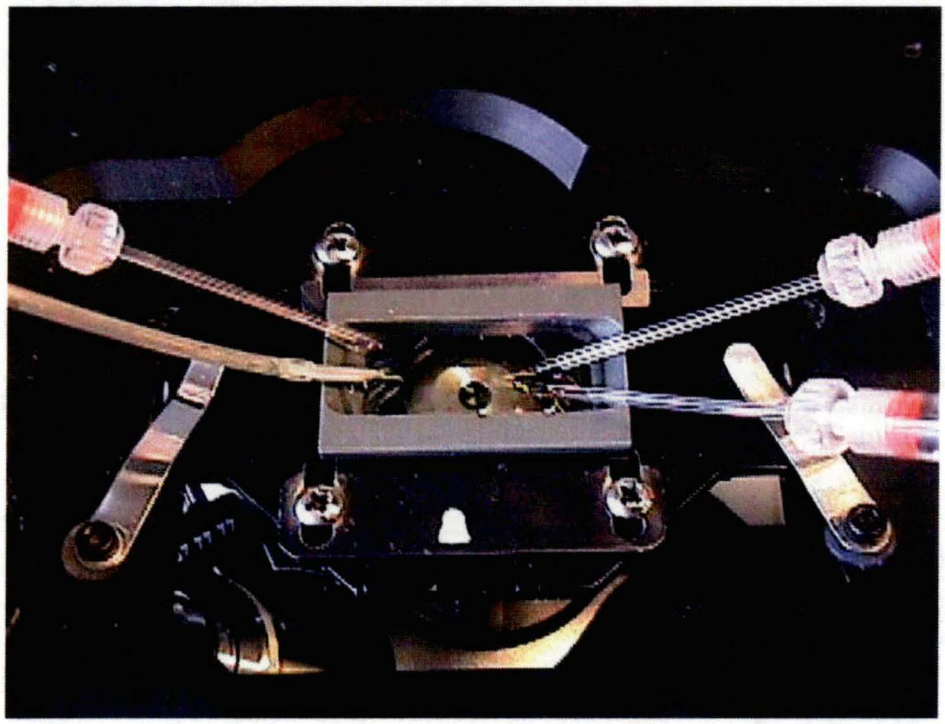

Fig. 2-5. Individually assembled chamber (V=1 mL). Two measuring microelectrodes are situated on the right-hand side, a reference electrode and a tube for perfusion of solution through the chamber are situated on the left-hand side. The chamber is situated in a holder and its position is fixed by four screws. The holder is attached to the microscope table by two clips.

Bacterial cells were immobilised on a large glass cover-slip (22x32 mm, Vitromed, Basel, Germany). A shaped teflon form with the external perimeter similar to that of the cover-slip was used for an individually assembled chamber formation. Immobilisation and washing procedures were as described above followed by sealing the teflon form to the prepared cover-slip using silicone grease. The perfusion chamber was thus formed (of approximately 1 mL volume) and then filled with the experimental solution of desired composition. This type of chamber did not rely on water-tension and, consequently, a top glass-cover was not used to ensure proper solution volume. The former chamber type enables smaller experimental solution volumes to be used in the measuring chamber, while the latter chamber type was more convenient for handling.

2.2.4 Advantages of the immobilisation procedure developed

The approach developed for cell immobilisation has a number of advantages:

(i) It achieves an even distribution of bacteria and creates a uniform monolayer of "standard" density (Fig. 2-6). This enabled comparative measurements from different 'sites' (see Fig. 3-3, Chapter 3.2).

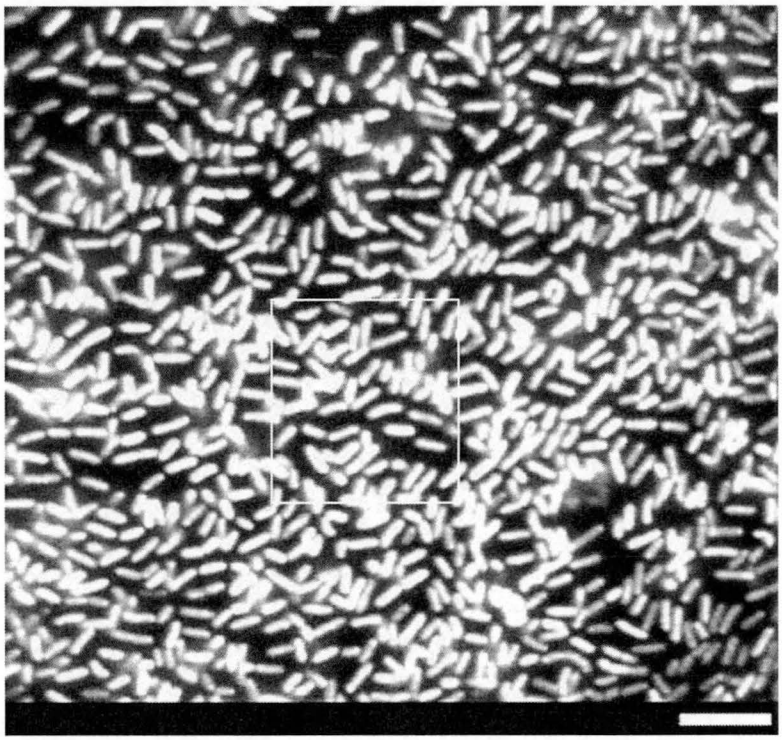

Fig. 2-6. Immobilised *L. monocytogenes* cells. A scale bar indicates 5 μm. The rectangle shown (10x10 μm) contains ~75 cells.

(ii) Once attached, cells adhered to the cover-slip was strongly enough to perform changes of solution without washing out the cells. Fig. 2-7 represents cells before and after the change of solution in a measuring chamber with a rate of flow up to 6 mL min^{-1} thus demonstrating that even the spatial distribution of cells remained unchanged. On average, less than 5% of cells were washed out after perfusion of 10 volumes (10 mL) of experimental solution through the chamber. The latter was determined by FRIM examination of microscope slides (n = 4-5).

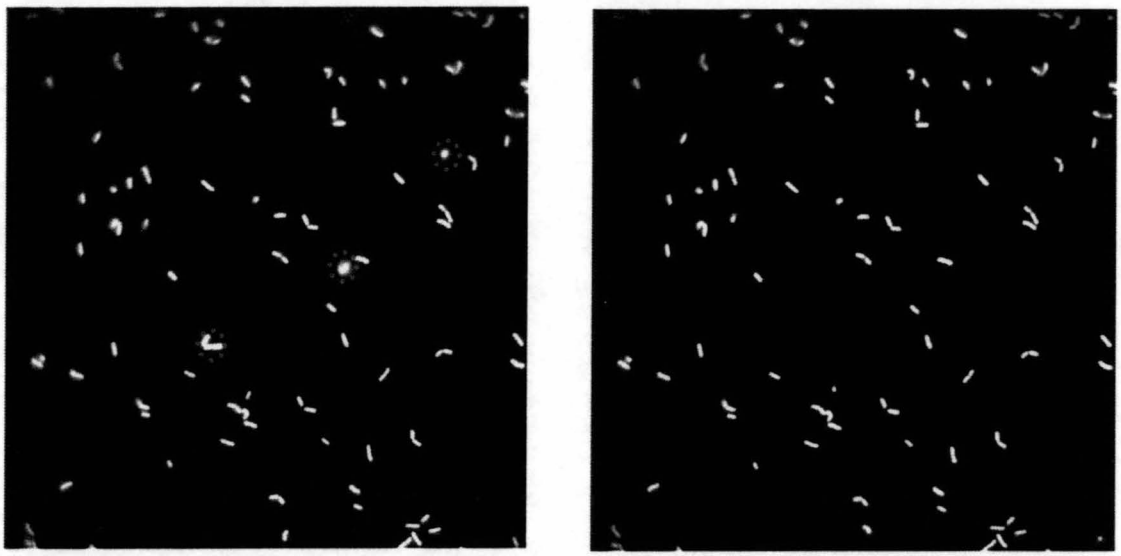

Fig. 2-7. Immobilised *L. monocytogenes* cells before **(A)** and after **(B)** change of solution in kinetic experiments (flow rate of solution up to 6 mL min^{-1}). The Fluorescence Ratio Image Microscopy was employed to assess position of immobilised cells at the bottom of a chamber before and after solution change. Low cell density was required for FRIM measurements to enable analysis of individual cells. The circled cells represent cells that were washed out after the change of experimental solution.

The immobilisation procedure developed in the present work has increased the diversity of MIFE applications by introducing a possible change of the experimental solution and thus allowing kinetic studies of essentially the same cells. This also opened opportunities for kinetic studies using FRIM by eliminating delays in bacterial response caused by using a filter for cell immobilisation (see Chapter 2.2.1). Furthermore, this enabled measurements using both FRIM and MIFE of essentially the same cells.

2.3. Microelectrode Ion Flux Measurement (the MIFE) technique

2.3.1 Principles of the MIFE system

If an ion is taken up by living cells, its concentration in the proximity of the cell surface will be lower than that further away. *Vice versa*, if the ion is extruded across the plasma membrane (PM), there will be a pronounced electrochemical potential gradient directed away from the cell surface.

Ions in solution move down a concentration gradient (from high to low concentration) and also down an electrical potential (from high to low potential). Consequently, if the combined electrochemical potential gradient is measured, the net ion movement can be calculated from that gradient using the known mobility and concentration of the ion in solution (Newman, 2001). Ions crossing the cell surface in solution are carried to or from that surface by diffusion. In static or slowly changing conditions, when the convection or water uptake are negligibly small, measurements of the net diffusive flux of the ion in solution close to the sample indicates the net flux of the ion across the sample surface.

Thus, the principle of the MIFE technique is the slow square-wave movement of ion-selective microelectrode probes between two positions, close to (position 1), and distant from (position 2) the sample surface (Fig. 2-8).

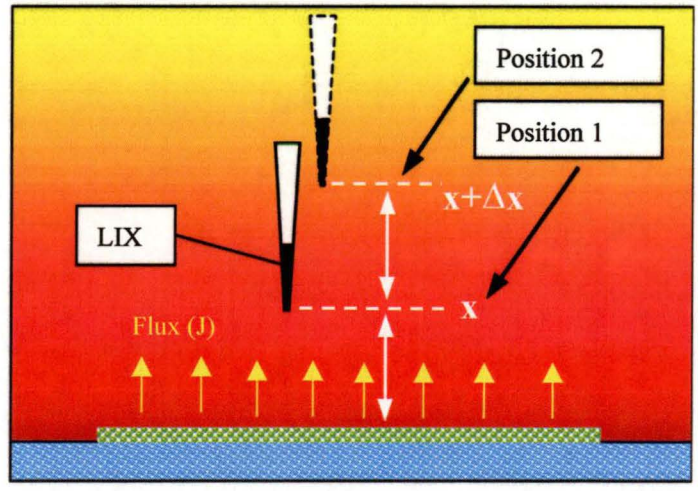

Fig. 2-8. Schematic diagram illustrating principles of MIFE ion flux measurements (ion-selective "vibrating probe").

The recorded voltages at positions 1 and 2 (Fig. 2-8) are converted into concentrations using the calibrated Nernst slopes of the electrodes. Net fluxes of specific ions can then be calculated from measured voltage gradient at the surface. Depending on the diffusion geometry, different equations are used. For the simplest case of a planar surface (e.g. immobilised bacterial cells), net flux, J (nmol $m^{-2}s^{-1}$) of a specific ion can be calculated as follows (Newman, 2001):

$$J = c\ u\ F\ (58/\text{Nernst slope})(\Delta V/\Delta x), \quad (1)$$

where c is average concentration (mol m^{-3}) of the ion of interest between positions 1 and 2; u is ion mobility (speed per unit force, m s^{-1} per newton mol^{-1}); F is Faraday number (96500 C mol^{-1}); $\Delta V/\Delta x$ is the voltage gradient measured by the ion-selective probe between positions 1 and 2; and Nernst slope is the slope of the calibration graph for the probe.

For a large unicellular organism, a spherical or cylindrical diffusion geometry can be used instead. The equation used with spherical cells (as for *Thrasutocytrium*), where r is the radius of the sphere, is obtained by replacing Δx in Eqn 1 with

$$\Delta x = r^2\ (1/(r+x) - 1/(r+x+\Delta x)) \quad (2)$$

MIFEFLUX software (a component of the MIFE setup) automatically performs the required calculations based on the geometry of the measured cell (cell diameter and probe distance above cell surface) and provides the tabulated results of measurements as net ion fluxes (nmol $m^{-2}s^{-1}$) for import into a spreadsheet.

2.3.2 The MIFE apparatus

A new MIFE experimental setup was designed at the School of Agricultural Science, University of Tasmania to enable measurement of net ion fluxes from bacteria immobilised on a cover-slip. The MIFE system consists of several parts (Fig. 2-9).

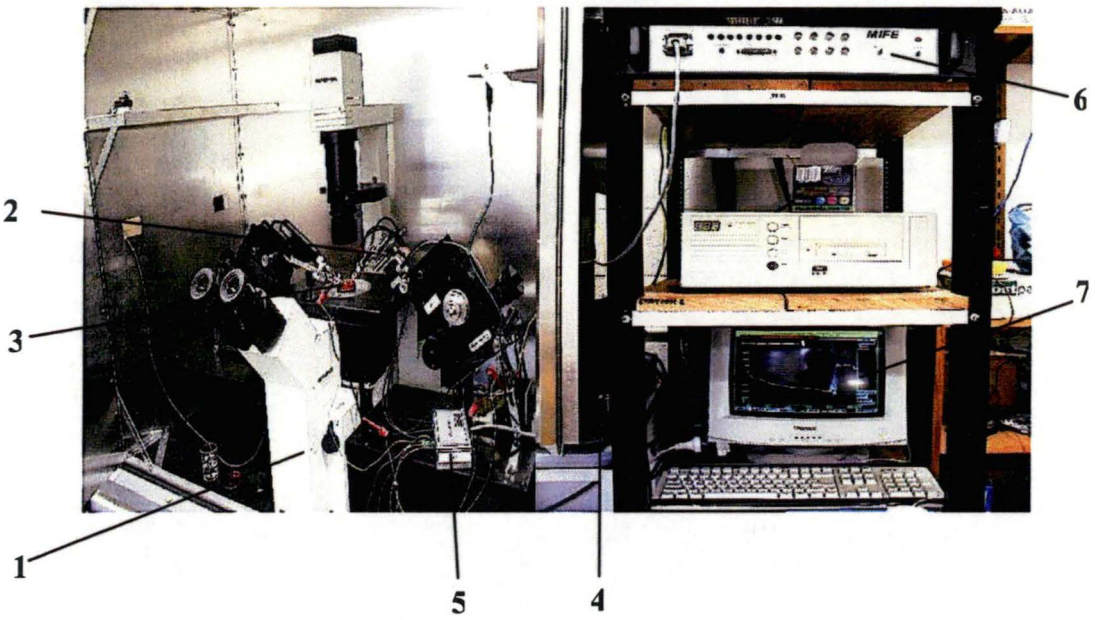

Fig. 2-9. The MIFE setup: microscope (1); an electrode holder (2); a measuring chamber (3); a stepper motor and controller (4); a pre-amplifier (5); a main amplifier and controller (6) connected to a personal computer (7).

The apparatus was built around an inverted microscope system (IX50, Olympus Optical Co., Ltd, Tokyo, Japan) with long working distance objectives, providing total magnification of up to 500x. Microelectrodes were held in E45P-F15PH electrode holders (CDR Clinical Technology, Middle Cove, Australia) mounted on a 3-dimensional micromanipulator. Two types of perfusion chamber were used in this study (Fig. 2-4, Fig. 2-5). Both of them introduced an open-type perfusion chamber enabling easy access to both sides of the measured object. The chamber was inserted on the microscope stand (Fig. 2-9).

The rate of solution flow through the perfusion chamber was not more than 6 mL min^{-1}. All measurements were made under steady state conditions after solution flow stopped. This was done to satisfy the requirements of the theoretical basis of the MIFE method (ie no convection or water uptake) and meant that measurements started a few minutes after solution changes were completed (see Chapter 3.3 for details). The standard non-polarising Ag/AgCl reference electrode was positioned in the chamber 10 to 30 mm away from the measured cells.

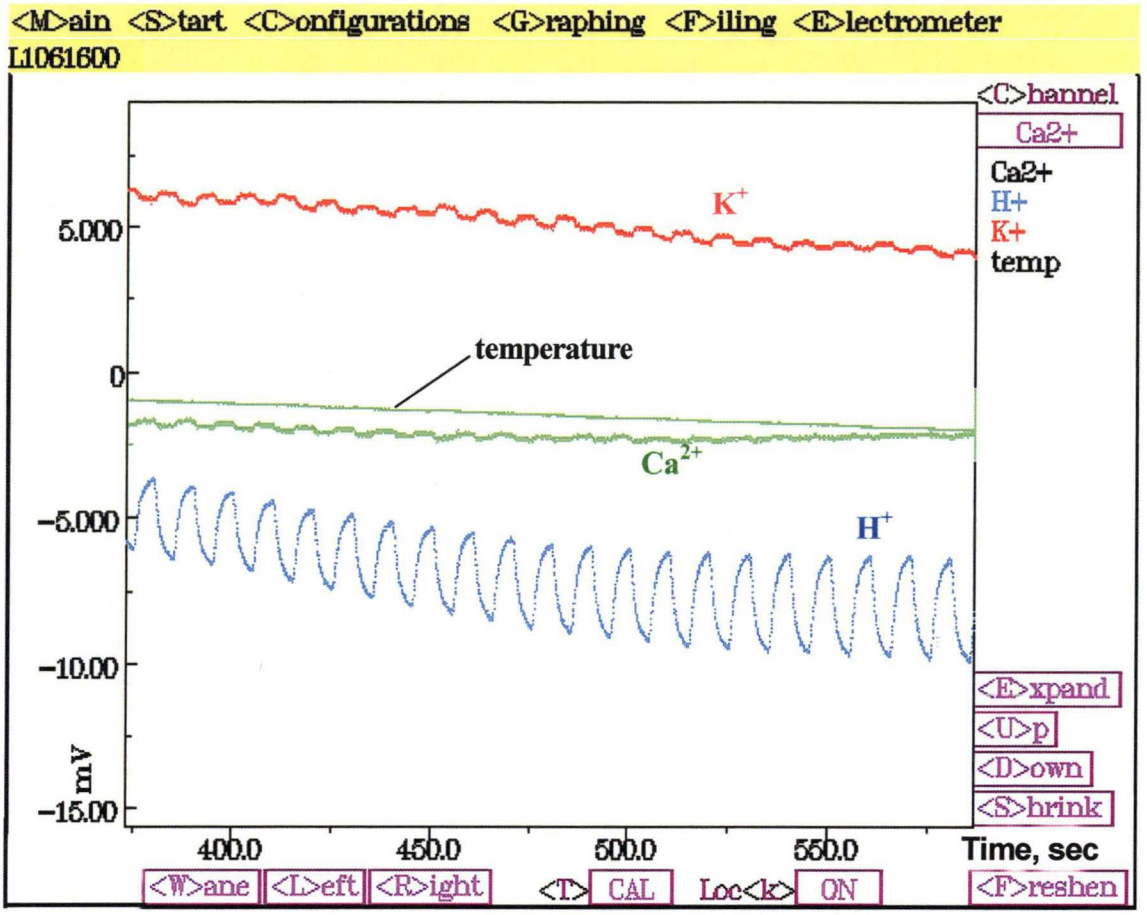

Fig. 2-10. Computer screen display of the MIFE recordings. A (reverse colour) screen is pictured showing four concurrent voltage records for Ca^{2+}, H^+, K^+, and temperature. Fluxes of ions were calculated from the voltage (ΔV) using recorded concentration values. H^+ and K^+ concentrations are decreasing slowly. K^+ and H^+ fluxes are steady, while Ca^{2+} flux decreases to zero. Temperature (reversed scale) increases slowly.

The voltage output from the electrodes is amplified and digitised using an analogue-to-digital interface card (DAS 08, Computer Boards Inc.) on an IBM-compatible PC. The card also controlled the stepper motor of the manipulator and was used for offset adjustment of the 4 channel electrometer. A custom designed software, the CHART program (University of Tasmania), was used to control the interface, collection and storage of the digitised output. The electrodes were oscillated at either 0.1 or 0.05 Hz moving between the two positions (usually 10 and

30 μm) above the surface of the object under study in the experiments. An example of a trace produced by the output of the electrodes during the measurements is demonstrated in Figure 2-10.

2.3.3 Microelectrode fabrication

Good ion-selective microelectrode fabrication is a crucial step in MIFE measurements. Several different approaches for microelectrode preparation are available in the literature (Smith et al., 1999; Shabala and Newman, 1997 a, b; Newman, 2001). A shorter procedure was used in this study that also enabled storage of the prepared electrode blanks at room conditions for up to six weeks without loss of microelectrode performance in contrast to other methods (eg. Smith et al., 1999).

Microelectrode fabrication included several distinct steps:

- pulling out electrode blanks;
- baking and salinising the blanks;
- filling the electrodes with an appropriate liquid ion exchanger (LIXs).

(i) ***Pulling out electrode blanks***. The electrode blanks were made using 1.5 mm (OD) non-filamentous borosilicate glass capillaries (GC150-10, Harvard Apparatus Ltd, Kent, UK). The blanks were pulled to <1 μm diameter tips using a vertical pipette puller (PP 830, Narishige, Japan).

(ii) ***Baking and salinising the blanks***. Electrode blanks were placed upright, base down, in a stainless steel rack and oven dried at 220 °C overnight. Ten to fifteen minutes before silanisation, electrodes were covered by a steel lid that created a closed container with the blanks, and 2 drops (approximately 15 μL) of tributylchlorosilane (90796, Fluka Chemicals) were injected under the lid. The lid was removed after 10 min and electrode blanks baked at 220 °C for a further 30 min. By this procedure, the surface of the electrode was made hydrophobic. Freshly pulled electrodes are hydrophilic due to the surface hydroxyl groups (Ammann, 1986). LIXs are organic cocktails and hydrophobic. Hydrophobic coating of an electrode blank enables entry of the LIX into the tip of the prepared microelectrode (Fig. 2-11).

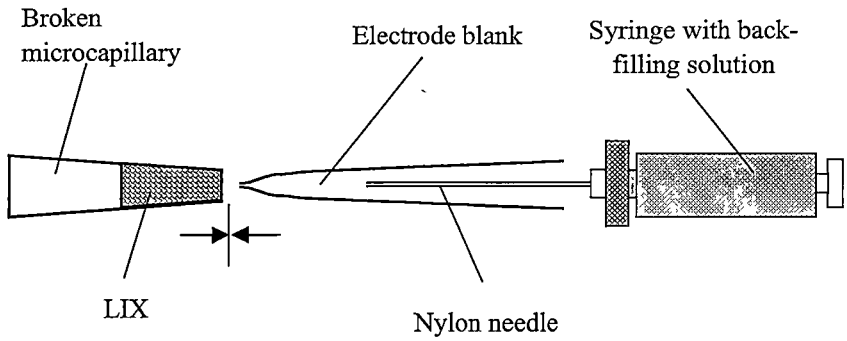

Fig. 2-11. Scheme of ion-sensitive microelectrode fabrication.

(iii) ***Filling the electrodes with an appropriate ion-selective resin (LIXs).*** Dried and cooled electrode blanks were then filled with LIX as depicted in Figure 2-11 and described below. A LIX-containing tube is first constructed using a broken back glass mirocapillary (tip diameter approximately 100 μm), which was dipped into the stock LIX taking up a column of cocktail of approximately 1 mm. The microelectrode blank was mounted horizontally on a three-dimensional micromanipulator and the electrode tips were flattened to achieve tip diameter of 2-3 μm. To do that, the electrode blank was gently placed against a flat glass surface under a stereo microscope. Blanks with proper tip size were back filled with appropriate back-filling solutions using a syringe with a custom made nylon needle. The latter was pulled out from 0.1 mL nylon pipette tip after flaming it. The use of the flexible nylon needle for the microelectrode back-filling, significantly simplified the procedure. Immediately after back-filling, the electrode tip was front-filled with the corresponding LIX. To do that, the back-filled electrode blank was positioned co-axially with the broken mirocapillary containing the appropriate LIX in its tip. The blank was briefly put in contact with LIX, and resin flowed into the electrode tip. The column length of the LIX in the prepared electrode was 100 to 200 μm. Immediately after filling, electrodes were immersed in solution and kept there until use (up to 8-10 hours).

Most of the prepared microelectrodes can be used immediately after preparation, while others (eg., H^+ and Cl^-) need some conditioning time (~1h) to ensure a stable response.

2.3.4 Calibration of the microelectrodes

Electrodes were fitted to the electrode holder and then calibrated in a set of three standards with a series of concentrations covering the expected range of the ion in question before and after use. Specific details about the type of commercially available LIX, composition of back-filling solutions and range of calibration standards used, are given in Table 2-2.

Table 2-2. Fabrication details of ion-selective microelectrodes used in experiments.

Ion	*LIX (Fluka catalogue No)*	*Back-filling solution (mM)*	*Calibration set*
Hydrogen	95297	15 NaCl + 40 KH_2PO_4	3.5 – 4.8 - 6.4 (pH)
Potassium	60031	200 KCl	0.1 - 0.5 – 1.0 (mM)
Calcium	21048	500 $CaCl_2$	0.1 - 0.2 – 0.5 (mM)
Ammonium	09882	500 NH_4Cl	0.1 - 0.5 – 1.0 (mM)

Electrodes with responses less than 50 mV per decade for monovalent ions and 25 mV per decade for calcium, and with correlation coefficients less than 0.999 were discarded. Both the slope and intercept of the calibration line are used to calculate the concentration c in Equation 1 from the value of V measured during the experiment. The resistance of the electrodes was typically 1-5 GΩ. The values of electrode resistance and the length of the LIX in the tip of the electrode are critical for the

quality of the prepared electrode. High values result in an increase in 'noise' of electrode response.

An Ag/AgCl reference electrode was fabricated in a similar way from a pulled and broken glass micro-capillary and filled with 1 M KCl in 2 % agar. A chlorided silver wire (galvanised in 0.25 N HCl for 15 min) was inserted in a length of a glass micro-capillary and sealed with parafilm. A small tip diameter (approximately 50 µm) ensured little K^+ leakage from the reference electrode.

2.3.5 Flux measurements

The electrode tips were positioned in one plane, separated laterally by 1-2 µm, under the microscope. A measuring chamber with immobilised bacteria or thraustochytrid cells was positioned on the microscope stage and the electrodes were set the required distance away (about 20 µm for experiments on bacterial "monolayers", and 10 µm for measurements on thraustochytrid cells) above measured cells. The electrode holders were positioned at an angle of 30° to the surface of the cover-slip and moved axially by a computer-driven hydraulic manipulator, providing electrode movement of 30 µm (for bacteria) and 20 µm (for thraustochytrid cells) from the primary position at a frequency of either 0.05 Hz (a 20 sec cycle) or 0.1 Hz (a 10 sec cycle). The recorded voltages were converted into concentration differences using the calibrated Nernst slopes of the electrodes. Two to four seconds (depending of the frequency of data acquisition) were allowed after each movement for the response to stabilize before data were used to calculate fluxes (see Chapter 2.3.6 for details and Fig. 2-12). Flux of an ion was then calculated by the MIFE software, assuming planar diffusion geometry for bacteria and spherical geometry for thraustochytrid cells.

Two major types of measurements were performed.

In "static" experiments, net ion fluxes were measured for a short time (ca. 3 min) at each bacterial site, or from each individual thraustochytrid cell. Electrodes were then re-positioned to another site (typically 100-200 µm aside), or to another cell, and measurements were resumed. On average, for each run, 5 to 7 sites of the immobilised bacteria or individual thraustochytrid cells were measured in the same

chamber.

In "kinetic" experiments, a chosen bacterial site or an individual thraustochytrid cell were monitored for a prolonged interval (up to several hours). Fluxes were measured in steady state conditions first; then the treatment was applied, and transient flux kinetics was monitored. In most experiments, the basic experimental solution was replaced by a new one, with altered ionic or chemical composition. Typically 5 to 10 chamber volumes were pumped through a chamber to ensure full replacement of the experimental solution in the chamber by the new one.

2.3.6 Flux calculation

Measured voltage records were stored on a Pentium PC. Net ion fluxes were then calculated essentially as described elsewhere (Shabala et al., 1997; Newman, 2001). Figure 2-12 details the output from an individual electrode.

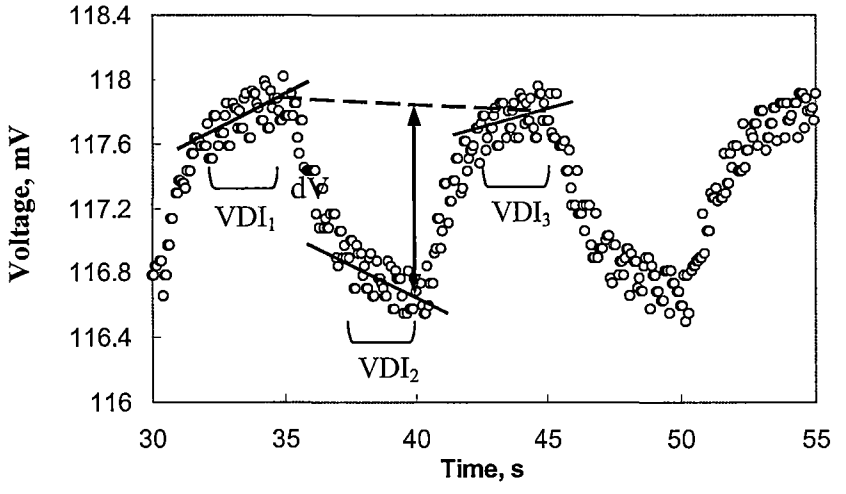

Fig. 2-12. Fragment of the "raw" voltage data recorded from a H^+ selective microelectrode. Frequency of the data sampling was 0.1 Hz, and electrode was moved between position 1 and 2 every 5 sec. (Modified from Shabala et al., 1997).

The electrode was rapidly (every 5 s) moved from position 1 (10 μm above the measured surface) at t=35 s to position 2 (30 μm above the measured surface) (Fig.

2-12). Concurrently, the electrochemical potential decreased. At t = 40 s the electrode moved back to position 1 and electrochemical potential increased again. These cycles were repeated with a period of 10 s. Flux calculations are based on voltage differences between the two positions (10 and 30 μm here) measured by the microelectrode. Part of a voltage trace associated with changing position and stabilisation (2.5 sec in Fig. 2-12) is discarded, thus only valid data intervals (VDI) are used for analyses.

2.3.7 Membrane potential measurements

The electrode blanks were made from 1.5 mm (external diameter) filamentous borosilicate glass capillaries (GC150-10, Harvard Apparatus Ltd, Kent, UK). The blanks were pulled to <1 μm diameter tips using a vertical pipette puller (PP-830, Narishige, Japan) followed by backfilling with 0.5 M KCl. The prepared microelectrodes were connected to the MIFE electrometer for the voltage measurement. Membrane potentials of thraustochytrid cells were measured in steady state conditions. A microelectrode was impaled into the cell, and voltage characteristics were recorded.

2.4. Fluorescence Ratio-Imaging Microscopy (FRIM)

2.4.1 Principles

Intracellular labeling with fluorescein is based on the assumption that only cells which have an intact membrane and esterase activity are able to accumulate the fluorescent probe (Breeuwer and Abee, 2000). The fluorescent probe can be easily taken up by bacteria during incubation with the diacetate ester, cFSE. Once cFSE is incorporated, its succinimidyl group forms conjugates with aliphatic amines. Fluorescence can be detected after intracellular esterase activity. It was shown that its fluorescence is pH dependent (Breeuwer et al., 1996). Leakage of probe to the external environment may be minimised by the application of fluorescein derivatives such as carboxyfluorescein (cF), calcein and BCECF, which are more negatively charged at physiological pH, and are thus less likely to leak from the cells.

2.4.2 Procedure of cell staining with fluorescent probe

Fluorescent probe preparation. A 10 mM stock solution of 5(6)-carboxyfluorescein diacetate siccinimidyl ester (cFSE) (Molecular Probes Inc., Eugene, Or) was prepared by dissolving in DMSO. The 10 µM aliquots of the cFSE prepared from the stock solution were stored at -20 °C.

Cell staining with the fluorescent probe. A 1ml volume of stationary phase culture was harvested by centrifugation at 10,000 x g for 5 min followed by pellet resuspention in 1ml sterile cold 50 mM phosphate-buffered saline containing per litre: 1.5 g of Na_2HPO_4 (Merck), 0.22 g of NaH_2PO_4 (Merck), and 8.5 g of NaCl (Merck) (pH 7.4). The fluorescent probe (pH indicator) at a concentration of 30 µM was added to the cell suspension, vortexed, and the preparation incubated at 37 °C for 30 min. The cell suspension was centrifuged at 10,000 x g for 5 min, re-suspended in experimental solution N2 (see Appendix A) containing different concentrations of glucose (0, 1 mM, 10 mM) adjusted to pH 6.0, vortexed, and further incubated at 30 °C for 30 min. Subsequently, the cell suspension was centrifuged at 10,000 x g for 5 min, then re-suspended in equivalent volume of the same experimental solution. Cells not analyzed immediately were stored on ice in the dark for a maximum of 30 min.

2.4.3 Measurements of pH_i of individual cells

An individually assembled chamber (see Figure 2-5) was mounted on an appropriate platform (type PH1; Warner Instrument Corporation, Denmark) and placed on the stage of the microscope (Zeiss model Axiovert 135 TV; Brock & Michelsen A/S, Birherod, Denmark). Solutions entered the chamber by gravity via a silicone tube and were removed via another tube using a peristaltic pump. Solutions were perfused through the chamber at a rate of up to 6 mL/min.

The pH_i of individual cells was measured by ratio imaging using a fluorescence microscope as described by Budde and Jakobsen (2000). Stained cells were excited at 490 and 435 nm with exposure time of 1 s. The excitation source was an optical fiber-connected monochromator with a 75 W short-arc xenon lamp (Monochromator B; TILL Photonics GmbH, Planegg, Germany). The inverted epifluorescence microscope (Zeiss Axiovert 135 TV) was equipped with a Zeis Fluar 100 x objective (numerical aperture 1.3), a band-pass emission filter (515-565 nm) (Zeiss type BP 515-565; Brock & Michelsen A/S, Birkerød, Denmark), a beam splitter (Zeiss model BSP 510; Brock & Michelsen A/S, Birkerød, Denmark), and a dichroic mirror (510 nm). Fluorescence emission was recorded at wavelengths between 515 and 565 nm by using a cooled charge-coupled device camera (CCD) (EEV 512 X 1024, 12-bit frame-transfer camera; Princeton Instruments Inc., Trenton, N.J.). To minimize photobleaching of the stained cells, a 2.5% neutral-density filter was used. Ratio imaging of emission signals collected from excitation at 490 and 435 nm was performed using the software package MetaFluor, version 3.5 (Universal Imaging Corporation, West Chester, Pa, USA). Ratio imaging was initiated at time zero before perfusion of a solution through the chamber. Images of the same region were recorded at intervals indicated in individual experiments, and each experiment was terminated within 60 min.

2.4.4 Image acquisition and pH_i calculation

Digital images were stored on a Pentium PC. Data analysis was carried out on the saved data. To analyse single cells, regions were drawn along the perimeter of the cell using MetaFluor 3.5 (Universal Imaging Corporation, West Chester, Pa, USA).

Cells were randomly selected on the 435 nm image which is pH independent (to avoid selection based on high intensity of the 490 nm image, which is pH dependent). A region without cells was subtracted as background. The ratios $R_{490/435}$ were corrected for background signal. The data region was directly logged into a spreadsheet. The ratio $R_{490/435}$ calculations for each cell examined were performed by dividing the intensity of individual pixels on the 490 nm image by the intensity of the corresponding pixels on the 435 nm image. The pH_i calculations were performed using a calibration curve. In each experiment between 15 and 25 randomly selected individual *L. monocytogenes* cells were analyzed. Each experiment was repeated at least twice. For presentation, ratio images were saved as TIF files, and Adobe Photoshop 5.5 was used for contrast enhancement. An example is given in Figure 2-13. The images demonstrate changes in pH_i of *L. monocytogenes* cells exposed to acidic pH. Stationary phase cells were adapted in experimental solution N2 (Appendix A) without glucose (pH 6.0) (image #1 in Fig. 2-13). Acidic stress was introduced by change of experimental solution in a chamber for one of the same composition at pH 4.0. The images shown demonstrate changes in pH_i after acidic treatment at indicated times. Change of solution is taken as a zero time. A colour-coded pH_i scale is shown in each panel. The data demonstrates rapid decrease in pH_i of *L.monocytogenes* in the absence of glucose in the medium that is in accord with the results presented in Chapter 5.5.

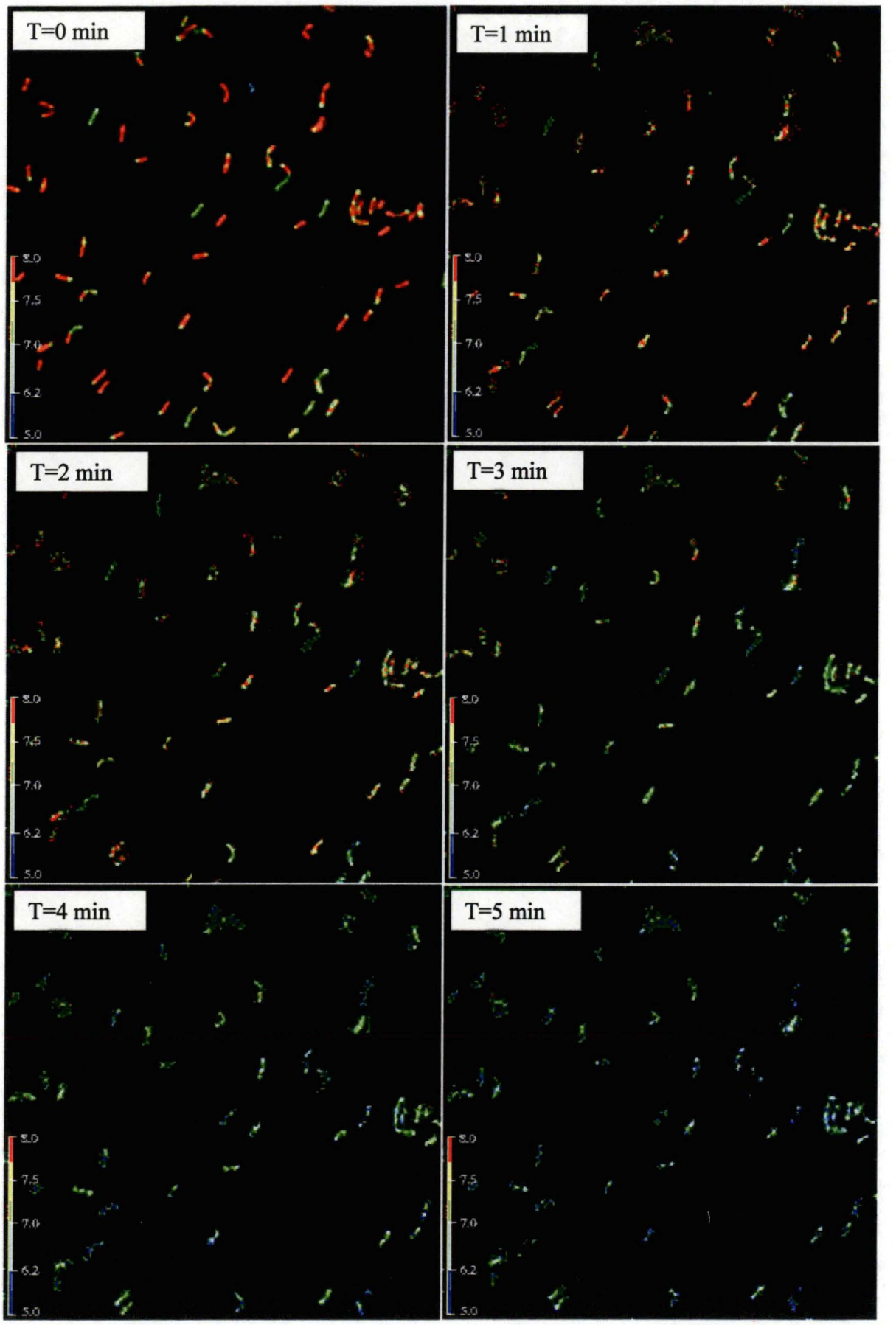
T=0 min
T=1 min
T=2 min
T=3 min
T=4 min
T=5 min
8.0
7.5
7.0
6.2
5.0

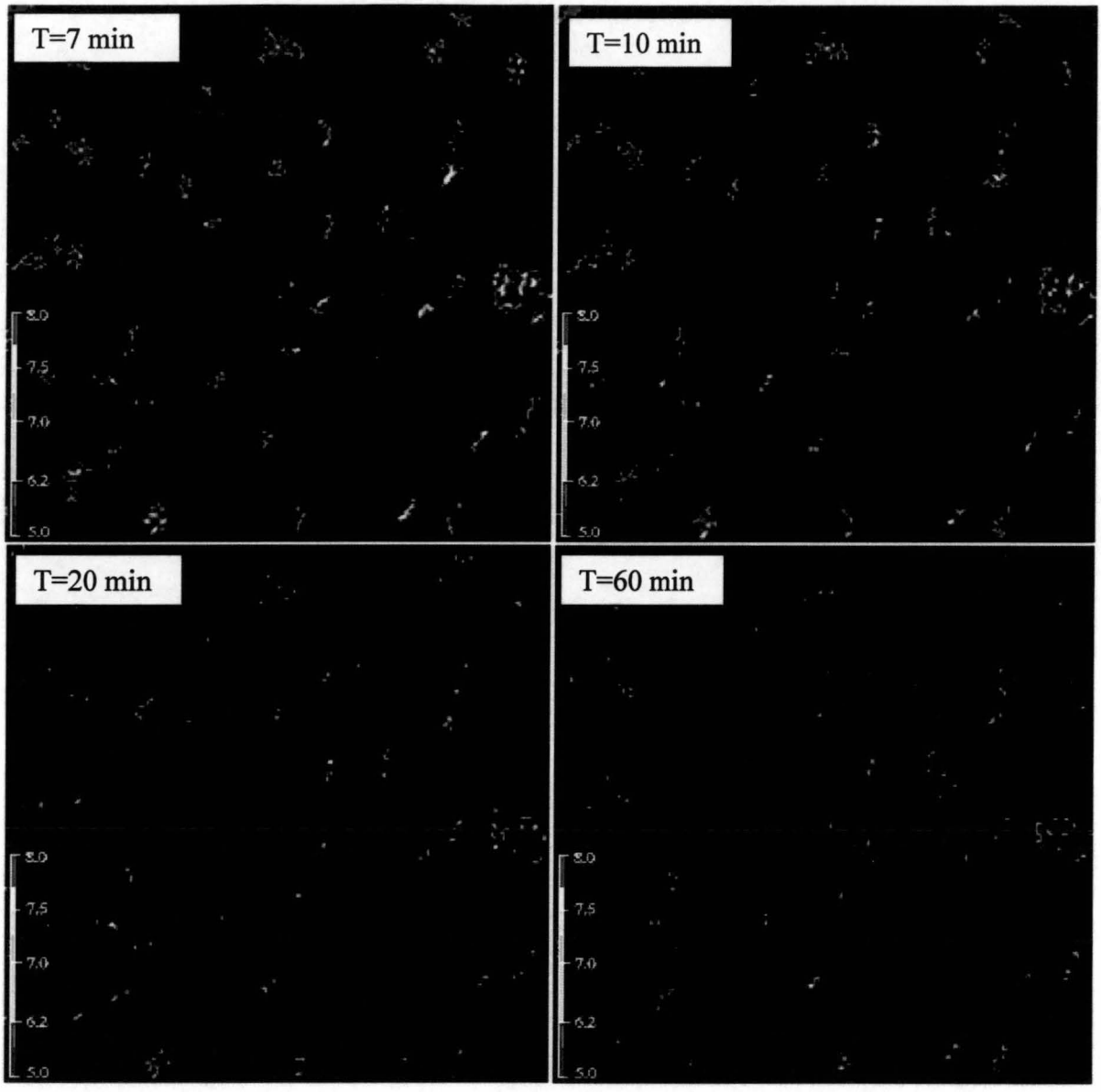

Fig. 2-13. Changes in ratio images of *L. monocytogenes* 4140 exposed to acidic stress. Acidic stress was introduced by change of experimental solution in a chamber of pH 6.0 without glucose for one of the same composition at pH 4.0. Image #1 represents cells at pH_o 6.0. Change of solution was made after image #1 was taken (indicated as a zero time). Images thereafter demonstrate changes in pH_i after acidic treatment at indicated times. A color-coded pH_i scale is shown in each panel.

2.4.5 Calibration curve establishment

To construct a calibration curve for pH_i estimation, pH_i was equilibrated with pH_o adjusted to pH in the range 4.5-9.0 and a corresponding ratio $R_{490/435}$ was estimated (Fig. 2-14).

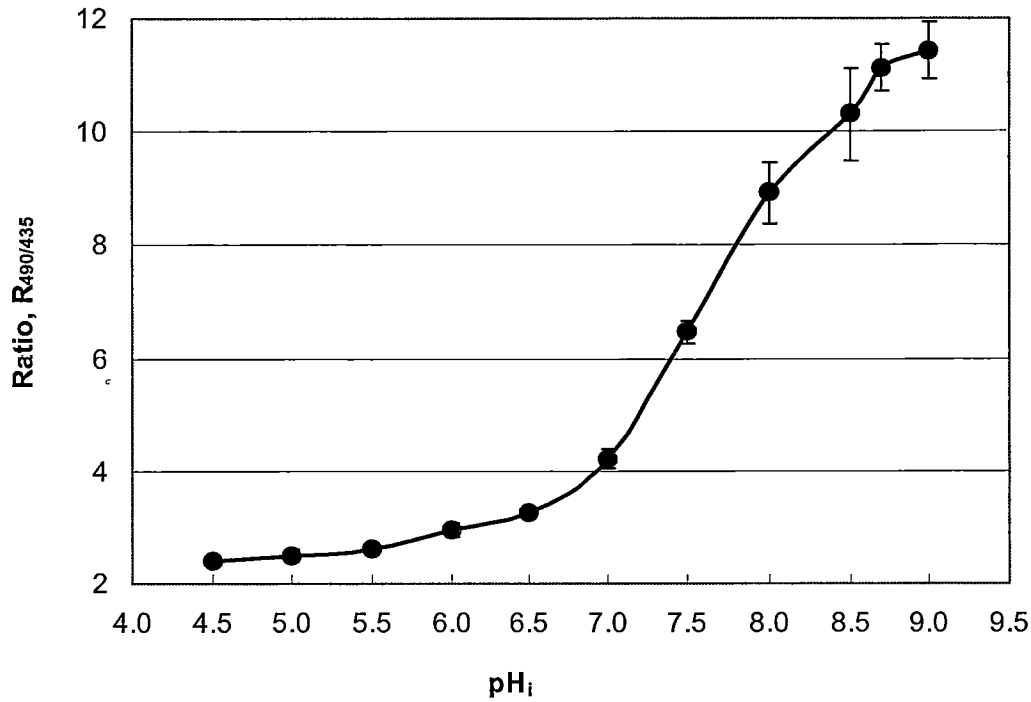

Fig. 2-14. Calibration curve for pH_i determination in *L. monocytogenes* 4140. The ratio values are averages based on 40 single cells. The error bars indicate SEM.

To equilibrate the pH_i and the pH_o of cells, ethanol (63%, v/v) was added to stained cells to dissipate the ΔpH irreversibly. The mixture was incubated at 30 °C for 30 min. Subsequently, the cells were harvested by centrifugation at 10,000 x g for 5 min and resuspended in buffers having pH ranging from 5.0 to 9.0 with a step of 0.5 pH unit. Details are given in Table 2-3.

Table 2-3. Details of buffer solutions used for FRIM calibration.

pH range	*Buffer type*	*Chemical composition*
4.5 – 5.0	phthalate buffer	0.2 M KH phthalate + 0.2M NaOH
5.0 - 8.0	potassium phosphate buffer	50 mM KH_2PO_4-K_2HPO_4
8.5 - 9.0	sodium borate buffer	50 mM $Na_2B_4O_7.10H_2O$ + 0.1 M HCl

The ratios $R_{490/435}$ were determined as described previously. Ratios less than 2.1 were recorded as pH 5.0 due to the dye pH sensitivity range (Fig. 2-14). A relationship between pH_i and $R_{490/435}$ was established for the range from pH 4.5 to 9.0 (assuming $pH_i = pH_o$ for equilibrated cells). Interpolation between calibration points was used to calculate the pH_i of each cell.

2.5. Measurements of glucose availability

Glucose availability in growth medium from inoculation to the stationary phase of growth was determined by spectrophotometric measurements of glucose oxidation at 340 nm using a commercial kit (Boehringer Mannheim, Cat. No. 139106). The growth medium used was a defined MM (Table 2-1) supplemented with glucose. A sample of 1 mL was aseptically withdrawn from the batch culture at different times after inoculation, filtered through 0.22 μm filter, and a supernatant was used for analyses. To determine the concentration of D-glucose in the medium, 0.1 ml of the filtered supernatant was combined with 1 ml of triethanolamine buffer pH 7.6 containing ATP, NADP, and magnesium sulfate, 0.02 ml of suspension containing hexokinase and glucose-6-phosphate dehydrogenase, and 1.9 ml of redistilled water. The mixture was incubated for 15 min and the absorbance was read at 340 nm against a reagent blank with distilled water. The standard calibration curve was constructed and used to determine the amount of glucose in the supernatant (Fig. 2-15). The glucose concentrations used for construction of the calibration curve ranged from 0 to 0.1% to cover the actual glucose concentration in the medium.

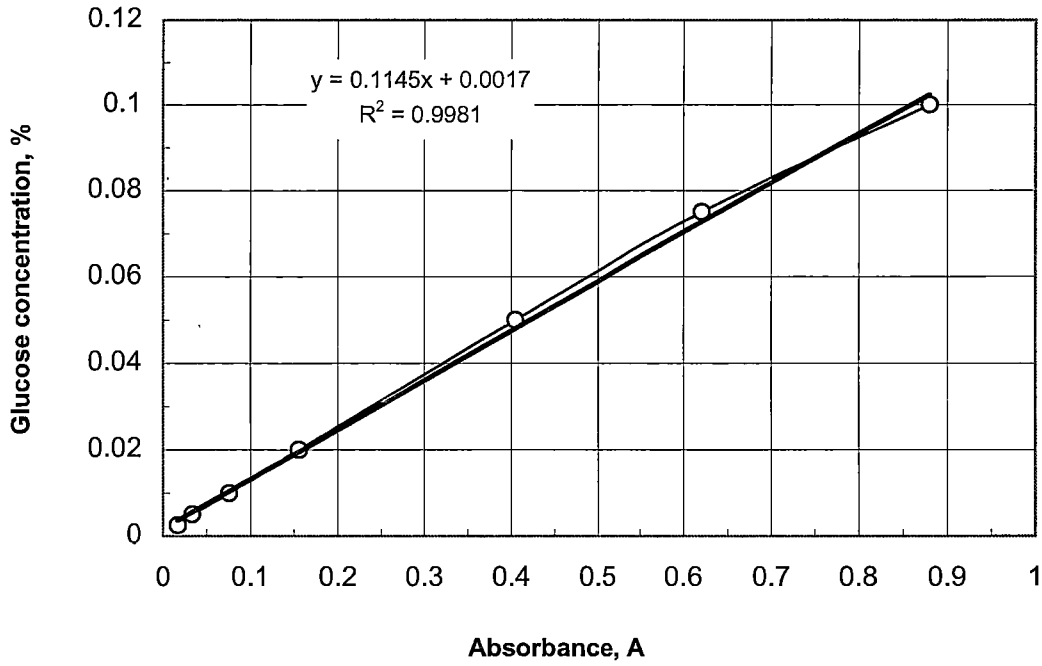

Fig. 2-15. Calibration curve for determination of glucose concentration in the medium (n=3).

2.6. Data analysis

2.6.1. Statistical analysis

Statistical significance of differences in data was determined by the standard Student's t-test. In all kinetic experiments, comparison was made between net ion flux or pH_i values before and 20-30 min after the treatment. Details, including the sample size numbers, are given in the text and figure legends.

2.6.2 Spectral analysis

Spectral analysis of ion flux oscillations was performed by applying the Discrete Fourier Transform (DFT) using an EXCEL 4.0 package. The "data window" contained 512 or 1024 data points (either 42.6 or 85.2 min intervals). Using the IMABS tool in EXCEL 4.0, the moduli of the complex amplitudes were returned from the DFT spectra. These moduli were later plotted against the period (T) of the

harmonic components for the discrete frequencies $\nu = 0, 1/T, 2/T, \ldots\ldots, (n-1)/T$. For some data, the high frequency noise (above 0.05 Hz) was filtered by using a low pass filter in the SANTIS package (University of Aachen, Germany). In that case, all the analysed ions were treated the same way and DFT, available in the SANTIS package, was used to plot the oscillatory spectra. The resulting spectra revealed by EXCEL and SANTIS were identical when applied to the same data series.

2.6.3. Cross-correlation analysis

Cross-correlation analysis (CCA) was used to quantify the relationship between fluxes of two different ions. Large positive or negative cross-correlation means that influx of one ion was associated with influx or efflux of another ion, respectively. Correlation near zero means fluxes of the two ions are unrelated. To assess the possibility of a causal link between the activity of the plasma membrane ion transporters, maximum values of the cross-correlation coefficient (ρ_{max}) and corresponding phase shifts (φ_{max}) were determined. The values of the cross-correlation coefficients were plotted against phase shifts, and the magnitude and the sign of φ_{max} were analyzed to determine which ion was leading, and which one was following.

Chapter 3

METHODOLOGICAL ASPECTS OF *MIFE* MEASUREMENTS IN BACTERIAL AND FUNGAL CELLS

As discussed in the preceding sections, since 1995 the MIFE technique has become a popular tool in studies on plant adaptive responses. Its application to bacteria, however, is entirely novel. Differences between plants and bacteria inevitably required significant modifications of experimental protocols, thus potentially introducing confounding effects associated with MIFE application in microbiology. Therefore, before commencing studies of membrane-transport processes in bacteria or fungi, methodological issues should be addressed.

The most remarkable difference between plant and bacterial cells is their rate of growth and, consequently, the duration of their life cycle. The rapid change of bacterial cell physiological "status" imposes some restrictions on the timing aspects of ion flux measurements. Therefore, it was important to establish the time scale required for "static" and kinetic experiments on bacterial cells.

Another important methodological aspect relates to cell immobilisation and associated confounding effects of ion fluxes from the supporting surface used to attach bacterial cells. Lew (2000) has mentioned significant K^+ efflux from the surface of the gelan gum, used to anchor root hairs in *Arabidopsis* seedlings. Some type of plastics, or even a freshly cut glass surface, may be a significant source of H^+ efflux (S. Shabala, personal communication). It was, therefore, crucial to ensure that such artifacts were eliminated or, at least, taken into account in microbial studies.

Finally, the effects of temperature, metabolic inhibitors, ionic strength of solution etc on LIX properties had to be investigated before studies on bacterial or fungal physiology were undertaken.

3.1. Confounding effects of measuring chambers

As described in Chapter 2, the MIFE technique is based on measurements of electrochemical potential gradient profiles near the cell surface. To enable ion flux measurements, cells must be immobilised in the measuring chamber. Depending on the method used, several confounding effects might be expected. The major ones relevant to this study are:

- possible leak of ions from the "supporting" surface (cover slip; see Chapter 2.2);
- confounding effects of adhesive agent (poly-L-lysine).

To ensure that the experimental methods involved in immobilisation of bacterial cells did not induce artefactual ion fluxes, net ion fluxes (illustrated by H^+) were measured from a plain clean glass surface, from a glass surface coated by poly-L-lysine, and from adherent *E. coli* cells prepared from a batch culture at the exponential phase of development (OD_{540}=0.3 A). No fluxes were present in the absence of bacteria, while immobilised cells exhibited significant net H^+ efflux (Fig. 3-1) indicating a high level of cell metabolic activity.

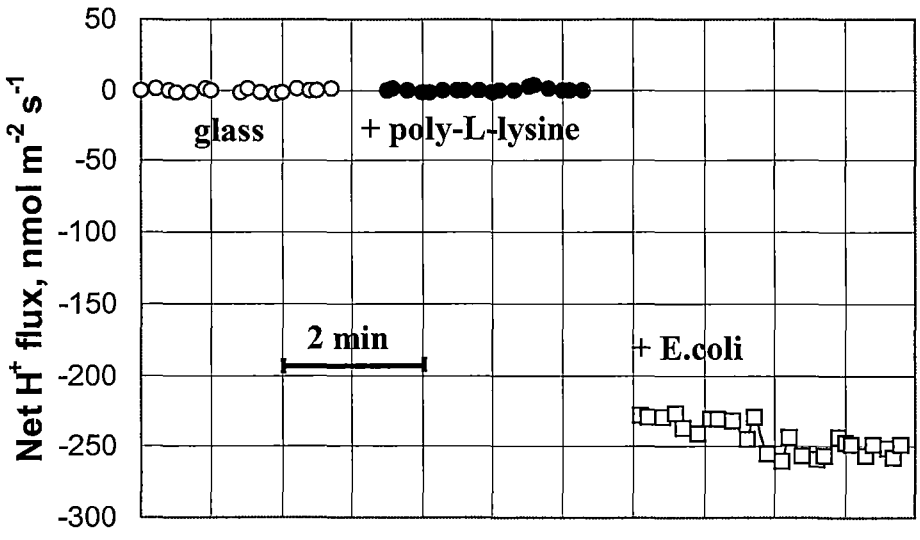

Fig. 3-1. Validation of the applicability of the MIFE technique to measure net ion fluxes from immobilised bacteria. Net H^+ flux (inward positive) measurements for the glass surface, for the glass surface coated by poly-L-lysine (used to attach cells to the glass surface), and for the immobilised *E. coli* cells prepared from an exponential phase culture (OD_{540}=0.3 A). Experimental solution N1 (Appendix A) was used for the study.

Similar results were observed for all other ions measured. Figure 3-2 shows the absence of significant net fluxes of Ca^{2+}, H^+, and K^+ from the glass surface, measured at two different levels of Na^+ (low- and high ionic strength solution, respectively).

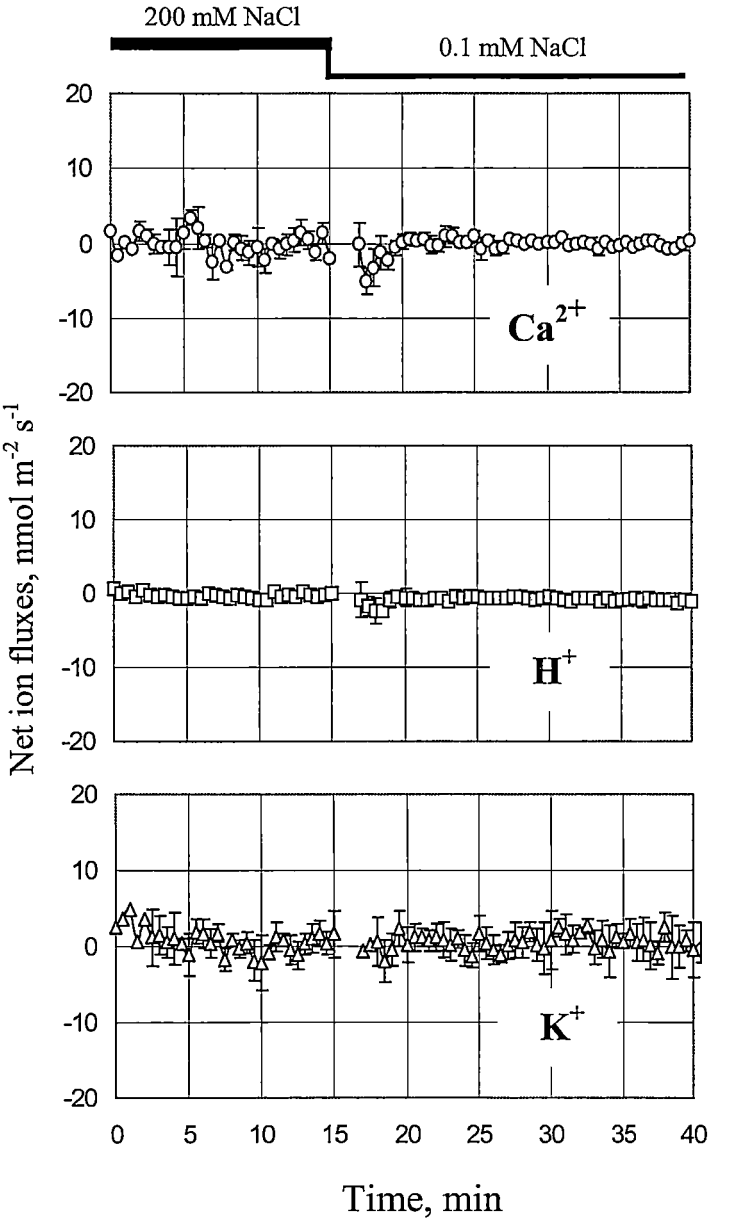

Fig. 3-2. Net fluxes of Ca^{2+}, H^+, and K^+ from the glass surface, measured at two different levels of Na^+, 200 and 0.1 mM NaCl, respectively. thraustochytrid experimental solution (Appendix A) was used throughout the study. Solution was changed at 15 min. Data are means ± SE (n=3).

No artifactal ion fluxes were caused by changing the ionic strength of solution in the absence of fungal or bacterial organisms, validating the experimental protocol used. The only difference observed was higher noise level of all fluxes measured in

200 mM NaCl. The latter may be explained by the imperfect selectivity of LIX used (for details, see LIX characteristics in Fluka catalogue).

3.2. Effect of cell viability on flux value

To ensure the measured fluxes were due to the activity of living cells, measurements were conducted using viable and dead (killed by heating) bacterial cells (Fig. 3-3).

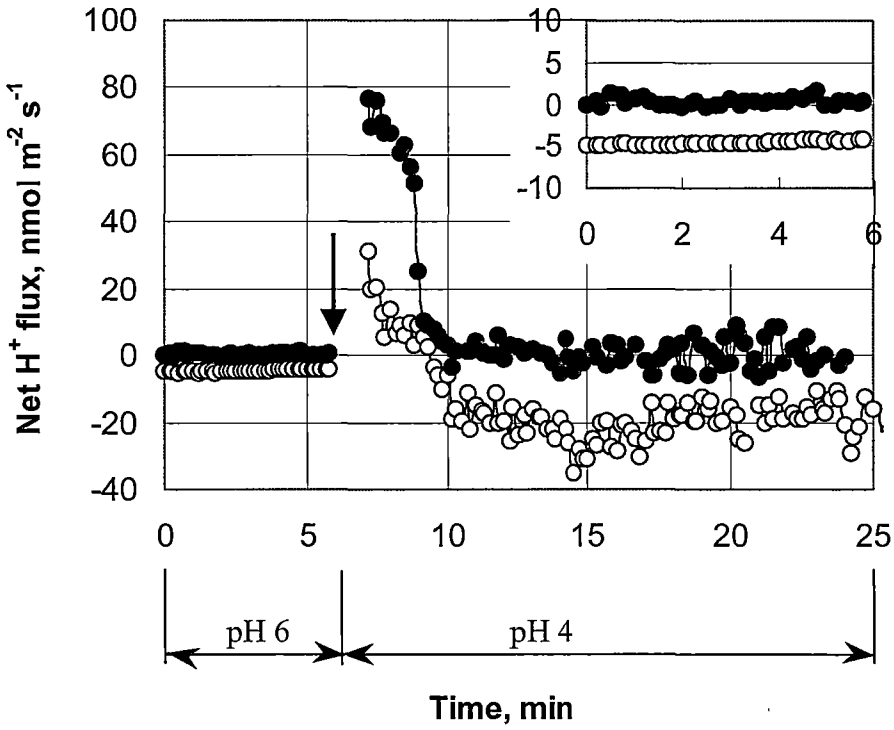

Fig. 3-3. Net H^+ fluxes from viable (open symbols) and dead (closed symbols) *L. monocytogenes* 4140 cells. Culture in the stationary phase of growth was used (see Table 2-1). Experimental solution N2 (Appendix A) at pH_o 6 or pH_o 4 containing 10 mM glucose was used for flux measurements. Change of solution for pH_o 4 is indicated by arrow. An enlarged insert shows net H^+ fluxes at pH_o 6.

To kill the cells, an aliquot of the culture was autoclaved at 121 °C for 15 min under a pressure of 1 atm. Immobilisation procedure and flux measurements were performed similarly for both trials.

Zero net H^+ flux was observed from the dead cells (Fig. 3-3; from 0 to 6 min). Immediately after pH_o was shifted from 6 to 4, a brief (less than 5 min) transient uptake of H^+ was observed. This may be explained by the loss of bacterial plasma membrane semi-permeability in dead cells, leading to a quick equilibration of internal (~7.0) and external (4.0) pH. Once concentrations of H^+ at both sides of the PM are in equilibrium, zero H^+ flux is observed (from 10 min onwards in Fig. 3-3, closed symbols). Therefore, in this situation we are dealing with a passive process of H^+ entry into the killed cell.

In contrast, viable cells of *L. monocytogenes* 4140 extruded H^+ at pH_o 6 at the level typical for these experimental conditions (see also Figs. 5-10 and 5-20). Furthermore, a shift from pH_o 6 to pH_o 4 resulted in a transient net H^+ influx (7-9 min in Fig. 3-3, open symbols) followed by H^+ extrusion due to pH homeostasis known to occur in *L. monocytogenes* (see Sections 5.1, 5.3, and 5.5 for details).

This data demonstrates that only viable cells are able to extrude H^+ against a concentration gradient, thus validating the MIFE studies.

3.3. Variability of flux measured from different spots

This part of the study addressed the variability of flux measurements and their dependence on duration of measurement. Both of these issues were addressed by measurements from different sites of the same cover-slip with immobilised bacterial cells. Figure 3-4 illustrates measurements of net H^+ fluxes from 3 different sites of immobilised *E. coli* SB1 cells derived from two different batch cultures harvested during early exponential growth (OD_{540}=0.17 A). Experimental solution N1 (Appendix A) was used in the study. Flux was measured for 1-2 min at each site in turn. The data is highly reproducible. The flux patterns are quite uniform between different spots, but have a tendency to increase with time (see the difference between samples 1 and 3, or 4 and 6). This may be explained by increasing activity of cells in the perfusion chamber and associated changes in the H^+ transport activity.

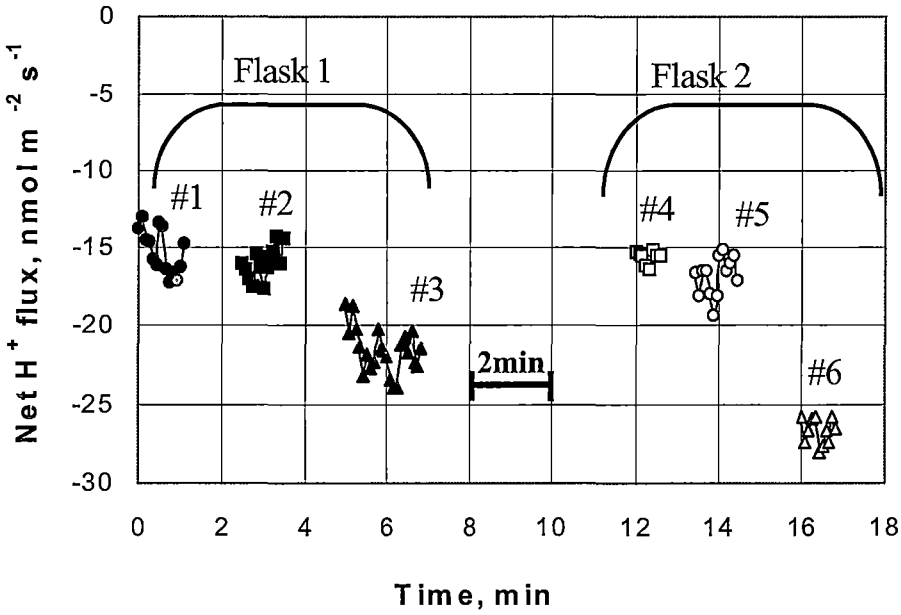

Fig. 3-4. Net H^+ fluxes from 3 different sites (different symbols) of immobilised cells from duplicate cultures (open and closed symbols, respectively) of exponential phase (OD_{540}=0.17 A) *E.coli* SB1 cells. The time scale represents relative time with bars indicating units.

3.4. Effect of solution change

Most kinetic experiments performed in this study involved replacement of the bath solution (acid and osmotic treatment; application of metabolic inhibitors etc). As MIFE theory assumes non-stirred layer conditions (Shabala et al., 1997; Newman 2001), it was important, therefore, to estimate quantitatively the timing required for this procedure. Figure 3-5 shows the response time of a microelectrode after solution change, measured in the absence of bacteria.

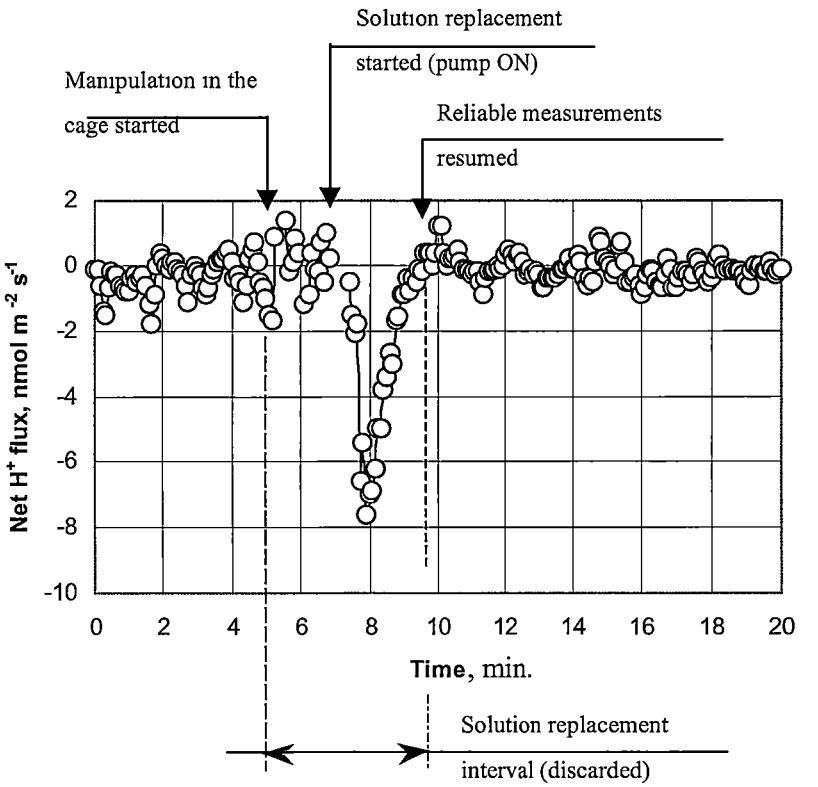

Fig. 3-5. Effect of solution change on a microelectrode response. Net H^+ fluxes measured from the cover slip in the absence of bacteria. Manipulations in the chamber were started at 5 min, and fresh solution (N2 for bacteria; see Appendix A) of the same composition was added at about 7 min. At about 9.5 min, solution replacement was fully completed, and no turbulent flow was observed. The interval from 5 to 10 min was later discarded from subsequent flux analyses.

From these data, it is apparent that the complete procedure of solution replacement in the experimental chamber took about 5 min (as tested for the large volume chamber). By that time, all turbulent flow ceased (misinterpreted by the MIFE system as net H^+ efflux from the surface (Fig. 3-5; between 7 and 9 min). The interval from 5 to 10 min was not used in subsequent flux analyses.

3.5. Effect of fluorescent dye loading

Measurements of cytosolic pH_i using the FRIM technique, employed in this study for bacteria (see Chapter 5.5), requires the pH-sensitive fluorescent probe to be loaded into the cell. In preliminary experiments, the MIFE technique was used to evaluate potentially confounding effects of the presence of the fluorescent probe cFSE, on membrane-transport activity of *L. monocytogenes*.

L. monocytogenes cells were prepared and immobilised as described in the Chapter 2.2. Experimental solution N2 (Appendix A) was used in the study. Bacterial cells were stained with the fluorescent probe cFSE by the procedure described in Chapter 2.4. Control cells were prepared in a similar way but without adding cFSE. Kinetic experiments were conducted using the MIFE technique to monitor net H^+ flux at pH_o 6.0 and after the medium change to pH_o 4.0 without glucose in the medium (Fig. 3-6).

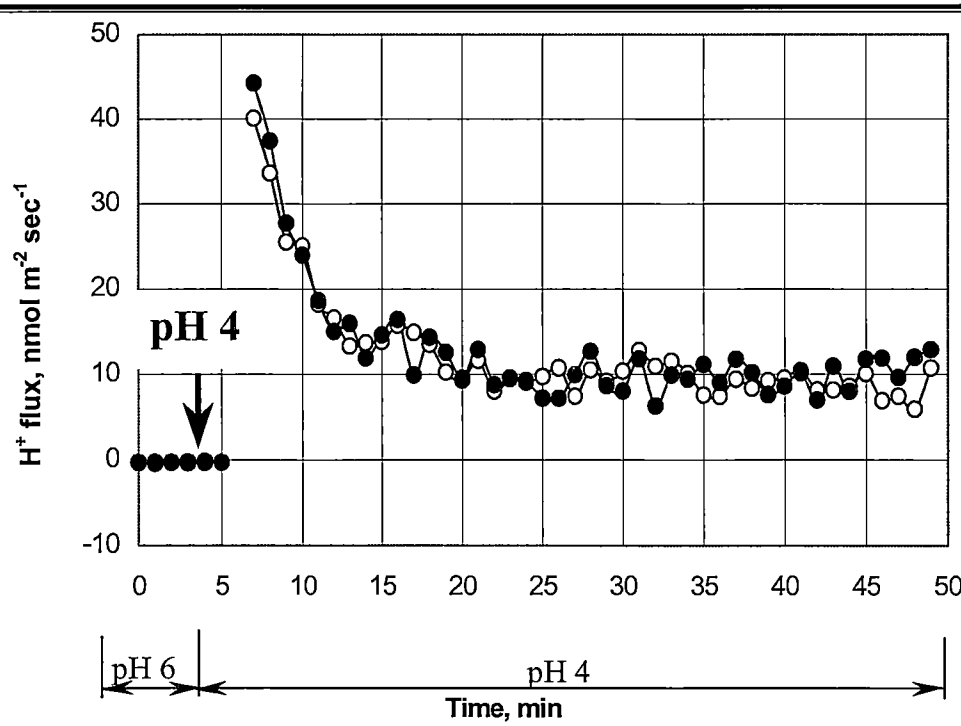

Fig. 3-6. Effect of the presence of fluorescent probe on net H^+ flux changes and response to solution pH change. Experimental solution N2 (Appendix A) without glucose was used. Data was taken every 0.1 min. Each point represents the average value over 1 min. Open symbols represent the trial with 30 μM cFSE; closed symbols represent control.

The results demonstrated an almost identical response between control cells and cells loaded with the fluorescent dye. It is concluded that net H^+ flux response is not affected by the fluorescent probe used.

3.6. Effect of ionic strength change

Variations in ionic strength of solutions might significantly affect characteristics of ion selective electrodes and result in inaccurate estimates of ionic concentrations and, ultimately, net ion fluxes. For example, high levels of Na^+ in the bath solution were expected to decrease the activity of other cations (K^+, Ca^{2+}) (Nobel, 1974). The experimental data obtained support these phenomena as shown in Table 3-1 and Figure 3-7. In Table 3-1, characteristics of a Ca^{2+}-selective microelectrode are given for several levels of NaCl added to 100 μM $CaCl_2$ standard.

Table 3-1. Characteristics of Ca^{2+}-selective microelectrodes as a function of ionic strength of the experimental solution.

NaCl, mM	Electrode potential, mV	Calculated Ca^{2+} concentration, μM	Electrode calibration characteristics		
			Slope	Intercept	Correlation
0	-87.0	168	-27.51	-31.82	-0.9997
20	-89.8	139			
50	-92.3	113			
90	-93.5	100	-27.92	25.33	-0.9999
150	-94.2	96			

Electrodes were calibrated in two sets of Ca^{2+} standards, of low and high (90 mM NaCl added) ionic strength. Data for electrode potential and calculated Ca^{2+} concentrations refer to a calibration set including 90 mM NaCl.

In this example, Ca^{2+} selective microelectrodes were calibrated in two sets of Ca^{2+} standards, with (90 mM) or without (0 mM) NaCl. No significant change in

the Nernst slope of electrodes was found, but the electrode intercept was significantly affected. As a result, calculated Ca^{2+} concentrations in a solution with different ionic strength, were inaccurate. The only accurate reading of Ca^{2+} standard (100 μM) was for 90 mM NaCl solution, e.g. for the ionic strength for which the electrode was calibrated. The actual Ca^{2+} concentrations were overestimated for solutions with lower ionic strength than one for the standard, and underestimated *vice versa*.

The underestimation of cation concentrations in solutions with high ionic strength might have resulted in significant errors in net flux calculation. Figure 3-7 shows examples of net Ca^{2+} flux kinetics measured from thraustochytrid cell in response to hypoosmotic shift.

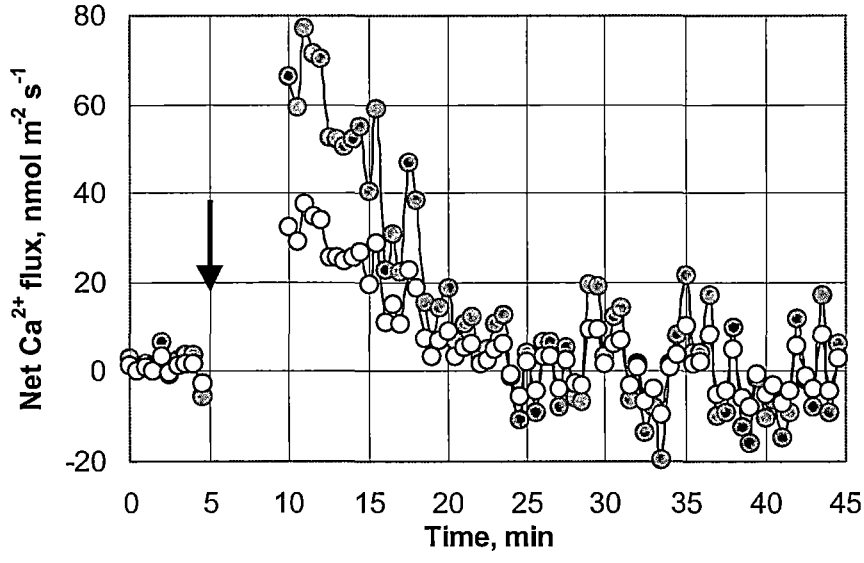

Fig. 3-7. Effect of ionic strength of the bath solution on quantitative estimation of net Ca^{2+} fluxes from thraustochytrid cell. Incubation solution, containing 200 mM NaCl, was replaced by one with 0 mM NaCl (indicated with arrow). Flux values were calculated using two different calibration sets for Ca^{2+}, with (closed symbols) or without (open symbols) 200 mM NaCl added.

Starting measurements were undertaken in an experimental solution for thraustochytrid (Appendix A) with addition of 200 mM NaCl (0 to 5 min). The experimental solution was changed at 5 min (indicated by arrow in Fig. 3-7) for one

of the same composition but without NaCl. Flux values were calculated using two different calibration sets for Ca^{2+}, with (closed symbols) or without (open symbols) 200 mM NaCl added. Net Ca^{2+} fluxes were significantly overestimated if NaCl was included in the standards of the calibration solutions for the experiments in low ionic strength solutions. Similarly, changes in solution ionic strength affected flux measurements of other ions employed in this study (H^+, K^+, NH_4^+; data not shown). As a result, this effect was taken into account in all subsequent measurements by including NaCl in the calibration set for each of the ions measured in all experiments in which NaCl concentration was a variable. Practically, each electrode was calibrated in two sets of standards and flux was calculated separately for data segments obtained before and after osmotic stress was applied.

3.7. Temperature sensitivity of ion-selective microelectrodes

Another methodological issue, important for studying temperature-induced ion flux kinetics from thraustochytrid, was the effect of temperature on LIX characteristics. It was expected that both the slope and the intercept of the calibration curve for ion-selective electrodes might be slightly affected by the changing temperatures.

Two possible options existed. First, these changes might be taken into account by the CHART software used for ion flux calculations (calibration and measurement solution temperatures are included in the defined parameters). Practically it meant flux data would have to be re-calculated a large number of times for the appropriate temperature range. Consequently, methodological experiments were carried out to evaluate the degree to which ion-selective microelectrodes were affected by the changing temperatures. It was found that correction for temperature was not required, as is illustrated in Figure 3-8.

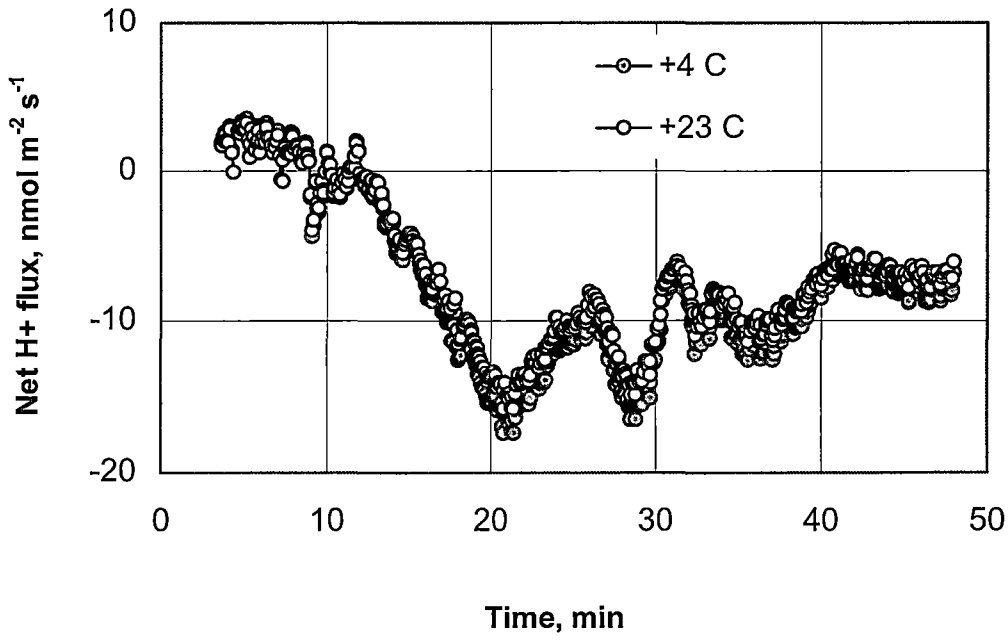

Fig. 3-8. Kinetics of net H^+ flux recovery from thraustochytrid ACEM C calculated by using two sets of pH calibrating standards, at 23 ^{0}C (open symbols) and 4 ^{0}C (closed symbols), respectively.

The maximum deviation in pH readings of 0.03 pH was observed for the first 2-3 min of measurements, which resulted in about 4.5% underestimation of the net flux values. For temperatures ≥ 10 ^{0}C (characteristic for all reported apparent critical temperatures (ACT) values in this study), the systematic error of ion flux estimation was less than other uncontrolled variability.

Therefore, even in the worst case scenario (e.g. when fluxes are compared for samples measured at + 4 and + 23 ^{0}C), the difference in the ion flux estimate did not exceed 5% for all ions. Even more important is that these temperature changes affected only the magnitude of the net flux values, but not the time course of flux kinetics. Therefore, there was no effect of temperatures on the estimation of ACT and real critical temperature (RCT) values (crucial for this work, see Chapter 4.5).

3.8. Confounding effect of metabolic inhibitors on LIX sensitivity

Pharmacological approaches to "dissecting" underlying membrane-transport processes is a cornerstone of electrophysiology, and specifically patch-clamp studies

(Garrill and Davies, 1994; Ward, 1997). Various specific metabolic inhibitors or channel blockers were used in combination with the MIFE technique (Shabala et al., 2000; Tyerman et al., 2001; Shabala et al., 2001a, b; Shabala and Shabala, 2001). Some of them, however, might interfere with LIX in the microelectrode tip and significantly affect its selectivity, Nernst slope, or intercept (S. Shabala, personal comm.). This is further illustrated by Figure 3-9, where the effect of CCCP (a known protonophore) on K^+ LIX sensitivity is shown. It is obvious that LIX sensitivity was significantly reduced in the presence of 100 μM CCCP. The effect was reversible, and after CCCP was removed from the solution, electrode characteristics returned to normal.

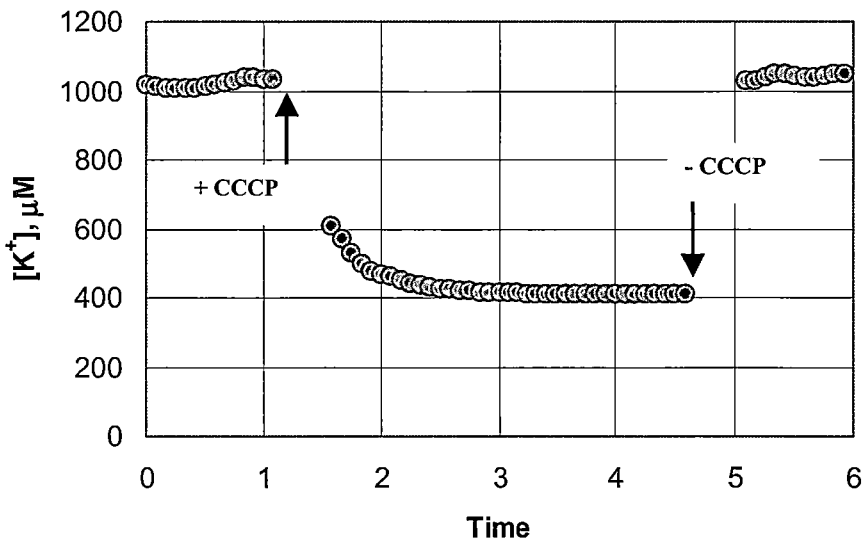

Fig. 3-9. Confounding effects of 100 μM CCCP on the sensitivity of the K^+ LIX. Potassium electrode was calibrated in the normal set of K^+ standards, and concentration measurements were undertaken using 1 mM KCl solution, with or without CCCP added.

By contrast, CCCP application had no effect on the sensitivity of H^+ LIX as indicated by absence of any pH changes after CCCP application (Fig. 3-10).

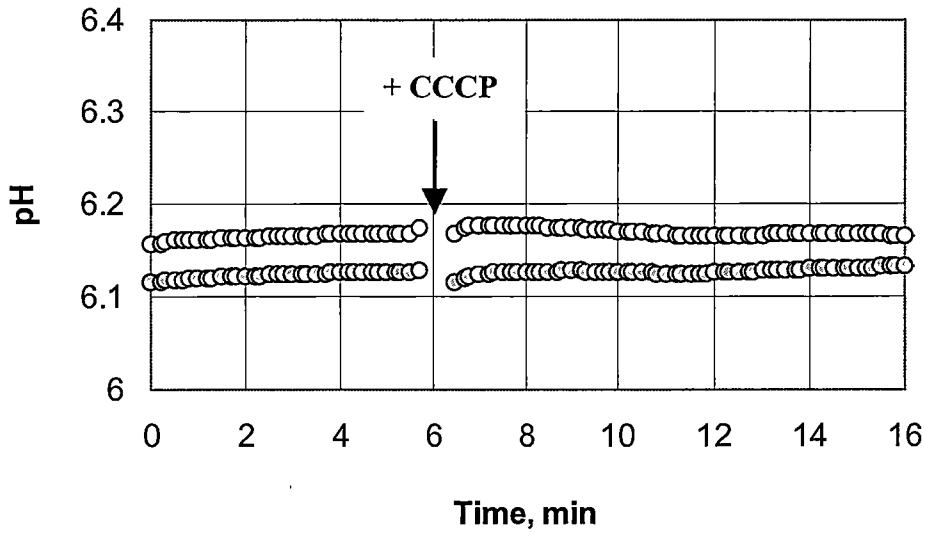

Fig. 3-10. Confounding effects of CCCP on the sensitivity of the H^+ LIX. Experimental solution N2 (Appendix A) containing 10 mM glucose was used. CCCP preparation is given in Appendix C. CCCP (final concentration 100 µM) was added to a chamber and solution mixed using a 5 mL pipette. Two replicates are shown.

The absence of confounding effect of DCCD application, a known inhibitor of H^+-ATPase, on both K^+ and H^+ LIX is illustrated by Figure 3-11 A and B, respectively .

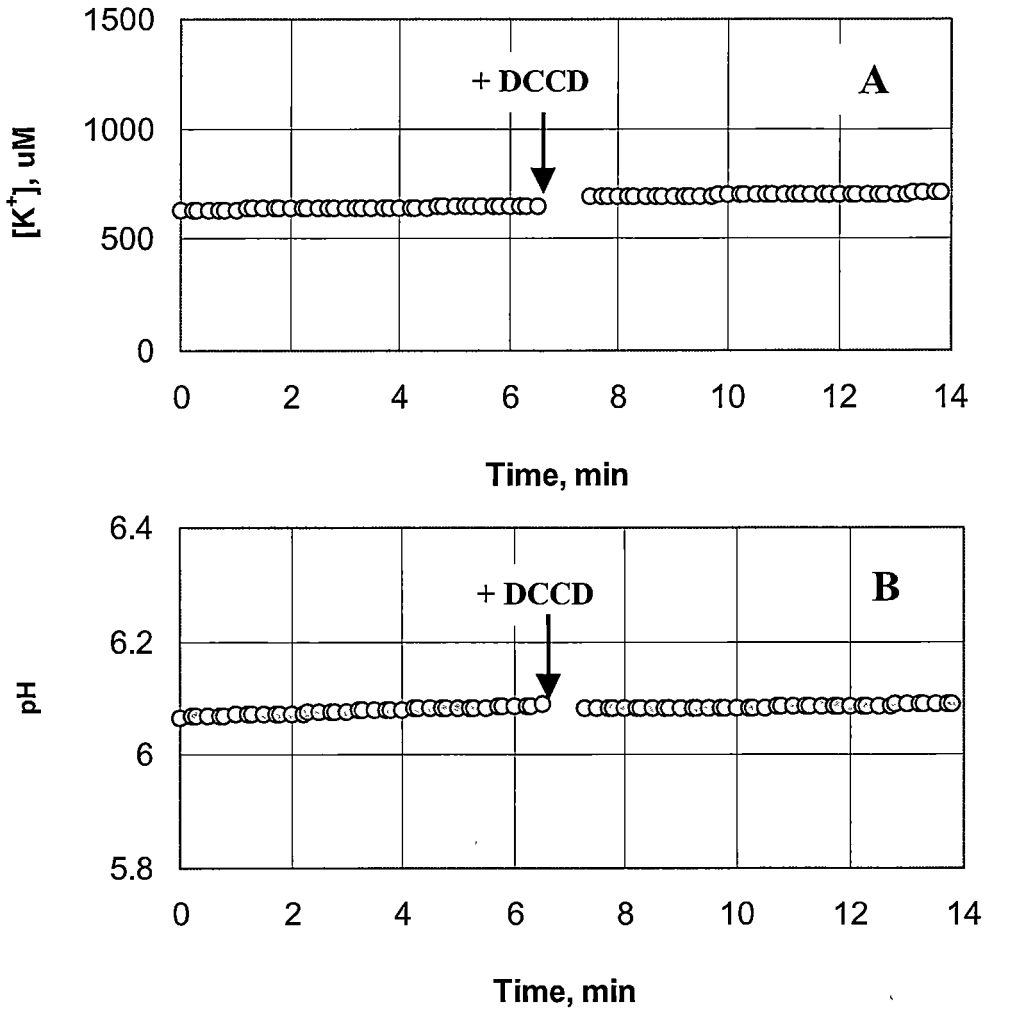

Fig. 3-11. Confounding effects of 100 μM DCCD on sensitivity of the K^+**(A)** and H^+ **(B)** LIX. Experimental solution N2 (Appendix A) was used. Procedures for preparation and application of DCCD is given in Appendix C. Arrow indicates application of 100 μM DCCD.

Overall, several specific metabolic inhibitors or channel blockers were used in this study. Of these, only CCCP was found to significantly modify LIX properties (Table 3-2). Due to high sensitivity of Ca^{2+} LIX to CCCP, calcium flux measurements were impossible in the presence of CCCP.

Table 3-2. Effect of metabolic inhibitors/channel blockers used in this study, on sensitivity and characteristics of various LIX.

LIX	Inhibitor/blocker			
	La^{3+}	*vanadate*	*CCCP*	*DCCD*
H^+	No effect	No effect	No effect	No effect
K^+	No effect	No effect	Correction factor required	No effect
Ca^{2+}	No effect	No effect	Application impossible	Not tested
Cl^-	No effect	No effect	Not tested	Not tested
NH_4^+	No effect	No effect	Not tested	Not tested

Chapter 4

APPLICATION OF THE MIFE TECHNIQUE TO STUDY MEMBRANE – TRANSPORT PROCESSES AT THE SINGLE CELL LEVEL: A CASE STUDY FOR THE THRAUSTOCHYTRID ACEM C

In this chapter, the feasibility of MIFE measurements in microbiology at the cellular level is demonstrated, using the marine protist ACEM C (a thraustochytrid) as an example. The major objective of this chapter was to demonstrate how the application of the MIFE technique might provide new, valuable information about physiological processes associated with the growth and adaptation of the thraustochytrid ACEM C, and to provide some insights into the underlying ionic mechanisms. Because of their ability to produce large amounts of polyunsaturated fatty acids (PUFA), thraustochytrids have recently attracted considerable attention as a potential single-cell source of these oils. A better understanding of thraustochytrid physiology might advance the biotechnology. Several specific issues were addressed in this study, particularly:

- Membrane-transport activity and ion flux kinetics associated with the cell cycle;
- Ion flux profiles over the plasma membrane surface and the issue of polarity in thraustochytrid ACEM C cells;
- Underlying ionic mechanisms and the functional role of ultradian membrane oscillations in thraustochytrid ACEM C cells;
- Membrane-transport processes associated with cell adaptation to hypoosmotic shock;
- Kinetics of post-chilling adaptation.

4.1. Thraustochytrids and their importance to food microbiology: an overview

4.1.1 Ecology and phylogenetic position

Thraustochytrids are unicellular, zoospore-producing species of non-photosynthetic marine protists characterised by the presence of a sagenogenetosome, an ectoplasmic net and a cell wall composed of non-cellulosic scales (Weete et al., 1997). Though originally classified as fungi, they are ultrastructurally closest to the labyrinthulids, which have often been treated as protozoa. Chamberlain and Moss (1988) suggested that the thraustochytrids should be placed in a group of their own and not assigned to the Saprolegniales as was done originally by Sparrow (1943) and subsequently by Dick (1973) and Gaertner (1977). The controversial taxonomic position of the thraustochytrids was clarified by genetic studies of the 18s rRNA (Cavalier-Smith et al., 1994), confirming earlier suggestions based on ultrastructure that thraustochytrids constitute a deeply divergent branch of the phylum Heteroconta, which is currently classified in the kingdom Chromista.

Thraustochytrids are abundant in waters and sediments of coastal areas and in estuaries, while populations of variable densities also occur in open ocean where they are major constituents of the marine mycoflora (Goldstein, 1963; Bahnweg, 1979; Miller and Jones, 1983; Raghukumar, 1992; Porter and Lingle, 1992). Thraustochytrids are a common component of the marine microbiota that have been associated with surfaces of organic substrates like algae, pollen, and seagrasses (Miller and Jones, 1983; Porter and Lingle, 1992). The role of thraustochytrids in marine ecosystems is poorly understood. Many reports suggest that they are involved in the decay of seaweed (Miller and Jones, 1983; Raghukumar et al., 1994 and ref. within). They may also disintegrate calcareous shells and carbonate rocks, thus remineralising the organic matter that comprises a significant portion of many marine sediments and coastlines (Porter and Lingle, 1992; Raghukumar, 1992).

4.1.2 DHA production

The ability of the thraustochytrids to produce docosahexaenoic acid [22:6(n-3)] (DHA) has recently attracted considerable attention in relation to the industrial application of long-chain polyunsaturated fatty acids (PUFAs).

PUFAs are important dietary constituents for humans (reviewed by Takahata et al., 1998). Their beneficial effects on human health are widely accepted and have thus led to extensive nutritional and clinical studies on their effects on human physiology (Dyerberg, 1986; Chilton et al., 1993; Takahata et al., 1998). These fatty acids have been utilised in the prevention and treatment of heart disease and high blood pressure, moderation of the inflammatory response (for example, treatment of asthma, arthritis and psoriasis) and some cancer treatments (Ward, 1980). DHA appears to be essential for normal growth and functional development of the brain and cornea (Connor et al., 1990).

Although DHA has been found in algae, fungi and bacteria of marine origin, their content of PUFA is generally very low (Iida et al., 1996). The largest commercial source of DHA is fish oil, which contains 7-14% DHA. In contrast, thraustochytrids produce up to 40% of DHA of the total fatty acids of the cells (Singh and Ward, 1996; Iida et al., 1996). In addition, there are several factors which encourage the use of organisms like fungi for lipid production. Fungi need limited space for cultivation, a short time to reach maximum lipid yield, and the growth cost is low (Farag et al., 1983).

The demand for oils and fats for industry or consumption is increasing annually. Thraustochytrids have already been used for commercial production of PUFA-rich products for human consumption and aquaculture feeding (reviewed by Lewis et al., 1999). They are also a potential substitute for fish oil in the world market and are expected to play an essential role in the future of the pharmaceutical industry (Lewis et al., 1999).

4.1.3 Adaptive responses

The physiology and nutrition of the thraustochytrids play a key role in understanding the ecology of this unique group of marine organisms. In spite of their significance, little is known in the area, and many important aspects of thraustochytrid physiology are yet to be revealed. The recently recognised importance of the thraustochytrids for biotechnology should sharpen the interest towards the understanding of the physiology of their growth, the mechanisms of

transport processes and their obvious effect on growth. A large number of variables affect production of fatty acids (FAs), including medium composition (Farag et al., 1983; Bajpai et al., 1991; Li and Ward, 1994; Singh and Ward, 1996; Iida et al., 1996), nutrient starvation (Peberdy and Toomer, 1975), FA precursor addition (Radwan and Soliman, 1988), pH (Iida et al., 1996), temperature (Neidelman, 1987), light intensity (Cohen et al., 1987) and oxygen supply (Davies et al., 1990). To date, all the improvements in DHA production in thraustochytids have been made by empirical medium optimisation, a lengthy and often unproductive way of dealing with the problem. A better understanding of the physiology of this protist might open some alternative ways for biotechnological optimisation.

In this Chapter the MIFE technique is applied to study membrane-transport processes in thraustochytrid ACEM C associated with the cell cycle and adaptive responses to key stress factors.

4.2. Membrane-transport activity and ultradian ion flux oscillations associated with cell cycle

The life-cycle of the thraustochytrids is poorly understood (Chamberlain and Moss 1988). In this Chapter findings on membrane transport activity associated with growth and nutritional status of thraustochytrid cells are reported. Thraustochytrid ACEM C was grown as described in Chapter 2.1.1. Culture preparation and immobilisation for MIFE measurements are described in Chapter 2.2.2. The experimental solution for thraustochytrids (Appendix A) was used for the MIFE measurements. The procedure of microelectrode preparation, MIFE measurements and data analysis used are given in Chapters 2.3 and 2.6.

A pharmacological study using sodium orthovanadate (referred here as vanadate), a known inhibitor of PM H^+-ATPase (Cid and Serrano, 1988; Davies et al., 1990; Kollmann and Altendorf, 1993), was performed. After 10 min of H^+ flux measurements at the surface of a thraustochytrid cell, an aliquot of vanadate stock solution (Appendix B) was added to a measuring chamber to give the final concentration of 1 mM. Experimental solution in the chamber was mixed by suction and ejection using a pipette. The H^+ flux measurements from the same cell were continued for a further 30 min.

Net fluxes of H^+, Ca^{2+}, and Na^+ were monitored as the cell progressed from the zoospore to sporangium stages of development. A change of membrane transport activity associated with cell growth and development, the topography of net H^+ fluxes over the thraustochytrid cell surface, and the possible association between cell development and ultradian oscillatory activity in membrane-transport processes are discussed.

4.2.1 Morphology and growth stages of thraustochytrid ACEM C

The typical mature thraustochytrid cell has a cytoplasm filled with multiple oil globules and therefore appears to be granular (Fig. 4-1).

The cells are heterogeneous in size and appearance, with diameters ranging from about 6 to 50 μm, depending on the age and stage of development. The

thraustochytrids reproduce asexually by laterally heterokont zoospores formed during the progressive cleavage of the cytosol (Moss 1985; Iida *et al.* 1996).

No standard classification of thraustochytrid growth stages is accepted. For convenience, a five-stage scale is used in this study illustrated in Figure 4-1.

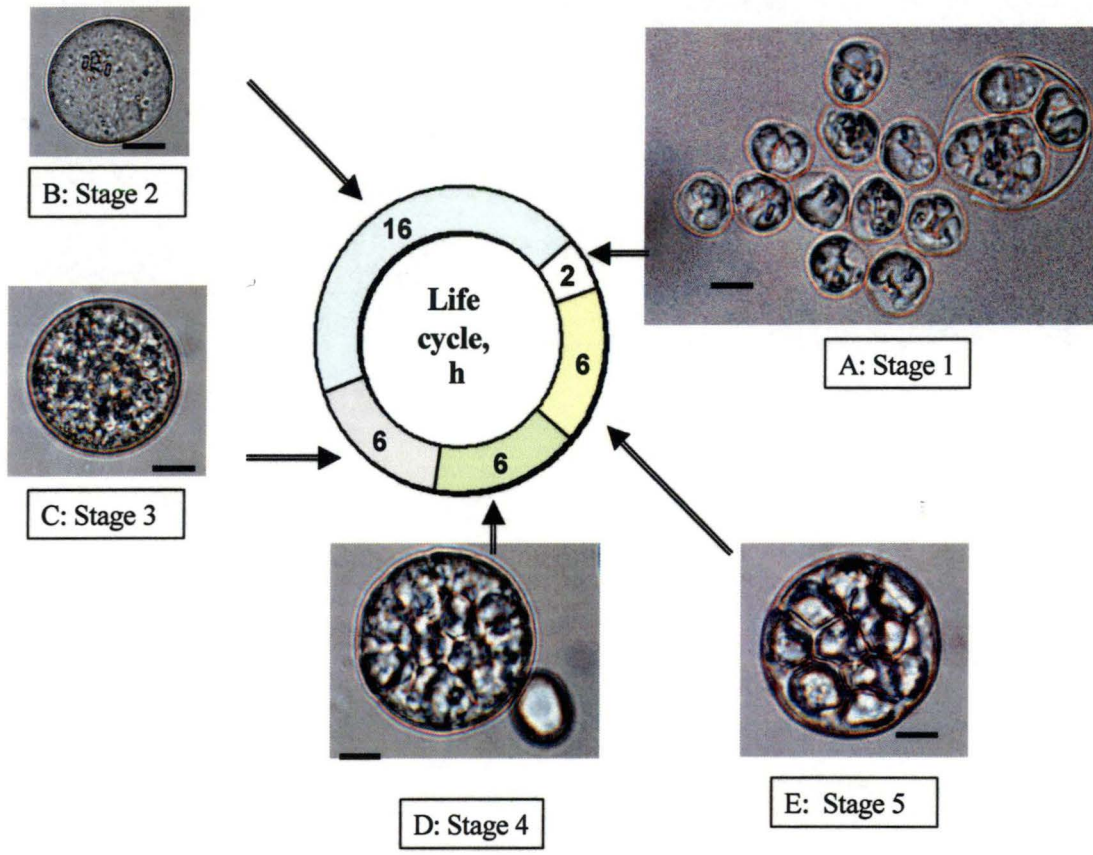

Fig. 4-1. The life cycle of the thraustochytrid ACEM C and a five-stage time scale employed in this study. *A* to *E* show the consecutive stages of cell development from the zoospore to the sporangium. More details are given in the text. The bar is 10 μm.

(1) The zoospore stage (Fig. 4-1, *A*). Due to the relatively small zoospore size (typically 6 to 12 μm), simultaneous measurements of several ions from the same zoospore were not feasible.

(2) The zoospore becomes quiescent. The cyst is formed and gradually enlarges to form the sporangium (Fig. 4-1, B).

(3) The granular structure of the sporangium becomes evident (Fig. 4-1, C). Oil droplet formation starts, and cell wall formation is also in progress.

(4) The number of oil bodies increases. The thallus continues to expand, and a thick capsular wall forms around the sporangium. The formation of cleavage line begins (Fig. 4-1, D).

(5) Cleavage lines delimiting the individual planonts become evident (Fig. 4-1, E). This process is then followed by the disruption of the cell wall and discharge of zoospores into the medium (Fig. 4-1, A).

In total, the life cycle of the thraustochytrid ACEM C was quite variable and lasted from 28 to 40 h (depending on nutritional status and aeration conditions). These times are consistent with other reports (Goldstein, 1963). Net ion fluxes were measured for stages 2 to 5, respectively, in this study.

4.2.2. Membrane transport activity associated with cell growth and development

As the cells progressed in their development from the zoospore to the sporangium stages (Fig. 4-1), regular changes in the activity of ion transport across the plasma membrane (PM) were evident. For all ions measured (H^+, Na^+, and Ca^{2+}), there was a significant ($P < 0.01$ for H^+ and Na^+ and $P < 0.05$ for Ca^{2+}) decrease in the net influx of these ions into the cell (Table 4-1) associated with cell aging.

Table 4-1. Average fluxes of H^+, Na^+, and Ca^{2+} (nmol m^{-2} s^{-1}) measured from the surface of thraustochytrid ACEM C associated with cell aging. Results are mean ± SE. The sample size is indicated in brackets.

Growth stage	Net H^+ flux	Net Na^+ flux	Net Ca^{2+} flux
Stage 2	48.7 ± 5.5 (42)	196 ± 22 (42)	16.2 ± 2.2 (20)
Stage 3	23.7 ± 6.1 (55)	115 ± 31 (55)	13.2 ± 9.2 (16)
Stage 4	9.2 ± 6.9 (56)	99 ± 38 (56)	8.6 ± 5.6 (22)
Stage 5	1.4 ± 6.1 (36)	22 ± 36 (36)	6.1 ± 3.3 (18)

However, even within the same variant (e.g. for cells at the same developmental stage), there was a wide variation in both the magnitude and direction of the net ion movement. Generally, the ion flux distribution within the variant was close to normal. Data for net H^+ fluxes are illustrated in Fig. 4-2A.

The possible reasons for such variability are discussed in the following sections of this Chapter.

Without exception cells at stage 2 exhibited net H^+ uptake. However, as the development progressed, fewer cells took up hydrogen ions. At stage 5, more than 60% of the cells exhibited net H^+ efflux (Fig. 4-2, B). Similar regularities were found for other ions measured (Ca^{2+} and Na^+; data not shown).

Interpretation of the H^+ flux data is always complicated by the large number of potentially contributing mechanisms. Both biochemical (fluxes of CO_2 or bicarbonate, or weak acid extrusion) and biophysical (PM hydrogen transporters) mechanisms could be involved. However, there are several lines of evidence suggesting that in our case the observed net H^+ fluxes may originate essentially from the activity of PM H^+-ATPase. First, Garrill and co-workers (1992) showed that such a pump does exist at the PM of *Thraustochytrium* sp. and plays a key role in nutrient transport into the cell. Second, experiments with photosynthesising plant tissues suggested that fluxes of bicarbonate or CO_2 occur much more quickly and do not produce pronounced pH gradients in the proximity of living tissue (Shabala and Newman, 1999). Third, net H^+ efflux in thraustochytrid was significantly suppressed by 1 mM vanadate, a specific inhibitor of H^+-ATPase (see Fig. 4-12).

Therefore, it would be reasonable to suggest that the measured net H^+ fluxes were at least partially attributable to the activity of the PM H^+-pump.

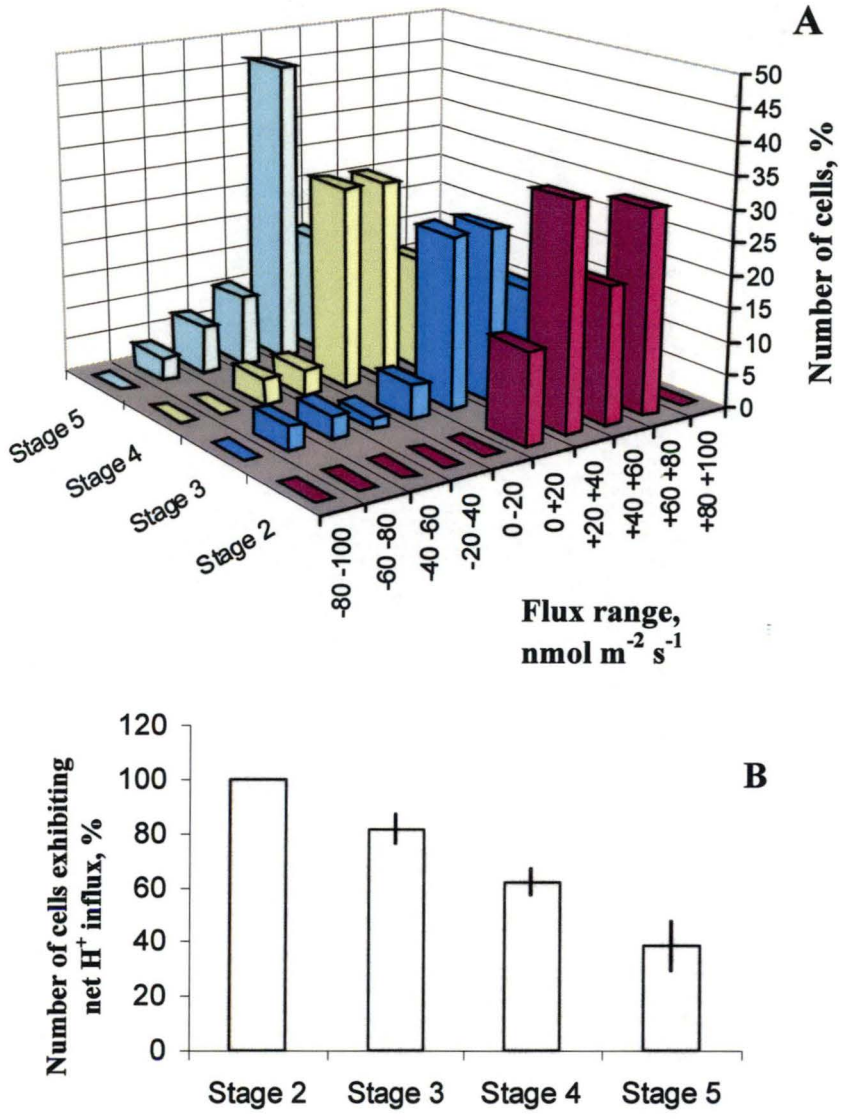

Fig. 4-2. A - Net H^+ flux distribution within variants as a function of growth development. The flux values for each individual cell were grouped into 20 nmol m^{-2} s^{-1} intervals, and the total number of cells was plotted as a function of the median flux value. A clear shift towards net H^+ efflux as cells aged towards stage 5, as well as a wide flux variation within the same variant, are seen. **B** – a histogram showing progressive decrease in a number of cells exhibiting net H^+ influx at the thraustochytrid ACEM C plasma membrane as cells progressed from the zoospore to the sporangium stages of development. Results of measurements of 174 individual cells (4 batches of 10 to 12 replicates x 4 different stages of growth in each) are shown. Data are mean ± SE (n = 4 is the number of batches).

Recent findings show that plasma membrane transporters play a crucial role in fungal hyphal extension in many species (Lew, 1998). It was also hypothesized (Van Brut and Harold, 1980) that univalent cations may trigger encystment and germination of *Blastocladiella* (water mould) zoospores and, therefore, control the developmental processes in this species. Of particular importance seem to be hydrogen ions (Bachewich and Heath, 1997). Changes in internal pH have been implicated in the control of cellular differentiation in *Dictyostelium* (Gross et al., 1983; Jamieson et al., 1984), germination of yeast ascospores (Barton et al. 1980), and control of starvation and refeeding in *S. cerevisiae* (Den Hollander et al., 1981). Germ tube formation in *Candida albicans* was associated with dramatic alkalinization of the cell cytosol (Stewart et al., 1988). Here a significant shift towards net H^+ efflux is reported (in more than 60% of the total cell number; Fig. 4-2B), likely to lead to cytosol alkalinisation, associated with sporogenesis in thraustochytrid ACEM C.

One possible explanation to the observed correlation between net ion flux value and cell developmental stage may be the changing thickness of the cell wall (acting as a barrier for ion diffusion). However, even within the same variant (for cells of the same age and, therefore, the same wall thickness), there was wide variation in net H^+ fluxes measured in the range of –100 to +100 nmol m^{-2} s^{-1} (Fig. 4-2A). Therefore, it is more reasonable to suggest that the progressive decrease in average H^+ flux value (Table 4-1) has physiological origins.

Mechanisms of pH control over the cell cycle are still elusive. At least two possible components may be suggested. One is the pH regulation of the cytoskeleton. It is known that several actin-binding proteins (e.g. myosin) are pH-sensitive (Bachewich and Heath ,1997). Those authors reported that acidification of the cytosol in *Saprolegnia* caused growth inhibition which was accompanied by changes in positioning and morphology of mitochondria and nuclei, condensation of chromatin, and disruption in peripheral actin. Raising the cytosolic pH could also affect cytoplasmic gelation, actomyosin contraction, actin filament cross-linking and signal transduction by cGMP (Jamieson et al., 1984 and refs within). It is reasonable

to assume that both karyokinesis and cytokinesis require significant rearrangement of cytoskeleton assembly (Moss, 1985).

Another possibility is pH control over cell wall degradation. It is known that the thraustochytrid cell wall is of variable thickness, depending upon the stage of development (Goldstein, 1963; Moss, 1985). It is usually very thin in newly formed zoospores and is progressively transformed into the multilamellate structure in the older cysts before it begins to disappear in the fully cleaved sporangium. In higher plants, recent findings suggest that cell expansion is strongly dependent on cell wall loosening controlled by a special group of enzymes called expansins (Cosgrove, 1998). Such expansins are known to exhibit an acidic pH optimum and, therefore, their activity could be controlled by H^+ extrusion from the cell. A similar scenario might take place in thraustochytrid at the later stages of organism development facilitating the breakage of the cell wall and resulting in zoospore release.

The functional role of other ions is less clear. It is known that thraustochytrids require sodium as an essential element (Jennings, 1983; Garrill et al., 1992). A progressive decrease in net Na^+ uptake with cell aging observed (Table 4-1) may therefore be partially explained by the diminishing requirements for this ion at the later stages of development.

Calcium is considered to be a ubiquitous second messenger in both the plant and animal tissues (Bush, 1993). Calcium gradients were found to be essential for hyphal growth (Hyde and Heath, 1997) and regulation of hyphal branch induction (Grinberg and Heath, 1997) in *Saprolegnia*. There is also some evidence of Ca^{2+} control over H^+ transport in microorganisms (Giraldez-Ruiz et al., 1999). Therefore, the observed changes in net Ca^{2+} fluxes across the PM of thraustochytrid ACEM C (Table 4-1) may be associated with a signalling role in organism development.

4.2.3 Topography of net ion fluxes

There are many reports that polar growing cells show asymmetric location of ion transporters, including those for Ca^{2+} and H^+ (Jaffe, 1980; Levina et al., 1995; Bachewich and Heath, 1997; Lew, 1998). A complex mosaic of ion flux topography over the surface of corn coleoptile protoplasts has been shown by Shabala et al.

(1998). To explain the large variability of measured net ion fluxes within the same variant (from –100 to + 100 nmol m^{-2} s^{-1} for H^+; Fig. 4-2A), it was hypothesized that thraustochytrid cells may possess a polarity.

To test this hypothesis, net H^+ fluxes from opposite sides of individual thraustochytrid cells were measured simultaneously. In total, about 60 cells, at stage 3 and 4, were studied. The H^+ flux ratio distribution had a normal character (Fig. 4-3). The median value of about 0.9 (trend line slope in Fig. 4-4) could probably be explained by methodological problems of electrode positioning.

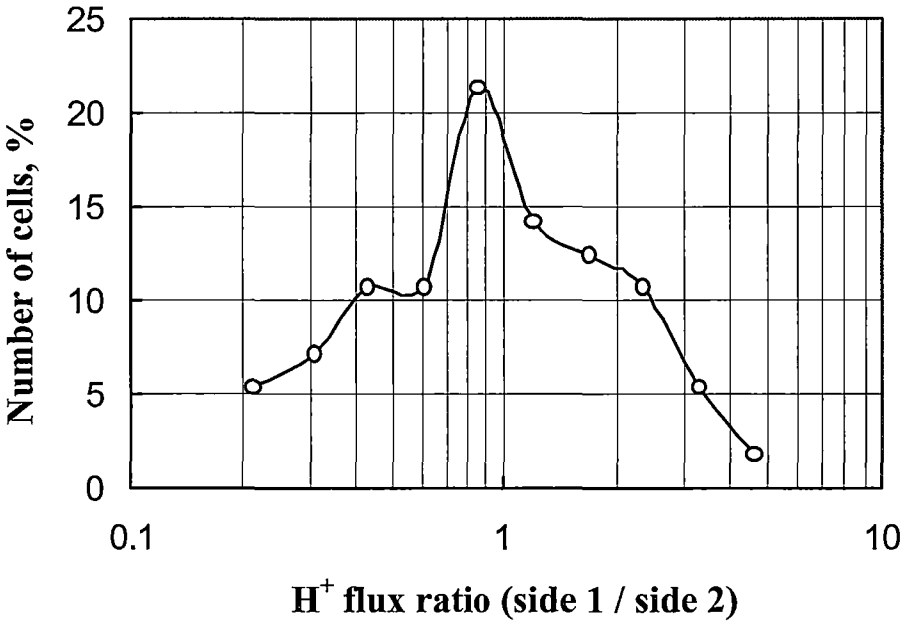

Fig. 4-3. Topography of ion flux profile over the cell surface. Net H^+ fluxes were measured from opposite sides of the cell, and the frequency distribution was then plotted.

The absence of polarity to a spherical shape of a thraustochytrid cell may indicate an equal expansion of the cell surface during growth. However, about 10% of the measured cells had oppositely directed fluxes (e.g. net H^+ influx on one side and net H^+ efflux on the opposite site) as illustrated in Fig. 4-4 (filled symbols). Therefore, although in the majority of measured cells pronounced polarity was absent, it is possible that such polarity may appear at the later stages and be

associated with the spatial positioning of the place where zoospores are then released. Perhaps the 10% of the cells possessing opposite H^+ fluxes might be more advanced in their development compared to the majority of the cells studied (stages 3 and 4).

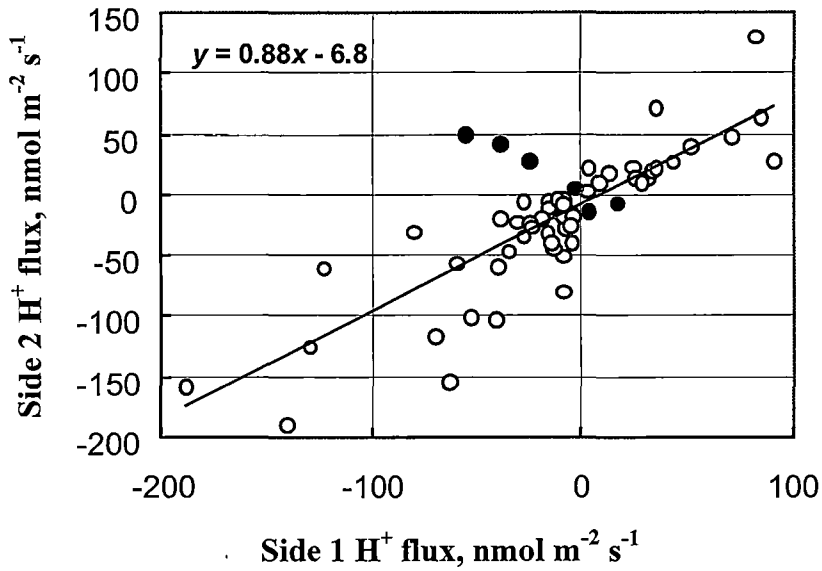

Fig. 4-4. The stoichiometry between net H^+ fluxes on opposite sides of individual thraustochytrid cells. Each point represents a measurement from one individual cell (stages 3 and 4). Filled symbols indicate cells exhibiting oppositely directed net H^+ fluxes.

Other evidence supporting the possibility of polar ion transport in thraustochytrid ACEM C is that the kinetics of flux changes could be strikingly different when measured from two different sides of the cell (Fig. 4-5).

In the example shown in Fig. 4-5, net H^+ fluxes from opposite sides of seven individual cells were measured (denoted as #). Cells #1 and #7 showed steady fluxes of H^+, of the same magnitude, when measured from opposite sides (no "polarity"). Cells #4 and #6 showed different mean H^+ flux values, but the kinetics of their changes were similar. Finally, in cells # 3 and # 5, fluxes on opposite sides of the cell were behaving independently (steady fluxes at one "pole", open symbols, and oscillating fluxes at the other "pole", closed symbols). Therefore, although not

polarity in the classical sense, at least independent activity of plasma membrane transporters does occur in thraustochytrid ACEM C cells.

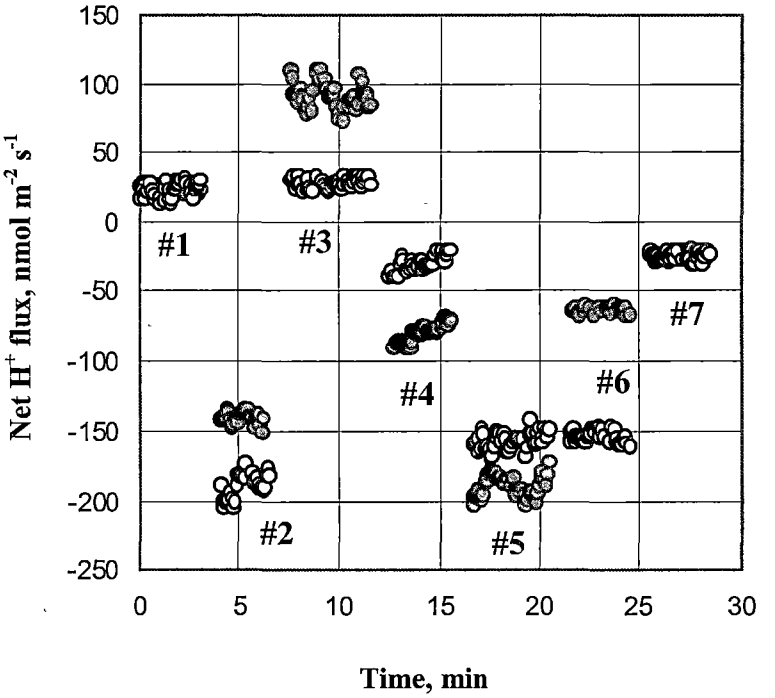

Fig. 4-5. Experimental evidence for asymmetric location and/or activity of ion transporters at the plasma membrane of thraustochytrid ACEM C. In this example, net H^+ fluxes were measured from opposite sides (open and closed symbols, respectively) of seven individual cells (denoted as #). Note the different (asynchronous) flux kinetics for cells ## 3 & 5.

4.2.4 Ultradian oscillations in net ion fluxes across the plasma membrane

Ultradian oscillations are believed to be crucial for the synchronization and coordination of spatially separated physiological processes (Lloyd and Kippert, 1993) as well as for the separation of incompatible processes within the same cell compartment (Rapp, 1987). Theoretical models show that oscillatory control is more accurate, stable and noise-immune than analog control (Rapp et al., 1981) and may provide increased energy efficiency in various biochemical systems (Termonia and Ross, 1982). Propagation of oscillatory signals is postulated to be central to

morphogenetic processes providing positional information for cell aggregation and differentiation (Gross, 1975).

Despite this, the role of rhythmical processes in plant and fungal physiology has always been underestimated. Most of the above mentioned papers are theoretical in nature. Experimental evidence is not as abundant, and most of it is relevant at the population level, not that of individual cells. Even then, most studies deal with diurnal or circadian rhythms in membrane-transport activity. Ultradian oscillations have always been treated as "Cinderellas". Experimental data reporting a causal link between cell ultradian oscillations in membrane-transport activity and growth, adaptation, or morphogenesis of the single cell organism are lacking.

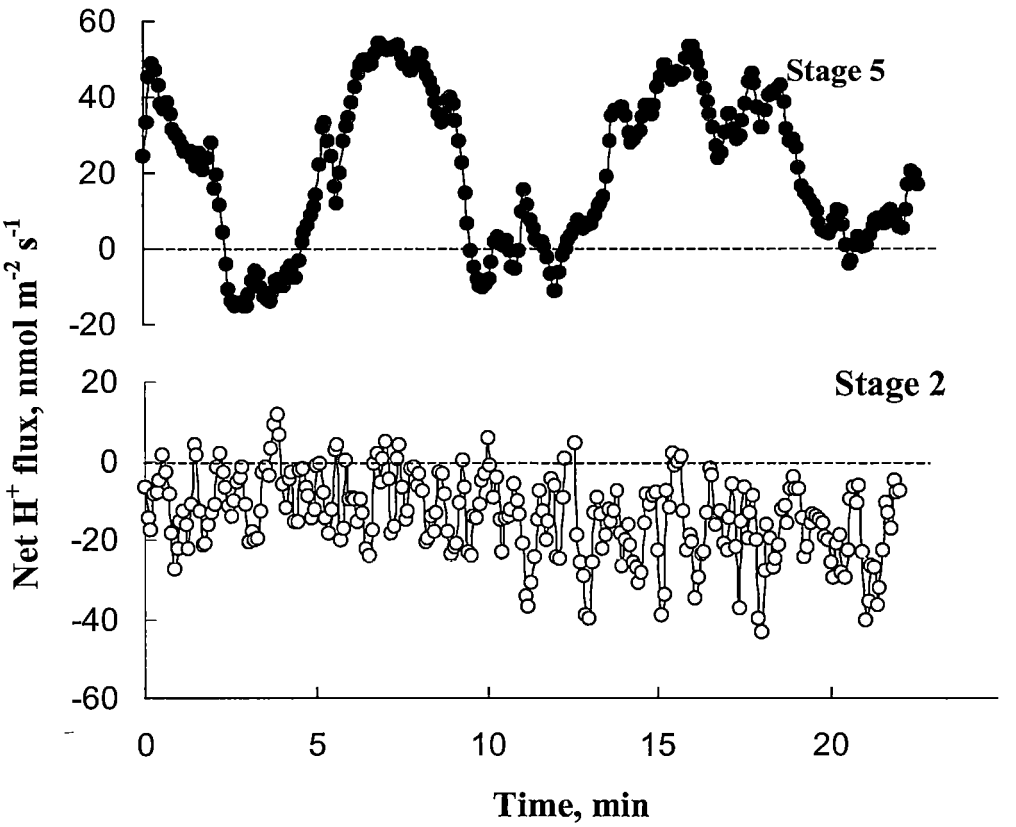

Fig. 4-6. Ultradian oscillatory activity in membrane-transport processes at the plasma membrane of thraustochytrid ACEM C. A typical example of endogenous H^+ flux oscillations (dark symbols) for cell at the stage of sporangium (stage 5). No oscillations are evident for immature cells at stage 2 (open symbols).

Ultradian oscillations (minute range of periods) in net ion fluxes measured non-invasively near the cell surface of thraustochytrid cells were observed in this study. A typical example of such oscillations for net H^+ flux is shown in Fig. 4-6 (upper trace).

Such oscillatory activity was characteristic for mature cells at advanced stages of their development. For example, only 10% of the total cell number exhibited ultradian H^+ oscillations when measured at stage 2. This number progressively increased as cells aged, and at the last stage as many as 85% of cells possessed oscillatory activity (Table 4-2).

Table 4-2. Correlation between the developmental stage of thraustochytrid ACEM C and number of cells exhibiting rhythmical activity.

Growth stage	*Cell number, %*
Stage 2	10.1 ± 0.7
Stage 3	14.4 ± 2.9
Stage 4	54.6 ± 6.8
Stage 5	85.5 ± 1.5

Collated data represents results of measurements of 174 individual cells (4 batches of 10 to 12 replicates x 4 different stages of growth in each). Results are mean ± SE (n = 4 is the number of batches).

The period range of ultradian ion flux oscillations was typically 6 to 10 min for cells measured in low Na^+ solution (1 mM) (Fig. 4-7). These oscillations were undoubtedly of endogenous nature as Fourier analysis revealed no oscillatory harmonics for the majority of cells at earlier stages of their development when measured under the same experimental conditions (Fig. 4-6, open symbols). Based on these data, it is suggested that ultradian ion flux oscillations in thraustochytrid ACEM C may be causally linked with cell developmental processes.

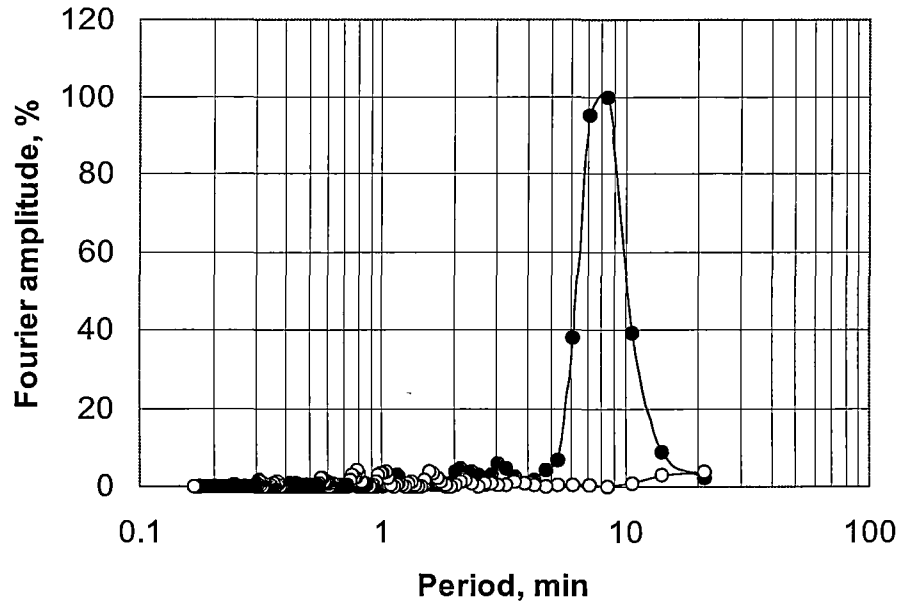

Fig. 4-7. Discrete Fourier Transform for two traces shown in Fig. 4-6. A clear resonant peak at about 8 min is seen for developmentally advanced cell (closed symbols) while a typical "white noise" is characteristic for immature cells (open symbols).

Ultradian oscillations in the minute range of periods have been found in a large number of microorganisms. The best known are oscillations in glycolysis (Lloyd and Stupfel, 1991; Wang et al., 1998) reported for many yeast and fungi species. Other examples may include energy-yielding processes, protein turnover, motility and the timing of the cell division cycle processes (Jenkins et al., 1989; Lloyd and Stupfel, 1991; Lloyd and Rossi, 1992; Kippert and Lloyd, 1995; Kippert, 1996). As for membrane-related oscillations, there are reports on rhythmical changes in cell membrane potential (Gradmann and Slaymann, 1975; Brownlee, 1984; Slaymann et al., 1976; Gradmann and Boyd, 1995), but (to my knowledge) no direct evidence of rhythmical ion exchange similar to that reported in this study. However, as the period range reported elsewhere is very consistent with the observations reported here, it is very likely that the above mentioned oscillations in the membrane potential (MP) were caused by rhythmical activity of ion transporters at the cell plasma membrane.

4.2.5 Ionic basis for ultradian membrane oscillations in thraustochytrid ACEM C

As most of the ion transporters located at the PM are coupled via membrane potential (Gradmann and Buschmann 1997), it comes as no surprise that rhythmical changes in the activity of one of these transporters may cause oscillatory flux patterns for other ions. This is illustrated in Fig. 4-8 where fragments of endogenous ultradian oscillations in net H^+, Na^+, and Ca^{2+} fluxes are shown.

As discussed in the above sections, membrane transport activity of thraustochytrid cells was quite variable in terms of the absolute flux values. Also, ion flux oscillations are usually very far from being harmonic. Altogether, that was expected to result in significant variations in the periods and the absolute values of oscillatory harmonics between different cells and therefore to complicate their interpretation.

A unique advantage of the MIFE system used for ion flux measurements in this study is its high temporal resolution (5 sec) and the ability to measure fluxes of several ions in the same experiment and essentially in the same site (the maximum distance between electrode tips did not exceed 8 μm). With this experimental design, even small deviations in the resultant Fourier spectra for different ions (measured simultaneously) may be considered significant.

Discrete Fourier Transform (DFT) spectra for H^+, Na^+, and Ca^{2+} flux oscillations are shown in Figure 4-9.

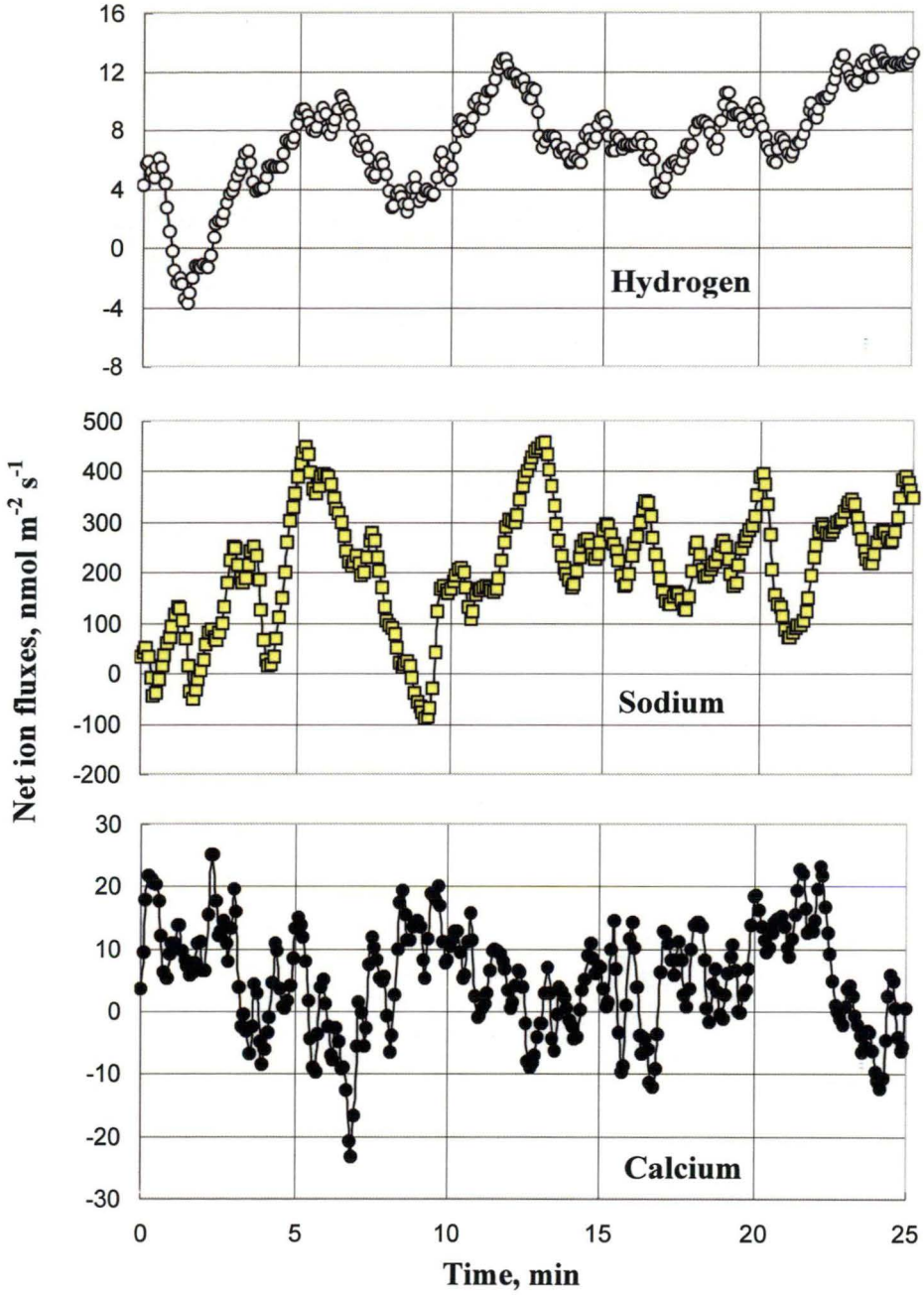

Fig. 4-8. Fragments of endogenous ultradian oscillations in net H^+, Na^+, and Ca^{2+} fluxes measured concurrently from the same thraustochytrid ACEM C cell. One representative example (out of 12) is shown (stage 5 of growth). The raw data were collected at 5 sec intervals and then smoothed by low pass filtering (0.05 Hz) using SANTIS software.

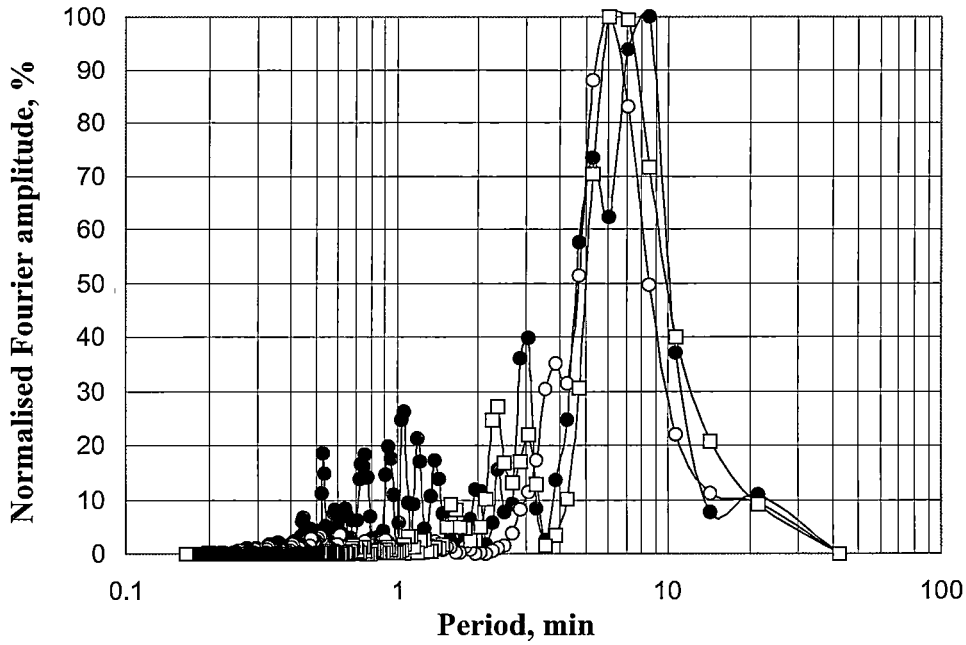

Fig. 4-9. Normalised DFT spectra for H^+ (O), Na^+(□), and Ca^{2+} (●) flux oscillations shown in Fig. 4-8. It appears that both H^+ and Na^+ ions have the same major peak at 6.1 min while for Ca^{2+} this value was shifted to 8.5 min period. Additional peaks at about 1 min and 3 min period are also evident for Ca^{2+} flux oscillations.

It appears that both H^+ and Na^+ ions have the same major peak at 6.1 min while for Ca^{2+} this value was shifted to 8.5 min period. Although rigorous statistical analysis was not possible, there is much evidence to suggest this difference is significant. One of the strongest arguments *pro* is the fact that in most of the cells studied the major resonant harmonic for Ca^{2+} flux oscillations was always shifted towards the longer period by 1.5 to 3 min compared with that for H^+, regardless of its modal value (data not shown). Also, additional resonant components at about 1 min and 3 min are also seen in the Ca^{2+} spectrum (Fig. 4-9, dark circles). The latter is not an artifact of the measuring system as DFT of Ca^{2+} flux for cells not-exhibiting ultradian oscillatory activity (at stages 2 or 3) was typical "white noise" similar to that reported for H^+ in Fig. 4-6 (data not shown). H^+ and Na^+ flux oscillations may be mediated by the same transport mechanism, while oscillations in the net Ca^{2+} flux are likely to be attributed to another physiological process. Further support for this suggestion is given by cross-correlation analysis of ion flux oscillations (Fig. 4-10).

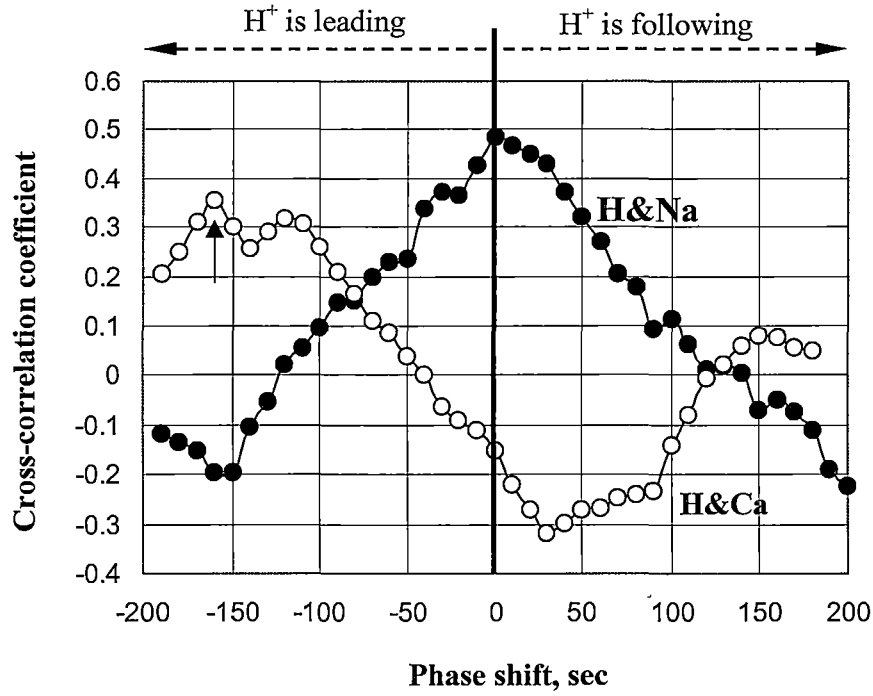

Fig. 4-10. Cross-correlative analysis of ultradian ion flux oscillations shown in Fig. 4-9. The cross-correlation coefficient (CCC) for variable pairs (H^+ & Na^+; H^+ & Ca^{2+}; Na^+ & Ca^{2+}) was calculated for different phase shifts between two data series ranging between –200 and +200 sec with 10 sec increments. The CCC-values were then plotted against the phase shifts, and the maximum values of the cross-correlation coefficient (ρ_{max}) and the corresponding phase shifts (φ_{max}) were determined (shown as an arrow for H^+ & Ca^{2+}). It was demonstrated that H^+ was the leading ion.

The maximum correlation between H^+ and Ca^{2+} flux oscillations occurred when fluxes were shifted by about 2.5 min (H^+ is leading; Fig. 4-10, open symbols). At the same time, the phase shift between H^+ and Na^+ flux oscillations is zero. The difference in the values of cross-correlation coefficients for H^+ & Na^+ and H^+ & Ca^{2+} pairs is statistically significant at $P = 0.01$ level (Fig. 4-11).

Shabala et al. (1997) also reported a phase shift of about 1.5 min between Ca^{2+} and H^+ flux oscillations in corn root which was attributed to protonation of the cell wall and displacement of Ca^{2+} by hydrogen ions as a result of the Donnan interaction. However, in that case Ca^{2+} flux oscillations were leading and oscillatory

periods for both ions were the same. Here the correlation between two of these ions is negative (Fig. 4-11), and oscillations have apparently different periods. Therefore, the involvement of the cell wall is excluded and the Ca^{2+} flux oscillations are attributed to some (still unidentified) cellular process. This question will require further studies using a pharmacological approach.

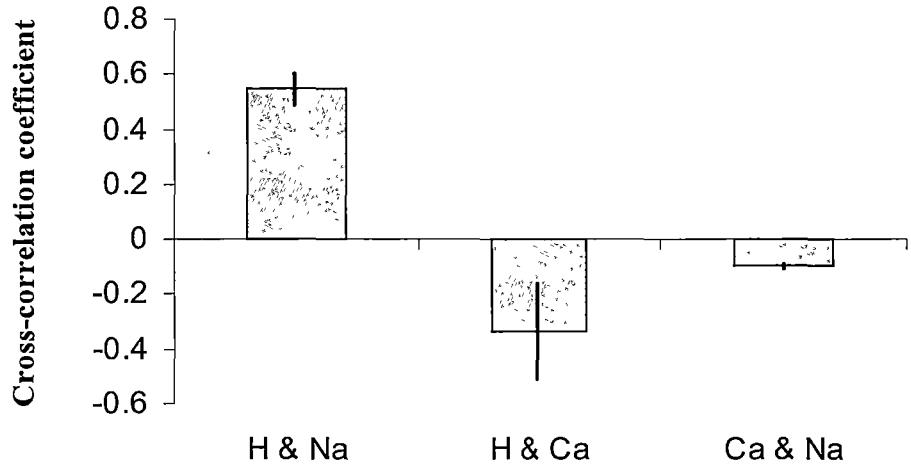

Fig. 4-11. Average CCC-values for $\Delta\varphi = 0$. Error bars are SEM (n = 4 to 7). Significant positive correlation between H^+ and Na^+ flux oscillations is evident.

By contrast, oscillations of H^+ and Na^+ flux seem to be tightly coupled (Figs. 4-10, 4-11). Several possibilities might explain their origin.

(1) It could be that net H^+ flux oscillations are caused by oscillatory activity of an H^+-pump. Such an idea was put forward by Gradmann and Slayman (1975) to explain membrane potential oscillations found in a *Neurospora poky* mutant. A similar conclusion was made from the study of pH effects on ion flux oscillations in corn roots (Shabala et al., 1997). Following that scenario, Na^+ flux oscillations might be driven simply via membrane voltage. If membrane coupling operates within the time frame of ≤1 sec, the temporal resolution of the MIFE system (5 sec) is inadequate to distinguish between these two processes. Additional evidence supporting the possible involvement of the H^+ pump as a potential source of cell rhythmical activity comes from concurrent measurements of the net H^+ fluxes during patch-clamp studies of protoplasts isolated from wheat roots (Tyerman et al., 2001).

In the latter study, half the protoplasts measured were reported to possess rhythmical activity lasting up to 5 h. Measured in the current-clamp mode, the resting potential (RP) oscillated between -160 and + 40 mV with period from 10 to 60 min without significant changes in the IV–curve slopes and, therefore, channel conductance. These RP oscillations were accompanied by significant (amplitude up to 200 nmol m^{-2} s^{-1}) oscillations in the net H^+ flux from the protoplast surface.

If H^+-pump activity is central to ion flux oscillations, the ultradian H^+ flux oscillations should be strongly affected by known inhibitors of H^+-ATPase activity. However, 1 mM vanadate had no apparent effect on net H^+ flux oscillations within one hour of being added in the bath medium (Fig. 4-12, open symbols).

Net Na^+ flux oscillations were also not affected significantly (data not shown). At the same time, vanadate almost completely suppressed the cell's ability to respond to temperature variations (see Fig. 4-26, Chapter 4.6) indicating its efficient control over H^+-ATPase activity in thraustochytrid ACEM C. It was concluded that the observed ultradian ion flux oscillations in thraustochytrid cells are vanadate-insensitive and not likely to originate from the oscillatory activity of the plasma membrane H^+-ATPase pump.

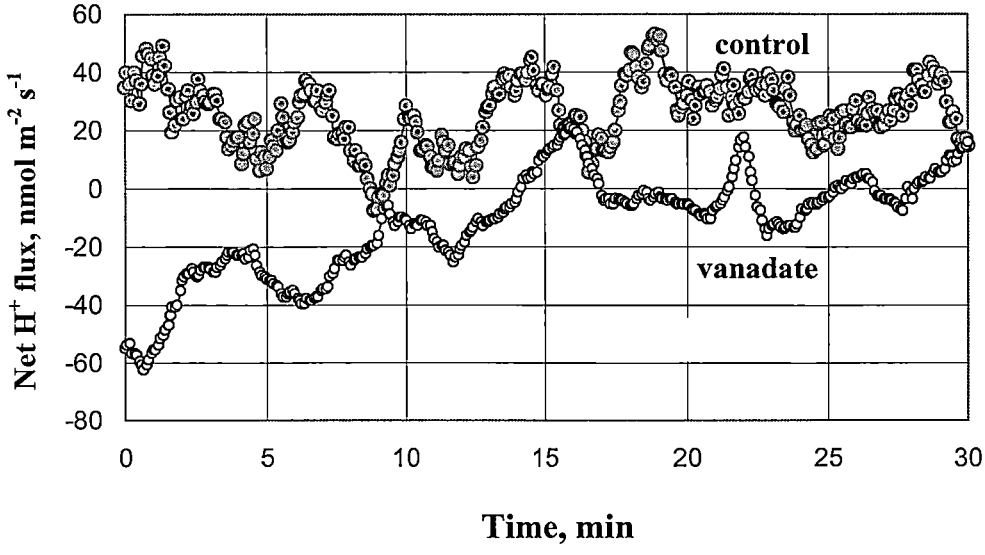

Fig. 4-12. Effect of 1 mM orthovanadate (a known inhibitor of plasma membrane H^+-ATPase) on net H^+ flux in thraustochytrid ACEM C. Fragments of ultradian H^+ flux oscillations before (closed symbols) and 30 min after (open symbols) vanadate treatment.

(2) Observed oscillations might be a consequence of rhythmical activity of the Na^+/H^+ co-transport system.

Sodium is considered an essential element for thraustochytrid growth and it is therefore present in the cytosol of thraustochytrid cells in large quantities (between 30 and 50 mM; Garrill *et al.* 1992). For the experimental conditions described (1 mM Na^+ in the bath), the Nernst potential for sodium E_{Na} is therefore between –85 and –100 mV. The membrane potential of thraustochytrid ACEM C cells was in the range –60 to –80 mV. In such conditions, passive Na^+ uptake is not possible. Nonetheless, net Na^+ influx was measured in all experiments (Table 4-1). Therefore, a significant part of such Na^+ influx must be mediated by some co-transport system operating at the plasma membrane. A high degree of synchronism between Na^+ and H^+ flux oscillations (absence of phase shift, Fig. 4-10) makes it tempting to suggest that the putative co-transport system could be a Na^+/H^+ cotransporter. Garrill *et al.* (1992) suggested that movement of Na^+ and H^+ occurs in antiport in *Thraustochytrium aureum*. Katz *et al.* (1989) reported similar findings for unicellular halotolerant alga, *Dunaliella salina*. For these organisms in their normal habitat (hypersaline environments), Na^+ enters down a large electrochemical gradient, driving the active export of H^+. At low NaCl conditions, this process could probably be reversed.

However, the correlation between net Na^+ and H^+ flux oscillations was positive, not negative (Fig. 4-11), which undermines the plausibility of the antiport hypothesis. Therefore, some other possibilities require consideration.

(3) Another option is that ion flux oscillations are driven by rhythmical variations in Na^+ channels conductance, and H^+ flux simply follows these changes. A plausible scenario is periodical switching between inward- and outward rectifying Na^+ channels. As most of the data concerning the actual values of cytosolic Na^+ concentration come from atomic absorption spectroscopy (Garrill et al., 1992), it could well be that the actual level of cytosolic Na^+ may fluctuate around the "basic" numbers reported. This will cause rhythmical changes in E_{Na} values and, therefore, alter energy requirements for the passive Na^+ uptake. The question should be further studied by concurrent patch-clamp and ion flux measurements.

Under this scenario, the oscillatory feature of H^+ flux is expected to originate from voltage coupling (Gradmann and Buschmann, 1997). Experimental support for the concept is now presented. Figure 4-13 illustrates ultradian H^+ flux oscillations measured from opposite sides of the same cell. The synchronism is striking.

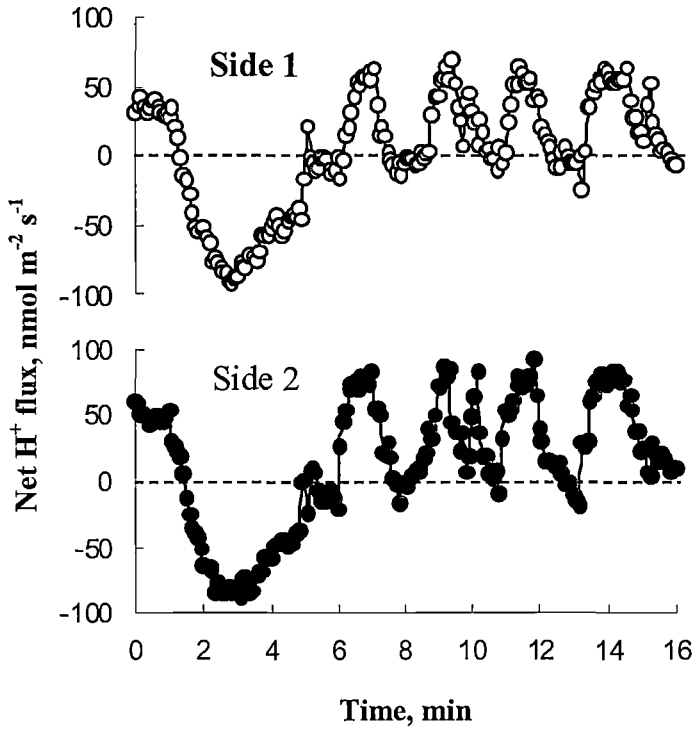

Fig. 4-13. Evidence for the coupling between different membrane transporters via membrane potential. In this example, ultradian H^+ flux oscillations, measured from opposite sides of the same cell, have a striking degree of similarity. One (out of 8) typical examples are shown.

4.2.6 Functional role of ultradian membrane oscillations

The question of the functional role of the observed ultradian ion flux oscillations remains to be answered. At the current level of knowledge, it is only possible to state that the oscillatory behaviour is different at various stages of cell development. To establish a causal link between these two processes, more experimentation is required. Two possibilities are suggested.

On the one hand, the oscillations might be directly involved in control of physiological processes. One such process is sporogenesis. Here it is shown that the highest rhythmical activity in thraustochytrid ACEM C was observed at the stage of the sporangium. In some microorganisms (e.g. *Fusarium*), rhythmical Ca^{2+} oscillations play a central role in the cyclic assembly and disassembly of cytoplasmic actin filaments and, ultimately, in shuttle streaming (Smith and Saldana, 1992). It could well be that a similar scenario is applicable to actomyosin contraction or rearrangement of cytoskeleton assembly in thraustochytrid cells resulting in a rupture of the plasma membrane and zoospore release. Direct experiments are required to assess this hypothesis.

Another possibility is that the oscillations may be of adaptive significance. A clear trend in dependence of periods of net H^+ and Na^+ flux oscillations on the external Na^+ concentrations in the bathing medium was observed (Figs. 4-14 and 4-15). The higher was the concentration of Na^+, the shorter was the oscillatory cycle.

Cell treatment with 200 mM NaCl shifted the resonant peak from 6.5 min observed in the control (1 mM NaCl solution; Fig. 4-14A; 4-15A) to 4-min (Fig. 4-14B; 4-15B). The difference in the period of H^+ flux oscillations between 1 mM and 200 mM NaCl variants was highly significant (7.09 ± 0.17 and 3.99 ± 0.09 min respectively; $n = 60$).

Many papers suggested that environmental signal specificity may be encoded by the amplitude and the frequency of oscillations in some cellular processes. This is expected to result in an increase in accuracy of control over intracellular processes, enhanced stability and better signal to noise ratio than analog control (Rapp et al., 1981). Best known are oscillations, or repetitive spikes, in cytosolic free Ca^{2+} concentrations found in many organisms in response to various stimuli (McAinsh *et* al., 1995; Hajnoczky et al., 1995; De Koninck and Schulman, 1998; McAinsh and Hetherington, 1998). Often the frequency of such oscillations showed a dose-response dependence on the external medium composition (McAinsh et al., 1995; Bauer et al., 1998). Understanding the mechanisms of such encoding and its physiological implications is a great challenge for future studies.

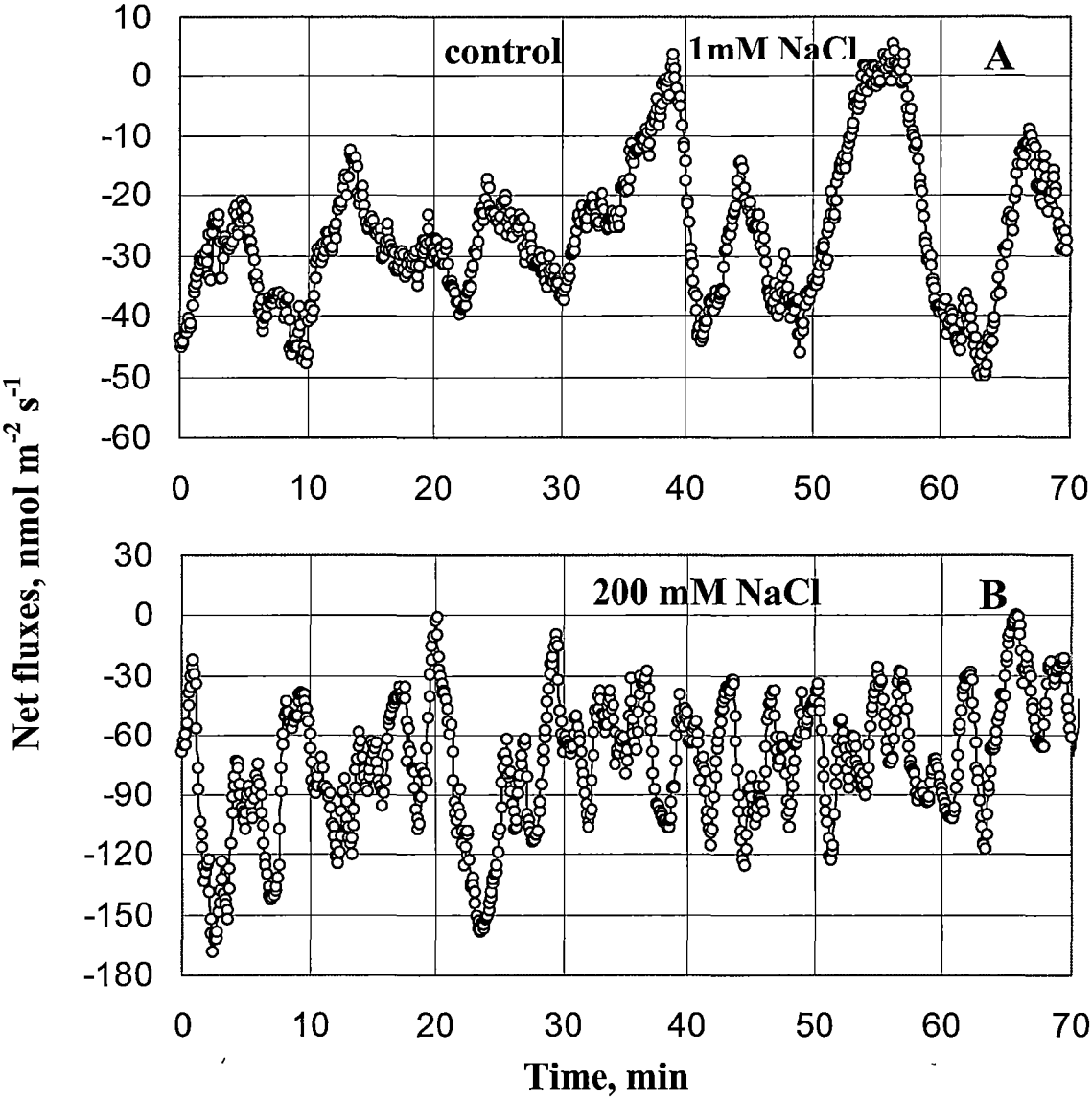

Fig. 4-14. Evidence for the presence of a frequency-encoding mechanism in thraustochytrid ACEM C cells. Two fragments of ultradian H^+ flux oscillations are shown for 1 mM (Control) (*A*) and 200 mM (*B*) NaCl in the bath medium.

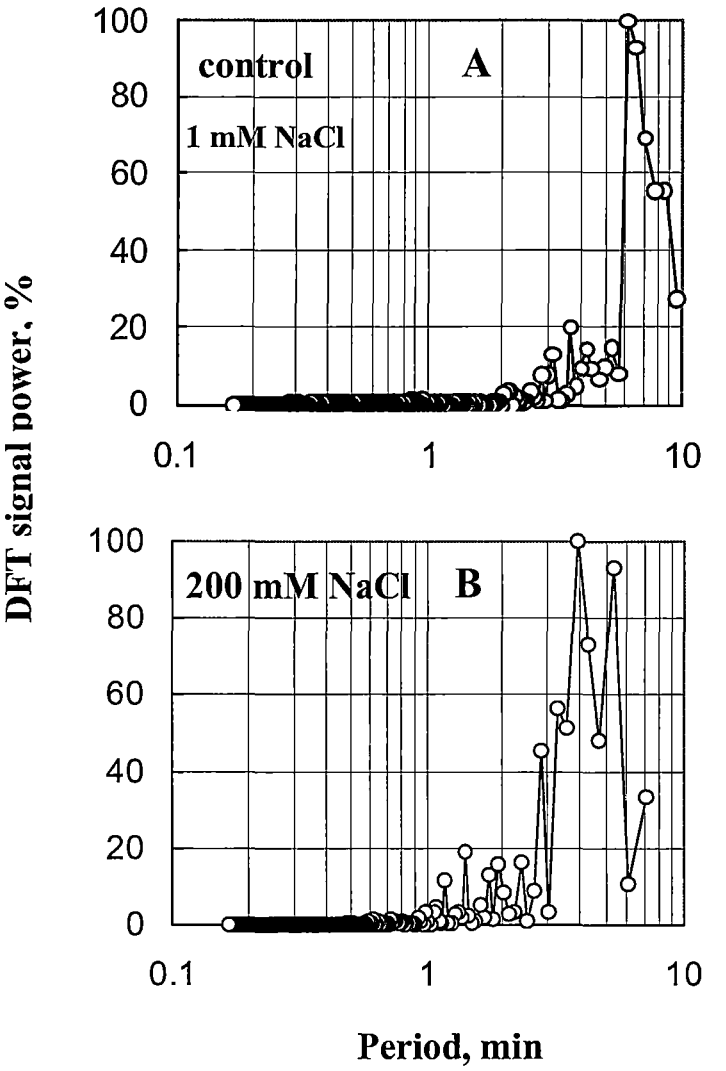

Fig. 4-15. Evidence for the presence of frequency-encoding mechanism in thraustochytrid ACEM C cells. Results of spectral analysis are shown in panels A – 1 mM NaCl (Control) and B – 200 mM NaCl. For each of these the power of the DFT signal is plotted against the corresponding harmonic Fourier component. A significant shift in the resonant Fourier harmonic is evident. The higher the NaCl concentration, the shorter was the oscillatory cycle.

4.2.7 Conclusion

In this study the MIFE technique was applied to study membrane-transport processes associated with cell growth and nutritional status of thraustochytrid ACEM C. Several important phenomena, such as development of polarity at the later stages of cell development and the presence of pronounced oscillatory patterns in ion transport across the plasma membrane (period range of several minutes) were revealed. Some evidence that a frequency-encoding mechanism might be present in thraustochytrid cells was found. The high spatial and temporal resolution of the MIFE technique, as well as the ability to measure simultaneously several different ions, provided insights into the underlying mechanisms responsible for the observed changes. Taken together, these findings illustrate the power of the MIFE technique to study membrane-transport processes in unicellular organisms similar to thraustochytrid ACEM C. Further studies might lead to greater progress in balancing the nutritional requirements and optimization of other growth culture conditions (pH, osmoticum, temperature etc), eventually leading to an increase in production of PUFA.

4.3. Osmotic adjustment in thraustochytrid ACEM C: literature review

4.3.1 Background significance

Thraustochytrids and other inhabitants of terrestrial waters are exposed to frequent variations in osmolarity during their life cycle. Consequently, they are expected to have developed an adaptive mechanism for osmotic adjustment to the changing environment.

Two marine species, namely *Dendryphiella salina* and *Debaryomyces hansenii*, have been proposed as model organisms to study fungal adaptive responses to salt and osmotic stresses (Clipson and Jennings, 1992). This suggestion, however, is supported primarily by the large number of studies performed on these organisms, rather than by their "universal" physiological features. It is difficult to indicate to what extent the models, based on these higher fungi, are applicable to the thraustochytrids. The latter are often referred to as the lower fungi (Jennings, 1995) and were shown to require macro amounts of sodium for growth (Jennings, 1983; Garrill et al., 1992).

The importance of studies into thraustochytrid adaptive responses to salinity and osmotic stress are at least two-fold. First, these organisms form a significant component of the marine biota (Goldstein, 1963; Bahnweg, 1979; Porter and Lingle, 1992); second, thraustochytrids have minimal cell walls with almost naked membranes (Clipson and Jennings, 1992) and, therefore, can be an ideal model organism for membrane studies in marine organisms. In most other marine fungi, the large volume of the hyphal wall makes work on the plasma membrane problematic.

In the marine environment, the water potential is dominated by sodium and chloride, resulting in an external water potential of around –2.3 MPa (Clipson and Jennings, 1992). Maintenance of turgor pressure is essential for an increase in cell volume and thus for growth of the thraustochytrid cell. Furthermore, intracellular water potential of cells must be maintained more negative than the external one to enable an inwardly directed flux of water, ions, and nutrients (for importance of membrane transport processes see Chapter 1.2).

4.3.2 Cell responses to hypoosmotic shock

In their natural habitats, microorganisms are often exposed to significant osmotic changes. The osmotic stress must be sensed and converted into an activity change of specific enzymes and transport proteins, and/or must trigger their synthesis in a way that the osmotic imbalance can be rapidly restored.

Goldstein (1963) proposed that *Thraustochytrium roseum* is an obligatory marine organism. However, it was shown later that this protist may inhabit a wide range of osmolarities and ion compositions (Booth, 1971). Fluctuations of salinities within a habitat (particularly an estuary) are expected to have resulted in the development of efficient mechanisms of osmotic adjustment. Specific details of the latter, however, remain to be revealed. Transport processes across the PM play an important role in osmotic adjustment of fungal cells in response to osmotic stress (Burgstaller, 1997). The mechanism involved in the response to hypoosmotic shock has been established using mammalian cells (for review see Lang et al., 1998), bacteria (for reviews see Blount and Moe, 1999) or algae (Bisson and Gutknecht, 1975; Okazaki and Tazawa, 1990; Beilby et al., 1999; Shepherd and Beilby, 1999), while marine fungi remain unexplored.

When cells are affected by hypoosmotic shock they are subject to substantial inward flows of water. A decrease in the external solute concentration from 250 mM to near zero would increase the intracellular pressure by more than 6 atmospheres (Blount and Moe, 1999). Unless steps are taken, these drastic forces will cause the cell to rupture.

Organisms employ a number of strategies when confronted with hypoosmotic stress. One of them is opening large pores in the cell membranes, the so-called 'mechanosensitive channels' (MSCs), and release of cytoplasmic solutes into the medium, thus equilibrating the turgor pressure (Blount and Moe, 1999; Levina et al., 1999). Thus, MSCs act as 'emergency release valves' (Blount and Moe, 1999). This efflux is believed to be a universal response in both prokaryotes and eukaryotes (for reviews see Sukharev et al., 1993; Blount and Moe, 1999; Hamill and Martinac, 2001). Although some metabolic solutes are lost, this is a small cost compared with the prospects of cell death due to potential rupture. The re-shrinking of hypotonically swollen cells is termed regulatory volume decrease (RVD). These changes in cell

volume are caused by the activation of ion transport pathways as well as by osmotically driven water movement such that the cell volume returns to normal levels.

Another way to cope with hypoosmotic shock is transporting the ions via ion channels thus reducing the turgor pressure (Bisson and Gutknecht, 1975; Beilby et al., 1999; Shepherd and Beilby, 1999).

Finally, an organism regulates the water flow via water channels (aquaporins) that are found in both eukaryotic organisms and bacteria (Calamita et al., 1995). Aquaporins facilitate rapid water movement across the cytoplasmic membrane and are repressed during growth at high osmolarity. Such repression might be beneficial for any cell unfortunate enough to undergo hypoosmotic shock as this might slow down the rate of water penetration and the consequent pressure build up during the transition from high to low osmolarity.

4.4. Ion fluxes and hypoosmotic adjustment in thraustochytrid ACEM C

Response to hypoosmotic stress (or osmotic down-shock) requires an increase in osmotic potential within the protoplasm of an organism. This increase is usually achieved by reducing the internal concentration of solutes. Ion transport across the cell membrane is the most efficient and rapid means of altering cellular osmolarity (Lang et al., 1998). The MIFE technique was used to assess the involvement of transport processes in response of traustochytrid ACEM C to hypoosmotic shock. The culture was prepared and cells were immobilised as described in Sections 2.1.1 and 2.2.2, respectively. Detailed description of microelectrode preparation, flux measurements, and data analysis are given in Section 2.3. Four day old culture was used (if not stated otherwise) in the study to minimise the variability of cellular response. Thraustochytrid experimental solution (Appendix A) containing 5% glucose and various NaCl concentrations was used throughout this study. Thraustochytrid cells were adapted in an experimental solution containing 200 mM NaCl for 2 h. Hypoosmotic shock was introduced by changing the experimental solution using a peristaltic pump (rate of solution flow up to 6 mL min^{-1}) in a measuring chamber with immobilised cells. At least 6 chamber volumes were pumped through the chamber to substitute the experimental solution. Net ion fluxes were measured for 10 min before solution change (at high osmolarity) and for 60 min after the change of experimental solution for low osmolarity. The kinetics were monitored for up to 3 different ions were measured simultaneously from the surface of a thraustochytrid ACEM C cell.

Lanthanum chloride, which blocks PM Ca^{2+} channels, was used at 200 μM concentration. The preparation of $LaCl_3$ stock solution is described in Appendix B. The kinetics of Ca^{2+} flux were measured at the surface of thraustochytrid cells pretreated in an experimental solution containing 200 μM $LaCl_3$ at two levels of NaCl in the solution: at 200 mM NaCl (for 10-15 min) and after a shift to 0 mM NaCl concentration (for 40-50 min).

The ions monitored in the present study were divided into two groups:

(i) ions known to be involved in osmotic adjustment (K^+, Na^+, and Cl^-);

(ii) ions not directly contributing to osmotic adjustment (H^+ and Ca^{2+}).

The first group of ions were selected for their role in osmotic adjustment in a number of organisms. As other ionic movements must provide for overall charge balance, the second group of ions was studied also. Involvement of Ca^{2+}, known for its signalling role in a number of responses, was of special interest.

4.4.1 Changes in net K^+, Na^+, and Cl^- fluxes

The kinetics of K^+, Na^+, and Cl^- flux of thraustochytrid ACEM C in response to hypoosmotic shock are shown in Fig. 4-16.

When the NaCl concentration in the medium was reduced from 200 mM to near 0 mM, transient net efflux of K^+, Na^+, and Cl^- was observed. This efflux gradually decreased, and returned to the original values 15 to 20 min after the hypoosmotic stress onset.

Animal cells (Ikehara et al., 1992; Orlov et al., 1993; Hoffmann and Dunham, 1995), yeast (Thome-Ortiz et al., 1998), algae (Bisson and Krist, 1995; Beilby and Shepherd, 1996; Bielby et al., 1999; Shepherd et al., 1999) and marine fungi (Rauferova et al., 1997) are all reported to lose mainly K^+, Cl^-, and Na^+ in response to hypoosmotic shock. The overall contribution of the above three ions, however, might be different in various organisms. Usually, more K^+ and Na^+ than anions Cl^- are lost from cells in animal tissues in response to hypoosmotic stress (Lang et al., 1998). Most marine algae have an inward Cl^- pump (Bisson and Gutknecht, 1975), and turgor-sensitive Cl^- transport is believed to be prevalent in these organisms (Gutknecht et al., 1977; Bisson and Gutknecht, 1975). In some species, such as *Valonia* or *Chaetomorpha*, however, the most significant changes relate to K^+ permeability (Steudle et al., 1977). A recent report of La Spada et al. (1999) demonstrates that the regulatory mechanisms of *Aiptasia diaphana* (a marine species) to hypoosmotic shock consist mainly of an increase in conductance to K^+ and Cl^-. The three ions mentioned above were also claimed to be the major contributors to turgor regulation in plant cells (Jones and Pritchard, 1990; Shabala et al., 2000). Hyperosmotic stress usually reverses fluxes of these ions, as was shown both in plants and fungi (Clipson and Jennings, 1992).

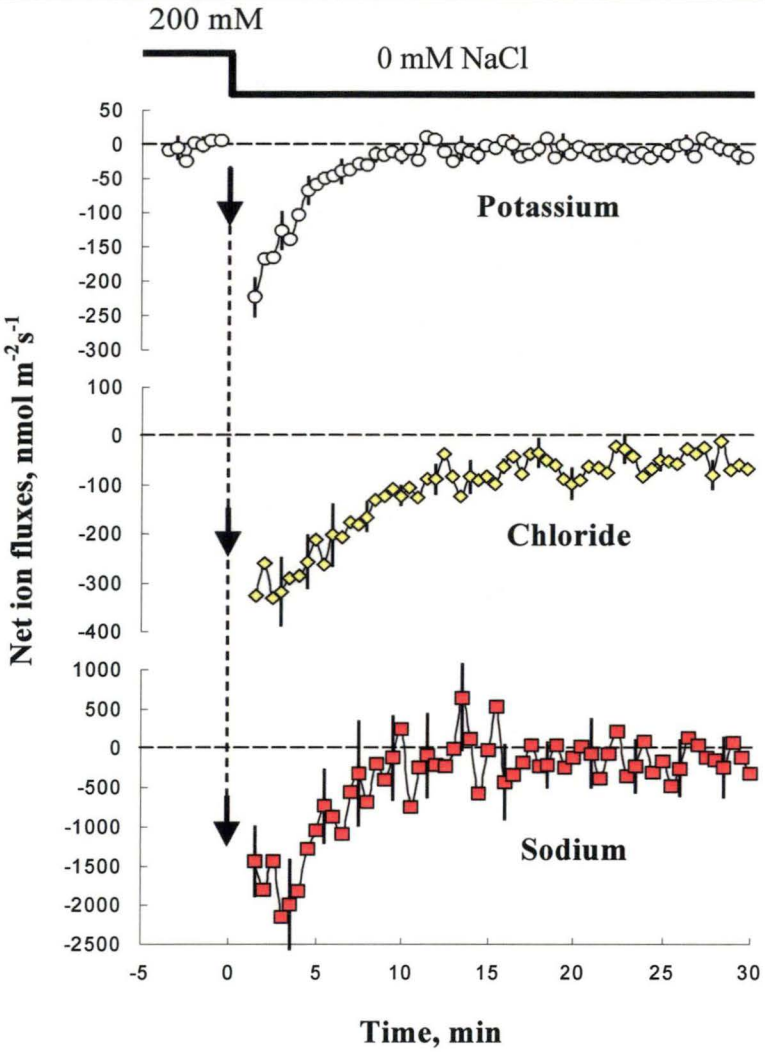

Fig. 4-16. Kinetics of net K^+, Na^+, and Cl^- flux in response to hypoosmotic shock in thraustochytrid ACEM C. Cells adapted to 200 mM NaCl for 2 h were subjected to hyposmotic shift by a change of experimental solution in a chamber for a new one without NaCl using a peristaltic pump. Error bars are SEM (n=8). Due to low signal to noise ratio, measurements of steady Cl^- and Na^+ flux values at 200 mM NaCl concentration in the experimental solution were not possible.

Apart from MSCs, intracellular solutes may leave an organism via other routes. For example, an exchange mechanism (K^+/H^+ and Na^+/Ca^{2+}) was shown to be involved in volume regulation of mammalian cells (Lang et al., 1998). Furthermore, it was shown that in HeLa cells K^+ and Na^+ were released through the K^+-channel and the Na^+-pump, respectively (Ikehara et al., 1992). Similar pathways for efflux

were reported in marine fungi (Rauferova et al., 1997). However, Garrill et al. (1992) presented some evidence for the absence of the sodium pump in *Thraustochytrium roseum.* Therefore, some other pathway of Na^+ efflux from the cell must be operating in thraustochytrids.

An additional factor that influences ion flux across the plasma membrane of thraustochytrids is the depolarisation of the PM known to occur in a variety of cells in response to hypoosmotic shock (Bisson et al., 1995; Lang et al., 1998; Wood, 1999; Shepherd and Beilby, 1999; Shepherd et al., 1999; Stento et al., 2000). Based on cell volume and membrane potential measurements under various experimental conditions, it was concluded that hypoosmotic shock activates independent, conductive transport pathways for K^+ and for Cl^-, respectively (Sarkadi et al., 1984). Membrane depolarisation has been proposed to be one of the early events responsible for the stimulation of the efflux of ions involved in cell volume regulation (Brochiero et al. (1995). Indeed, depolarization of the cell membrane was shown to be responsible for the opening of anion channels (Caldwell et al., 1986) as well as voltage sensitive K^+ and Ca^{2+} channels (Lang et al., 1998) in cells after hypoosmotic shock. For example, depolarisation of the PM in the 'lower fungus' *Blastocladiella emersonii* resulted in the opening of an anion channel which was able to pass chloride among other anions (Caldwell et al., 1986). The authors postulated the control role of the anion channel in turgor regulation.

4.4.2 Quantitative assessment of ion flux contribution to osmotic adjustment in thraustochytrid ACEM C.

Among the cytoplasmic solutes that may be released upon hypoosmotic shock are inorganic ions and solutes of organic origin (proline, trehalose, and even small proteins) (Sukharev et al., 1993; Cui and Adler, 1996; Blount and Moe, 1999; Jones et al., 2000). Wethered and Jennings (1985) demonstrated that ions made the major contribution (around 90%) to solute potential of *Thraustochytrium* spp. sporangia when grown at different seawater salinities. This is a far higher contribution than that for the higher marine fungus *Dendrypliella salina.* Clearly, ionic contribution is predominant in turgor regulation of thraustochytrids. Qualitative data presented here

(Fig. 4-16) supports this, demonstrating that all these ions were extruded after the application of a hypoosmotic shock to thraustochytrid ACEM C.

High spatial resolution and a unique opportunity of the MIFE system to measure concurrently fluxes of three ions in the same experiment and from the same cell enabled the contribution of efflux of each specific ion (Na^+, K^+ and Cl^-) in the osmotic adjustment of thraustochytrid cells to be quantified.

Assuming average cell radius R= 10 μm, the cell volume (V) is

$V = 4/3\ \pi R^3 = 4.18\ 10^{-15}\ m^3$

and the cell surface area (S)

$S = 4\ \pi R^2 = 1.25\ 10^{-9}\ m^2$

From Fig. 4-16, the average net efflux of ions over the 30 min interval, observed during the transient response, is

K^+ efflux = 25 nmol m^{-2} s^{-1}

Na^+ efflux = 390 nmol m^{-2} s^{-1}

Cl^- efflux = 150 nmol m^{-2} s^{-1}

Assuming surface area of the thraustochytrid cell $S = 1.25\ 10^{-9}\ m^2$ (see above), and the flux being uniform over the cell surface, then in 30 min, the total loss of ions from the cell will be

ΔN = Flux x Surface area x Time

$\Delta N = 5.65\ 10^{-14}$ mol of K^+

$\Delta N = 8.79\ 10^{-13}$ mol of Na^+

$\Delta N = 3.39\ 10^{-13}$ mol of Cl^-

According to van't Hoff's law, the loss of each of these ions will cause a drop $\Delta\Psi$ in the cell turgor (Shabala et al., 2000)

$\Delta\Psi = \Delta N * R * T / V,$

where R = 8.31 is the universal gas constant; T = 296 K is the ambient temperature; and $V = 4.18\ 10^{-15}\ m^3$ is an average cell volume (see above).

Then

$\Delta\Psi$ = 0.04 mPa for K^+

$\Delta\Psi$ = 0.51 mPa for Na^+

$\Delta\Psi$ = 0.20 mPa for Cl^-

Overall, efflux of these 3 ions will result in the drop of cell turgor by about 0.75 mPa. At the same time, transition from 200 mM to near 0 mM NaCl is expected to cause the change in osmotic potential of about 0.8 mPa (CRC Handbook, 1974). Therefore, almost complete osmotic adjustment is achieved within the first 30 min by efflux of Na^+, K^+ and Cl^- ions in thraustochytrid cells. Of these, sodium is a major contributor (more than half of the total osmotic adjustment), with chloride being the second major contributor. The role of K^+ in the process of osmotic adjustment appears to be relatively small. Involvement of other ions for charge balance is discussed below.

According to Bisson et al. (1995), turgor regulation in *Chara* occurs in two distinct phases:

- the fast phase, lasting ca 5 min, during which about 25% of initial turgor is recovered;
- the slow phase, when the remaining balance of the turgor pressure is achieved.

The duration of the second phase was strikingly different between different cells, and showed very strong dependence on cell size (volume). In small cells, its duration was about 40 min, while in larger cells full turgor restoration required up to several days. The calculations presented above suggest that almost complete cell turgor was restored within 30 min of stress onset. Due to small cell size, the efficacy of turgor regulation in thraustochytrids should be much higher than in giant algae (similar to response of *Chara* cells of different size, Bisson et al., 1995).

The observation that Na^+ plays a key role in the process of osmotic adjustment in thraustochytrid ACEM C is consistent with the crucial role of Na^+ for normal cell growth and development. Various studies (Goldstein, 1963; Bahnweg, 1979; Garrill et al., 1992) have shown that thraustochytrids can grow in salinities ranging from 10 to 100% sea water but cannot grow at zero salinity. Moreover, the requirement for Na^+ can be met only partly by potassium (Jennings, 1983; Garrill et al., 1992).

It is apparent, however, that the role of Na^+ is not limited by its involvement in cell osmoregulation. Garrill et al. (1992) showed that protoplasmic Na^+ concentration was very stable ranging from 40 to 50 mM at different external NaCl concentrations, indicating an efficient mechanism of intracellular Na^+ homeostasis. Increase in sodium chloride concentration in the medium up to 500 mM correlated with an

almost proportional increase in dry weight production and in cell numbers (Garrill et al., 1992). Part of the requirement for sodium appears to be the facilitation of phosphate uptake (Siegenthaler et al., 1967 a, b; Belsky et al., 1970).

Quantitative information on the contribution of inorganic ions to turgor regulation in thraustochytrids is controversial. Wethered and Jennings (1985) reported that inorganic ions contributed about 90% of the osmotic potential of solutes within the protoplasm of *T. aureum* grown at 50% seawater. In contrast, Garrill et al. (1992) showed that at around sea water salinity, sodium and potassium contributed less than 25% of the osmotic potential of *T. roseum* required for osmotic balance. However, the input of Cl^- into the osmotic adjustment of *T. roseum* was not considered by those authors. Meanwhile, many of the reports reviewed above, as well as the present study, demonstrate an important role for Cl^- in the process of osmotic adjustment. Keeping in mind the small contribution of organic solutes to the osmotic potential of thraustochytrid cells (~0.5%) (Wethered and Jennings, 1985), our data demonstrates the importance of inorganic ions to osmotic adjustment of thraustochytrids exposed to hypoosmotic stress.

4.4.3 Changes in net H^+ fluxes

The second group of ions studied, namely H^+ and Ca^{2+}, does not directly contribute to the osmotic adjustment of an organism.

It was found that the onset of hypoosmotic stress (transition from 200 to near 0 mM NaCl) induced significant (~150 nmol m^{-2} s^{-1}) net H^+ influx into the thraustochytrid ACEM C cell, peaking 5 to 7 min after the treatment, followed by a gradual decline in net H^+ flux back to the initial value (Fig. 4-17).

In steady-state experiments, net H^+ fluxes were measured from the thraustochytrid surface after cell pre-incubation in an appropriate experimental solution (Appendix A) for 1 h. Net H^+ extrusion increased progressively with an increase in NaCl concentration in the solution. Protons were taken up at NaCl concentration below 10 mM and actively extruded above this concentration (Fig. 4-18).

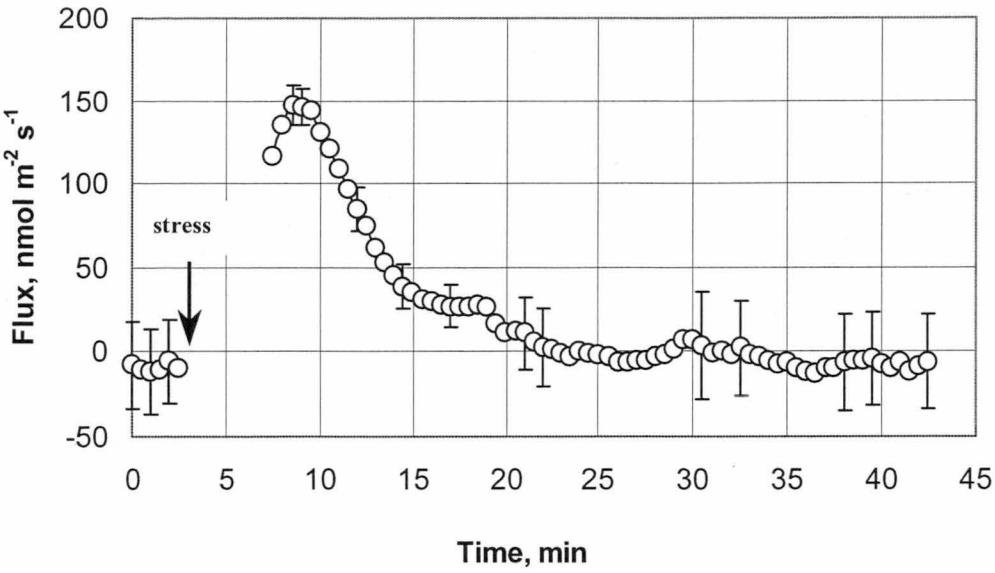

Fig. 4-17. Kinetics of net H^+ flux in response to hypoosmotic shock. Adapted to 200 mM NaCl, the thraustochytrid cells were shifted to 0 mM NaCl by a change of solution in the measuring chamber using a peristaltic pump. Error bars are SEM (n =8).

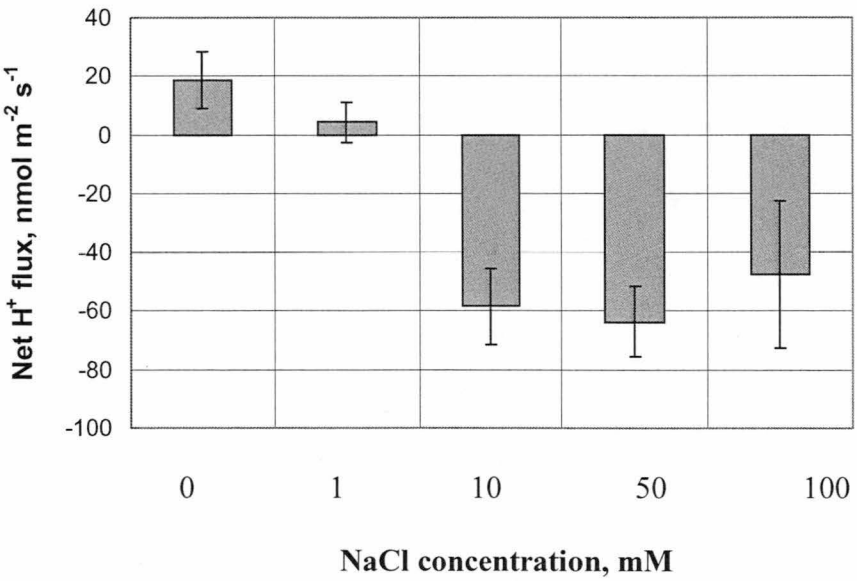

Fig. 4-18. Net H^+ flux as a function of NaCl concentration. Net H^+ flux was measured at static conditions after 1 h adaptation at indicated salinities. Error bars are SEM of 2-4 replicates with n=10 in each.

A number of studies have demonstrated that cell swelling in response to hypoosmotic shock leads to cytosolic acidification. This was reported for a number of organisms including animal cells (Lang et al., 1998), bacteria (Berrier et al., 1992; Schleyer et al., 1993), fungi (Luard, 1982) and plants (Li and Delrot, 1987). Several possible mechanisms were suggested.

First, MSCs display little ion or solute preference. The changes in cytoplasmic pH strongly support the notion, derived from patch clamping, that the solutes can move in both directions through the open channel (Schleyer et al., 1993). MSCs were also reported to facilitate H^+ entry (Schleyer et al., 1993). This is consistent with a dramatic H^+ influx in response to hypoosmotic shock observed in Figure 4-17.

Secondly, modulation of H^+-pump activity by the changes in external osmotic concentration and/or cell turgor has been reported (Rubinstein, 1982; Reinhold et al., 1984; Li and Delrot, 1987). Passive H^+ transport is also affected (Bisson and Gutknecht, 1975; Rubinstein, 1982; Lew, 1996) implying a multicomponent osmo-regulatory system (Berrier et al., 1992).

Acidification of the cytosol was also reported to activate H^+-ATPase (Nannen and Hutkins, 1991; Miwa et al., 1997; Amachi et al., 1998; O'Sullivan and Condon, 1999). That is particularly important for restoration of otherwise depolarised PM potential (Bisson et al., 1995). The gradual decrease in net H^+ influx within 20-30 min of stress onset (Fig. 4-17) might be explained by such H^+-pump activation. Moreover, PM depolarisation by itself also increases the activity of H^+-ATPase (Sanders, 1988). The triggers that were found to regulate the H^+-ATPase exert their effect within different time scales. The time scale for membrane depolarisation due to an osmotic shock was reported to reach the order of minutes (Slayman, 1992). By this time most internal solutes are extruded and over-regulation of transport processes with a return to equilibrium is required. Activation of H^+-ATPase fulfills this requirement by pumping H^+ from the cell and thus stabilising the net H^+ flux at the optimal value. Garrill et al. (1992) suggested the presence of an electrogenic proton pump in the thraustochytrids. The results reported here (Figs 4-17; 4-18) are consistent with this idea.

4.4.4 Transient Ca^{2+} kinetics

At 200 mM NaCl in the medium thraustochytrid ACEM C had net Ca^{2+} flux close to zero. This is a common feature for all living organisms (Norris et al., 1996; Sanders and Bethke, 2000). The shift in medium osmolarity from 200 mM to near 0 mM NaCl resulted in net Ca^{2+} influx of up to ~80 nmol m^{-2} s^{-1} followed by decrease to the original value in ~15 min (Fig. 4-19).

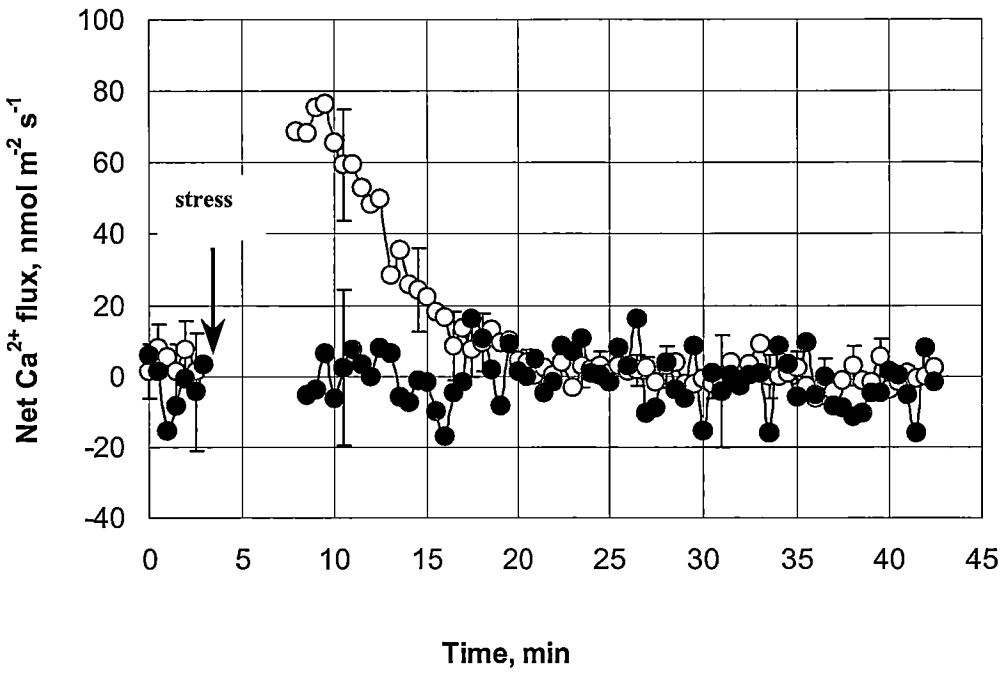

Fig. 4-19. Kinetics of net Ca^{2+} change to hypoosmotic shock. Adapted to 200 mM NaCl, the cells were shifted to ~0 mM NaCl. Open symbols represent the control experiment. Effect of 200 μM $LaCl_3$ pretreatment on hypoosmotically-induced transient Ca^{2+} flux is indicated by closed symbols. Error bars are SEM (n =8).

A similar increase in cytosolic free calcium ion concentration in response to hypoosmotic shock was reported for a number of cells of different origin: in plant cells (Takahashi et al., 1997a,b; Cessna and Low, 2001), marine organisms (nematocytes and alga, respectively) (La Spada et al., 1999; Stento et al., 2000), yeast (Lichko et al., 1980; Eilam, 1982), and mammalian cells (Mongin et al., 1997; Lang et al., 1998). In certain cell types, extracellular Ca^{2+} was shown to be essential

for cell volume regulation (Wong et al., 1995, Cessna and Low, 2001). The nature of the observed elevation in cytosolic free Ca^{2+} is unclear, and both Ca^{2+} influx from the extracellular medium and Ca^{2+} release from internal organelles were suggested (Shepherd and Beilby, 1999; Cessna and Low, 2001). In this study, significant net Ca^{2+} influx (Fig. 4-19) supports the idea of Ca^{2+} entry into the hypoosmotically stressed cell from the external solution.

However, due to Donnan exchange in the cell wall (Arif et al., 1995), the observed Ca^{2+} uptake might be a result of increased H^+ uptake in response to hypoosmotic stress (Fig. 4-17). To eliminate the potentially confounding effect of the cell wall as a source of measured Ca^{2+} flux, lanthanum chloride, a known blocker of PM Ca^{2+} channels, was used. In contrast to the control experiment (Fig. 4-19; open symbols), presence of 200 μM $LaCl_3$ in the medium resulted in the absence of calcium influx in response to hypoosmotic shock indicating that the observed Ca^{2+} influx was via the Ca^{2+} channels (Fig. 4-19; closed symbols). This is consistent with literature reports, when other Ca^{2+} channel blockers were used (Stento et al., 2000)

The physiological role of the observed hypoosmotically-induced Ca^{2+} uptake might be at least three-fold.

First, many ion channels are Ca^{2+}-dependent. Shepherd and Beilby (1999) have shown the presence of Ca^{2+}-activated Cl^- and K^+ channels in the marine algae *Lamprothamnium papulosum*. Similar observations were made on other organisms. Omission of Ca^{2+} from the medium was reported to inhibit RVD in animal cells (Ikehara et al., 1992; Lang et al., 1998), suggesting an involvement of Ca^{2+}-dependent K^+ channels in turgor regulation.

Secondly, calcium is known to be a ubiquitous second messenger in living cells (see Chapter 1.2.5). The regulation of intracellular Ca^{2+}concentration by cell volume may interfere with signaling of Ca^{2+}-recruiting hormones, as shown in both animal and plant cells (Lang et al., 1998; Cessna and Low, 2001). Alterations in cytosolic free Ca^{2+} were suggested to be part of the signal transduction chain in osmotically-stressed marine algae (Okazaki and Tazawa, 1990; Bisson et al., 1995; Stento et al., 2000).

Finally, the observed Ca^{2+} influx might provide the charge balance. Compensatory ion fluxes are necessary for repolarisation of the PM after depolarisation. In fungi, two main compensatory ion fluxes were shown to be the uptake of potassium and the backflow of protons (Slayman, 1977). It was also suggested that electrogenic entry of Ca^{2+} in response to hypoosmotic shock might represent the involvement of the ion in charge balancing (Hunter and Segel, 1973; Eilam and Chernichovsky, 1987).

4.4.5 Conclusion

This work demonstrates the evidence for turgor regulation in thraustochytrid ACEM C in response to hypoosmotic shock. Major ions involved in osmotic adjustment were Na^+ and Cl^- and, to some extent, K^+. Significant net efflux of these ions was measured immediately after stress onset. Together these ions almost completely compensated the changes in osmotic potential of thraustochytrid ACEM C within 30 min of treatment being applied. Two other ions studied, Ca^{2+} and H^+, exhibited net influx in response to hypoosmotic shock. The Ca^{2+} influx occurred via calcium channels and suggests that it either plays a signalling role, or is used as a charge balancer.

4.5. Homeostasis of plasma membrane at low temperature: an overview

As mentioned above (Chapter 4.1), thraustochytrids have recently attracted special interest as a valuable source of polyunsaturated fatty acids (PUFA). The reason for the high level of PUFA in this protist is unknown. Low temperatures are known to have lipid-solidifying effects (Evans et al., 1998; Holler et al., 1998) and high levels of PUFA would ameliorate this effect. Thraustochytrids were first found in sediments in coastal waters of areas with temperate climate like the North Sea and the Norwegian Sea (Booth, 1971). Some of them were reported to withstand temperatures of –20 °C for 7 h (Booth, 1971). Thraustochytrids were also discovered in Antarctic fast ice close to the Weddell Sea (Riemann and Schaumann, 1993). Based on the above evidence, high PUFA levels might result from the evolution of thraustochytrids in low temperature environment that was conserved later. This is in accordance with a report by Dunstan et al. (1999) who observed an increase in PUFA and monounsaturated fatty acids (MUFA) production in antarctic marine species *v/s* temperate and tropical marine species that contained more saturated fatty acids (SFA). Nichols et al. (1995) stated that the benefit of PUFA to cold adapted organisms derives from their fluidising effect and stabilisation of the lipid phase at low temperature.

Even within their normal habitat, thraustochytrids more or less frequently experience periods of sub-optimal temperatures that might severely limit their growth. A large number of physiological processes affected by low temperature were shown to depend on temperature-induced changes in membrane structure and activity similar to those shown in plants (Nishida and Murata, 1996; Murata and Los, 1997), fungi (Stein, 1990; Dunstan et al., 1999), and bacteria (Russell, 1990; Nichols et al., 1994; Nichols et al., 1997). It is not surprising, therefore, that temperature has an enormous effect on nutrient uptake and transport in all poikilothermic organisms. Consequently, alterations in membrane transport activity due to low temperature stress are an obvious starting point for investigations of thraustochytrid ACEM C adaptive responses to temperature extremes.

Temperature variations are ubiquitous in nature (Thieringer et al., 1998). Due to direct effects of temperature on all metabolic process within the living cell, adaptations to temperature fluctuations are of paramount importance for all organisms. When the cell is faced with temperature extremes, numerous biochemical and physiological alterations occur. Among the most important changes in poikilotherms caused by cell exposure to low temperature are (i) changes of fatty acid (FA) composition in cellular membranes and (ii) changes in protein profile leading to biosynthesis of so-called cold-shock proteins (CSPs).

4.5.1 Changes in fatty acid composition

A change in the lipid composition of membranes is a universal response to low temperatures in poikilotherms. It is well documented that microorganisms adjust the fatty acids (FA) composition of their membrane phospholipids in response to changes in growth temperature (De Mendoza and Cronan, 1983; Nichols et al., 1994, 1997; Russell et al., 1995; Thieringer et al., 1998). Fluidity of the lipid bilayer is crucial for normal cell functioning. As temperature is decreased, the FA chains of the membrane lipids undergo a lipid phase transition (change of state from a fluid, disordered state, to a more ordered gel state of the FA chains) (De Mendoza and Cronan, 1983; Russell, 1990; Berry and Foegeding, 1997). The temperature at which these changes occur is called the phase transition temperature (Burgstaller, 1997).

There is a large number of mechanisms that can alter the membrane phospholipid composition in response to temperature change (for reviews see Russell, 1990; Berry and Foegeding, 1997). Many organisms have developed mechanisms to compensate for the transition from the liquid crystalline to gel phase by changing the degree of saturation of the hydrocarbon chains of membrane phospholipids (Nakayama et al., 1980; Russell et al., 1995; Nichols et al., 1994, 1997; Evans et al., 1998; Holler et al., 1998). Phospholipids with unsaturated fatty acids have lower melting points and a greater degree of flexibility than phospholipids containing saturated fatty acids. For example, Jackson and Cronan (1978) showed that *E. coli* can grow normally with as much as 20% of its membrane lipids in the ordered state; the growth ceases if more than 55% of the lipids are ordered. In bacilli

a decrease in temperature resulted in increased synthesis of membrane bound desaturase, along with the increased stability of the enzyme (Aguilar et al., 1998). Null mutant strains were unable to synthesise unsaturated FAs upon a shift to low growth temperatures indicating the significance of this enzyme.

Another change in lipid composition in response to reduced growth temperature is the shortening of its acyl chain length (Evans et al., 1998; Holler et al., 1998). This lowers the melting temperature and, hence, helps to maintain membrane fluidity at the lower temperatures (Russell, 1989; Russell et al., 1995; Holler et al., 1998). Also, the organism may exhibit a change in the ratio of phospholipids to proteins of their membrane as a response to cold shock as was shown for bacteria (Garbay and Lonvaud-Funel, 1996).

An increase in the ratio of cis-form of FAs is yet another of the characteristic changes in FA composition in response to chilling (Marr and Ingraham, 1962; Garwin and Cronan, 1980; Holler et al., 1998). Other FA changes at low temperatures include increases in branched-chain FAs and the proportion of anteiso- FAs (Mastronicolis et al., 1998; Klein et al., 1999; Edgcomb et al., 2000).

Surprisingly, there is no apparent link between membrane lipid fluidity and minimum growth temperature in some microorganisms. For example, an *E. coli* may grow near its minimum growth temperature, having a fatty acid composition characteristic of a cell grown at 37 °C (Shaw and Ingraham, 1965). Direct measurements of membrane fluidity in psychrotrophic and mesophilic bacteria indicate that the lipid phase transition temperature of their membrane lipids can be lower than their minimum growth temperature (Lepock et al., 1990; Tsuchido et al., 1995).

The time course for thermal modulation of FA composition (e.g. increase in the ratio of unsaturated to saturated FA) was reported to be within 30 sec (Garwin and Cronan, 1980). These changes in membrane fatty-acid composition did not require new protein synthesis (Garwin and Cronan, 1980; Mastronicolis et al., 1998). In addition to the above FA alterations, some organisms may stabilise membrane structure by using low molecular weight protectants (amino acids, sugars, quaternary amines etc. (Storey and Storey, 1988; Franks et al., 1990; Ko et al., 1994).

4.5.2 Alterations in protein profile and associated changes in membrane-transport activity

In bacterial cells, low temperature stress causes initial arrest in growth. Then fatty acid composition is altered, RNA synthesis is enhanced, and cell growth is resumed (Jeffreys et al., 1998). A specific pattern of gene expression occurs in response to chilling stress. This includes the induction of cold-shock proteins, continued synthesis of proteins involved in transcription and translation despite the lag period, and repression of heat-shock proteins (Jones et al., 1987; Jones and Inouye, 1994; Graumann et al., 1996; Kandror and Goldberg, 1997; Panoff et al., 1997). Disturbance of membrane lipoprotein complexes was shown to be involved in the perception of temperature shock in yeast leading to the transcription of genes implicated in the thermal response (Carratu et al., 1996).

The above changes in FA and protein composition are aimed to increase membrane fluidity, which is essential for maintaining the physiological functioning of biological membranes at lower temperatures (Leder, 1972; Murata and Wada, 1995). One of the most important consequences of alterations in membrane lipid composition in microorganisms is the modulation of the activity of transport proteins involved in numerous functions such as electron transport, ion pumping and nutrient transport across various cellular membranes (Hochachka and Somero, 1984). It was demonstrated in *Lactococcus lactis* that membrane fluidity affected H^+-coupled leucine translocation (Zheng et al., 1988). The rate of carrier-mediated solute transport across the membrane is proportional to the diffusion constant of the protein in the membrane. This diffusion constant is inversely proportional to microviscosity (Veld et al., 1993). Temperature-controlled alteration of membrane fluidity is widespread, indicating that it does serve an important adaptive function and must offer some selective advantage.

4.5.3 The plasma membrane as a primary target

Cold shock is defined as irreversible damage expressed shortly after exposure to low temperatures. The primary target of it is thought to be the PM (Arav et al., 1996). Evidence of membrane damage caused by cold stress is numerous and has

been demonstrated by using different experimental techniques such as measurements of electrolyte leakage, electron spin resonance and fluorescence depolarisation, changes in lipid composition, freeze-fracture electron microscopy, and X-ray diffraction (Lyons, 1973; DuPont, 1989; Sharom et al., 1994; Yoshida, 1994). It is now accepted that electrolyte leakage denotes irreversible cell damage and appears long after many other events in the cell membranes (Yoshida, 1991). Therefore, attention must be given to the primary mechanisms of ion transport across cell membranes.

The most sensitive appear to be the H^+-transporting systems. Cold inactivation of H^+-transporting systems occurs much sooner than the appearance of injury to cells (Yoshida, 1991, 1994). The effect of temperature on H^+ transporting systems seems to be complex, and involves different types of transporters, passive and active, as well as their different locations within the cell (Raison, 1979; DuPont and Mudd, 1985; Kasamo et al., 2000; Prasad et al., 1994). Temperature is likely to have direct effects on the fluidity, viscosity, or phase-state of membrane lipids (Lyons, 1973; DuPont, 1989) and so will directly modify H^+ transporter properties. Indirect effects on H^+ transporters may also come from temperature responses of other systems in cell membranes.

Despite a large number of studies having been conducted, temperature effects on ion uptake and transport across membranes appear contradictory. Bravo-F and Uribe (1981) have reported strong temperature dependence of uptake of potassium ($Q_{10} = 9$) and phosphate ($Q_{10} = 4.3$) by plant tissues (Q_{10} determines change of a chemical reaction's rate when an ambient temperature is changed by 10 degrees Celsius). At the same time, Petterson (1995) found that low (10 ^{0}C) temperature had no impact on uptake or transport of potassium, magnesium, nitrogen, and phosphate by plant roots. Even for the same element (K^+ in particular), dependence of uptake rate on temperature was shown to be either linear (White et al., 1987), sigmoidal/exponential (Bravo-F and Uribe, 1981), or even hyperbolic (Carrey and Berry, 1978). Obviously, many factors including ionic composition of experimental solution, membrane composition, exposure temperature(s), duration of temperature

treatment, rate of temperature changes, genetic variability etc affect membrane transport processes, and therefore, contribute to this apparent controversy.

It is also unclear whether different ion transporters have different sensitivity to chilling temperatures. Wang et al. (1993) have reported that high (<1 mM) and low (1-40 mM) affinity transport systems for NH_4^+ had very different Q_{10} (2.5-2.6 and 1.5, respectively), in the temperature range of 5-10 ^{0}C. The break in the Arrhenius plots for NO_3^- and NH_4^+ uptake also occurred at two different critical temperatures, 13.5 and 10 ^{0}C respectively (Clarkson et al., 1988). In bacteria and algae, the specific affinity for NO_3^- was strongly dependent on temperature (Q_{10} = 3) and consistently decreased at temperatures below the optimum temperature. In contrast, the specific affinity for NH_4^+ exhibited no clear temperature dependence (Reay et al., 1999). Engels and Marschner (1992) have found that phosphorous uptake is usually more depressed than uptake of other nutrients. Does it mean that different ion transporters have different sensitivity to chilling temperatures? Direct evidence for such a conclusion is lacking. This is considered in the next section.

4.6. Net ion flux kinetics in thraustochytrid ACEM C in response to chilling stress

In this section, the MIFE technique was used to study adaptive responses of thraustochytrid ACEM C to low temperature stress. For these purposes, the recovery of net H^+ and Na^+ fluxes during warming after several hours of low temperature treatment was monitored. H^+ and Na^+ ions were chosen for the study because of their importance in thraustochytrid physiology. H^+ is known to be involved in PMF generation and energy transduction, while Na^+ is an essential macro-element crucial for the growth of this organism. Measurements of net flux kinetics were used to establish critical temperatures associated with changes in ion fluxes studied.

4.6.1 Experimental protocol

Cells grown as described (see Chapter 2) were transferred to the experimental solution (see Appendix A) and left there for 2 h for adaptation at either 17 or 23 °C. Then cells were immobilised in a chamber as described in Section 2.2.2 at one of the selected ambient temperatures (either 17 or 23 °C). Flux measurements were performed for 5-10 min (control). Then the chamber containing immobilised thraustochytrid cells was transferred to a refrigerator (+ 4 °C). After 2 h of chilling treatment, cells were returned to ambient temperature, and flux measurements resumed immediately. The same cell was measured before and after the chilling treatment.

Temperature increase in the experimental chamber was measured from 4 °C to its return to room temperatures using a miniature thermistor inserted into the chamber. The thermistor was connected to a MIFE channel that enabled the corresponding voltage to be recorded and stored with the flux data on disk. Systematic error of temperature measurements was less than 0.2 °C. A delay of ~2-3 min between removal of the chamber from the refrigerator and the start of data acquisition occurred. This was the time required to transfer the measuring chamber with immobilised cells from the refrigerator to the microscope stage, fixing the chamber on a hydraulic manipulator, and adjusting the microscope focus and

electrodes position above the cell. As a result, flux measurements normally started when the temperature of the solution, and presumably that of the cell, had increased to about 6-7 °C. Measurements continued as the solution temperature gradually grew towards the ambient temperature. The measurements lasted for ~ 40-50 min. This was sufficient for the bulk solution temperature to reach a steady-state level. The changes in solution temperature over time for two ambient temperatures used are shown in Fig. 4-20.

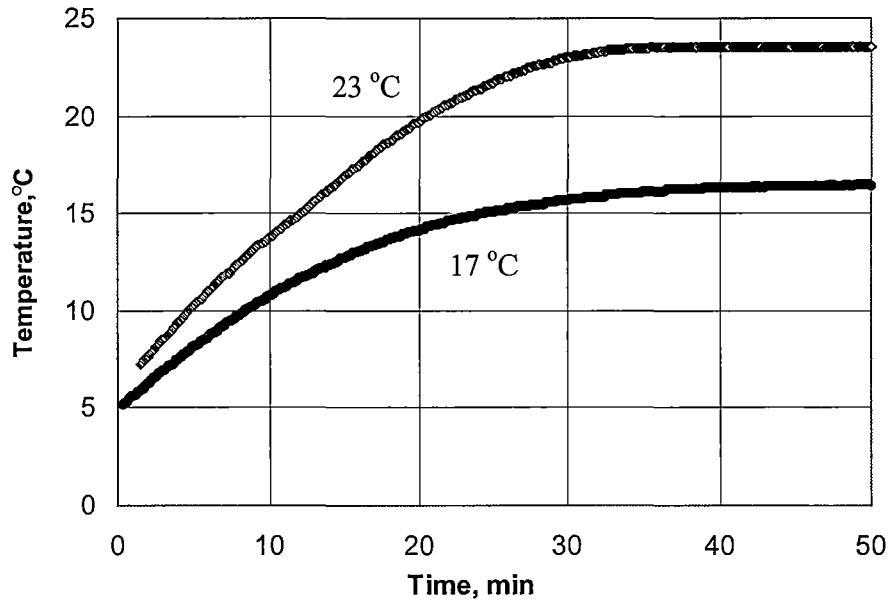

Fig. 4-20. Temperature changes of the bath solution for two ambient temperatures, 17 and 23 °C, respectively. Typical examples for the two ambient temperatures used are shown (n=7). Data acquisition was every 5 sec.

A calibration curve was constructed to enable temperature determination at any given time using voltage output data (Fig. 4-21). For that reason temperature and the corresponding voltage changes were recorded in a chamber using a digital multimeter and a miniature thermistor, respectively, inserted into the chamber. The calibration curve was used to establish the relationship between the net ion flux and temperature changes.

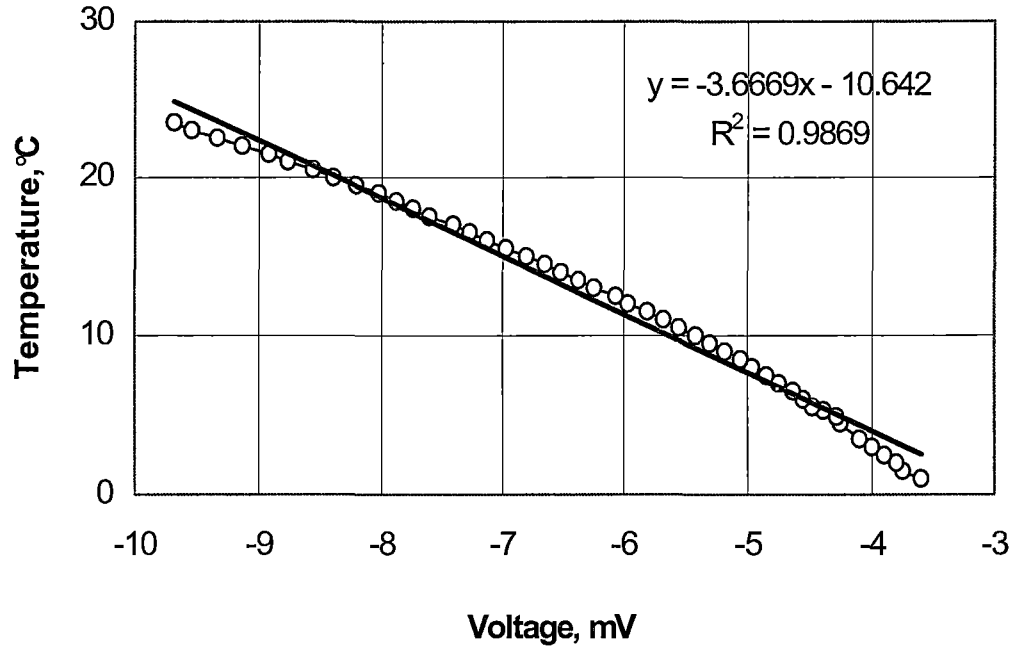

Fig. 4-21. Calibration curve. The chamber with measuring solution was kept at 4°C for 2 h followed by a return to room temperature. The temperature in the chamber was measured by a hermocouple and the corresponding voltage was recorded using the MIFE electrometer. The calibration curve is based on three individual experiments. Indicated SEM (n=3) are smaller than symbols. The calibration curve was used during the experiments for temperature change estimation in the chamber by recording the voltage with a miniature thermistor inserted into the chamber.

The rate of temperature change (V_t) was determined as the average rate of temperature increase during the first 10 min of measurements. The temperature rose at different rates for the two room temperatures used. Mean temperature rate was 0.34 ± 0.02 °C min^{-1} for 17°C (n=10) and 0.99 ± 0.02 °C min^{-1} for 23°C (n=15).

4.6.2 Temperature-induced ion flux kinetics

Chilling treatment was found to significantly modify the magnitude of net fluxes of both measured ions. When a chamber with immobilized thraustochytrid

cells was returned to ambient temperature after two hours of exposure at low (+4 ^{0}C) temperature, complex flux kinetics of recovery were measured (Fig. 4-22) and several apparent critical temperatures denoted as ACT_1 were observed.

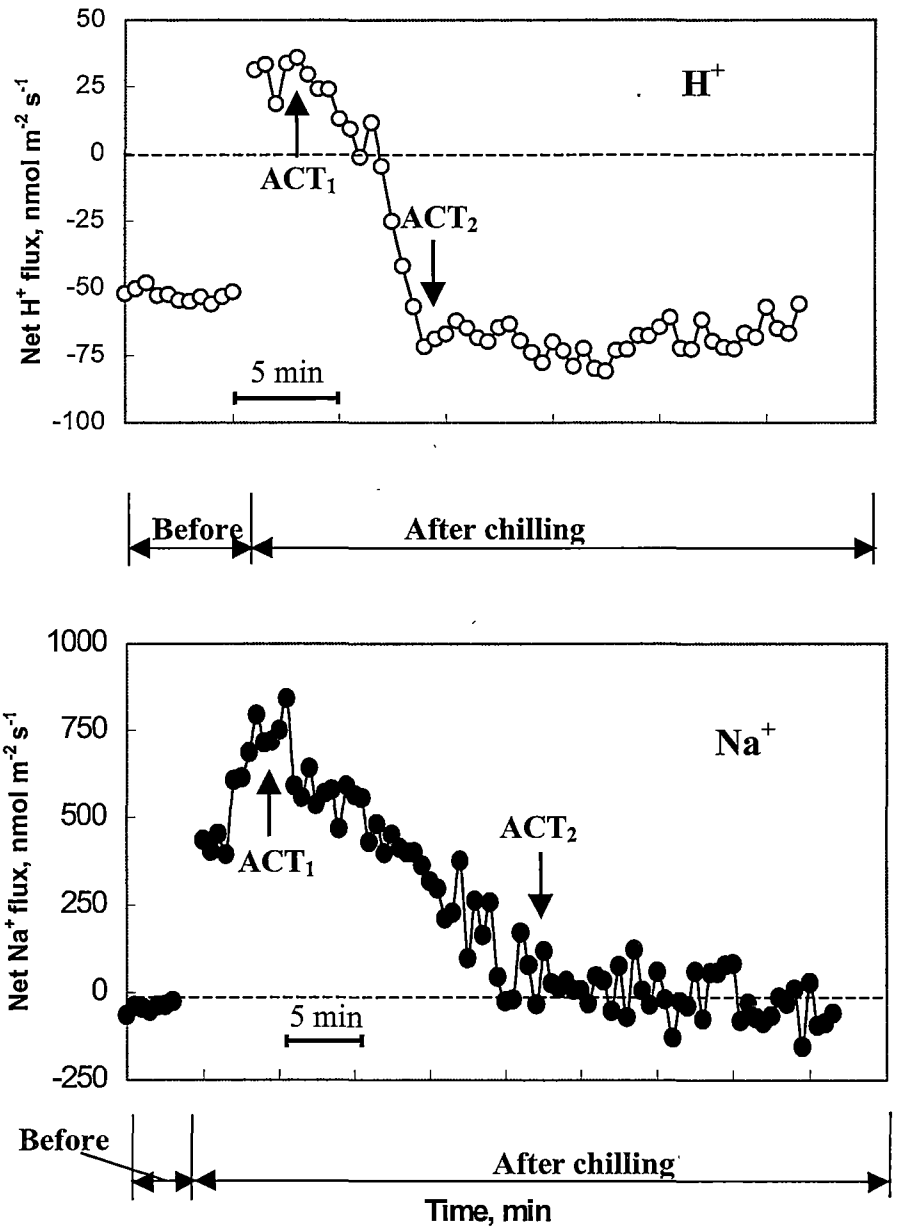

Fig. 4-22. Kinetics of H^+ and Na^+ flux responses to post-chilling as a function of time. One (out of 7) typical example is shown. Ambient temperature was 23 °C. Net ion fluxes from the same cell before and after 2 h chilling are shown. Time scale is indicated by a bar.

Low temperature caused a significant shift towards net H^+ and Na^+ influx (Fig. 4-22). Immediately after the chamber was transferred to room temperature, a dramatic influx of both ions was observed. As the cell temperature reached some threshold (ACT_1), changes in flux kinetics occurred. This resulted in a significant drop in net flux of both ions towards an efflux (Figs. 4-22, 4-23).

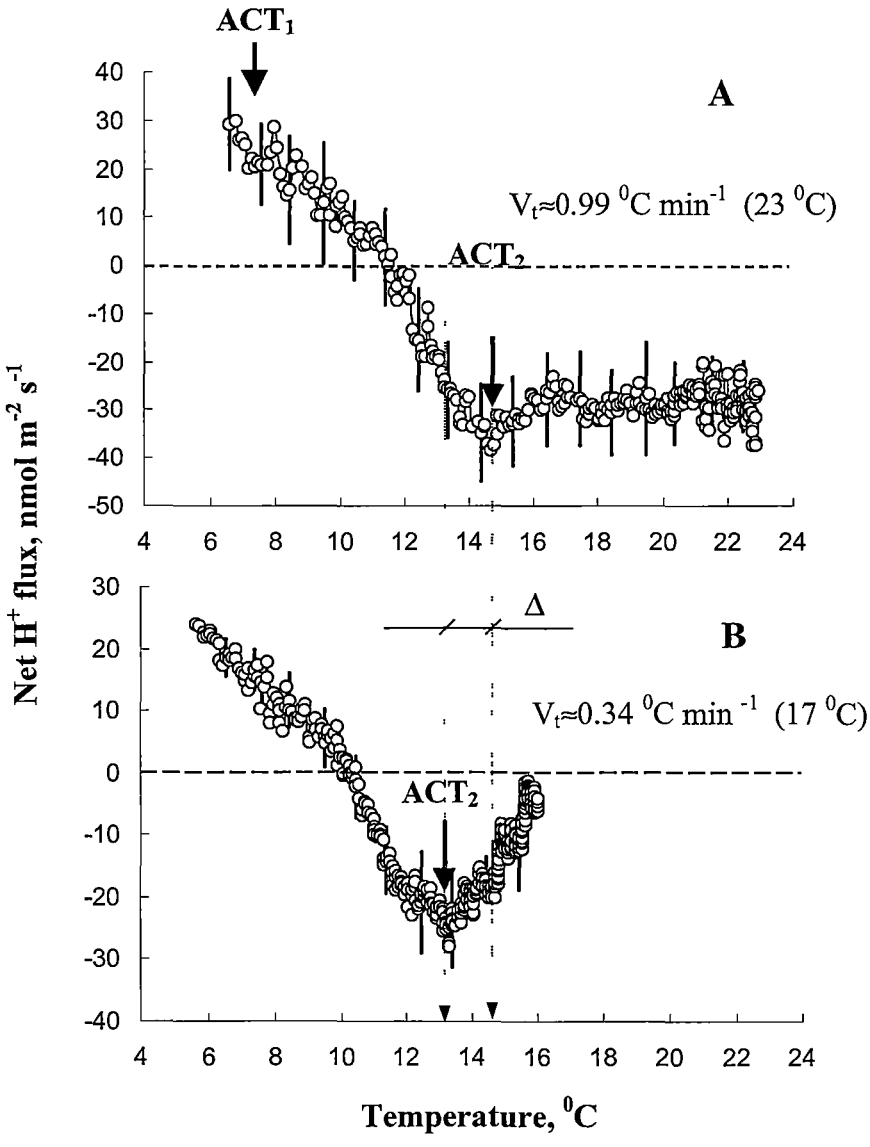

Fig. 4-23. Kinetics of net H^+ flux recovery for two different ambient temperatures. Rates of temperature change were estimated for both ambient temperatures as an average for measured cells (see Figs. 4-24 and 4-25). Data are SEM (n=4).

When the cells reached another critical threshold (ACT_2), the net efflux of H^+ and Na^+ reached its extreme value and either stabilised, or slightly reversed (Fig. 4-23B).

Metabolic processes that contribute to the observed flux changes are not instantaneous and require time before the resultant changes in the activity of PM transporters become evident outside the cell (and measured with microelectrodes). A strong dependence of ACT values on the ambient temperature used (and, consequently, rates of temperature change) was found. This is further illustrated in Figure 4-23, where traces of H^+ flux recovery from thraustochytrid cells are shown for two ambient temperatures.

It is obvious that the absolute values of ACT_2 showed a strong dependence on the rate of ambient temperature changes (Fig. 4-23). The slower the temperature recovery, the more accurate was the estimation of ACT values.

To avoid misleading conclusions based on the dependence of ACT on the rate of temperature changes, the real critical temperature (RCT) was calculated. RCT is associated with the actual temperature when the recovery of PM transporters takes place. Shabala and Newman (1997a) showed mathematically that the RCT value may be determined as the intercept of the line of best fit for a graph where ACT values are plotted against the rate of temperature changes. Using this approach, a relationship between ACT_1 and the rate of temperature change (V_t) was established for ACT_1 (Fig. 4-24) and ACT_2 and V_t for ACT_2 (Fig. 4-25) for both H^+ and Na^+.

Remarkably, despite the variation between ACT_1 values for H^+ and Na^+, the RCT_1 values were very close for both ions measured (7.82 ± 0.21 °C; intercepts for the lines of best fit in Fig. 4-24). A similar trend was observed for RCT_2 values for H^+ and Na^+ (Fig. 4-25) with an average value of 11.1 ± 0.22 °C.

These data are consistent with the observations on plant tissue, where six different ions measured had the same RCT near 7 ^{0}C (Shabala and Shabala, 2001).

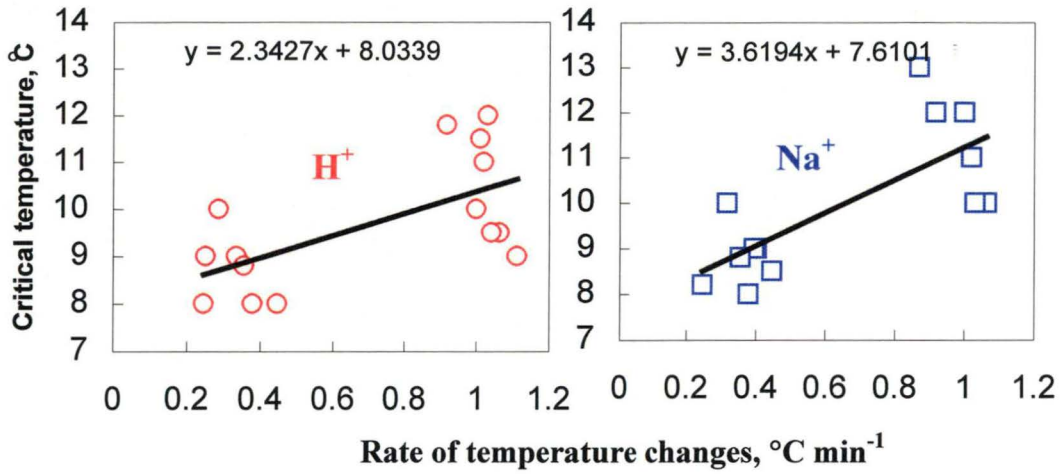

Fig. 4-24. Relationship between apparent critical temperature ACT_1 and the rate of temperature changes, V, for H^+ and Na^+. Each point on the graph represents an ACT value from an individual thraustochytrid cell. The real critical temperature (RCT) is defined as the intercept of the line of best fit with the Y-axis (shown as a constant term in the equation for each graph). The RCT values were similar for both ions measured (8 and 7.6 ^{0}C).

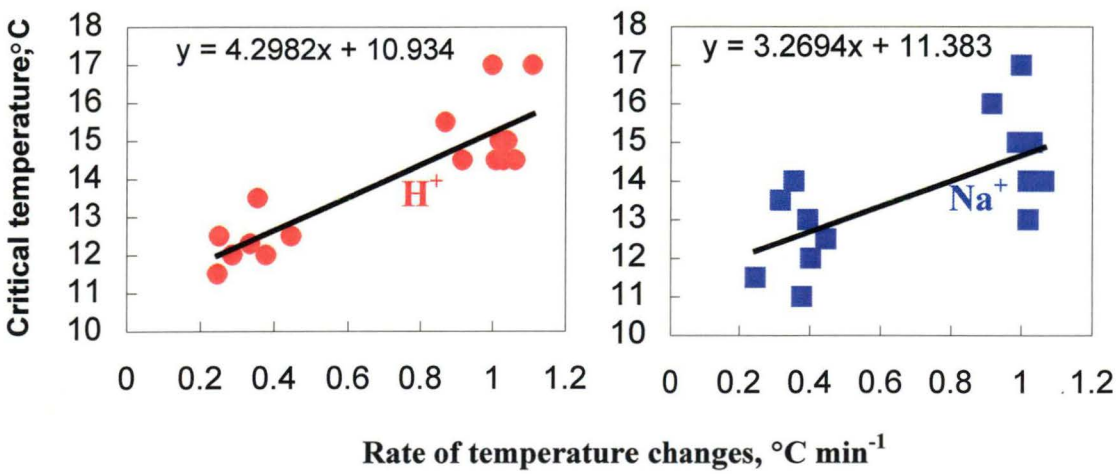

Fig. 4-25. Relationship between apparent critical temperature ACT_2 and the rate of temperature changes for H^+ and Na^+ fluxes. The RCT values were defined as indicated in Fig.4-24. They are 10.9 and 11.4 °C for H^+ and Na^+, respectively.

To elucidate the ionic mechanisms involved in post-chilling recovery of net H^+ fluxes measured from the thraustochytrid ACEM C cell, a series of experiments were conducted using orthovanadate, a specific inhibitor of P-type H^+-ATPases were conducted. Pretreatment was performed for 15 min after adaptation of cells at room temperature prior to chilling at 4 °C. Preparation of the stock solution of orthovanadate is given in Appendix B.

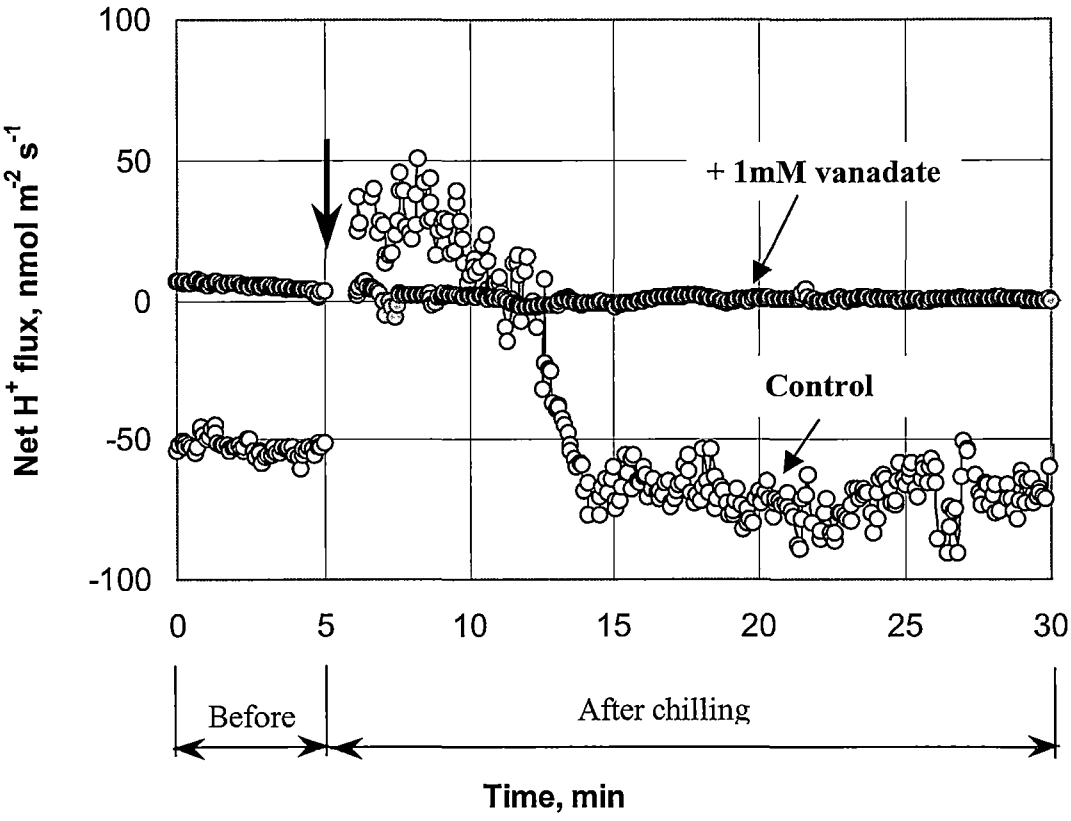

Fig. 4-26. Net H^+ flux responses to temperature changes. At the moment indicated by the arrow, cells were transferred from 4 ^{0}C to 23 ^{0}C. Recovery of H^+-pump activity (resulting in increased net H^+ efflux) is seen in control (open symbols) while in vanadate-treated cells (closed symbols) such recovery did not occur. The same cell was monitored before (0 to 5 min in a graph) and after 2 h chilling treatment (after 7th min in a graph).

Vanadate (1 mM) treatment resulted in an almost complete elimination of the H^+ response to post-chilling recovery, indicating the involvement of the H^+-ATPase in the observed kinetics of H^+ flux (Fig. 4-26). This supports the possible involvement of the H^+-pump in mediation of thraustochytrid ACEM C responses to chilling stress.

4.6.3 Underlying mechanisms

The ability of the cell to control membrane transport processes may be important in determining the temperature kinetics for a particular organism. Membrane permeability to ions was reported to be temperature dependent (Svobodova et al., 1995; Gruwel et al., 1998; Van de Vossenberg et al., 1995, 1999). The control of membrane permeability represents an important part of adaptation to high and low temperatures (Svobodova et al., 1995; Van de Vossenberg et al., 1995, 1999). Van de Vossenberg et al. (1999) demonstrated that bacterial cells were able to maintain the proton permeability of the cytoplasmic membrane at a low value within the range of growth temperatures (16-50 °C). Membrane permeability to both proton and sodium was reported to increase with temperature and was comparable for the species of different optimum growth temperatures at their respective growth temperatures (Van de Vossenberg et al., 1995, 1999).

Temperature dependent changes were also reported for the transport of a number of ions (Clarkson et al., 1988; Gruwel et al., 1998; Andjus et al., 1999; Stinner and Hartzler, 2000). Lowering temperature was shown to reduce proton and sodium transport (Clarkson et al., 1988; Dinno and Nagel, 1988; Morgunov and Hirsch, 1991). It is commonly found that diffusive efflux of ions increases in the cold (Wasserman et al., 1986; Clarkson et al., 1988). For example, sodium loss at 2 °C and the consequent influx at 37 °C was reported for animal cells (Wasserman et al., 1986).

The issue of whether ion transporters at the PM of thraustochytrid ACEM C exhibit similar temperature dependence was the topic of this study. To my knowledge, no attempt to directly measure the flux kinetics of different ions *in situ* as a function of temperature has been undertaken in a unicellular organism. Using the

unique advantage of the MIFE technique, it was demonstrated that post-chilling recovery resulted in a dramatic influx of both proton and sodium ions followed by the efflux. Moreover, the absolute values of RCT_1 for thraustochytrid ACEM C were very similar to those found for H^+, K^+, NH_4^+, Na^+, Ca^{2+} and Cl^- in plant tissues (Shabala and Shabala, 2001; Fig. 4-26).

Changes in lipid composition, carrier activity, and permeability have been shown to occur at the membrane level (Clarkson et al., 1988; Hällgren and Öquist, 1990; Mustafa et al., 1999 and references therein). Lowering the tissue temperature may directly affect the structure and function of the PM transport enzymes (Hawley, 1971; Mustafa et al., 1999) and porins (De et al., 1997). Recent work by De and coworkers (1997) suggests that a change in the structure and function of porins could be responsible for the differential permeability of the membrane at different temperatures. These authors showed that the outer membrane permeability of the psychrotrophic bacterium *Pseudomonas fluorescens* is increased at the optimum growth temperature (28 ^{0}C) when compared to the low growth temperatures (8 ^{0}C).

There is much evidence in the literature that cold inactivation of H^+ transporting systems is among the most sensitive membrane-transport processes (Clarkson et al., 1988; Kennedy and Gonsalves, 1988; Kasamo et al., 2000). When the principal processes generating ATP temporarily collapsed under chilling conditions, the ATP-driven efflux of H^+ was shown to decrease (Clarkson et al., 1988). That is expected to cause significant membrane depolarisation. Evidence for such a depolarisation in response to cold shock has been previously reported in the literature (Apte and Thomas, 1986; Clarkson et al., 1988; Lewis et al., 1997; Imada and Oosawa, 1999; Piotrowska et al., 2000). A subsequent shift in the values for the Nernst potential will enhance passive cation leakage from the cells, - a phenomenon observed by Shabala and Shabala (2001) in experiments with plants. The opening of voltage-dependent channels, highly selective for sodium ions, was shown to underlie the depolarization obtained in *Xenopus* oocytes (Charpentier, 1999). The opening of the oocyte sodium channels was reported to be modulated by the temperature of the bathing medium. Cells were reported to become leaky and membranes less fluid immediately after cold shock (Apte and Thomas, 1986; Barbaro et al., 1999). *Vice*

versa, post-chilling recovery might result in a reverse transport of ions, resulting in initial net H^+ and Na^+ influx as shown in the present study. The involvement of mechanosensitive stretch-activated channels in temperature response and ion transport regulation was suggested (Reifarth et al., 1999). The probabilities of these channels being open in oocytes of *Xenopus laevis* increased strongly when temperature was raised from 21 to 27 °C and the channels were shown to be cation non-selective. Temperature dependence of monovalent cation fluxes in isolated rat hearts using NMR was reported to correlate well with previously observed membrane phase transitions in these systems (Gruwel et al., 1998).

Restoring membrane fluidity was reported to be accompanied by taking K^+ into the cell (Barbaro et al., 1999). Potassium entry in response to warming the external solution was reported to occur instantaneously (Willis and Anderson, 1998). The time course for Na^+ loss from animal cells after a shift from 37 to 2 °C was shown to consist of two components: a rapid efflux that was completed after 30 min, and a slow component that required at least 24 h for completion (Wasserman et al., 1986). Here a similar timeframe is reported for ion flux recovery (Fig. 4-22).

For many years, phase transition in membrane lipids was believed to be central to chilling stress perception (see reviews by Nishida and Murata, 1996; Russell, 1990). This phase transition was shown to occur within a wide range of temperatures (15 to 35 °C in bacteria) (Stein, 1990). However, more recent reports indicate that the phase transition temperature is kept below the growth temperature due to the changes in FA composition that distort membrane order (van de Vossenberg et al., 1999). For example, the phase transition temperature of membrane lipids in zebrafish (*Brachydanio rerio*) oocytes was shown to be 10 °C below the normal physiological range for this organism (Pearl and Arav, 2000). Thermotropic phase transitions were reported to be related to the temperature at which direct chilling injury affected the integrity of the membranes. Lipid phase transition, which was evaluated using Fourier transform infrared microscopy, occurred at the temperatures at which membrane integrity damage was maximal (Arav et al., 2000; Pearl and Arav, 2000).

Specific mechanisms underlying the effects of membrane phase transition on activities of PM transporters remain to be elucidated. Several possibilities including

conformational changes of transport proteins (changing affinity), or indirect effect due to modification of the physical properties of the lipid environment, have been suggested (Clarkson et al., 1988). As most membrane transporters are coupled via membrane potential, conformational changes in one transport protein will most likely have a domino effect on the activity of the others.

Experiments with vanadate suggest that H^+-ATPase might be a primary "suspect" for such a role. This is in accord with the reports in the literature which suggest that active H^+ transporters are among the most sensitive to temperature stress, as was shown for plants (DuPont, 1989; Yoshida, 1994; Yoshida et al., 1999) and yeast (Panaretou and Piper, 1992; Coote et al., 1994). Decrease in pH_i was shown to stimulate ATPase activity (Kobayashi et al., 1986; Anand and Prasad, 1989; Holyoak et al., 1996). Net H^+ efflux, reported in the present study immediately after re-warming the chamber at room temperature (Figs. 4-22 and 4-23) is expected to be reversed in the chilling situation. Therefore, net H^+ influx would take place in response to temperature decrease that is expected to result in cytosol acidification. That might lead to activation of H^+-ATPase and subsequent H^+ extrusion. This scenario agrees with the observation of increased H^+ efflux followed after H^+ influx (Fig. 4-23). The cumulative evidence leads to the conclusion that membrane H^+-ATPase is essential for thermoadaptation.

Based on literature data discussed above, RCT_1 determined (7.8 °C) might be attributed to the phase transition temperature in the plasma membrane of thraustochytrid ACEM C. At this temperature, significant changes in activity of PM transporters for different ions begin. As soon as the temperature returns to the optimal range required for the activity of cellular enzymes, the pumps and ion exchange systems operate at the optimal rate (Mustafa et al., 1999). Therefore, it might be suggested that the second critical point, ACT_2, when flux stabilization occurs, indicates the temperature required for complete recovery of the transporters after low temperature treatment.

4.6.4 Conclusion

Application of the MIFE technique was extended to study membrane transport processes in post-chilling recovery. Strong relationship between temperature and the activity of the ion transport system was demonstrated. The post-chilling recovery was associated with a dramatic H^+ and Na^+ influx. The kinetics of both ions showed two apparent critical temperatures that have been used to estimate the corresponding RCT values. These were found to be similar for both ions and it was suggested that RCT_1 (7.8 °C) may be associated with the phase transition of the PM lipids of thraustochytrid ACEM C. The physical interpretation for the observed apparent critical temperatures is that at ACT_1 H^+ and Na^+ transporters are re-activated, while ACT_2 is associated with their complete recovery after chilling. Evidence for involvement of H^+-ATPase in regulation of post-chilling recovery was demonstrated by experiments with vanadate. The practical significance of this work includes the ability to determine critical temperatures of ion transporters by estimation of RCT_1 in a one-step experiment, adding a new dimension to better understanding of thraustochytrid cell physiology.

Chapter 5

APPLICATION OF THE MIFE TECHNIQUE TO STUDY MEMBRANE – TRANSPORT PROCESSES AT THE BACTERIAL POPULATION LEVEL

Due to their small size, application of non-invasive microelectrode measurements on a single bacterial cell will be very difficult, if not impossible. To overcome the problem, the candidate developed a novel approach, where ion fluxes were measured from the surface of bacterial "monolayers" (a population of cells, immobilised on the supporting surface and forming a dense single-cell layer). The MIFE technique was applied to study specific features of membrane-transport processes in these monolayers, associated with bacterial growth and adaptive responses. The major focus was on three different types of bacteria: *Escherichia coli*, *Listeria monocytogenes* and *Lactobacillus bulgaricus*.

L. monocytogenes and *Lb. bulgaricus* are Gram-positive bacteria that employ different strategies to adapt their metabolism to an acid environment. In this study, H^+ flux kinetics from these organisms were studied in response to acid treatment.

In another case study, *L. monocytogenes* was used as a model organism to explore the potential of MIFE to study the mode of action of nisin, an antimicrobial additive used to control Gram-positive bacteria including *L. monocytogenes* in the food industry.

The association between membrane-transport activity and cell growth was studied using another food-borne bacterium, *E. coli*, as an example. The fluxes of 4 ions (H^+, Ca^{2+}, K^+, and NH_4^+) were measured at different stages of cell growth as a function of substrate (glucose) availability.

Finally, the feasibility and prospects of combining the MIFE technique with another method employed to study bacterial adaptive responses, specifically, Fluorescence Ratio Imaging Microscopy (FRIM) was investigated. Again, *L. momocytogenes* responses to acid stress were used as a case study.

5.1. Non-invasive microelectrode ion flux measurements on immobilised bacteria: a feasibility study

Before specific issues related to bacterial adaptive responses were addressed, a general study on feasibility of ion flux measurements from bacterial cells was conducted. Bacteria are diverse in structure, and it was considered possible that this diversity could impose limitations on the applicability of the MIFE technique. For example, the double membrane system in Gram-negative bacteria like *E. coli* might impose limitations on ion movement from the cell. The different thickness of the cell is another potentially confounding factor. It is known that it is more difficult to make and patch giant spheroplasts from Gram-positive, than from Gram-negative bacteria (B. Martinac, pers. comm.).

Apart from a general feasibility study, enabling further research on specific aspects of bacterial physiology, the effect of the growth phase on bacterial membrane-transport activity was evaluated by comparing the net H^+ flux measured at two distinct phases of growth (exponential and stationary). Several bacteria, differing in both cell wall structure (Gram-negative and –positive) and cell morphology, were used.

5.1.1 Feasibility of MIFE flux measurements from different bacteria

The specific characteristics and growth conditions of bacteria used in this study are given in Table 2-1. Culture preparation and cell immobilisation are described in Section 2.1.2 and 2.2.3, respectively. Microelectrode preparation, flux measurements and data analyses are described in Section 2.3. Experimental solution N2 (Appendix A) was used for flux measurements. Net H^+ flux was measured from immobilised cells at two distinct phases of growth: exponential and stationary. The growth phase of bacterial populations was determined using a spectrophotometer as described in Section 2.1.2 and shown in Figure 2-1. Flux measurements were performed under static conditions: 4 to 7 sites were assessed from a glass-slide with immobilized bacteria. Measurements at each site lasted for 2-3 min followed by re-positioning of the microelectrodes to another site typically 100-200 μm apart. The average values of

net H^+ fluxes for a number of bacteria in the exponential and stationary phases of growth are presented in Table 5-1.

Table 5-1. Net H^+ flux in the exponential and stationary phases of growth defined for different bacteria

Species	Exponential phase		Stationary phase	
	Net H^+ flux, nmol m^{-2} s^{-1}	SEM	Net H^+ flux, nmol m^{-2} s^{-1}	SEM
Escherichia coli M23	-9.29	0.57	-2.08	0.39
Salmonella typhimurium	-6.00	0.08	-1.8	0.43
Klebsiella oxytoca	-9.67	0.66	-3.26	0.12
Enterobacter sp.	-7.31	0.24	-4.37	0.13
Staphylococcus aureus	-13.92	0.79	-6.67	0.52
Listeria monocytogenes Scott A	-9.01	0.65	-2.67	0.08
Bacillus cereus	-0.23	0.07	0	0.04

Cultures were prepared and immobilized on a cover slip as described in Sections 2.1.2 and 2.2.3. Experimental medium for bacteria N2 (Appendix A) with the addition of 10 mM of glucose was used. SEM is standard error of 2-4 experiments with measurements from N=4-7 bacterial sites in an individual experiment.

Significant ($P < 0.01$) differences in net H^+ fluxes between exponential and stationary stages of growth were observed for all bacteria studied (Table 5-1). This may be caused by a decreasing metabolic activity of stationary-phase cells (i.e. cessation of growth). Increased acid tolerance in stationary-phase populations was shown to correlate with a decrease in permeability of the cell envelope to protons (Jordan et al., 1999a). This implies that both efflux and influx of protons are reduced resulting in a decrease in the net H^+ flux value.

The magnitude of net H^+ flux of several bacteria belonging to the Enterobacteriaceae (viz: *Escherichia coli*, *Salmonella typhimurium*, *Klebsiella oxytoca*, *Enterobacter* sp.) was similar for each growth phases studied, respectively.

The magnitude of net H^+ flux of a Gram-positive bacterium *L. monocytogenes* was similar to one of the Enterobacteriaceae family (difference not significant). Differences might be observed under stress conditions if the strategy of survival is different. This could be the subject for future studies while the aim of the present work was to establish the method and demonstrate its applicability to different bacteria.

Staphylococcus aureus, another Gram-positive bacterium, demonstrated a higher level of proton extrusion then any other bacterium studied in both growth phases with $P<0.01$ (Table 5-1).

In contrast, the net H^+ flux of *Bacillus cereus* was close to zero for both the exponential and stationary-phase cells (Table 5-1). *Bacillus cereus* is known for its feature to form endospores, and a consequent resistance to many adverse conditions. The small net H^+ flux might be the result of a balanced state of this bacterium.

5.1.2 Effect of growth phase on flux magnitude

A significant body of information supports the notion that the ability of bacterial cells to survive a number of stresses depends on growth phase. It is generally accepted that stationary-phase cultures acquire natural resistance to a variety of environmental stresses. Growth-phase-dependent acid, heat, and salt tolerance of *E. coli* and *S. typhimurium* requires the stress-specific sigma factor RpoS for full induction (Cheville et al., 1996). RpoS is a regulatory factor that is necessary for the transcriptional activation of a large number of genes required for tolerance to environmental stress (reviewed by Lowen and Hengge-Aronis, 1994). A similar general stress transcription factor, called sigma B, was found in the Gram-positive bacteria *B. subtilis*, *L. monocytogenes*, and *S. aureus* (Becker et al., 1998; Wiedmann et al., 1998).

Stationary-phase *E. coli* have higher levels of acid tolerance compared to their exponential-phase counterparts (Arnold and Kasper, 1995; Benjamin and Datta,

1995; Jordan et al., 1999b). Similar patterns have been reported for *S. typhimurium* (Rowbury, 1995) and *L. monocytogenes* (Davis et al., 1996; O'Driscoll et al., 1996).

E. coli cells are also known to increase the cyclopropane fatty acids (CPFA) content of their membranes upon entry into the stationary phase (Cronan, 1968). A similar increase in cFA was demonstrated in acid-adapted *E. coli* cells that was correlated with better survival following an acidic shock (Brown et al., 1997) as was a change in the lipid composition of a Gram-positive bacterium *Clostridium acetobutylicum* grown at an acidic pH (LePage et al., 1987). Changes in the lipid composition of membranes have been suggested to affect proton conductance reducing the leakage of protons across the membrane when the external proton concentration is high (Jordan et al., 1999a).

5.1.3 Conclusion

The feasibility of net H^+ flux measurements for both Gram-negative and Gram-positive bacteria was demonstrated. This opens the possibility to study membrane-transport processes, associated with bacterial growth and adaptive responses, in a variety of food-borne microorganisms. Significant differences were found in the magnitude of net H^+ fluxes for bacteria in the exponential and stationary phase of growth. As bacterial cells progressed from the exponential to stationary stage of their growth, a significant decrease in net H^+ efflux through the plasma membrane was measured.

5.2. Ion flux kinetics associated with bacterial growth: a case study using *E. coli*

In this study, several issues relevant to growth and nutritional status of *E. coli* were addressed. As ion-flux measuring technique is novel to food microbiology, net ion flux measurements were compared with traditional concentration measurements in batch cultures at analogous stages of the population growth cycle and with different concentrations of glucose. Four major ions (H^+, K^+, NH_4^+, and Ca^{2+}), important in bacterial cell homeostasis, were studied.

5.2.1 Bacterial strain and culture conditions

E. coli SB1 cultures for experiments were grown and prepared as described in Section 2.1.2 and Table 2-1. Cultures were harvested at the exponential phase of growth (OD_{540}=0.3 A), late exponential (OD_{540}=0.8 A), and stationary phases (culture grown for 16 h, OD_{540}=1.4 A), washed and suspended in bacterial experimental solution N1 (Appendix A), and kept on ice for up to 2 h until use. The concentration of glucose varied from 0.1% (w/v) ("high") to 0.05% (w/v) ("intermediate"), and 0.01% (w/v) ("low"), depending on the design of the experiment. Cell immobilisation on a cover-slip and following flux measurements are described in details in Sections 2.2.3 and 2.3.

In some experiments, carbonyl cyanide-*m*-chlorophenyl hydrazone (CCCP) (C 2759, Sigma Chemical Co.) was included in the medium (concentration range 10-200 μM). Preparation of stock CCCP is described in Appendix B.

5.2.2. Concentration changes *vs* ion flux measurements

A series of experiments was undertaken to elucidate a possible association between ion flux kinetics and the phase of population growth cycle in liquid culture. Aliquots (≈3 mL) of the culture were aseptically transferred from a 125 mL flask containing 30 mL of the culture into sterile vials at 15 min intervals, and concentrations of four ions (H^+, K^+, Ca^{2+}, and NH_4^+) were measured for 3-4 min with the same microelectrodes used for flux measurements. In a parallel experiment,

growth parameters of *E. coli* batch cultures were estimated by measuring absorbance at λ=540 nm using a spectrophotometer.

Under the experimental conditions, the bacteria possessed classical biphasic growth patterns (Fig. 5-1), reaching the stationary phase in 2 to 6 h (depending on glucose concentration in the media) after inoculation.

High correlations (R> 0.9) of the growth patterns were found with changes in both the glucose uptake into the cell (Fig. 5-1 D) and with pH and Ca^{2+} changes in the media (Figs. 5-1 B, C). No lag phase was observed for any of the measured parameters. Both the growth patterns and associated concentration changes were dependent on glucose availability in the external medium.

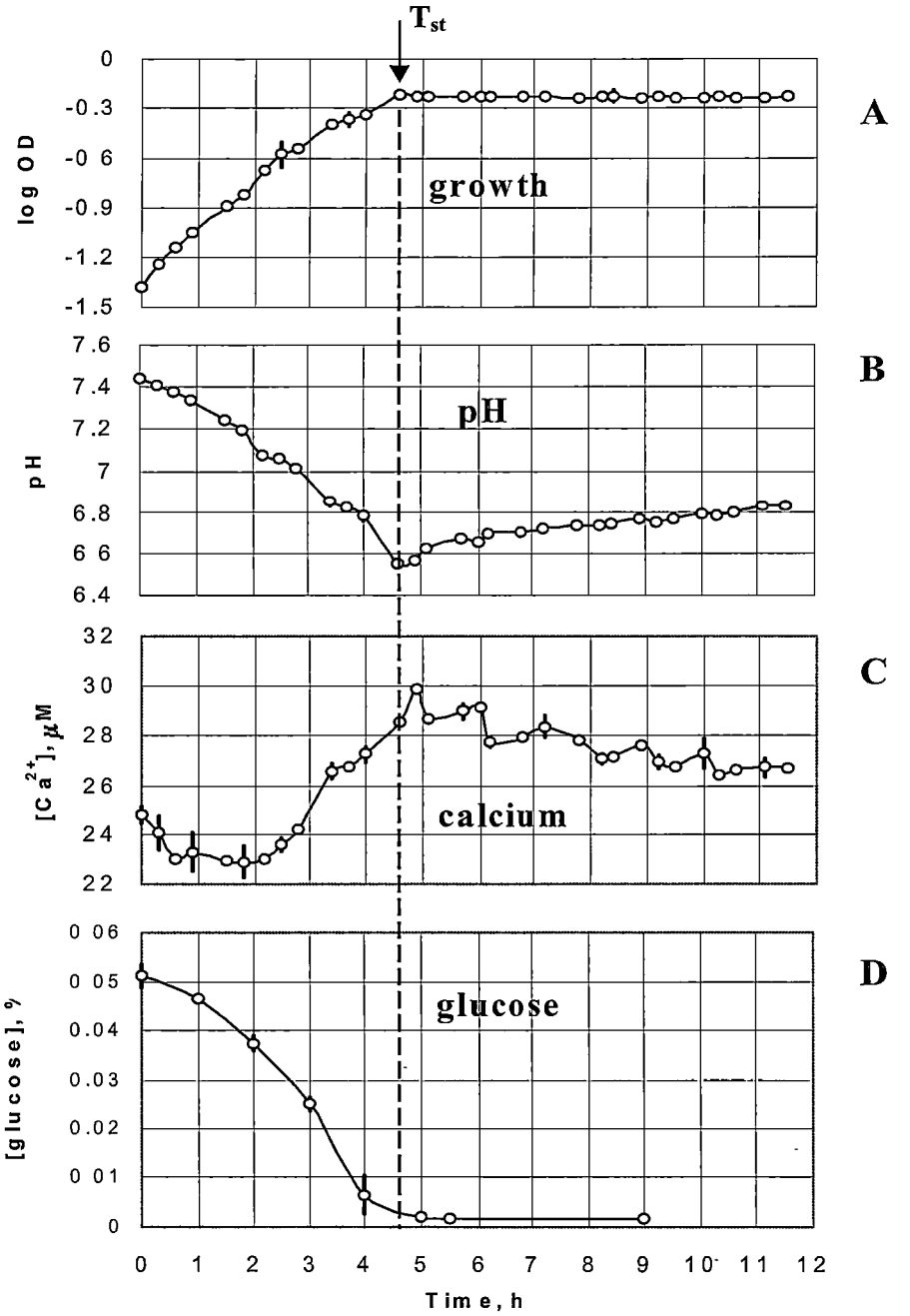

Fig. 5-1. Changes in OD (A), medium pH (B), Ca^{2+} (C) and glucose (D) concentrations in the batch culture of *E.coli* SB1 grown in modified minimal medium containing 0.05% (w/v) of glucose. Cultures were incubated in a water bath at 30° C with shaking at 60 rpm. Flasks were taken from the water bath for measurements at the indicated time. Each point represents the average value of 8 flasks from inoculation time up to 5 hours after reaching the stationary phase (indicated as T_{st} in the figure). Error bars are SEM (n=8).

Figure 5-2 illustrates differences in pH kinetics at three different levels of glucose in the batch culture. Quantitative information on the timing for onset of the stationary phase (T_{st}) as well as the magnitude of observed changes, are given in Figure 5-3.

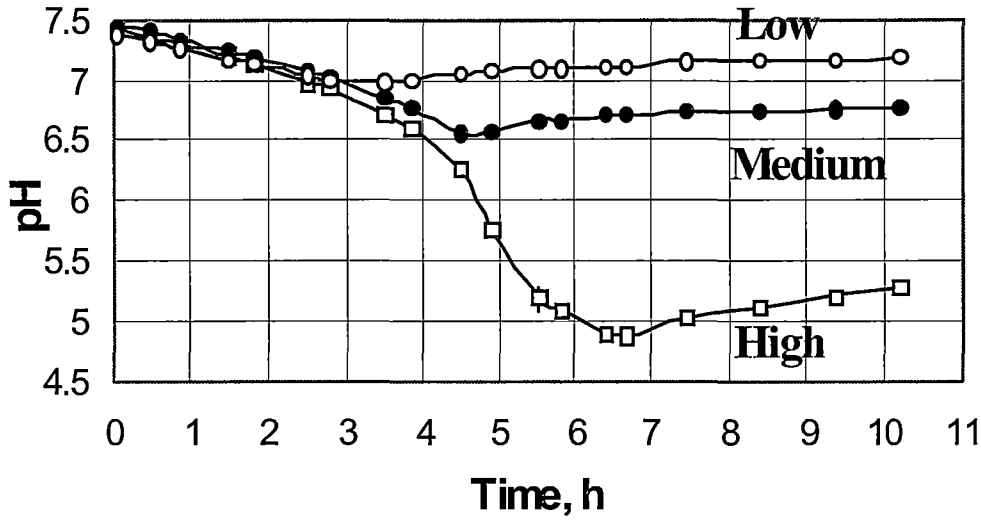

Fig. 5-2. Kinetics of external pH changes in the batch culture of *E.coli* SB1 grown at low (0.01%), medium (0.05%) and high (0.1%) glucose levels. Error bars are SEM (n=8).

Dependence of *E.coli* growth kinetics on glucose availability has been reported elsewhere. In aerobic conditions, such growth is usually accompanied by a fall in pH_o while pH_i is believed to remain constant (Russell and Rosenberg, 1979; Kashket, 1981; Booth and Kroll, 1983).

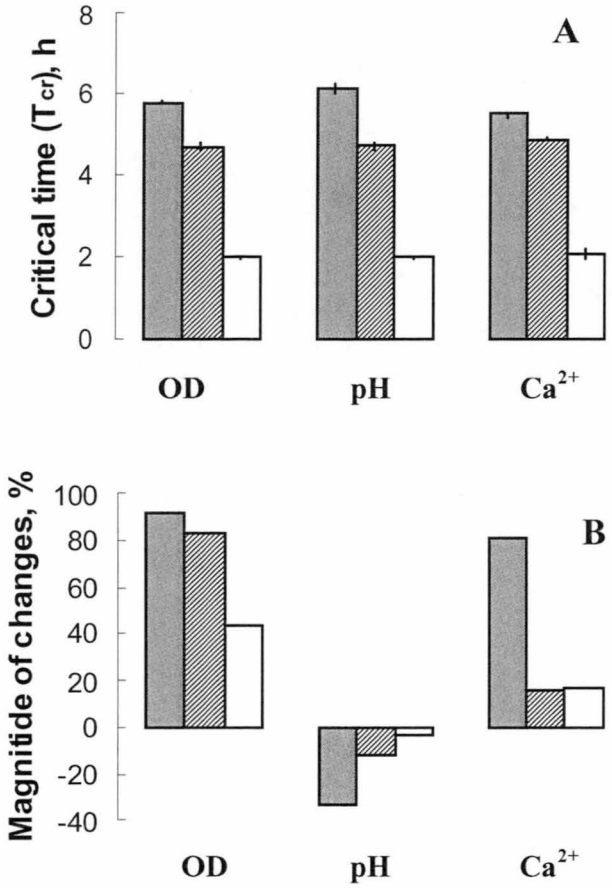

Fig. 5-3. A - Effect of glucose content on the time to onset of the stationary phase (determined as critical time, T_{st}).

B - the magnitude of observed changes (% of initial value) at T_{st}. Error bars are SEM (n=8).

Dark bars – high glucose;
dashed bars – medium glucose;
open bars – low glucose.

Also, most reported data describe the resultant pH changes at the exponential phase of growth, while a reversal of pH kinetics as the cells reach the stationary phase (Figs. 5-1B, 5-2) is described here. Several different mechanisms could be involved.

First, it could be a result of the changing transport activity at the plasma membrane of *E. coli* cells. In aerobically growing *E. coli*, H^+ ions are expelled by the respiratory chain (Harold and Maloney, 1996). Therefore, the acidification could be the consequence of increased respiratory activity of the *E. coli* population at the exponential stage of their growth (as a result of increased number of cells). Also, *E. coli* maintains a cytoplasmic pH of 7.5 to 7.8 over a wide range of external pH values (Padan and Schuldiner, 1987; Booth, 1999). One of the major sources of cytoplasmic pH perturbation are the essential metabolic processes associated with growth and metabolism (Booth, 1985). Apart from internal buffering, pH_i homeostasis may be maintained by controlled movement of cations across the plasma membrane. In

particular, K^+ transport is believed to play a major role in pH homeostasis in *E. coli* and other bacteria living at neutral pH (Booth, 1999). Other co-transport systems may also be involved (Na^+/H^+ and H^+/P_i ; Russell and Rosenberg, 1979).

Another reason for acidification of the medium could be the formation of acidic by-products by growing cells. Under aerobic conditions, glucose is transported into *E. coli* cells by the phosphotransferase system (PTS). As the result of growth on excess glucose, acetate and lactate are formed and exported (Luli and Strohl, 1990) and, therefore, may contribute to the decline in pH_o. The observed acidification of the batch culture during the late exponential phase of growth (Fig. 5-1B) is consistent with literature reports (Kashket, 1981; Booth and Kroll, 1983; Luli and Strohl, 1990).

When cells reached the stationary phase (T_{st}), a gradual alkalinization of the media was observed (Fig. 5-1B). This might also have several causes. First, part of the glucose converted into acetate and released into the medium might be reabsorbed and metabolized (Neijssel et al., 1996), causing the pH_o to rise. Cell lysis during the stationary phase is another possibility. NH_3 diffusion out of the cell can also contribute to the alkalinization process (Buurman et al., 1991). Finally, H^+ might be removed from the external medium in co-transport with some other inorganic ions.

The biphasic changes in Ca^{2+} concentration in the external medium (Fig. 5-1C) are an artifact of the changing pH, as discussed below.

5.2.3. Effect of CCCP on growth parameters

To elucidate the mechanisms of pH changes associated with *E. coli* growth, a known metabolic inhibitor of H^+ transport was used. CCCP in μM concentrations strongly affects H^+ transport across the PM acting as a protonophore and dissipating the PMF. Figure 5-4 demonstrates that addition of CCCP to the medium strongly affected growth parameters of *E. coli* SB1.

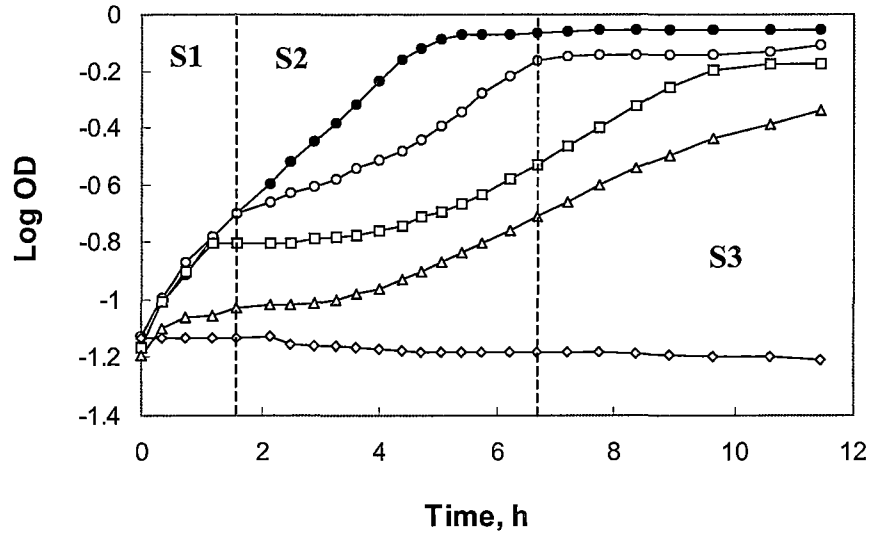

Fig. 5-4. Effect of protonophore CCCP on changes in log OD of the medium containing high concentration of glucose. Different concentrations of CCCP were added to flasks containing 0.1% glucose 15 min prior to inoculation. Flasks were incubated at 30 ^{0}C with shaking. Symbols: ● - control; ○ - 10 μmol l^{-1} CCCP; □ - 20 μmol l^{-1} CCCP; Δ - 50 μmol l^{-1} CCCP; ◊- 80 μmol l^{-1} CCCP. Zones divide the growth curve into stages according to sensitivity to CCCP (shown for 10 μmol l^{-1} CCCP).

Dose-response studies (Fig. 5-4) revealed that *E. coli* SB1 growth was completely arrested at CCCP concentrations of 80 μM and above. For concentrations below 80 μM, *E. coli* SB1 grew, however with significantly altered growth characteristics. Three stages in *E. coli* growth were evident in response to CCCP treatment below 80 μM (see for example 10 μM CCCP treatment in Fig. 5-4).

During the first stage (S1), a small difference in growth between the control and treated cells was noted. The duration of this stage was 0.35 to 1.6 h and showed a very strong negative correlation with CCCP concentration used (Fig. 5-4) as well as positive correlation with glucose concentration in the medium (data not shown). The second stage (S2) of bacterial growth, lasted for 5 to 11 h and was characterized by a significant increase in generation time and induced lag time. The magnitude of this increase was also directly dependent on CCCP concentration used. In the last stage (S3), both the control and treated cells reached almost the same OD, but at very

different times, also showing very strong concentration dependence. Similar patterns were observed for the middle- and low- glucose levels (data not shown).

In full agreement with the findings above (Fig. 5-4), the kinetics of pH changes correlated strongly with growth kinetics in experiments with CCCP. No characteristic biphasic pH changes were evident for variants treated with CCCP in concentrations of 80 μM and above (Fig. 5-5) implying a possible association between PM H^+ transport processes (affected by CCCP), and *E. coli* growth.

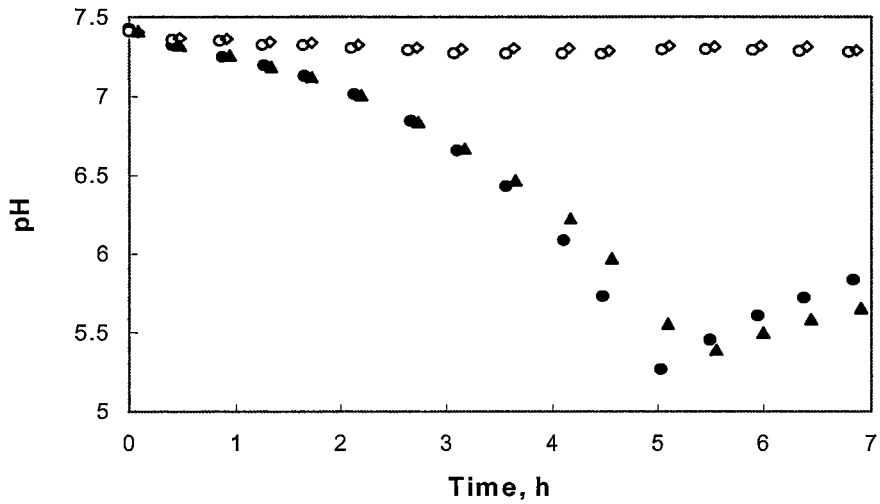

Fig. 5-5. pH changes associated with *E. coli* SB1 growth in control (closed symbols) and after 80 μM CCCP pretreatment (open symbols). Two replicates are shown.

Diez-Gonzalez and Russell (1997) reported that low concentrations of CCCP stimulated glucose consumption by *E. coli* cells, but higher concentrations were inhibitory. This is consistent with the above findings. The significance of glucose availability is supported by the fact that growth rates, viability, and protein concentrations of *E. coli* were not affected by the addition of 100 μM CCCP if bacteria were grown in the absence of glucose (Nagata, 1995). High efficiency of CCCP lethality for *E. coli* cells in the presence of glucose was attributed to the acidic pH of the culture due to metabolites from glucose, mainly lactic acid. The results are also consistent with those of Kinoshita et al. (1984) who showed that bacterial growth

was stopped immediately after a shift in the medium pH from 7.4 to 6.2 in the presence of 50 μM CCCP. When pH_o is not significantly different from pH_i values (stage S1 in the experiments), the effects of CCCP are also insignificant, and bacterial growth is slightly, or not at all affected (depending on CCCP concentration) (Fig. 5-4). As cell growth progresses, the metabolism of glucose by bacterial cells result in acidification of the external medium, and thus active H^+ extrusion becomes more critical (stage S2 in Fig. 5-4). Under these conditions, dissipation of the PMF by CCCP becomes a serious problem. The more CCCP is originally present, the higher the pH at which growth inhibition occurs. At CCCP concentrations above 80 μM, bacterial cells can not maintain pH_i homeostasis, and the cell growth is arrested.

However, the CCCP data must be interpreted with caution. It is unclear if membrane-transport processes are the only ones affected. If cell growth inhibition was among the primary targets, then non-growing cells consume much less glucose and, therefore, produce much less acetate and lactate. This could explain the lack of pH changes in CCCP-treated variants (Figs. 5-4, 5-5) assuming that acid production is responsible for acidification of the external medium. It is obvious that an unambiguous explanation of the involvement of membrane-transport systems in regulation of pH kinetics will come only from ***direct*** measurements of the net H^+ fluxes across the bacterial membrane.

5.2.4. Net fluxes at immobilised bacterial monolayers.

Kinetics of net H^+ fluxes associated with bacterial growth

Concentration measurements alone do not allow unambiguous interpretation of these results. Several mechanisms, including changes in respiratory activity (Harold and Maloney, 1996), membrane-transport processes at the plasma membrane (Padan and Schuldiner, 1987; Benjamin and Datta, 1995; Booth, 1999), formation of acid by-products (Luli and Strohl, 1990; Neijssel et al., 1996), cell lysis (Buurman et al., 1991) and others might be involved. However, when net H^+ fluxes were measured, a progressive increase in the net H^+ extrusion peaking at –150 nmol $m^{-2}s^{-1}$ for OD_{540}= 0.3A was found followed by a gradual return to zero net flux at late stationary phase (Fig. 5-6).

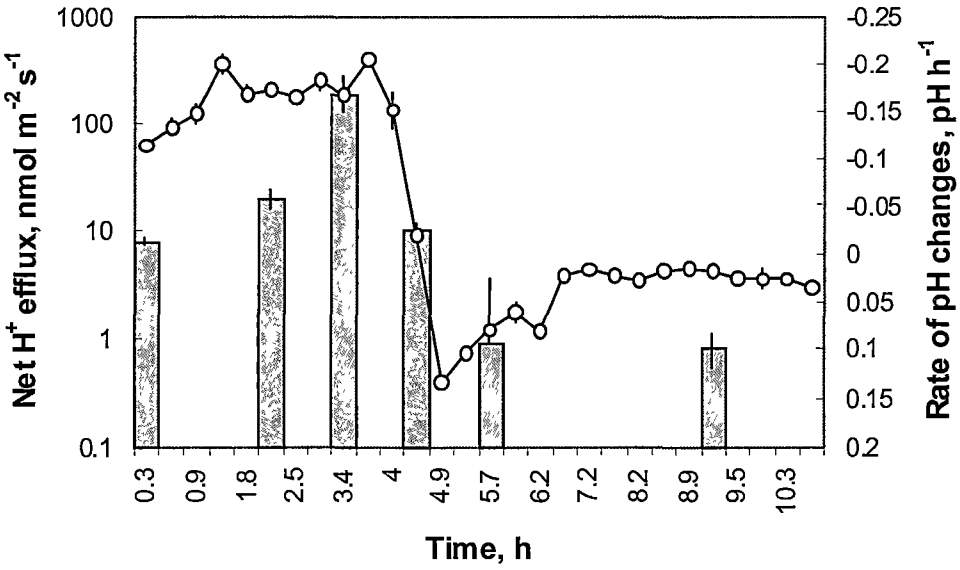

Fig. 5-6. Kinetics of pH changes for the *E. coli* SB1 cells in batch culture (open symbols) and associated net H^+ fluxes (bars) measured from the surface of immobilised cells prepared from confluent batch culture. Note the logarithmic scale for H^+ fluxes. Error bars are SEM (n=6).

There is close association between net H^+ flux changes and acidification of the medium (Fig. 5-6), with the magnitude of the net H^+ flux leading the resultant pH changes. This offers strong evidence that the observed acidification of the external media during exponential growth of *E. coli* originates mainly from net H^+ movement across the bacterial membrane. It appears that membrane-transport processes are major contributors during the exponential stage of growth. This conclusion was further supported by experiments with manipulation of substrate (glucose) concentration, where a strong dependence of net H^+ fluxes on external glucose concentration was found, and by experiments with CCCP (see above; Fig. 5-4, 5-5), a known protonophore dissipating the PMF across the PM.

5.2.5. Net ion fluxes at steady-state conditions

Fluxes of other ions also exhibited consistent changes associated with population growth. Figure 5-7 shows average flux values measured for H^+, K^+, NH_4^+, and Ca^{2+} for middle exponential (OD_{540}=0.3 A), late exponential (OD_{540}=0.8 A), and stationary phase (16 h old culture) of development.

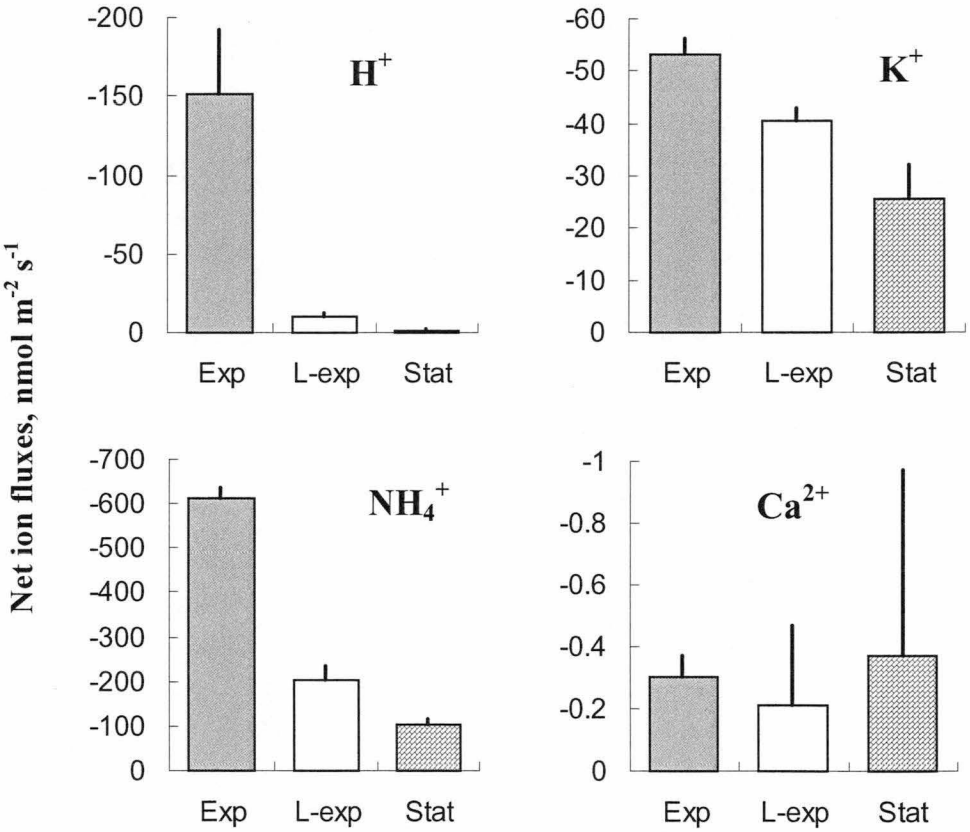

Fig. 5-7. Net fluxes of H^+, K^+, NH_4^+, and Ca^{2+} measured from immobilised bacterial cells prepared from middle exponential (Exp), late exponential (L-exp), and stationary (Stat) phases of culture development. Experimental solution N2 (Appendix A) was used to reduce the noise during flux measurements. Data are mean ± SE (n = 10, 8, 6, and 11, respectively).

Fluxes of K^+ and NH_4^+ displayed regular changes and showed strong dependence on glucose availability (Fig. 5-7). This is consistent with the essential roles of these ions in maintaining the homeostasis in *E. coli* cells (Neijssel et al., 1996). Note that the scale of the Ca^{2+} flux response is 1-2 orders of magnitude less

than other ions measured, and is of the same order as the background noise level. That indicates the absence of significant variation in net Ca^{2+} flux at different stages of bacterial growth.

5.2.6. Changes in Ca^{2+} concentrations

Unlike H^+, K^+, and NH_4^+, it was found that there were no significant net Ca^{2+} transport across the bacterial membrane (Fig. 5-8). Concentration measurements in batch cultures, however, showed complex biphasic kinetics (Fig. 5-1C), highly correlated (R=0.96) with population growth (Fig. 5-1A).

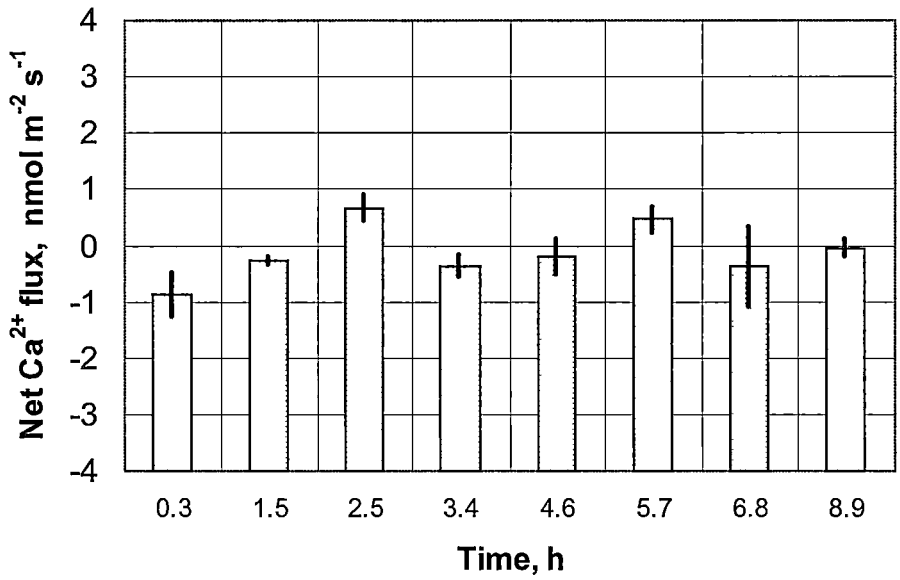

Fig. 5-8. Net Ca^{2+} fluxes from immobilised cells associated with different stages of growth of *E. coli* SB1 batch culture. Experimental solution N1 containing high (0.1%) glucose concentration was used. Error bars are SEM (n=5-8).

To explain the biphasic changes in the external Ca^{2+} concentrations in the medium (Fig. 5-1), it was hypothesized that such changes originate from Ca^{2+} binding to phosphate, known to be a pH-dependent process. Changes in the concentration of free Ca^{2+} in the cell-free medium were measured at different pH values (Fig. 5-9A). Figure 5-9B shows the striking similarity in the measured

changes in Ca^{2+} concentration and those changes calculated from observations in cell-free medium due to pH-dependent binding with phosphate. Therefore, it is suggested that biphasic Ca^{2+} concentration changes are merely a reflection of the changes in Ca^{2+} binding to phosphate due to modulation of the external pH in the batch culture.

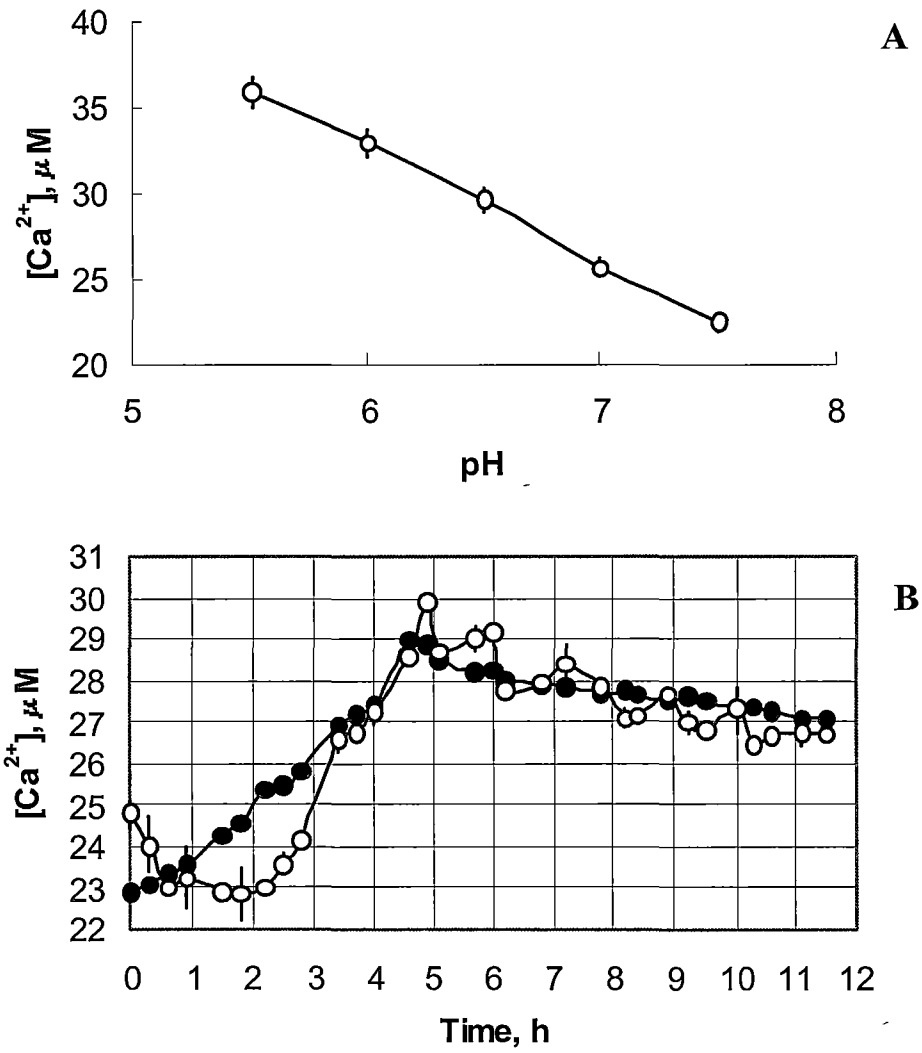

Fig. 5-9. A - pH dependent Ca^{2+} concentration measured in bacteria-free solution. **B** - measured changes in Ca^{2+} concentration (open symbols) in batch cultures compared with changes calculated from curve A (closed symbols) assuming pH changes as shown in Fig. 5-1B.

These examples illustrate advantages of net ion flux measurements over simple concentration measurements with ion-selective electrodes.

5.2.7. Conclusion

Non-invasive ion flux measurements, taken at different stages of bacterial growth, provided a less ambiguous interpretation of concentration changes in a culture medium. Regular changes in net H^+ fluxes, supported by pharmacological studies, showed that activity of PM H^+ transporters is a major contributor to the observed pH changes. The absence of significant variation in net Ca^{2+} flux at different stages of bacterial growth suggested that the biphasic Ca^{2+} kinetics, observed in culture media, originate merely from pH-dependent calcium-to-phosphate binding. Flux measurements were shown to avoid misleading interpretations of calcium concentration changes.

5.3. Ion flux kinetics associated with bacterial responses to acid stress: a comparative study using *L. monocytogenes* and *Lb. delbrueckii subsp. bulgaricus*

From a pragmatic point of view, acid stress responses and adaptation of bacterial organisms to low pH are of high importance for food microbiologists. Organic acids and their derivatives are widely used in the food industry as food preservatives. Examples include acetic, propionic, and lactic acids. In this section, some aspects of bacterial responses to acid stress were examined by application of the MIFE technique to *Listeria monocytogenes* and *Lactobacillus delbrueckii* subsp. *bulgaricus*.

The acquired acid tolerance of *L. monocytogenes* and *Lb. bulgaricus* can have important implications for their survival in environments and food products and for bacterial colonisation in the human gut. Bacteria have a variety of genetic mechanisms that respond to changes in environmental pH (Hall et al., 1995), but the physiology of pH adaptation is still poorly understood. Bacteria can be divided into three groups with respect to the preferential growth pH, namely: acidophiles, neutrophiles, and alkalophiles. Both bacteria studied grow fastest at neutral pH, while the minimum pH that permits growth differs. Both the literature (Farber et al., 1989) and data presented in this thesis suggest that *L. monocytogenes* is able to maintain growth at pH levels as low as 4.3-4.4. Below these values *L. monocytogenes* was only able to survive. The corresponding value for lactobacilli, fermentative bacteria, was reported to be as low as pH_o 3.5 (Kashket, 1987; McDonald et al., 1990). Bender et al. (1986) reported that *Lactobacillus casei* was even more resistant to environmental acidification with gross membrane damage being evident only below pH_o 3.0. The strategies of survival at low pH of these two organisms are different. Understanding the mechanism(s) of adaptation and survival is important for the food industry in order to develop methods for control of growth and inactivation of undesired bacteria or to enhance the growth and survival of beneficial organisms.

5.3.1 Experimental design

The MIFE technique was used for a comparative study of kinetics of *L. monocytogenes* and *Lb. bulgaricus* responses to acidic treatment. Net H^+ flux was measured from immobilised bacteria at normal conditions (pH_o 7.0 or 6.0) and after a shift to lower pH_o. The effects of glucose availability on the ability of bacterial cells to respond to low pH treatment were also evaluated. Two glucose concentrations (0 and 10 mM) were used throughout the study with bacteria in the stationary phase of growth (see Fig. 2-1). Growth conditions for both bacteria are indicated in Table 2-1. Cultures were prepared and immobilised as described in Chapters 2.1.2 and 2.2.3. Net H^+ flux was measured and data analysed as stated in Chapter 2.3. Experimental solution N2 (Appendix A) was used for flux measurements. Acidic treatment was performed by a change of experimental solution (pH 6 or 7) in a measuring chamber for a new one at pH 4 using a peristaltic pump (flow rate up to 6 mL min^{-1}). The kinetics of H^+ flux were monitored for 10-15 min before the solution change and up to 60 min after a change of solution. The glucose concentration of the experimental solutions is indicated in figure legends. Introduction of glucose into the measuring chamber with immobilised cells was achieved by a change of an experimental solution for a new one in a way similar to that described above.

Pharmacological studies were performed using 1mM DCCD. Details on DCCD stock solution preparation is given in Appendix B.

5.3.2 Response to acidic treatment in the presence of glucose

The kinetics of the response of *L. monocytogenes* Scott A to lowered pH_o in the presence of 10 mM of glucose in the medium is shown in Figure 5-10. A shift from pH_o 7.0 to pH_o 4.0 resulted in increased H^+ extrusion from about zero to -20 nmol m^{-2} s^{-1}.

L. monocytogenes, like other neutrophilic bacteria seeks to maintain a relatively constant pH_i. As pH_o decreases, the pH gradient (ΔpH, the difference between pH_i and pH_o) increases. Ita and Hutkins (1991) reported ΔpH of 0.5 to 0.7 pH units over a pH range of 5.0 to 6.0 for *L. monocytogenes*. The pH_i was

maintained above 7.0 in the range of pH_o 4.0 to 7.0 in the present experimental conditions (Fig. 5-18; and also by Siegumfeldt et al., 1999; Budde and Jakobsen, 2000). However, at some critical pH_o the bacteria are not able to maintain constant pH_i, the ΔpH collapses and bacteria start to die. Christensen and Hutkins (1992) reported that *Listeria* cells remained viable as long as a ΔpH could be maintained.

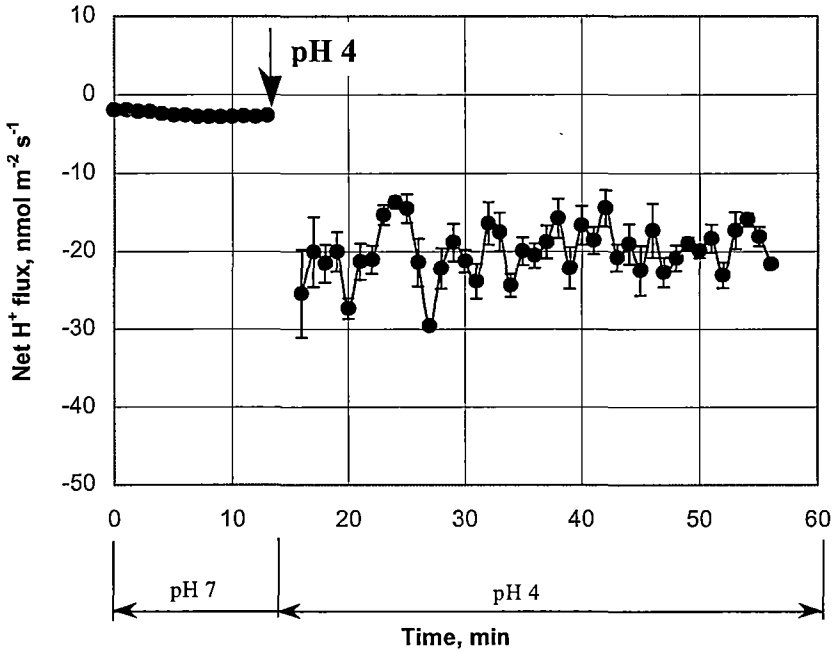

Fig. 5-10. Kinetics of *L. monocytogenes* responses to lowered pH_o in the presence of 10 mM of glucose. Experimental medium used was N2 (Appendix A). Error bars are SEM (n=2).

In contrast to *L. monocytogenes*, *Lb. bulgaricus* response to acid stress in the presence of 10 mM of glucose in the medium resulted in a significant decrease in net H^+ extrusion from –38 nmol m^{-2} s^{-1} to –20 nmol m^{-2} s^{-1} (a decrease in net H^+ efflux is interpreted as an increased H^+ influx) (Fig. 5-11).

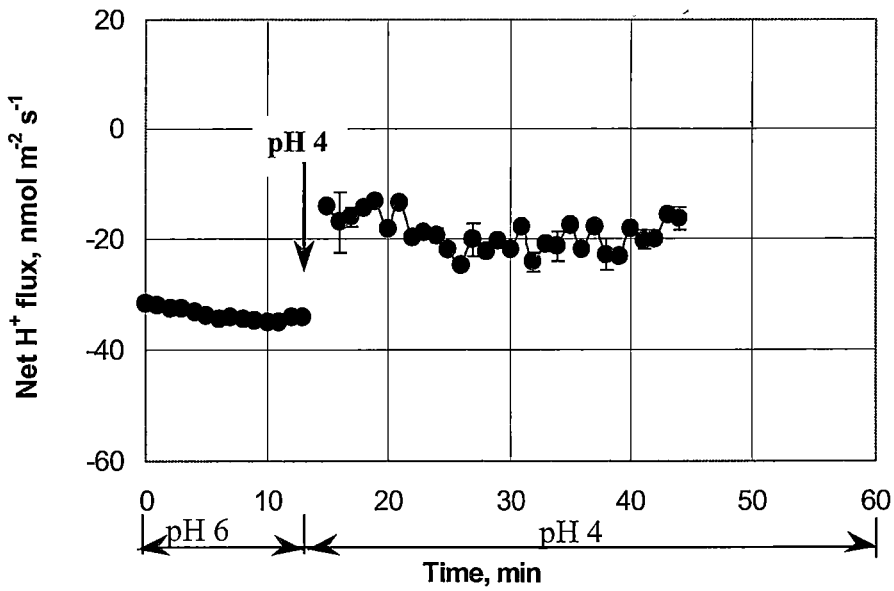

Fig. 5-11. Kinetics of *Lb. bulgaricus'* response to lowered pH_o in the presence of 10 mM glucose. The experimental solution used was N2 (Appendix A). Error bars are SEM (n=2).

Siegumfeldt et al. (1999) demonstrated the different magnitude of pH_i changes in *L. innocua* and *Lb. bulgaricus* in response to a pH_o shift from 7.0 to 5.0. The reported pH_i decrease was 1.5 pH units for *Lb. bulgaricus* compared with only 0.8 pH for *L. innocua*. This indicates different strategies of coping with acid stress in these two bacteria. It was also shown that in growing cultures of fermentative LAB, pH_i decreases as a function of pH_o, and ΔpH (difference between pH_i and pH_o) never exceeds 1.0 (Kashket, 1987; McDonald et al., 1990; Cook and Russell, 1994; Russell and Diez-Gonzalez, 1998). The proton translocating H^+-ATPase enzyme complex was claimed to play an important role in pH homeostasis in fermentative LAB (Kobayashi et al., 1986; Bender et al., 1986; Bender and Marquis, 1987; O'Sullivan and Condon, 1999). H^+-ATPase activity was shown to increase with a decrease in pH_o (Kobayashi et al., 1984; Kobayashi et al., 1986; Nannen and Hutkins, 1991; O'Sullivan and Condon, 1999). Nannen and Hutkins (1991) demonstrated that

optimal H^+-ATPase activity of *Lacobacillus casei* occurred at pH_o 5.0 and the H^+-ATPase activity was greatest when the pH_i was less than the optimum for the enzyme. Moreover, the aciduric lactic acid bacterium, *Lacobacillus casei*, was shown to have higher basal levels of ATPase than the less acid tolerant streptococci and lactococci (Nannen and Hutkins, 1991). Together with the fact that lactobacilli grow at lower pH_o than other LAB (Kandler and Weiss, 1984; Mundt, 1984), these reports suggest that H^+-ATPase may be involved in regulation of pH homeostasis of lactobacilli.

Detailed discussion of the mechanisms underlying the acid-stress response in *L. monocytogenes* is given in section 5.5.

5.3.3 Pharmacological studies

Pharmacological studies were carried out to further elucidate the ionic mechanisms of bacterial responses to acid stress and to investigate the possible involvement of H^+-ATPase in the observed response to lowering the pH_o in *Lb. bulgaricus*. The addition of 1mM DCCD, a specific inhibitor of F0F1 ATPase, resulted in a transient net H^+ influx followed by stabilisation around zero (Fig. 5-12).

Kobayashi et al. (1986) reported that inhibition of H^+-ATPase in LAB resulted in a marked decrease in pH_i thus indicating proton entry into the cells. Bender et al. (1986) also demonstrated that DCCD noticeably increased the permeability of *Lactobacillus casei* and other LAB to protons. Experiments with mutant strains of LAB with reduced membrane-bound ATPase activity support the hypothesis of the essential role of the enzyme in these organisms surviving low pH (Yokota et al., 1995; Amachi et al., 1998; Takahashi and Yamada, 1999). It was reported that DCCD inhibited the synthesis of ATP in *Lactobacillus* by 70% (Cotter et al., 2000). Keeping in mind that the level of H^+-ATPase activity depends on the amount of the cellular ATP (O'Sullivan and Condon, 1999), data presented here offers strong evidence for the involvement of H^+-ATPase in the H^+ flux regulation of *Lb. bulgaricus* after acidic treatment.

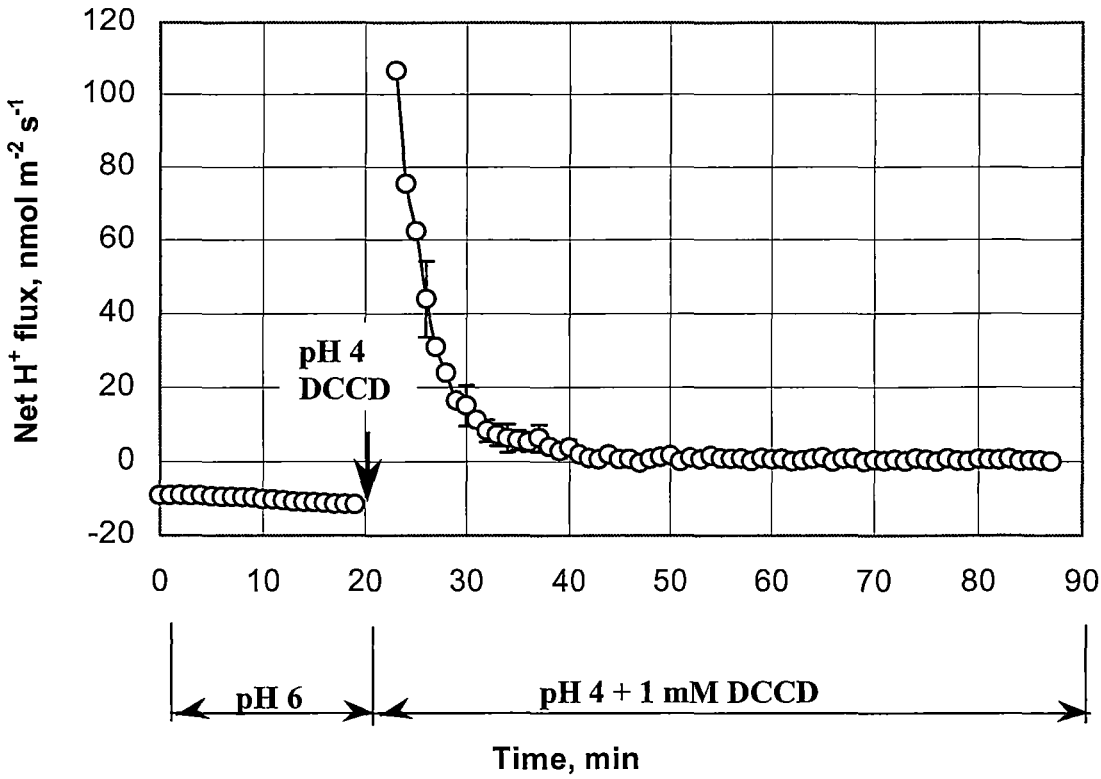

Fig. 5-12. Effect of 1 mM DCCD on response of *Lb. bulgaricus* to acid treatment. Cells were adapted to pH 6 in the presence of 10 mM of glucose. Acid treatment was performed by a change of the medium to one of the same composition at pH 4. The same cells were monitored throughout the experiment. The experiment was performed in duplicate. Data was taken every 0.1 min and is shown as 1 min average. Error bars are SEM (n=2).

5.3.4 Response to acidic treatment in the absence of glucose

The activity of H^+-ATPase is strongly dependent on cell energetic status. Therefore, glucose availability might significantly affect the responses of *L. monocytogenes* and *Lb. bulgaricus* to acid stress. The effect of glucose availability on the response to acidic treatment was studied.

The kinetics of *L. monocytogenes* response to acid treatment in the absence of glucose in the medium is shown in Figure 5-13.

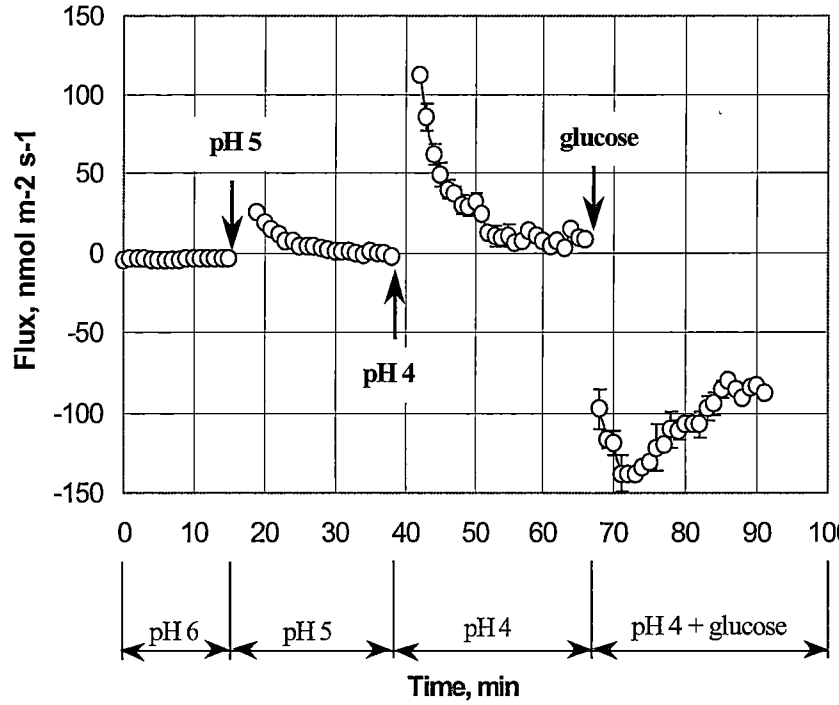

Fig. 5-13. Effect of glucose availability on kinetics of *L. monocytogenes* Scott A after acid treatment. Cells were adapted at pH 6.0 in the absence of glucose for 1 h. Acid treatment was applied by a change of the medium to one with desired pH. Glucose was added as indicated in amounts to achieve 10 mM in the experimental solution. Error bars are SEM (n=4).

The kinetics of *Lb. Bulgaricus* response to acidic treatment is shown in Figure 5-14.

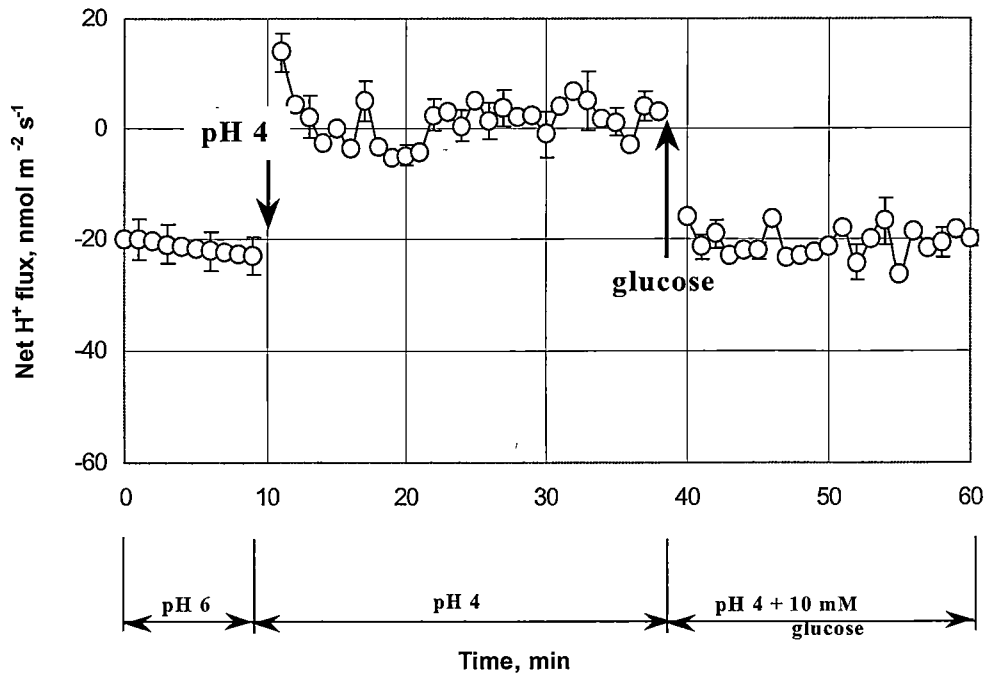

Fig. 5-14. Effect of glucose availability on kinetics of *Lb. bulgaricus* response to acidic stress. A glucose-deprived culture was shifted from pH_o 6.0 to pH_o 4.0, with 10 mM of glucose added at indicated times. Error bars indicate SEM (n=2).

Regardless of the availability of glucose, a decrease in pH_o led to a similar shift towards net H^+ influx in *Lb. bulgaricus* (Fig. 5-11). Extrusion of protons at pH_o 6.0 (before acidic treatment) in the presence of 10 mM of glucose was nearly 2-fold higher than the corresponding process for glucose-deprived cells due to fermentative activity of *Lb. bulgaricus*. A shift from pH_o 6.0 to pH_o 4.0 in the absence of glucose resulted in net H^+ influx followed by stabilisation around zero. Addition of 10 mM of glucose to acid-stressed glucose-deprived cells resulted in a significant extrusion of protons, as was observed for *L. monocytogenes* (Fig. 5-13).

The observed data is consistent with the hypothesis that resistance to acid stress is an energetically expensive process (Miyagi et al., 1994). Mechanisms of regulation of cytosolic pH_i are numerous and involve active H^+ extrusion via ATP-driven pumps, proton/cation exchange systems, buffering of the cytoplasm or decarboxylation processes (Booth, 1985; Lin et al., 1996; Booth, 1999; Dilworth and

Glenn, 1999). Buffering capacity of the cytoplasm was shown to play a limited role in pH_i homeostasis (Krulwich et al., 1985). Involvement of decarboxylation processes in the present experimental conditions can be dismissed because of the absence of amino acids in the experimental solution used. Transport processes require the proton motive force (PMF) that needs to be fuelled by glucose (or other energy sources).

From this point of view, *L. monocytogenes*' inability to maintain a high level of pH_i at pH_o 4.0 (Fig. 5-13) in the absence of an energy source may be interpreted as further evidence for the crucial role of proton extrusion in maintaining pH homeostasis in this organism. Addition of glucose (as an energy source) to the medium enabled cells to expel protons to restore pH_i (Fig. 5-13).

The fermentative bacterium *Lb. bulgaricus* uses another strategy to cope with acidic treatment by decreasing pH_i together with pH_o. This strategy is based on energy economy and enables *Lb. bulgaricus* to survive at lower pH_o. However, the absence of glucose in the medium results in zero net H^+ flux at pH_o 4.0. The addition of 10 mM glucose leads to net H^+ extrusion of a magnitude similar to that in the previous trial with 10 mM of glucose (Figs. 5-14 and 5-11, respectively).

Glucose-induced acid efflux has previously been shown to be a reflection of F0F1 ATPase activity in streptococci (Harold et al., 1970). It was also demonstrated that H^+-ATPase is involved in ATR of *L. monocytogenes* (Davis et al., 1996; O'Driscoll et al., 1996). H^+-ATPase activity was shown to correlate with the cytoplasmic ATP levels (Kobayashi et al., 1984; O'Sullivan and Condon, 1999) which depend on glucose concentration in the medium. Glucose is used as an energy source in both *L. monocytogenes* and lactobacilli. Addition of an energy source was reported to result in a dramatic increase in the intracellular ATP in *Lb. plantarum* (Wouters et al., 1998). Absence of H^+ extrusion in glucose-deprived *L. monocytogenes* cells and zero net H^+ flux in *Lb. bulgaricus* cells demonstrated in this study are in accord with other reports and suggest involvement of H^+-ATPase in acid stress responses in both organisms.

5.3.5 Conclusion

The MIFE technique was used for kinetic studies of *L. monocytogenes* and *Lb. bulgaricus* responses to acidic treatment. These two Gram-positive bacteria employ very different mechanisms in dealing with acid stress. As discussed above, other workers have shown that while *L. monocytogenes* expels protons to maintain constant pH_i, the fermentative bacterium *Lb. bulgaricus* does not employ a pH_i homeostasis strategy. Instead, *Lb. bulgaricus* allows proton entry after acidic treatment so that pH_i follows pH_o. This energy-saving strategy enables high acid tolerance in *Lb. bulgaricus*. That observation is supported and extended by the present results. The important role of ATP-driven H^+ pumps in *Lb. bulgaricus* was demonstrated using DCCD.

5.4. Ion flux kinetics associated with bacterial responses to bacteriocins: a case study for nisin

In their competition for nutrients and a place in their ecological niche, some Gram-positive bacteria produce peptides that inhibit competing bacteria, conferring a growth advantage. One of the peptides, the bacteriocin nisin, is produced by certain strains of *Lactococcus lactis* subsp. *lactis*. It helps this bacterium to compete against other Gram-positive bacteria, eg. *L. monocytogenes* (Jack et al., 1995; Montville and Winkowski, 1997). Since the emergence of *L. monocytogenes* as a food-borne pathogen, significant efforts have been applied towards preventing its presence in food products. Bacteriocins, in particular nisin, have been promoted as potential antimicrobial agents against *L. monocytogenes* in foods. Nisin is at present the only bacteriocin with commercial applications in the food industry (Leriche et al., 1999) and is used as a food preservative in more than 50 countries (Delves-Broughton et al., 1996).

5.4.1 Mode of nisin action

Nisin is a cationic peptide of 34 amino acids that contains five intramolecular rings (Moll et al., 1998). Nisin inhibits the growth of Gram-positive bacteria by interaction with anionic constituents of the negatively charged cell wall that results in a rapid and a specific efflux of cytoplasmic cell constituents. Both the transmembrane electrical potential ($\Delta\psi$) and the ΔpH stimulate nisin-mediated membrane permeabilisation (Moll et al., 1997, 1998; Montville and Chen, 1998).

Driessen's group proposed two models: the 'barrel-stave' model (Sahl, 1991) and the "wedge" model (Driessen et al., 1995). Both models argue that nisin initially binds to the target membrane through electrostatic interactions. The models differ with regard to the insertion of the molecule. In the barrel-stave model, nisin binds as a monomer, inserted into the lipid bilayers, and the inserted monomers aggregate laterally to form pores. In the wedge model, pore formation is caused by the local perturbation of the lipid bilayer that occurs when nisin molecules bind. Nisin is then pulled into the membrane by a PMF component, either $\Delta\psi$ or ΔpH. The hydrophobic residues of nisin are inserted shallowly into the outer leaflet of the lipid bilayer. It

remains unclear how initial electrostatic interactions between the positively charged nisin molecules and the anionic phospholipids in the target membrane transform to hydrophobic interactions in the wedge-pore structure.

Montville's group also proposed two models to describe the interaction of bacteriocin nisin monomers and the cytoplasmic membrane: the "detergent disruption" model and the "poration complex" model (Montville et al., 1995). It was hypothesised that nisin permeabilises target cell membranes through a multi-step process of binding, insertion, and pore formation (Montville and Chen, 1998). The "detergent disruption" model predicts random insertion of bacteriocin monomers into the membrane with a resulting disruption of the phospholipid bilayer. The "poration complex" model proposes that nisin monomers are bound and inserted into the membrane, followed by the congregation of other monomers in a barrel stave formation. Such interaction of monomers results in pore formation within the membrane (Montville et al., 1995).

The existence of different models reflects the complex nature of nisin-membrane interaction that are far from fully understood.

Pore formation by nisin does not require a protein receptor since it dissipates the PMF. This causes carboxyfluorescein (CF) efflux from lipid vesicles (Montville and Chen, 1998). The PMF plays a central role in ATP synthesis, active transport, and bacterial motion (for details see Chapter 1.2). PMF dissipation by nisin depletes intracellular ATP (Abee et al., 1994; Winkowski et al., 1994; Christensen and Hutkins, 1994; Chen and Montville, 1995; Waite and Hutkins, 1998) and blocks amino acid uptake (Ruhr and Sahl, 1985; Chikindas et al., 1993; Maftah et al., 1993). Nisin also induces the efflux of various small intracellular substances from sensitive cells like amino acids, potassium, inorganic phosphate, and partial efflux of intracellular ATP (Ruhr and Sahl, 1985; Abee et al., 1994; Waite et al., 1998).

While both models are consistent with membrane disruption and loss of PMF observed in bacteriocin-sensitive cells, evidence of saturation kinetics and bacteriocin inhibition mechanisms, such as leakage of intracellular ATP and other large molecules, favour the poration complex model (Winkowski et al., 1994; Montville et al., 1995).

It is well established that nisin is effective against vegetative cells of Gram-positive bacteria and not Gram-negative bacteria. However, it was demonstrated that both Gram-positive and Gram-negative bacteria are sensitive to nisin if the outer membrane of the latter is destroyed by chelates (Montville and Bruno, 1994). In addition, nisin was shown to be active against liposomes of both Gram-positive and Gram-negative bacteria (Garcera et al., 1993). Taken together, these suggest that access to the membrane is the only requirement for nisin efficacy.

5.4.2 Inhibitory effect of divalent cations on nisin efficiency

While many papers report inhibitory effects of nisin in *L. monocytogenes* (Abee et al., 1994; Winkowski et al., 1994; Montville and Bruno, 1994; Montville et al., 1995; Crandall and Montville, 1998; Waite and Hutkins, 1998), a number of questions remain unanswered. It appears that many factors might contribute to the mode of nisin action. One of these is the effect of divalent cations.

Divalent cations were shown to reduce the efficacy of nisin action against *L. monocytogenes* (Abee et al., 1994; Verheul et al., 1997b; Crandall and Montville, 1998). Crandall and Montville (1998) showed that inclusion of 10 mM $MgSO_4$, $MgCl_2$, $CaCl_2$, $MnSO_4$, or $BaCl_2$ into the medium reduced the lethality caused by nisin (Abee et al., 1994). However, divalent cations had no effect on cell viability in the absence of nisin. The trivalent cation gadolinium (Gd^{3+}) was even more efficient and completely suppressed nisin activity at a concentration of 0.2 mM (Abee et al., 1994). In contrast, monovalent ions (as tested by addition of KCl and NaCl to the medium) had no effect on the mode of nisin action (Crandall and Montville 1998). Inhibition of nisin activity by di- and trivalent cations was reversed by chelation with EDTA (Abee et al., 1994; Crandall and Montville, 1998).

5.4.3 Effect of calcium on proton extrusion

The MIFE technique was used to investigate the physiological response of *L. monocytogenes* to different concentrations of nisin as a function of the presence of 10 mM of a divalent cation Ca^{2+} in the medium.

Exponential phase *L. monocytogenes* Scott A (see Fig. 2-1), were used in this study. Culture maintenance and growth conditions were as reported in Section 2.1.2. Cultures adapted for 1 h at an appropriate nisin and $CaCl_2$ concentration, were immobilised on a cover-slip (see Section 2.2.3), placed into a measuring chamber, and net H^+ flux was measured. Experimental solution N2 (Appendix A) with addition of 10 mM of glucose was used as a basic solution throughout the study. Comparative analyses of net H^+ flux from immobilised *L. monocytogenes* in the presence or absence of $CaCl_2$ are shown in Figure 5-15.

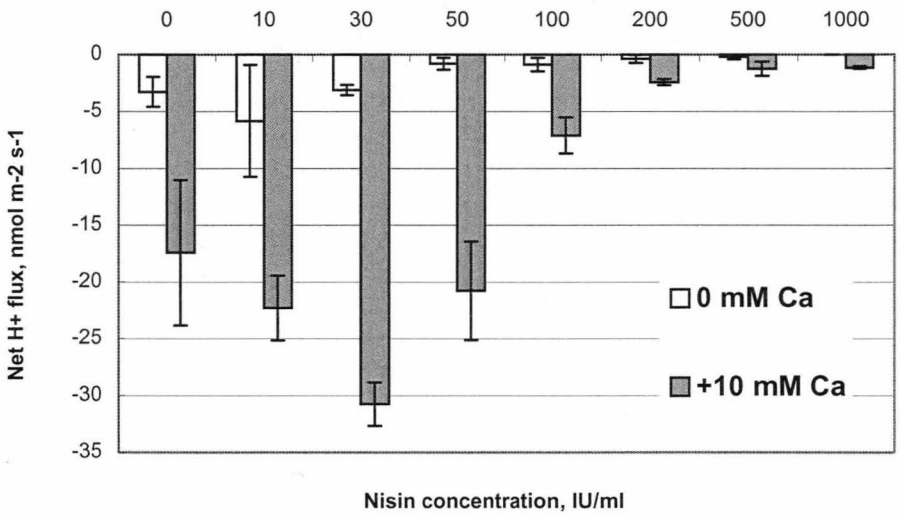

Fig. 5-15. Net H^+ flux from immobilised *L. monocytogenes* Scott A cells as a function of nisin concentration and calcium availability in the medium. Measurements were performed at pH 6.0 with or without 10 mM $CaCl_2$ in the experimental solution N2 (Appendix A) at indicated nisin concentrations. Cells were in the exponential phase of growth. Error bars are SEM (n=5-9).

Proton extrusion was activated by the presence of calcium in the medium (Fig. 5-15). Mean proton extrusion for a control (in the absence of nisin) in the presence of 10 mM $CaCl_2$ was ~4 -fold higher than a similar control in the absence of $CaCl_2$.

For all concentrations tested, the inhibitory effect of nisin on net H^+ efflux was significantly lower when Ca^{2+} was present in the medium (Fig. 5-15). That was

especially obvious at intermediate nisin concentrations (10 to 100 IU/ml). At higher concentrations, net H^+ extrusion was significantly suppressed, suggesting cell death.

Since the mode of nisin action relies on the interactions of cationic nisin molecules with anionic phospholipids of the target membrane, a major determinant for sensitivity to nisin is the relative amount of negatively charged lipids in the target membrane (Abee et al., 1994). It was reported that the major phospholipids of *L. monocytogenes* are phosphatidylglycerol and cardiolipin (Kosaric and Carroll, 1971; Mastronicolis et al., 1996). Fluorescence studies show that nisin tightly associates with the anionic surface of phosphatidylglycerol liposomes but not with the surface of phosphatidylcholine liposomes (Driessen et al., 1995). It was proposed that anionic phospholipids interact strongly with nisin and encourage nisin insertion (Giffard et al., 1996; Martin et al., 1996).

Di- and trivalent cations can bind to the negatively charged headgroups of phosphatidylglycerol and cardiolipin (Harwood and Russell, 1984). Neutralisation of negative charges induces condensation of these lipids, resulting in a more rigid membrane (Harwood and Russel, 1984). This may cause a decrease in efficiency of nisin insertion and pore formation (Abee et al., 1994).

The increase in net H^+ efflux observed from immobilised control cells in the presence of calcium, as compared to the trial without calcium, might be attributed to the known role of calcium in the structure and the function of several enzymes (eg. Ca^{2+} is an important cofactor of γ-carboxyglutomate decarboxylases; Martin, 1984) or to Ca^{2+} binding to negatively charged headgroups.

The pores formed by nisin were reported to be up to 1 nm in size and non-selective (Sahl, 1985). The monitored decreased ability of *L. monocytogenes* to extrude protons in the present experiments correlated with the increase in nisin concentrations to the values known to be inhibitory for *Listeria* survival (>100 IU/ml). The observed increase in proton extrusion for a given nisin concentration in the presence of 10 mM $CaCl_2$ in the medium may be due to decreased access of nisin molecules to bacterial phospholipids. The effect of calcium, significant for intermediate nisin concentration (30 to 100 IU/ml) was diminished with the increase in nisin concentrations (>100 IU/ml).

5.4.4 Conclusion

Calcium is present (often in large quantities) in a variety of food products, eg. dairy products. Therefore, the reported decrease in nisin efficacy due to Ca^{2+} should be taken into consideration while attempting to inhibit *L. monocytogenes* growth. Monitoring the resultant H^+ flux kinetics might be a sensitive tool in evaluating the efficacy of nisin action in a variety of food products and in combination with other factors.

5.5. Combination of the MIFE and FRIM techniques to study membrane-transport processes: a case study for *Listeria monocytogenes*

In the previous sections a number of applications of the MIFE technique to bacterial monolayers were demonstrated that offer new and exciting prospects to study the mechanisms underlying bacterial growth and adaptive responses. The power of this technique may be further significantly enhanced when ion flux measurements are combined with other electrophysiological or molecular biology techniques, concurrently applied to the same organism. One such technique is Fluorescence Ratio Image Microscopy (FRIM).

In recent years, FRIM has become a very powerful tool in microbial research (Siegumfeldt et al., 1999; Budde and Jakobsen, 2000). The advantages of the technique are outlined in Chapter 1.4.4. However, while it is able to detect the overall effect of applied stress on pH_i, the FRIM technique can not reveal the underlying mechanisms involved.

In this study, the FRIM and MIFE techniques were combined in one experimental set up to perform simultaneous measurements of pH_i and net H^+ fluxes in response to acidification of the medium. This novel combination of techniques enabled changes in H^+ concentrations at either side of the bacterial membrane to be measured concurrently and the contribution of plasma membrane H^+ transporters to bacterial pH homeostasis to be investigated.

5.5.1 Importance of *Listeria monocytogenes* acid stress studies

As described in Chapter 1, *Listeria monocytogenes* is a bacterium that poses a serious threat to public health and the viability of large segments of the processed food in the food industry. Among environmental conditions unfavourable for listerial growth, acidity is probably the most significant (Gahan and Hill, 1999). The ability of *L. monocytogenes* to adapt to low-pH environments is of particular interest because the organism encounters such environments during its passage through the stomach and also during its transient residence in the macrophage phagosome (Phan-

Thanh et al, 2000; Cotter et al., 2001). In addition, acids are often used in the food industry for food preservation. The phenomenon of acid tolerance in bacteria has been studied for many years. However, the majority of this research was carried out on *E. coli* and *Salmonella* (Booth, 1985; Foster, 1991; Lin et al., 1996; Brown et al., 1997). Work on *Listeria monocytogenes* and other Gram-positive bacteria is less extensive (Gahan et al., 1996; O'Driscoll et al., 1996).

Bacterial survival in acidic conditions is an energy requiring process. The role of carbohydrates in the survival of *L. monocytogenes* at low pH is particularly important because growth of this pathogen depends on carbohydrates for its primary energy source (Seeliger and Jones, 1986). Glucose is reported to be its preferred carbohydrate (Pine et al., 1989; Premaratne et al., 1991). In addition, as an intracellular parasite, *L. monocytogenes* also grows well within the cytoplasm of host tissue cells, where varying glucose concentrations might also be expected (Parker and Hutkins, 1997). Consequently, it is important to define the extent to which *L. monocytogenes* can survive low pH conditions and to determine the effect of energy in general on the process. Like other neutrophiles, *Listeria* maintains pH_i at around 8 even when the pH of the external medium decreases (Christensen and Hutkins, 1992; Siegumfeldt et al., 1999; Budde and Jakobsen, 2000). The maintenance of homeostasis requires an intact semipermeable cell membrane and expenditure of energy. Therefore, any treatments that disrupt membranes or interfere with generation of cellular energy will hinder or abolish homeostatic capacity and will eventually lead to cell degeneration and death (Mackey, 1999). Acid stress has a direct effect on the PMF and may result in instantaneous changes in the cell membrane potential (Young and Foegeding, 1993). Those changes will affect transport of all other major nutrients taken in cotransport with H^+ (Maloney and Wilson, 1996). Regulation of pH_i is a fundamental requirement for the survival and viability of *L. monocytogenes*.

As described in detail in Section 1.2.3, bacteria attempt to maintain their pH_i by minimising membrane permeability to H^+, buffering the cytoplasm, ameliorating the pH_o through catabolism or selective substrate utilisation, and using the H^+ pump and other transport systems (Booth, 1985; Lin et al., 1996; Booth, 1999; Dilworth

and Glenn, 1999). The literature does not suggest which, if any, of these mechanisms is predominant in *L. monocytogenes*. Consequently, it is important to study membrane-transport processes and their input into the process of *L. monocytogenes* pH homeostasis.

5.5.2 Importance of kinetic studies

At present, little is known of early events in the adaptive response of *L. monocytogenes* that occur at the cell membrane and enable survival in hostile environments or growth in foods. Of special importance are kinetic studies. Adaptive responses of bacterial cells are usually very fast. Synthesis of specific proteins in response to low pH treatment known as acid tolerance response (ATR) occurs about 60 min after stress onset (Davis et al., 1996; O'Driscoll et al., 1996). Long before *de novo* synthesis of stress-induced proteins becomes evident, biophysical responses take place (a time scale of minutes or even seconds) (Reich and Sel'kov, 1981). Kinetic studies might help to reveal the processes preceding the protein synthesis. However, a high rate of data sampling is required during that time in order to achieve temporal resolution and understand the underlying mechanisms of bacterial pH homeostasis. The MIFE technique offers advantages for kinetic studies, as will be demonstrated below.

5.5.3 Experimental protocol

The bacterial strain used throughout this study was *L. monocytogenes* 4140 in the stationary phase of growth (Table 2-1). The culture was prepared as described in Section 2.1.2. Washed cells were suspended in experimental solution N2 (Appendix A) adjusted to pH 6 and adapted to new conditions for 1 h. An experimental chamber depicted in Figure 2-5 was used. Staining cells for FRIM, immobilisation of cells and MIFE measurements are described in Sections 2.4, 2.2.3, and 2.3.5, respectively.

Net H^+ flux and pH_i were monitored at three conditions:

(i) In ***static*** experiments, the pH_i and H^+ flux measurements were taken after bacterial cells were pre-incubated for 1 h in a range of constant pH_o from 6 to 3 at intervals of 0.5 pH units;

(ii) In ***kinetic*** studies, continuous measurements were taken, starting at pH_o 6, and followed by a shift to pH_o 4 or 3;

(iii) In ***recovery*** experiments, cells were kept at pH_o 3.0 or 4.0 for at least 1 hour, followed by a shift to pH_o 6.0 and with measurements of subsequent H^+ flux and pH_i kinetics.

All experiments were carried out at three levels of glucose concentration (0, 1, and 10 mM).

Hydrogen electrodes were positioned 15 to 20 μm above the immobilised bacteria and moved 30 μm up and down in a square-wave manner. Under this design, the measured H^+ flux originated from the surface area of 300 to 400 μm^2, e.g. represented an average net flux from about 300 bacterial cells (Fig. 2-6). Each flux measurement lasted for about 3 min in static experiments. Electrodes were then re-positioned to another place on the bacterial layer about 200 μm away, and the measurements resumed. On average, 5 to 7 spots were measured from the layer of immobilised bacteria at every pH_o and glucose concentration studied. In kinetic experiments one spot was monitored throughout the experiment.

5.5.4 H^+ flux and pH_i at different pH_o and glucose concentrations

The acquired acid tolerance of *L. monocytogenes* can have important implications for survival in environments and food products and for bacterial colonisation in the human gut. Most of the reported information corresponds to survival in rich media which may confer protection to the bacteria by providing energy and metabolic precursors. *L. monocytogenes* survival in a defined medium and its relation to intracellular pH is considered here. Molecular mechanisms used by *L. monocytogenes* to survive low pH stress have not yet been established and in this respect the study of bacterial survival in a defined medium is of particular importance. Since glucose availability affects the energy status of bacteria, different glucose concentrations may exert an effect on the survival of *L. monocytogenes* at low pH.

Before the kinetics of net H^+ flux and pH_i changes were measured, the kinetics of bacterial growth and survival at various pH_o were studied. Stationary phase cells

of *L. monocytogenes* 4140 survived at pH 4.0 and 3.5 in the absence of glucose in the medium for more than 20 h at 25°C without a noticeable decline in their viability (Fig. 5-16).

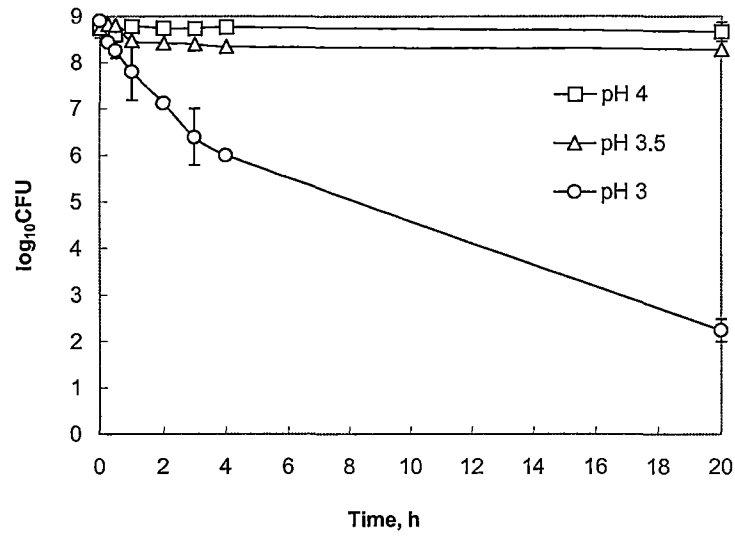

Fig. 5-16. Survival of *L. monocytogenes* 4140 at different pH values in the absence of glucose in the medium. The culture was grown in BHI adjusted to pH 6 at 37° C without agitation for 18 h. Washed cells were suspended in the experimental solution adjusted to pH 6 and adapted to new conditions for 1 h before imposing low pH steps. Error bars are SEM (n=3).

More cells were killed by the more severe treatment of pH 3.0 in the absence of glucose (log CFU cell count reduction of ~6 after 20 h). The magnitude of survival depended on the glucose concentration in the medium, with the highest survival observed in the presence of glucose (Fig. 5-17).

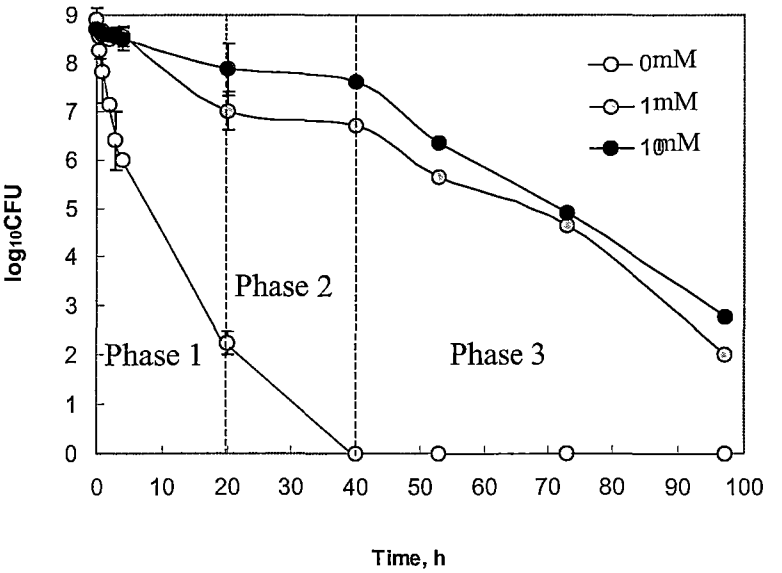

Fig. 5-17. Survival of *Listeria monocytogenes* 4140 at pH 3 at three levels of glucose in the medium (concentration of glucose is given in mM).The points are averages of three independent experiments. Error bars indicate SEM (n=2-4).

Inactivation curves showed regular changes and can be divided into three phases according to inactivation rate changes (Fig. 5-17). In phase 1 (0 to 20 h of treatment at pH 3.0), cell inactivation was found for all trials. This rate was related to glucose concentration in the medium and had a maximum value in the absence of glucose. The log reductions by the end of phase 1 were 6.3, 1.5, and 0.5 for 0 mM, 1 mM, and 10 mM of glucose, respectively.

In phase 2 (20-40 h), the curve flattened for the trials with glucose in the medium. In the absence of glucose, however, a progressive decrease in CFU values was observed, followed by cell death by the end of phase 2. At phase 3 (>40 h), the rate of cell inactivation increased again. An inhibitory effect of pH 3.0 on *L. monocytogenes* was reported for rich media (Ita and Hutkins, 1991; Kroll and Patchett, 1992; Davis et al., 1996; Datta and Benjamin, 1997) while reports for defined media are not as extensive. Phan-Thanh and Montagne (1998) showed no survival of *L. monocytogenes* after 1 h of treatment at pH 3.0 in their defined

minimal medium. Apart from strain specificity, the main reason for the disparity between their data and those in Figs. 5-16; 5-17 could be attributed to a different physiological state of the bacteria used for study. Phan-Thanh and Montagne (1998) used *L. monocytogenes* in the mid-exponential phase of growth, while bacteria in a stationary phase known to have enhanced acid resistance (Davis et al., 1996; O'Driscoll et al., 1996; Cotter et al., 2001) were used in this study. In addition, slightly acidic (pH_o 6.0) growth conditions used in these experiments might increase bacterial resistance to later lethal acid treatment. *L. monocytogenes* has been shown to exhibit an adaptive ATR following exposure to mild acid, which is capable of protecting cells from commonly lethal acid stress (Kroll and Patchett, 1992; Hill et al., 1995; Gahan et al., 1996; Datta and Benjamin, 1997; Cotter et al., 2000). The maximum protection from acidic treatment was reported to occur after adaptation at pH 5 and 5.5. However, adaptation at pH6.0 can also induce ATR.

Static experiments. *L. monocytogenes* cells were able to maintain constant pH_i between 7 and 8 for $pH_o > 4.0$ in trials with glucose in the medium, while pH_i decreased dramatically below pH_o 4 (Fig. 5-18). In the absence of glucose in the medium pH_i was lower than the corresponding data for the trials with glucose at all pH_o, and started to decline below pH_o 5.5.

Concurrently measured H^+ fluxes showed net H^+ extrusion at $pH_o > 4.0$ and net H^+ influx below pH_o 4.0 in the presense of glucose in the medium (Fig. 5-18). Maximum H^+ extrusion occurred at pH_o 5.5. For the trial without glucose net H^+ flux was zero at pH_o 6.0 and 5.5 followed by a net H^+ influx below pH_o 5.5.

The magnitude of both pH_i and net H^+ flux were related to glucose concentration in the medium with a higher pH_i and H^+ extrusion corresponding to a higher glucose concentration in the medium.

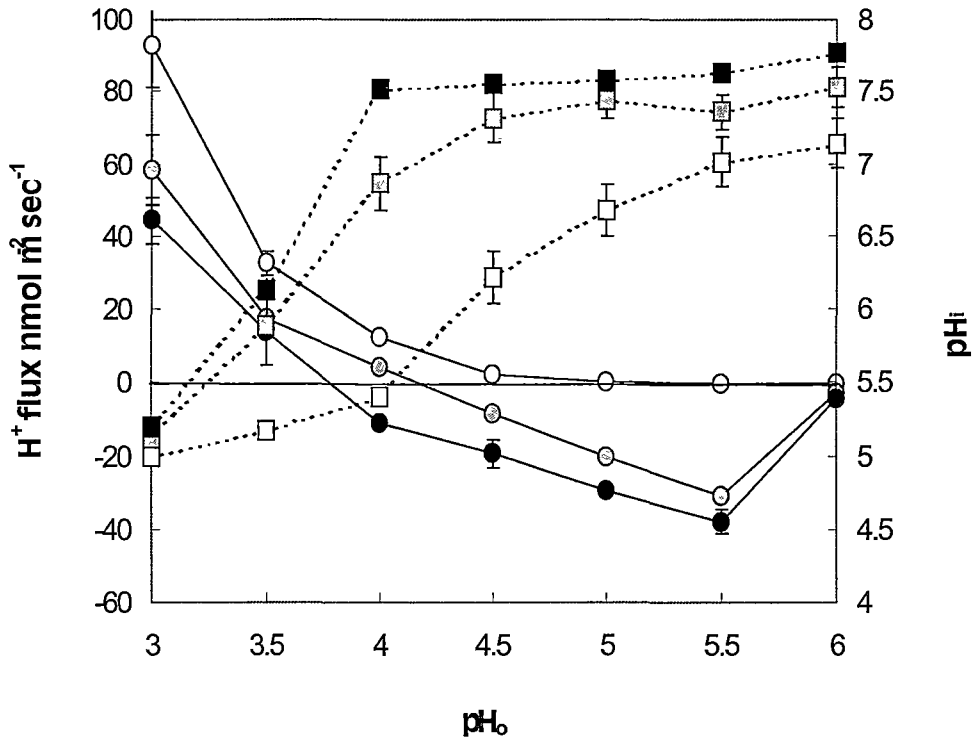

Fig. 5-18. Net H^+ fluxes (circles) and pH_i (squares) as a function of pH_o (static experiments). Cells were adapted for 1 h in the range of pH_o between 3.0 and 6.0 at 0.5 pH unit intervals at three levels of glucose in the media before measurements. Clear symbols represent 0 mM; grey symbols - 1 mM, and dark symbols - 10 mM of glucose. The pH_i values are averages of 40-60 single cells; net H^+ flux values are averages of 3-6 independent experiments with 4-6 distinct sites of immobilised cells measured in each. Error bars are SEM.

Kinetic studies. Kinetic experiments were crucial in evaluating the time constants of the mechanisms underlying cell ATR and contributing to *L. monocytogenes* pH_i homeostasis. Immediately after acid stress onset, hydrogen ions entered the cell regardless of the glucose availability in the medium (Figs. 5-19; 5-20).

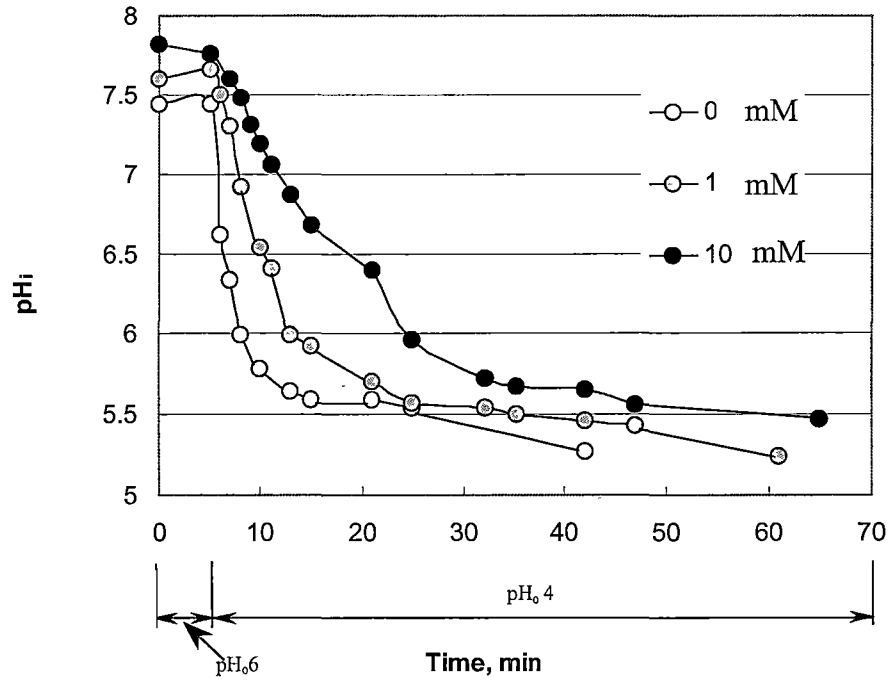

Fig. 5-19. Effect of pH_o change from 6 to 4 on the pH_i of individual *L. monoytogenes* 4140 cells at three levels of glucose in the medium. Symbols: clear – 0 mM; grey - 1 mM; dark - 10 mM glucose. Cells were adapted to starting experimental conditions (pH 6) for 1 h. Acid challenge was performed by perfusion experimental solution of pH 4 through the chamber (flow about to 6 mL/min).

The subsequent kinetics, however, were strikingly different for 0, 1 and 10 mM glucose variants. Glucose-rich cells (10 mM) were able to extrude H^+ at a significantly higher rate than those low in glucose (1 mM) (3.3 nmol m^{-2} s^{-1} and 0.5 nmol m^{-2} s^{-1} per min, respectively). As a result, 5 min after acid stress onset, glucose-rich cells pumped out excess H^+ (net H^+ efflux after 10 min; Fig. 5-20, dark symbols). Glucose-deprived cells (clear symbols in Fig. 5-20) continued to display net H^+ influx for the whole period of measurements (50 min). Cells incubated with intermediate glucose concentration were able to extrude H^+ only 20 min after stress onset (Fig. 5-20, grey symbols).

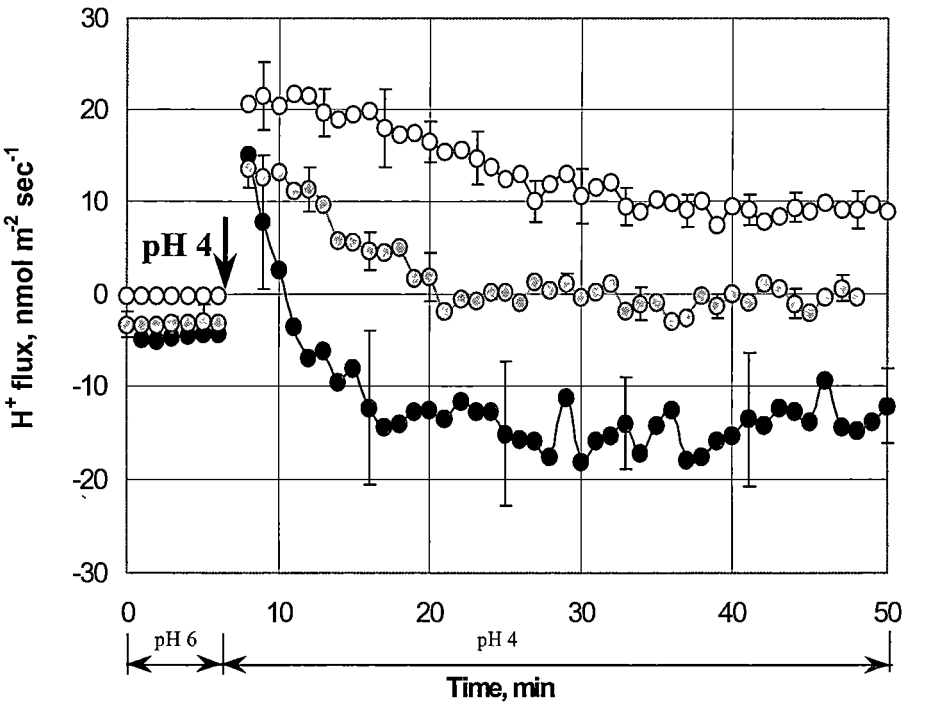

Fig. 5-20. Kinetics of net H^+ fluxes from immobilised *L. monocytogenes* in response to change of pH_o from 6 to 4 at three levels of glucose in MM: 0 mM glucose - clear symbols, 1 mM - grey symbols, and 10 mM - dark symbols. Data was taken every 0.1 min. Each point represents 1 min average value of 3-7 independent experiments. Error bars are SEM.

As H^+ ions flowed into the cell, intracellular pH_i declined sharply for 2-3 min after stress onset (Fig. 5-19). The resulting drop in pH_i (of about 2 pH units) reduced the magnitude of electrochemical gradients ($\Delta\mu_{H+}$) and resulted in a decreased ingress of H^+ into the cell (Fig. 5-20). The rate of pH_i change was inversely related to glucose concentration in the medium with the fastest stabilisation after acid treatment occurring at the highest glucose concentration (Fig. 5-20). A linear correlation between pH_i and H^+ flux, based on Figure 5-18 was determined. There was a high ($R > 0.90$) correlation between pH_i and H^+ flux kinetics for the trials with glucose. For the trial in the absence of glucose in the medium the correlation was less marked.

Recovery experiments. After acid stress was removed, bacterial cells were able to recover their pH_i values. Immediately after the solution was changed from pH 3 to pH 6, net H^+ flux switched from influx to efflux (Fig. 5-21).

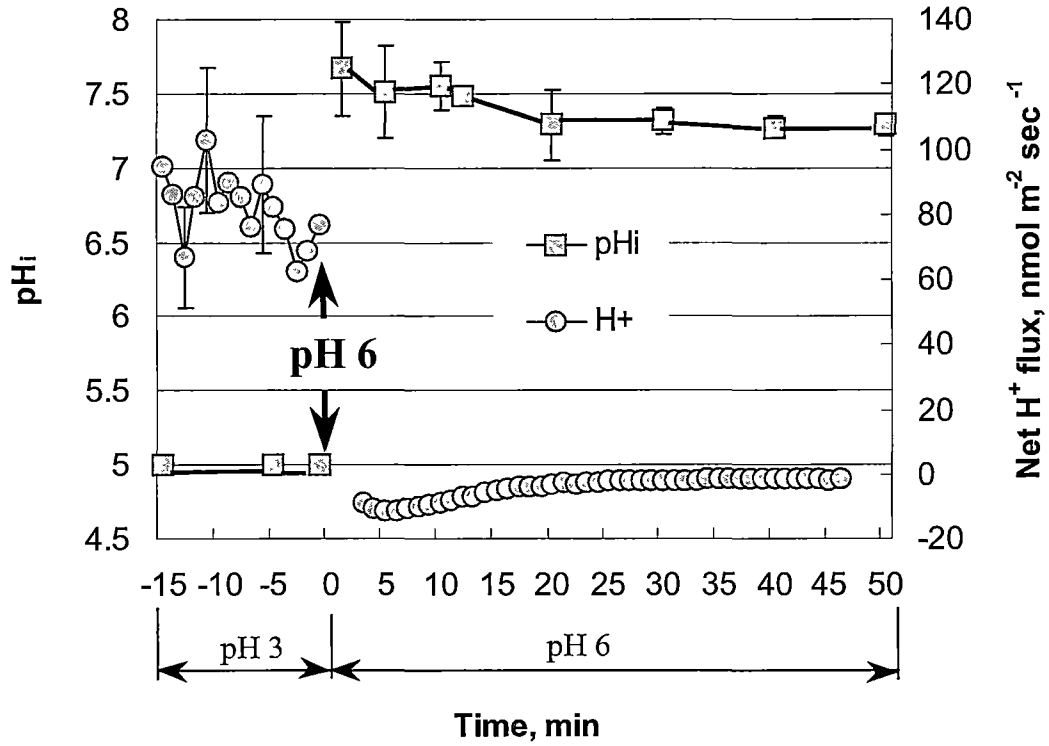

Fig. 5-21. Kinetics of recovery measured as pH_i and net H^+ flux change at pH_o 6.0 after an acidic stress at pH 3.0. The medium contained 1 mM of glucose for all treatments. 20 individual cells were monitored for pH_i analyses. The error bars indicate SEM (n=3).

The shift to pH 6.0 resulted in an almost complete recovery of pH_i values (around 7.5). The magnitude of response after recovery depended on the severity of the stress applied (pH_o of treatment), duration of acid stress and glucose concentration in the medium (data not shown).

5.5.5 Underlying mechanisms

In previous sections, the applicability of the MIFE technique to studying adaptive responses in several bacteria was demonstrated. Application of this technique was here extended by combining it with FRIM to elucidate the role of

plasma membrane H^+ transporters in acid stress responses and maintenance of pH_i homeostasis in *L. monocytogenes*.

It is generally accepted that pH_i exerts a feedback effect on cell metabolism. Cell membranes have low permeability to H^+ (Harold and van Brunt, 1978; Van de Vossenberg et al., 1999) and the regulation of pH_i implies control over this permeability. Protons enter and exit the cell by interacting with cell systems that control H^+ transport, such as H^+-ATPase, Na^+/H^+ antiporters, electron transport systems (Booth, 1999; Dilworth and Glenn, 1999; Cotter et al., 2000). In aerobic bacteria, the active transport of H^+ is coupled with the process of electron transport in respiratory chains. In anaerobic bacteria, H^+ transport is carried out by a H^+-ATPase molecule (proton pump) using energy from ATP hydrolysis. *L. monocytogenes*, a facultative anaerobic bacterium, may use both processes to achieve pH_i homeostasis (Phan-Thanh et al., 2000). Apart from cytoplasmic buffering capacity and proton transport processes, pH_i homeostasis is achieved by amelioration of pH_o via switching to decarboxylation of amino acids (Gale and Epps, 1942; Stim and Bennett, 1993; Lin et al., 1996; Dilworth and Glenn, 1999). As many different processes may contribute to pH_i regulation, the unambiguous interpretation of the underlying mechanisms is difficult. Until now, no precise role for any of these mechanisms has been clearly established.

Membrane-transport processes might be dominant in regulation of *L. monocytogenes* pH homeostasis. In the presence of glucose in the medium pH_i remained constant at intermediate pH_o values, while the corresponding net H^+ extrusion was increased. The maximum value occurring at pH_o 5.5 (Fig. 5-18). The activity of H^+-ATPase increases with a decrease in pH_o for a number of bacteria (Kobayashi et al., 1984; Nannen and Hutkins, 1991; O'Sullivan and Condon, 1999). The optimum pH_o for maximum H^+-ATPase activity varied between 5.0 and 6.5 depending on the species studied, as established for lactic acid bacteria (Nannen and Hutkins, 1991; O'Sullivan and Condon, 1999) and *Enterococcus faecalis* (Kobayashi et al., 1984). Keeping in mind the important role of H^+-ATPase in the ATR of *L. monocytogenes* (Cotter et al., 2000), the data here suggest that similar acid stress-induced activation of H^+-ATPase activity takes place in *L. monocytogenes*.

It was shown that the magnitude of response of both pH_i and H^+ flux depended on glucose concentration in the medium. The lowest pH_o at which ΔpH did not collapse occurred at the highest glucose concentration and reflected the ability of *L. monocytogenes* cells to expel protons (Fig. 5-18). Indeed, pH_i only started to decrease for $pH_o < 4$, 4.5, and 5.5 for 10, 1, and 0 mM of glucose, respectively. These values corresponded to H^+ influx below the indicated pH_o for similar glucose trials (crossing "zero" line in Fig. 5-18). The kinetics of net H^+-fluxes also demonstrated that the maximum rate of response occurred at the highest glucose concentration in the medium (Fig. 5-20). By contrast, glucose-deprived cells were not able to pump H^+ out even 50 min after stress onset (Fig. 5-20).

H^+-ATPase activity was shown to correlate with the cytoplasmic ATP levels (Kobayashi et al., 1984; O'Sullivan and Condon, 1999) which depend on glucose concentration in the medium. The absence of H^+ extrusion in the trial without glucose (Fig. 5-18) is in accord with this and suggests involvement of H^+-ATPase. The 1 mM and 10 mM glucose used in the present study correspond to high and low affinity transporters for glucose in *L. monocytogenes* that are fuelled by the PMF (Christensen and Hutkins, 1992). Consequently, the net H^+ flux responses observed in the experiments presented here at intermediate pH_o levels might be attributed to H^+-ATPase activity that was modulated by glucose concentration in the medium. The modulation of H^+ transport across the bacterial membrane was sufficient to maintain the pH_i at a constant level, with pH_o values within the pH range that permits growth of *L. monocytogenes*.

The interdependence of pH_i and net H^+ flux was also evident in the kinetics of acid stress and recovery (Figs. 5-19, 5-20, 5-21). Acidification of pH_o from 6 to 4 led to a decrease in pH_i followed by a net H^+ influx measured immediately after stress onset (Figs. 5-19, 5-20). During recovery, bacterial cells immediately (within the time resolution of the experiment; Fig. 5-21) switched from net H^+ influx to efflux which led to an almost complete recovery of pH_i. This demonstrates the complementary origin of the two processes and, therefore, implies a crucial role of plasma membrane H^+ transporters in acid stress responses and pH homeostasis in *L. monocytogenes*. This conclusion is further supported by the correlation (R=0.76

without glucose and R>0.90 with glucose; P<0.01) between pH_i and net H^+ flux changes for all glucose concentrations studied in the range of pH_o 3 to 6. Collectively, the data suggest that membrane-transport processes are the major contributors to the process of pH_i homeostasis in response to acidic treatments thus supporting the dominant role of "active homeostasis" (Booth, 1985). The above findings might be of importance in understanding the mechanism of ATR induction. Adaptation at intermediate pH_o induces ATR in bacteria including *L. monocytogenes* increasing its survival at lower pH_o values (Davis et al., 1996; O'Driscoll et al., 1996). ATR is known to occur after 60 min of the pH treatment being applied, and involves synthesis of specific proteins. However, the processes involved in bacterial adaptation prior to ATR induction are not known. This knowledge is of importance for understanding the early events in bacterial adaptation. The increase in net H^+ extrusion, observed after a treatment at intermediate pH_o for 1 h, might represent an early step in the adaptation process.

5.5.6 Conclusion

MIFE measurements of net H^+ from bacterial cells in response to acid treatment provide valuable information about the early stages of cell adaptive responses. However, due to a large number of contributing factors, unambiguous interpretation of mechanisms responsible for the measured pH changes (interpreted by the MIFE technique as net H^+ flux) is sometimes problematic. This problem has been overcome by the concurrent use of the MIFE and FRIM techniques.

The kinetics of pH_i and net H^+ fluxes were shown to be complementary in nature and provide evidence that plasma membrane H^+ transporters play a central role in *L. monocytogenes* pH homeostasis and ATR.

Combining the FRIM and MIFE techniques proved to be a powerful tool in studying bacterial response to acidic stress. To the candidates knowledge, this report is the first study of its kind in the literature. Further possible applications of the synergism of the two techniques used in this work include studies of bacterial response to other stresses like organic acids, salinity, temperature etc.

Chapter 6

GENERAL DISCUSSION

6.1. Advantages of non-invasive microelectrode ion flux measurements

In recent years, non-invasive microelectrode ion flux measurements have become a popular tool in studying adaptive responses of plant cells and tissues to a large number of abiotic stresses. Several laboratories around the world employ this technique, and their number is growing. In this work, the MIFE technique was first introduced to microbiology as a novel tool to study adaptive responses of bacteria and fungi. There are at least five major features that, taken together, confer the MIFE approach with a significant advantage over other methods for ion flux measurements.

(1) **Non-destructiveness**. In contrast to many other methods, the MIFE technique allows *in situ* measurements of net ion fluxes without requiring sub-samples of the batch culture to be taken and analysed. This is essential in situations when the experiment is carried out in a small volume, and where any sampling might significantly affect either the number of cells growing in the culture, or the substrate availability.

(2) **High spatial resolution**. This feature is especially important for microbiologists. The electrode tip is several (typically 2-3) μm in diameter, which makes it possible to measure net ion fluxes from organisms of comparable size or larger. Therefore, this technique is easily applicable in studies of membrane-transport processes in the majority of fungal and yeast cells. Only patch-clamp and FRIM techniques provide a similar capacity to carry out studies on individual organisms. Moreover, for some ionophores with high signal-to-noise ratio (like H^+), the electrode tip diameter can be further reduced to 0.8-1.0 μm. That might make it

theoretically possible to measure net ion fluxes from individual microorganisms, boosting studies of adaptive responses to a new level.

(3) **High temporal resolution.** In the present study, ion-selective microelectrodes were moved at either 0.1 or 0.05 Hz frequency, providing respectively 5 or 10 sec temporal resolution. This could be reduced without difficulty to 2 or 3 sec. Most other techniques (destructive sampling, NMR, radioactive tracers) operate on a time scale at least one order of magnitude slower. This gives the MIFE technique a unique opportunity to provide insights into very early (and fast) events associated with bacterial responses to environmental changes.

(4) **Duration of measurements.** There is essentially no limitation on how long ion fluxes could be measured from the cell. The technique is non-invasive, and its application is practically limited only by the lifetime of the ion-selective electrode (typically 15 to 20 h). Moreover, electrodes may be easily replaced, and measurements resumed after only a few minutes' break. None of the other techniques of the same time resolution (e.g. patch-clamp or FRIM) provide this opportunity. Due to dye bleaching, FRIM measurements are usually restricted to a limited number of images being taken. Maintaining a 'gigaseal' for several hours is also a big problem in every patch-clamp study.

(5) **Simultaneous measurements of several ions.** The possibility of measuring kinetics of fluxes of several ions simultaneously, and essentially at the same spot, is important to understanding the underlying ionic mechanisms of cell adaptive responses. By assessing stoichiometry ratios between various ions, valuable information about membrane transporters involved might be gained.

6.2. Feasibility of MIFE measurements in microbiology

The major technical advance of this study is demonstration of the feasibility of MIFE in microbiology. For the first time, net ion flux kinetics were measured from bacterial cells in response to various stresses (low pH; substrate availability;

bacteriocin). A few reports on non-invasive ion selective measurements from fungal and yeast cells are available in the literature (Lew, 1998), but is no report of the application of this technique to bacteria.

In this study, an efficient experimental protocol was developed to measure net ion fluxes from immobilised bacterial cells *in situ*. All methodological issues relevant to cell immobilisation procedure, potential confounding effects of changes in temperature, metabolic inhibitors, ionic strength of solution etc on LIX properties were thoroughly addressed. The feasibility of ion flux measurements from bacterial cells was demonstrated for a number of bacteria from different genera. By comparing flux data with those obtained by application of other techniques (such as growth studies, conventional concentration measurements or FRIM), the MIFE technique was validated for a wide range of physiological applications, relevant to bacterial responses to acid stress, nutritional status, or the mode of antibiotic action. These rigorous tests suggested the diverse origin of fluxes measured by the MIFE technique and highlighted some exciting prospects of its application in microbiology.

6.3. Outline of major findings

Apart from demonstrating the feasibility of MIFE ion flux measurements from fungal and bacterial cells, specific scientific phenomena were investigated. A brief summary of major findings was given after each experimental section. Summarised below are several key issues illustrating the power of the MIFE technique and the prospects of its application in microbiology.

Studies on thraustochytrid ACEM C:

- A close relationship between membrane-transport activity and cell growth and nutritional status was demonstrated. Evidence for polarity and the presence of pronounced oscillatory patterns in ion flux transport across the plasma membrane (period range of several minutes) were given. Further studies might lead to greater progress in balancing the nutritional requirements and optimization of culture growth conditions.

- The key role of membrane-transport processes in cell osmoregulation was reinforced. It was found that three cations (Na^+, Cl^- and K^+) are responsible for the bulk of osmotic adjustment in thraustochytrid ACEM C in response to hypoosmotic stress. The presented data also suggests that this process might be mediated by changes in cytosolic Ca^{2+} concentration.

- A strong relationship between the ambient temperature and activity of ion transport systems was found. The post-chilling recovery was associated with dramatic changes in net H^+ and Na^+ fluxes. Two critical temperatures were identified attributed to the re-activation of PM transporters for these ions and their complete recovery, respectively. These critical temperatures were found to be similar for the two ions investigated, suggesting the possible association of these processes with phase lipid transition in the plasma membrane.

Studies of bacterial cells

- Significant differences in membrane-transport activity were found for bacteria at different phases of growth. A significant decrease in the magnitude of net H^+, K^+ and NH_4^+ fluxes was found as cells progressed from middle exponential to late exponential and stationary phase of development. These measurements provided a possibility for interpretation of corresponding concentration changes in the medium.

- Studies on *L. monocytogenes* and *Lb. bulgaricus,* two Gram-positive bacteria of similar phylogenetic position, reinforced two different strategies employed by bacterial cells while dealing with acid stress, maintaining constant pH_i value (pH homeostasis) or ΔpH (pH homeokinesis), respectively. The strategy difference explains the different acid tolerance in these species.

- The important role of ATP-driven H^+ pumps in bacterial acid stress responses was shown. Activity of bacterial membrane H^+ transporters was found to be a major contributor to medium acidification observed by conventional methods.

- Experiments with nisin suggested that monitoring the resultant H^+ flux kinetics might be a sensitive tool in evaluating the efficacy of food additives in a variety of food products and in combination with other factors. That might significantly reduce time and labour-requirements to assess food formulations that prevent growth of *L. monocytogenes*.

- Combination of MIFE and FRIM demonstrated that pH_i and H^+ flux changes are complementary suggesting the central role of membrane transport processes in *L. monocytogenes* pH homeostasis.

6.4. Conclusions and prospects

In the present work, a comprehensive study on the feasibility of MIFE application in food microbiology was undertaken to shed light on adaptive responses of bacterial and fungal cells.

Similar to plants, application of the MIFE non-invasive ion flux measuring technique in food microbiology might provide unique opportunities to answer specific questions concerning how bacteria cope with environmental extremes. A better understanding of physiological processes might provide insights into early events associated with environmental perception and signalling in microorganisms. That might offer efficient measures to control bacterial growth with minimal doses of treatments used, further contributing to the "Hurdle Technology" approach to food safety. Ion flux measurements might also lead to greater progress in balancing the nutritional requirements and optimization of culture growth conditions (pH, osmoticum, temperature etc) for beneficial food microorganisms.

From the data presented in this work, it is apparent that the MIFE technique by itself is a powerful tool, capable of providing valuable information about the "blueprints" of cell adaptive responses to the environment. Its power, however, might be many-fold higher when combined with other electrophysiological or cellular techniques. Specifically:

- **Combining MIFE and FRIM techniques** proved to be a powerful tool in studying bacterial response to acidic stress. This report is the first study of its kind in the literature. Further, possible applications of the synergism of the two techniques used in this work include studies of bacterial response to other stresses like organic acids, salinity, temperature etc.

- **Combining MIFE and patch-clamp techniques.** This approach was shown to be extremely fruitful in plant physiology studies (Tyerman et al., 2001). Although restricted by the number of organisms suitable for patch-clamping, it might boost our knowledge about the nature and regulation of specific membrane transporters mediating bacterial adaptive responses.

- **MIFE studies on mutant strains.** Recent progress in molecular genetics has made available many mutant bacterial isolates and strains with altered adaptive response characteristics. For many of them, the genome sequence is known. These "structural genomics" data might, and should, be complemented by comprehensive studies into "functional genomics" of these organisms. The MIFE technique seems to be ideally suited for this purpose.

- **MIFE studies on natural biofilms.** There are many recent reports on *in situ* measurements of pH, dissolved oxygen, sulfide, and other chemical species within the biofilms (DeBeer et al., 1994, 1997; Lens et al., 1995; Rasmussen and Lewandowsli, 1998; Xu et al., 1998). The unambiguous interpretation of this data, however, is difficult due to many factors confounding the observed concentration changes. This problem might be overcome if ion *fluxes* are measured instead of concentrations. That might be achieved by impaling two identical ion-selective MIFE microelectrodes into the biofilm, followed by continuous monitoring of changes in measured concentration gradient between these two electrodes. Success in this activity will represent a quantum leap in development of strategies to control biofilms, as organisms contained therein display greatly enhanced resistance to antimicrobial agents.

In conclusion, due to its pioneering nature, this work has revealed only a very small "tip of the iceberg", namely the application of non-invasive ion-selective microelectrode technique in food microbiology. Further work in this direction might, and should, reveal the major bulk of the iceberg, preventing potential damage caused by food-borne pathogens to the "Titanic" of food industry. That might be an important step towards better understanding of the underlying mechanisms of bacterial adaptive responses and minimising billion-dollar losses imposed on the food industry. Customers' health will be the major beneficiary.

REFERENCES

Abee T, Rombouts FM, Hugenholtz J, Guihard G, Letellier L (1994) Mode of action of nisin Z against *Listeria monocytogenes* Scott A grown at high and low temperatures. *Appl Environ Microbiol* **60:**1962-1968.

Agranoff DD, Krishna S (1998) Metal ion homeostasis and intracellular parasitism. *Mol Microbiol* **28:**403-412.

Aguilar PS, Cronan JE, Demendoza D (1998) A *Bacillus subtilis* gene induced by cold shock encodes a membrane phospholipid desaturase. *J Bacteriol* **180:**2194-2200.

Altekruse SF, Cohen ML, Swerdlow DL (1997) Emerging foodborne diseases. *Emerg Infect Dis* **3:**285-293.

Amachi S, Ishikawa K, Toyoda S, Kagawa Y, Yokota A, Tamita F (1998) Characterization of a mutant of Lactococcus lactis with reduced membrane-bound ATPase activity under acidic conditions. *Biosci Biotechnol Biochem* **68:**1574-1580.

Ammann D (1986) Ion-Selective Microelectrodes. Berlin: Springer-Verlag.

Anand S, Prasad R (1989) Rise in intracellular pH is concurrent with 'start' progression of *Saccharomyces cerevisiae*. *J Gen Microbiol* **135:**2173-2179.

Andjus PR, Djurisic MR, Zujovic Z, Begovic N, Srejic R, Vucelic D (1999) Discontinuities in the temperature function of transmembrane water transport in *Chara*: relation to ion transport. *J Membr Biol* **167:**267-274.

ANZFA (1999) Food Safety Standards Costs and Benefits. AGPS, Canberra.

Apte SK, Thomas J (1986) Membrane electrogenesis and sodium transport in filamentous nitrogen-fixing cyanobacteria. *Eur J Biochem* **154:**395-401.

Arav A, Zeron Y, Leslie SB, Behboodi E, Anderson GB, Growe JH (1996) Phase transition temperature and chilling sensitivity of bovine oocytes. *Cryobiol* **33:**589-599.

Arav A, Pearl M, Zeron Y (2000) Does lipid profile explain chilling sensitivity and membrane lipid phase transition of spermatozoa and oocytes? *Cryo-Letters* **21:**179-186.

Arif I, Newman IA, Keenlyside N (1995) Proton flux measurements from tissues in buffered solution. *Plant Cell Environ* **18:**1319-1324.

Arneborg N, Salskou-Iversen AS, Mathiasen TE (1993) The effects of growth rate and other growth conditions on the lipid composition of *Escherichia coli. Appl Microbiol Biotechnol* **39:**353-357.

Arnold KW, Kasper CW (1995) Starvation- and stationary-phase-induced acid tolerance in *Escherichia coli* O157:H7. *Appl Environ Microbiol* **61:**2037-2039.

Atlas RM (1984) Microbiology : fundamentals and applications. New York : Macmillan. p. 879.

Babourina O, Shabala S, Newman I (1998) Auxin stimulates Cl^- uptake by oat coleoptiles. *Ann Bot* **82:**331-336.

Babourina O, Leonova T, Shabala S, Newman I (2000) Effect of sudden salt stress on ion fluxes in intact wheat suspension cells. *Ann Bot* **85:**759-767.

Bachewich CL, Heath IB (1997) The cytoplasmic pH influences hyphal tip growth and cytoskeleton-related organisation. *Fungal Genetics Biol* **21:**76-91.

Bahnweg G (1979) Studies on the physiology of Thraustochytriales. I. Growth requirements and nitrogen nutrition of *Thraustochytrium* spp., *Schizochytrium* sp., *Japonochytrium* sp., *Ulkenia* spp., and *Labyrinthuloides* spp. *Veroff Inst Meeresforsch, Bremerhaven* **17:**245-268.

Bajpai PK, Bajpai P, Ward OP (1991) Production of docosahexaenoic acid by *Thraustochytrium aureum. Appl Microbiol Biotechnol* **35:**706-710.

Bakker EP (1992) Cell K^+ and K^+ transport systems in prokaryotes. In: *Alkali Cation Transport Systems in Prokaryotes.* EP Bakker (ed.), CRC Press, Boca Raton, Fla, pp. 205-224.

Bakker EP, Booth IR, Dinnbier U, Epstein W, Gajewska A (1987) Evidence for multiple K^+ export systems in *Escherichia coli. J Bacteriol* **169:**3743-3749.

Barbaro SE, Trevors JT, Inniss WE (1999) Effect of different carbon sources on membrane permeability, membrane fluidity, and fatty acid composition of a psychrotrophic Acinetobacter sp HH1-1 during growth at low temperatures and after cold shock. *World J Microbiol Biotechnol* **15:**683-692.

Barnes EM, Jayakumar A (1993) NH_4^+ transport of systems in *Escherichia coli.* In: *Alkali Cation Transport Systems in Prokaryotes.* EP Bakker (ed.), CRC Press, Inc., Boca Raton, Fla, pp. 397-409.

Barton JK, den Hollander JA, Lee TM, MacLaughlin A, Shulman RG (1980) Measurements of the internal pH of yeast spores by ^{31}P nuclear magnetic resonance. *Proc Natl Acad Sci USA* **77:**2470-2473.

Bauer CS, Plieth C, Bethmann B, Popescu O, Hansen U-P, Simonis W, Schonknecht G (1998) Strontium-induced repetitive calcium spikes in a unicellular green alga. *Plant Physiol* **117:**545-557.

Becker LA, Cetin MS, Hutkins RW, Benson AK (1998) Identification of the gene encoding the alternative sigma factor sigma B from *Listeria monocytogenes* and its role in osmotolerance. *J Bacteriol* **180:**4547-4554.

Beilby MJ, Shepherd VA (1996) Turgor regulation in *Lamprothamnium papulosum*. 1. I/V analysis and pharmacological dissection of the hypotonic effect. *Plant Cell Environ* **19:**837-847.

Beilby MJ, Cherry CA, Shepherd VA (1999) Dual turgor regulation response to hypotonic stress in *Lamprothamnium papulosum*. *Plant Cell Environ* **22:**347-359.

Belsky MM, Goldstein S, Menna M (1970) Factors affecting phosphate uptake in the marine fungus *Dermocystidium* sp. *J Gen Microbiol* **62:**399-402.

Bender GR, Sutton SV, Marquis RE (1986) Acid tolerance, proton permeabilities, and membrane ATPases of oral streptococci. *Infect Immun* **53:**331-338.

Bender GR, Marquis RE (1987) Membrane ATPases and acid tolerance of *Actinomyces viscosus* and *Lactobacilluscasei*. *Appl Environ Microbiol* **53:**2124-2128.

Benjamin M, Datta AR (1995) Acid tolerance of enterohemorrhagic *Escherichia coli. Appl Environ Microbiol* **61:**1669-1672.

Berrier C, Coulombe A, Szabo I, Zoratti M, Ghazi A (1992) Gadolinium ion inhibits loss of metabolites induced by osmotic shock and large stretch-activated channels in bacteria. *Eur J Biochem* **206:**559-565.

Berry ED, Foegeding PM (1997) Cold temperature adaptation and growth of microorganisms. *J Food Prot* **60:**1583-1594.

Besser RE, Lett SM, Weber JT, Doyle MP, Barrett TJ, Wells JG, Griffin PM (1993) An outbreak of diarrhea and hemolytic uremic syndrome from *Escherichia coli* O157:H7 in fresh-pressed apple cider. *J Amer Med Assoc* **269:**2217-2267.

Bisson MA, Gutknecht J (1975) Osmotic regulation in the marine alga, *Codium decorticatum*. I. Regulation of turgor pressure by control of ionic composition. *J Membr Biol* **24:**183-200.

Bisson MA, Krist GO (1995) Osmotic acclimation and turgor pressure regulation in algae. *Naturwissenschaften* **82:**461-471.

Bisson MA, Kiegle E, Black D, Kiyosawa K, Gerber N (1995) The role of calcium in turgor regulation in *Chara longifolia. Plant Cell Environ* **18:**129-137.

Blatt MR, Thiel G (1994) K^+ channels of stomatal guard cells: bimodal control of the K^+ inward-rectifier evoked by auxin. *Plant J* **5:**55-68.

Blount P, Moe PC (1999) Bacterial mechanosensitive channels: integrating physiology, structure and function. *Trends Microbiol* **7:**420-424.

Booth IR (1985) Regulation of cytoplasmic pH in bacteria. *Microbiol Rev* **49:**359-378.

Booth IR (1999) The regulation of intracellular pH in bacteria. *Novartis Found Symp* **221:**19-37.

Booth IR, Kroll RG (1983) Regulation of cytoplasmic pH (pH_i) in bacteria and its relationship to metabolism. *Biochem Soc Trans* **601:**70-72.

Booth IR, Jones MA, McLaggan D, Nicolaev Y, Ness LS, Wood CM, Miller S, Totemeyer S, Ferguson GP (1996) Bacterial ion channels. In: WN Konings, HR Kaback, JS Lolkema (eds.) *Transport Processes in Eukaryotic and Prokaryotic Organisms*. Elsevier, Amsterdam, pp. 693-729.

Booth T (1971) Distribution of certain soil inhabiting chytrid and chytridiaceous species related to some physical and chemical factors. *Can J Bot* **49:**1743-1755.

Bravo -F P, Uribe EG (1981) Temperature dependence of the concentration kinetics of absorption of phosphate and potassium in corn roots. *Plant Physiol* **67:**815-819.

Breeuwer P, Abee T (2000) Assessment of viability of microorganisms employing fluorescence techniques. *Int J Food Microbiol* **55:**193-200.

Breeuwer P, Drocourt JL, Rombouts FM, Abee T (1996) A novel method for continuous determination of the intracellular pH in bacteria with the internally conjugated fluorescent probe 5 (and 6-)-carboxyfluorescein ester. *Appl Environ Microbiol* **62:**178-183.

Breeuwer P, de Reu JC, Drocourt JL, Rombouts FM, Abee T (1997) Nonanoic acid, a fungal self-inhibitor, prevents germination of *Rhizopus oligosporus* sporangiospores by disspation of the pH-gradient. *Appl Environ Microbiol* **63:**178-185.

Brochiero E, Banderali U, Lindenthal S, Raschi C, Ehrenfeld J (1995) Basolateral membrane chloride permeability of A6 cells – implication in cell volume regulation. *Eur J Physiol* **431:**32-45.

Brown JL, Ross T, McMeekin TA, Nichols PD (1997) Acid habituation of Escherichia coli and the potential role of cyclopropane fatty acids in low pH tolerance. *Int J Food Microbiol* **37:**163-173.

Brownlee C (1984) Membrane potential components of the marine fungus *Dendryphiella salina* (suth.) Pugh et Nicot. Possible involvement of calmodulin in electrophysiology and growth. *New Phytol* **97:**15-23.

Bruno MEC, Kaiser A, Montville TJ (1992) Depletion of proton motive force by nisin in *Listeria monocytogenes* cells. *Appl Environ Microbiol* **58:**2255-2259.

Budde BB, Jakobsen M (2000) Real-time measurements of the interaction between single cells of *Listeria monocytogenes* and nisin on a solid surface. *Appl Environ Microbiol* **66:**3568-3591.

Bunthof CJ, van den Braak S, Breeuwer P, Rombouts FM, Abee T (2000) Fluorescence assessment of *Lactococcus lactis* viability. *Int J Food Microbiol* **55:**291-294.

Burgstaller W (1997) Transport of small ions and molecules through the plasma membrane of filamentous fungi. *Crit Rev Microbiol* **23:**1-46.

Busa WB, Nuccitelli R (1984) Metabolic regulation via intracellular pH. *Amer J Physiol* **246:**409-438.

Bush DS (1993) Regulation of cytosolic calcium in plants. *Plant Physiol* **103:**7-13.

Buurman ET, Teixeira de Mattos MJ, Neijssel OM (1991) Futile cycling of ammonium ions via the high affinity potassium uptake system (Kdp) of *Escherichia coli. Arch Microbiol* **155:**391-395.

Calamita G, Bishai WR, Preston GM, Guggino WB, Agre P (1995) Molecular cloning and characterization of AqpZ, a water channel from *Escherichia coli.* **270:**29063-29066.

Caldwell JH, van Brunt J, Harold FM (1986) Calcium-dependent anion channel in the water mold *Blastocladiella emersonii. J Membr Biol* **89:**85-98.

Cardenas L, Feijo JA, Kunkel JG, Sanchez F, Holdaway-Clarke T, Hepler PK, Quinto C (1999) Rhizobium node factors induce increases in intracellular free calcium and extracellular calcium influxes in bean root hairs. *Plant J* **19:**347-352.

Carratu L, Franceschelli S, Pardini CL, Kobayashi GS, Horvath I, Vigh L, Maresca B (1996) Membrane lipid perturbation modifies the set point of the temperature of heat shock response in yeast. *Proc Natl Acad Sci USA.* **93:**3870-3875.

Cavalier-Smith T, Allsopp MTEP, Chao EE (1994) Thraustochytrids are chromists, not fungi: 18s rRNA signatures of heteroconta. *Phil Trans R Soc London* **346:**387-397.

Cessna SG, Low PS (2001) An apoplastic Ca^{2+} sensor regulates internal Ca^{2+} release in aequorin-transformed tobacco cells. *J Biol Chem* **276:**10655-10662.

Chamberlian AHL, Moss ST (1988) The thraustochytrids: a protist group with mixed affinities. *BioSystems* **21:**341-349.

Charpentier G (1999) Induction of membrane excitability in *Xenopus oocytes*. *J Soc Biol* **193:**517-22.

Chen Y, Montville TJ (1995) Efflux of ions and ATP depletion induced by pediocin PA-1 are concomitant with cell death in *Listeria monocytogenes* Scott A. *J Appl Bacteriol* **79:**684-690.

Cheville AM, Arnold KW, Bushrieser C, Cheng C-M, Kaspar CW (1996) *rpoS* regulation of acid heat, and salt tolerance in *Escherichia coli* O157:H7. *Appl Environ Microbiol* **62:**1822-1824.

Chikindas ML, Garciagarcera MJ, Driessen AJM, Ledeboer AM, Nissenmeyer J, Nes IF, Abee T, Konings WN, Venema G (1993) Pediocin PA-1, a bacteriocin from *Pediococcus-acidilactici* PAC1.0, forms hydrophilic pores in the cytoplasmic membrane of target cells. *Appl Environ Microbiol* **59:**3577-3584.

Chilton FH, Patel M, Fontch AN, Hubbard WC, Triggiani M (1993) Dietary n-3 fatty acids effects on neutrophil lipid composition and mediator production. Influence of duration and dosage. *J Clin Invest* **91:**115-122.

Christensen DP, Hutkins RW (1992) Collapse of the proton motive force in *Listeria monocytogenes* caused by a bacteriocin produced by *Pediococcus acidilactici*. *Appl Environ Microbiol* **58:**3312-3315.

Christensen DP, Hutkins RW (1994) Glucose uptake by *Listeria monocytogenes* Scott A and inhibition by pediocin JD. *Appl Environ Microbiol* **60:**3870-3873.

Cid A, Serrano R (1988) Mutations of the yeast plasma membrane H^+-ATPase which cause thermosensitivity and altered regulation of the enzyme. *J Biol Chem* **263:**14134-14139.

Clarkson DT, Earnshaw MJ, White PJ, Cooper HD (1988) Temperature dependent factors influencing nutrient uptake: an analysis of responses at different levels of organization. In: *Plants and Temperature* (SP Long and FI Woodward, eds.). XXXXII Symp Soc Exp Biol, Cambridge. pp. 281- 309.

Clipson NJW, Jennings DH (1992) *Dendryphiella salina* and *Debaryomyces hansenii* – models for ecophysical adaptation to salinity by fungi that grow in the sea. *Can J Bot* **70:**2097-2105.

Cohen Z, Vonshek A, Richmond A (1987) Fatty acid composition of Spirulina strains grown under various environmental conditions. *Phytochem* **26:**2255-2258.

Comas J, Vives-Rego J (1998) Enumeration, viability and heterogeneity in *Staphylococcus aureus* cultures by flow cytometry. *J Microbiol Methods* **32:**45-53.

Connor WE, Martha N, Lin DS (1990) Dietary effects on brain fatty acid composition, the reversibility of n-3 fatty acid deficiency and turnover of docosahexaenoic acid in brain, erythrocyte and plasma of rhesus monkey. *J Lipid Res* **31:**237-247.

Cook GM, Russell JM (1994) The effect of extracellular pH and lactic acid on pH homeostasis in *Lactococcus lactis* and *Streptococcus bovis*. *Curr Microbiol* **28:**165-168.

Coote PJ, Jones MV, Seymour IJ, Rowe DL, Ferdinando DP, McArthur AJ, Cole MB (1994) Activity of the plasma membarne H^+-ATPase is a key physiological determinant of thermotolerance in *Saccharomyces cerevisiae*. *Microbiol* **140:**1881-1890.

Cosgrove DI (1998) Cell wall loosening by expansins. *Plant Physiol* **118:**333-339.

Cotter PD, Gahan CGM, Hill C (2000) Analysis of the role of the *Listeria monocytogenes* F0F1-ATPase operon in the acid tolerance response. *Int J Food Microbiol* **60:**137-146.

Cotter PD, Gahan CGM, Hill C (2001) A glutamate decarboxylase system protects *Listeria monocytogenes* in gastric fluid. *Mol Microbiol* **40:**465-475.

Crandall AD, Montville TJ (1998) Nisin resistance in *Listeria monocytogenes* ATCC 700302 is a complex phenotype. *Appl Environ Microbiol* **64:**231-237.

CRC Handbook of Chemistry and Physics (1974). CRC Press: Cleveland, Ohio.

Cronan JE (1968) Phospholipid alterations during growth of *Escherichia coli. J Bacteriol* **95:**2054-2061.

Cui C, Adler J (1996) Effect of mutation of potassium-efflux system, KefA, on mechanosensitive channels in the cytoplasmic membrane of *Escherichia coli. J Membrane Biol* **150:**143-152.

Dalet K, Gouin E, Cenatiempo Y, Cossart P, Hechard Y (1999) Characterisation of a new operon encoding a Zur-like protein and an associated ABC zinc permease in *Listeria monocytogenes*. *FEMS Microbiol Lett* **174:**111-116.

Datta AR, Benjamin MM (1997) Factors controlling acid tolerance of *Listeria monocytogenes*: effects of nisin and other ionophores. *Appl Environ Microbiol* **63:** 4123-4126.

Davies JM, Brownlee C, Jennings DH (1990) Measurements of intracellular pH in hyphae using BCECF and digital imaging microscopy. Evidence for a primary proton pump in the plasmalemma of a marine fungus. *J Cell Sci* **96:**731-736.

Davies RJ, Holdsworth JE, Reader SL (1990) The effect of low oxygen uptake rate on the fatty profile of the oleaginous yeast *Apiotrichum curvatum*. *Appl Microbiol Biotechnol* **33:**237-247.

Davis MJ, Coote PJ, O'Byrne CP (1996) Acid tolerance in *Listeria monocytogenes*: the adaptive acid tolerance response (ATR) and growth-phase-dependent acid resistance. *Microbiology* **142:**2975-82.

De E, Orange N, Saint N, Guerillon J, Demot R, Molle G (1997) Growth temperature dependence of channel size of the major outer-membrane protein (oprf) in psychrotrophic *Pseudomonas fluorescens* strains. *Microbiol* **143:**1029-1035.

De Groot PWJ, Ruiz C, de Aldana CRV, Duenas E, Cid VJ, Del Rey F, Rodriquez-Pena JM, Perez P, Andel A, Caubin J, Arroyo J, Garcia JC, Gil C, Molina M, Garcia LJ, Nombela C, Klis FM (2001) A genomic approach for the identification and classification of genes involved in cell wall formation and its regulation in *Saccharomyces cerevisiae*. *Comparative and Functional Genomics* **2:** 124-142.

De Koninck P, Schulman H (1998) Sensitivity of CaM kinase II to the frequency of Ca^{2+} oscillations. *Science* **279:**227-230.

De Mendoza D, Cronan JE, Jr. (1983) Thermal regulation of membrane lipid fluidity in bacteria. Trends Biochem Sci **8:**49-52.

DeBeer D, Srinivasan R, Stewart PS (1994) Direct measurement of chlorine penetration into biofilms during disinfection. *Appl Environ Microbiol* **60:**4339-4344.

DeBeer D, Schramm A, Santegoeds CM, Kuhl M (1997) A nitrite microsensor for profiling environmental biofilms. *Appl Environ Microbiol* **63:**973-977.

Deere D, Porter J, Edwards C, Pickup R (1995) Evaluation of the suitability of bis-(1,3-dibutylbarbituric acid)trimethine oxonol, (DiBA-C_4(3)-), for the flow cytometric assessment of bacterial viability. *FEMS Microbiol Lett* **130:**165-170.

Delves-Broughton J, Blackburn P, Evans RJ, Hugenholtz J (1996) Applications of the bacteriocin, nisin. *Antonie Van Leeuwenhoek* **69:**193-202.

Den Hollander A, Ugurbil K, Brown TR, Shulman RG (1981) Phosphorus-31 nuclear magnetic resonanse studies of the effect of oxygen upon glycolysis in yeast. *Biochemistry* **20:**5871-5880.

DHHS/FDA/CFSAN (2001) Draft assessment of the relative risk to public health from foodborne *Listeria monocytogenes* among selected categories of ready-to-eat foods. 348 pp. http://www.foodsafety.gov/~dms/lmrisk.html (12.02.2001).

Dick MW (1973) Saprolegniales. In: *The Fungi - an advanced treatise* (Ainsworth GC, Sparrow FK and Sussman AL, eds.). Vol. 4B, pp. 113-144. Academic Press: New York.

Diez-Gonzalez F, Russell JB (1997) The ability of *Escherichia coli* O157:H7 to decrease its intracellular pH and resist the toxicity of acetic acid. *Microbiol* **143:**1175-1180.

Dilworth MJ, Glenn AR (1999) Problems of adverse pH and bacterial strategies to combat it. In: *Bacterial Responses to pH.* Novartis Found Symp **221:**4-18.

Dinno MA, Nagel W (1988) Temperature dependence of transcellular and intracellular parameters of frog skin. *Prog Clin Biol Res* **258:**103-120.

Dinsdale MG, Lloyd D, Jarvis B (1995) Yeast vitality during cider fermentation: two approaches to the measurement of membrane potential. *J Inst Brew* **101:**453-458.

Driessen, AJM, van den Hooven HW, Kuiper W, Van de Kamp M, Sahl H-G, Konings RNH, Konings WN (1995) Mechanistic studies of lantibiotic-induced permeabilization of phospholipid vesicles. *Biochem* **34:**1606-1614.

Dunstan GA, Olley J, Ratkowsky DA (1999) Major environmental and biological factors influencing the fatty acid composition of seafood from Indo-Pacific to Antarctic Waters. Recent Res Devel Lipids Res **3:**63-86.

DuPont FM (1989) Effect of temperature on the plasma membrane and tonoplast ATPases in barley roots. Comparison results obtained with acridine orange and quinacrine. *Plant Physiol* **89:**1401-1412.

DuPont FM, Mudd JB (1985) Acclimation to low temperature by microsomal membranes from tomato cell cultures. *Plant Physiol* **77:**74-78.

Dyerberg J (1986) Linoleate-derived polyunsaturated fatty acids and prevention of atherosclerosis. *Nutr Rev* **44:**125-134.

Edgcomb MR, Sirimanne S, Wilkinson BJ, Drouin P, Morse R (2000) Electron paramagnetic resonance studies of the membrane fluidity of the foodborne pathogenic psychrotroph *Listeria monocytogenes*. *Biochim Biophys Acta* **1463:**31-42.

Ehrenberg B, Montana V, Wei M-D, Wuskell JP, Loew LM (1988) Membrane potential can be determined in individual cells from the nernstian distribution of cationic dyes. *Biophys J* **53:**785-794.

Eilam Y (1982) The effect of monovalent cations on calcium efflux in yeasts. *Biochim Biophys Acta* **687:**8-16.

Eilam Y, Chernichovsky D (1987) Uptake of Ca^{2+} driven by membrane potential in energy-depleated yeast cells. *J Gen Microbiol* **133:**1641-1649.

Engels C, Marschner H (1992) Root to shoot translocation of macronutrients in relation to shoot demand in maize (*Zea mays* L.) grown at different root zone temperatures. *Z Pflanzenernahr Bodenk* **155:**121-128.

Epstein W, Schultz SG (1966) Cation transport in *Escherichia coli*. VI. K^+ exchange. *J Gen Physiol* **49:**469-481.

Evans RI, McClure PJ, Gould GW, Russell NJ (1998) The effect of growth temperature on the phospholipid and fatty acyl compositions of non-proteolytic *Clostridium botulinum*. *Int J Food Microbiol* **40:**159-167.

Fagan MJ, Saier MH (1994) P-type ATPases of eukaryotes and bacteria: sequence comparisons and construction of phylogenetic trees. *J Mol Evol* **38:**57-99.

Farag RS, Khail FA, Salem H, Ali LHM (1983) Effects of various carbon and nitrogen sources on fungal lipid production. *JAOCS* **60:**795-800.

Farber JM, Peterkin PI (1991) *Listeria monocytogenes*, a food-borne pathogen. *Microbiol Rev* **55:**476-511.

Farber JM, Sanders GW, Dunfield S, Prescott R (1989) The effect of various acidulants on the growth of *Listeria monocytogenes*. *Lett Appl Microbiol* **9:**181-183.

Felle HH, Hepler PK (1997) The cytosolic Ca^{2+} concentration gradient of *Sinapis alba* root hairs as revealed by Ca^{2+}-selective microelectrode tests and fura-dextran ratio imaging. *Plant Physiol* **114:**39-45.

Fliegel L, Frohlich O (1993) The Na^{+}/H^{+} exchanger: an update on structure, regulation and cardiac physiology. *Biochem J* **296:**273-285.

Francis MS, Thomas CJ (1997) The *Listeria monocytogenes* gene ctpA encodes a putative P-type ATPase involved in copper transport. *Mol Gen Genet* **253:**484-491.

Franks F, Mathias SF, Hatley RHM (1990) Water, temperature and life. *Phil Trans R Soc Lond* **B326:**517-533.

Fraser KR, Harvie D, Coote PJ, O'Byrne CP (2000) Identification and characterization of an ATP binding cassette L-carnitine transporter in *Listeria monocytogenes*. *Appl Environ Microbiol* **66:**4696-4704.

Gaertner A (1977) Revision of the Thraustochytriaceae (lower marine fungi). I. *Ulkenia* nov. gen. with description of three new species. *Veroffent Inst Meeresforsch Bremerhaven* **16:**139-157.

Gahan CG, Hill C (1999) The relationship between acid stress responses and virulence in *Salmonella typhimurium* and *Listeria monocytogenes*. *Int J Food Microbiol* **50:**93-100.

Gahan CGM, O'Driscoll B, Hill C (1996) Acid adaptation of *Listeria monocytogenes* can enhance survival in acidic foods and during milk fermentation. *Appl Environ Microbiol* **62:**3128-3132.

Gale EF, Epps HMR (1942) The effect of the pH of the medium during growth on the enzymic activities of bacteria (*Escherichia coli* and *Micrococcus lysodeikticus*) and the logical significance of the changes produced. *Biochem J* **36:**600-619.

Galinski EA (1995) Osmoadaptation in bacteria. In: *Advances in Microbial Physiology*. RK Poole (ed.) Academic Press, London, V. 37, pp. 273-328.

Gangola P, Rosen BP (1987) Maintenance of intracellular calcium in *Escherichia coli*. *J Biol Chem* **262:**12570-12574.

Garbay S, Lonvaudfunel A (1996) Response of *Leuconostoc oenos* to environmental changes. *J Appl Bacteriol* **81:**619-625.

Garcera JJG, Elferink GL, Driesen JM, Konings WN (1993) *In vitro* pore-forming activity of the lantibiotic nisin. Role of PMF and lipid composition. *Eur J Biochem* **212:**417-422.

Garrill A, Davies JM (1994) Patch clamping fungal membranes: a new perspective on ion transport. *Mycol Res* **98:**257.

Garrill A, Clipson NJW, Jennings DH (1992) Preliminary observations on the monovalent cation relations of *Thraustochytrium aureum*, a fungus requiring sodium for growth. *Mycol Res* **96:**295-304.

Garwin JL, Cronan JE, Jr (1980) Thermal modulation of fatty acid synthesis in *Escherichia coli* does not involve de novo enzyme synthesis. *J Bacteriol* **141:**1457-1459.

Gerhardt PN, Tombras Smith L, Smith GM (2000) Osmotic and chill activation of glycine betaine porter II in *Listeria monocytogenes* membrane vesicles. *J Bacteriol* **182:**2544-50.

Giffard CJ, Ladha S, Mackie AR, Clark DC, Sanders D (1996) Interaction of nisin with planar lipid bilayers monitored by fluorescence recovery after photobleaching. *J Membr Biol* **151:**293-300.

Gillies RJ (1994) NMR spectroscopy in Biomedicine. Academic Press, New York.

Giraldez-Ruiz N, Bonilla I, Fernandez-Pinaz F (1999) Role of external calcium in homeostasis of intracellular pH in the cyanobacterium *Anabaena sp.* strain PCC7120 exposed to low pH. *New Phytol* **141:**225-230.

Goldstein S (1963) Development and nutrition of new species of *Thraustochytrium*. *Amer J Bot* **50:** 271-279.

Gould RM, Lennarz WJ (1970) Metabolism of phosphatidylglycerol and lysylphosphatidylglycerol in *Staphylococcus aureus*. *J Bacteriol* **104:**1135-1144.

Gradmann D, Slayman CL (1975) Oscillations of an electrogenic pump in the plasma membrane of *Neurospora*. *J Membr Biol* **23:**181-212.

Gradmann D, Boyd CM (1995) Membrane voltage of marine phytoplankton, measured in the diatom *Coscinodiscus radiatus*. *Marine Biol* **123:**645-650.

Gradmann D, Buschmann P (1997) Oscillatory interaction between voltage gated electroenzymes. *J Exp Bot* **48:**399-404.

Graumman P, Schroder K, Schmid R, Marahiel MA (1996) Cold shock stress-induced proteins in *Bacillus subtilis*. *J Bacteriol* **178:**4611-4619.

Gray ML, Killinger AH (1996) *Listeria monocytogenes* and listeric infections. *Bacteriol Rev* **30:**309-382.

Grinberg A, Heath IB (1997) Direct evidence for Ca^{2+} regulation of hyphal branch induction. *Fungal Genet Biol* **22:**127-139.

Grishanin RN, Bibikov SI, Altschuler IM, Kaulen AD, Kazimirchuk SB, Armitage JP, Skulachev VP (1996) delta psi-mediated signalling in the bacteriorhodopsin-dependent photoresponse. *J Bacteriol* **178:** 3008-3014.

Gross D, Loew LM (1989) Fluorescent indicators of membrane potential: microspectrofluorimetry and imaging. In: *Methods in Cell Biology* (Lansing TD and Wang Y, eds.). London: Academic press. Vol. 30, pp.193-218.

Gross ID (1975) Periodic cyclic AMP signals and cell differentiation. *Nature* **255:**522-523.

Gross JD, Bradbury J, Kay RR, Peacey MJ (1983) Intracellular pH and the control of cell differentiation in *Dictyostelium discodeum*. *Nature* **303:**244-245.

Gruwel ML, Kuzio B, Xiang B, Deslauriers R, Kupriyanov VV (1998) Temperature dependence of monovalent cation fluxes in isolated rat hearts: a magnetic resonance study. *Biochim Biophys Acta* **1415:**41-55.

Guern J, Felle H, Mathieu Y (1991) regulation of intracellular pH in plant cells. *Int Rev Cytol* **127:**111-174.

Guldfeldt LU, Arneborg N (1998) Measurements of the effects of acetic acid and extracellular pH on intracellular pH of nonfermenting, individual *Saccharomyces cerevisiae* cells by fluorescence microscopy. *Appl Environ Microbiol* **64:**530-534.

Gustin MC, Martinac B, Saimi Y, Culbertson MR, Kung C (1986) Ion channels in yeast. *Science* **233:**1195-1196.

Gutknecht J, Hastings D, Bisson M (1977) Ion transport and turgor pressure relation in giant algal cells. In: *Transport across Biological Membranes*. G Giebisch, DC Tosteson, HH Ussing (eds.).

Haest CWM, de Gier J, Op den Kamp JAF, Bartels P, van Deenan LLM (1972) Changes in the permeability of Staphylococcus aureus and derived liposomes with varying lipid composition. *Biochim Biophys Acta* **255:**720-733.

Hajnoczky G, Robb-Gaspers LD, Seitz MB, Thomas AP (1995) Decoding of cytosolic calcium oscillations in the mitochondria. *Cell* **82:**415-424.

Hall HK, Karem KL, Foster JW (1995) Molecular responses of microbes to environmental pH stress. *Adv Microb Physiol* **37:**229-272.

Hällgren JE, Öquist G (1990) Adaptation to low temperature. In: *Stress Responses in Plants: Adaptation and Acclimation Mechanisms.* Wiley-Liss Inc. pp. 265-293.

Hama H, WilsonTH (1992) Primary structure and characteristics of the melibiose carrier of *Klebsiella pneumoniae. J Biol Chem* **267:**18371-18376.

Hamill OP, Martinac B (2001) Molecular basis of mechanotransduction in living cells. *Physiol Rev* **81:**685-740.

Harold FM (1986) The Vital Force: A Study of Bioenergetics. W. H. Freeman, New York.

Harold FM, van Brunt J (1978) Circulation of H^+ and K^+ across the plasma membrane is not obligatory for bacterial growth. *Science* **197:**372-373.

Harold FM, Maloney PC (1996) Energy transduction by ion currents, In: *Escherichia coli and Salmonella.* F Neidhardt (ed.) *Cellular and Molecular Biology.* ASM Press, Washington, DC, V., pp. 283-306.

Harold FM, Pavlasova E, Baarda JR (1970) A transmembrane pH gradient in *Streptococcus faecalis*: origin, and dissipation by proton conductors and *N,N'*-dicyclohexylcarbodiimide. *Biochim Biophys Acta* **196:**235-244.

Harwood J L, Russell NJ (1984) Lipids in plants and microbes. George Allen and Unwin, Ltd., London.

Hathcox AK, Beuchat LR, Doyle MP (1995) Death of enterohemorrhagic *Escherichia coli* O157:H7 in real mayonnaise and reduced-calorie dressing as influenced by initial population and storage temperature. *Appl Environ Microbiol* **61:**4172-4177.

Hawley SA (1971) Reversible pressure-temperature denaturation of chymotrypsinogen. *Biochem* **10:**2436-2442.

Hegemann P (1997) Vision in microalgae. *Planta* **203:** 265-274.

Hellingwerf KJ,. Konings WN (1985) The energy flow in bacteria: the main free energy intermediates and their regulatory role. *Adv Microb Physiol* **26:**25-154.

Hill C, O'Driscoll B, Booth I (1995) Acid adaptation and food poisoning microorganisms. *Int J Food Microbiol* **28:**245-254.

Hochachka PW, Somero GN (1984) Biochemical adaptation. New Jersey: Princeton University Press.

Hoffmann EK, Dunham PB (1995) Membrane mechanisms and intracellular signalling in cell volume regulation. *Int Rev Cytol* **161:**173-262.

Holler C, Witthuhn D, Janzen-Blunck B (1998) Effect of low temperatures on growth, structure, and metabolism of *Campylobacter coli* SP 10. *Appl Environ Microbiol* **64:** 581-587.

Holyoak CD, Stratford M, McMullin Z, Cole MB, Crimmins K, Brown AJP, Coote PJ (1996) Activity of the plasma membarne H^+-ATPase and optimal glycolytic flux are required for rapid adaptation and growth of *Saccharomyces cerevisiae* in the presence of the weak-acid preservative sorbic acid. *Appl Environ Microbiol* **62:**3158-3164.

Holyoak CD, Thompson S, Calderon CO, Hatzixanthis K, Bauer B, Kuchler K, Piper PW, Coote PJ (2000) Loss of Cmk1 Ca^{2+}-calmodulin-dependent protein kinase in yeast results in constitutive weak organic acid resistance, associated with a post-transcriptional activation of the Pdr12 ATP-binding cassette transporter. *Molecular Microbiol* **37:** 595-605.

Horn H (1994) Dynamics of a nitrifying bacteria population in a biofilm controlled by an oxygen microelectrode. *Water Sci Technol* **29:**69-76.

Huisman GW, Siegele DA, Zambrano MM, Kolter R (1996) Morphological and physiological changes during stationary phase. In: *Escherichia coli and Salmonella. Cellular and Molecular Biology.* F Neidhardt (ed.) ASM Press, Washington, DC, V. 2, pp. 1672-1682.

Hunter DR, Segel IH (1973) Effect of weak acids on amino acid transport by *Penicillium chrysogenum*: evidence for a proton or charge gradient as the driving force. *J Bacteriol* **113:**1184-1192.

Hyde GJ, Heath IB (1997) Ca^{2+} gradients in hyphae and branches of *Saprolegnia ferax. Fungal Genet Biol* **21:**238-251.

Iida I, Nakahara T, Yokochi T, Kamisaka Y, Yagi H, Yamaoka M, Suzuki O (1996) Improvement of docosahexaenoic acid production in a culture of *Thraustochytrium aureum* by medium optimization. *J Ferment Bioeng* **81:**76-78.

Ikehara T, Yamaguchi H, Hosokawa K, Takahashi A, Masuya T, Miyamoto H (1992) Different patterns of cell volume regulation in hypoosmotic media between attached and suspended HeLa cells. *Biochim Biophys Acta* **1111:**151-158.

Ilan N, Moran N, Schwartz A (1995) The role of potassium channels in the temperature control of stomatal aperture. *Plant Physiol* **108:**1161-1170.

Imada C, Oosawa Y (1999) Thermoreception of *Paramecium*: different Ca^{2+} channels were activated by heating and cooling. *J Membr Biol* **168:**283-287.

Ingraham JL, Marr AG (1996). Effect of temperature, pressure, pH and osmotic stress on growth. In: P Neidhardt (ed.) *Escherichia coli and Salmonella. Cellular and Molecular Biology*. ASM Press, Washington, DC, V. 2, pp. 1570-1578.

Ita PC, Hutkins RW (1991) Intracellular pH and survival of *Listeria monocytogenes* Scott A in Tryptic Soy Broth containing acetic, lactic, citric, and hydrochloric acids. *Int J Food Microbiol* **54:**15-19.

Jack RW, Tagg JR, Ray B (1995) Bacteriocins of Gram-positive bacteria. *Microbiol. Rev.* **59:**171-200.

Jackson MB, Cronan JE, Jr (1978) An estimate of the minimum amount of fluid lipid required for the growth of *Escherichia coli*. *Biochim Biophys Acta* **512:**472-479.

Jaffe LF (1980) Control of plant development by steady ionic currents. In: *Plant membrane transport: current conceptual issues* (Spanswick RM, Lucas WJ, and Dainty J, eds). pp. 381-388. Amsterdam: Elsevier.

Jamieson GA, Frazier WA, Schlesinger PH (1984) Transient increase in intracellular pH during *Dyctyostelium* differentiation. *J Cell Biol* **99:**1883-1887.

Jeffreys AG, Hak KM, Steffan RJ, Foster JW, Bej AK (1998) Growth, survival and characterization of cspA in *Salmonella enteritidis* following cold shock. *Curr Microbiol* **36:**29-35.

Jenkins HA, Griffiths AJ, Lloyd D (1989) Simultaneous operation of ultradian and circadian rhythms in *Chlamydomonas reinhardii. J Interdisciplin Cycle Res* **20:**257-264.

Jennings DH (1983) Some aspects of the physiology and biochemistry of marine fungi. *Biol Rev* **58:**423-459.

Jennings DH (1995) Water relations and salinity. In: *The physiology of fungal nutrition.* (Jennings DH, ed.) pp.398-443. Cambridge: University Press.

Jepras RI, Paul FE, Pearson SC, Wilkinson MJ (1997) Rapid assessment of antibiotic effect on *Escherichia coli* by bis-(1,3-dibutylbarbituric acid) trimethine oxonol and flow cytometry. *Antimicrob Agents Chemother* **41:**2001-2005.

Jones PG, Inouye M (1994) The cold-shock response – a hot topic. *Mol Microbiol* **11:**811-818.

Jones RGW, Pritchard J (1990) Stresses, membranes and cell walls. In: *Plants under stress*. (Jones HG, Flowers TJ, and Jones MB, eds). *Soc Exp Biol* **39:**95-114.

Jones PG, VanBogelen RA, Neidhardt FC (1987) Induction of proteins in response to low temperature in *Escherichia coli*. *J Bacteriol* **169:**2092-2095.

Jones SE, Naik RR, Stone MO (2000) Use of small fluorescent molecules to monitor channel activity. *Biochem Biophys Res Com* **279:**208-212.

Jordan KN, Oxford L, O'Byrne CP (1999a) Survival of low-pH stress by *Escherichia coli* O157:H7: correlation between alterations in the cell envelope and increased acid tolerance. *Appl Environ Microbiol* **65:**3048-3055.

Jordan S, Glover J, Malcom L, Thomson-Carter FM, Booth IR, Park SF (1999b) Augmentation of killing of Escherichia coli O157 by combinations of lactate, ethanol, and low-pH conditions. *Appl Environ Microbiol* **65:**1308-1311.

Kandler O, Weiss N (1986) Genus Lactobacillus. In: *Bergey's manual of systematic bacteriology* PHA Sneath, NS Mair, Sharpe ME, Holt JG (eds.), Williams and Wilkins, Baltimore, Md., V. 2, pp. 1209-1223.

Kandror O, Goldberg AL (1997) Trigger factor is induced upon cold shock and enhances viability of *Escherichia coli* at low temperatures. *Proc Natl Acad Sci USA* **94:**4978-4981.

Kaprelyants AS, Kell DB (1992) Rapid assessment of bacterial viability and vitality by rhodamine 123 and flow cytometry. *J Appl Bacteriol* **72:**410-422.

Kasamo K, Yamaguchi M, Nakamura Y (2000) Mechanism of the chilling-induced decrease in proton pumping across the tonoplast of rice cells. *Plant Physiol Biochem* **41:**840-849.

Kashket ER (1981) Effects of aerobiosis and nitrogen source on the proton motive force in growing *Escherichia coli* and *Klebsiella pneumoniae* cells. *J Bacteriol* **146:**377-384.

Kashket ER (1982) Stoichiometry of the H^+-ATPase of growing and resting, aerobic *Escherichia coli. Biochem* **21:**5534-5538.

Kashket ER (1985) The proton motive force in bacteria: a critical assessment of methods. *Annn Rev Microbiol* **39:**219-242.

Kashket ER (1987) Bioenergetics of lactic acid bacteria: cytoplasmic pH and osmotolerance. *FEMS Microbiol Rev* **46:**233-244.

Katz A, Pick U, Avron M (1989) Characterization and reconstitution of the Na^+/H^+ antiporter from the plasma membrane of the halotolerant alga *Dunaliella. Biochim Biophys Acta* **983:**9-14.

Kennedy CD, Gonsalves FAN (1988) H^+ efflux and trans-root potential measured while increasing the temperature of solutions bathing excised roots of *Zea mays. J Exp Bot* **39:**37-49.

Kim JH, Demaurex N, Grinstein S (1996) Intracelular pH: measurements, manipulation and physiological regulation. In: *Transport Processes in Eukaryotic and Prokaryotic Organisms*. WN Konings, HR Kaback, JS Lolkema (eds.) Elsevier, Amsterdam, pp. 447-472.

Kinoshita N, Unemoto T, Kobayashi H (1984) Proton motive force is not obligatory for growth of *Escherichia coli*. *J Bacteriol* **160:**1074-1077.

Kippert F (1996) A temperature-compensated ultradian clock of *Tetrahymena* – oscillations in respiratory activity and cell division. *Chronobiol Int* **13:**1-13.

Kippert F, Lloyd D (1995) A temperature-compensated ultradian clock ticks in *Schizosaccharomyces pombe*. *Microbiology* **141:**883-890.

Klein W, Weber MHW, Marahiel MA (1999) Cold shock response of *Bacillus subtilis*: Isoleucine-dependent switch in the fatty acid branching for membrane adaptation to low temperatures. *J Bacteriol* **181:**5341-5349.

Knight MR, Campbell AK, Smith SM, Trewavas AJ (1991) Recombinant aequorin as a probe for cytosolic free Ca^{2+} in *Escherichia coli*. *FEBS Lett* **282:**405-408.

Ko R, Smith LT (1999) Identification of an ATP-driven, osmoregulated glycine betaine transport system in *Listeria monocytogenes*. *Appl Environ Microbiol* **65:**4040-4048.

Ko R, Smith LT, Smith GM (1994) Glycine betaine confers enhanced osmotolerance and cryotolerance on *Listeria monocytogenes*. *J Bacteriol* **176:**426-431.

Kobayashi H, Suzuki TN, Unemoto T (1986) Streptococcal cytoplasmic pH is regulated by changes in amount and activity of a proton-translocating ATPase. *J Biol Chem* **261:**627-630.

Kobayashi H, Suzuki T, Kinoshita N, Unemoto T (1984) Amplification of the *Streptococcus faecalis* proton-translocating ATPase by a decrease in cytoplasmic pH. *J Bacteriol* **158:**1157-1160.

Kochian LV, Shaff JE, Kuhtreiber WM, Jaffe LF, Lucas WJ (1992) Use of an extracellular, ion selective, vibrating microelectrode system for the quantification of K^+, H^+, and Ca^{2+} fluxes in maize roots and maize suspention cells. *Planta* **188:**601-610.

Kocun FJ (1970) Amino acid containing phospholipids as major components of the phospholipids of *Streptococcus faecalis* 10Cl. *Biochim Biophys Acta* **202:**277-282.

Kollmann R, Altendorf K (1993) ATP-driven potassium-transport in right-side-out membrane vesicles via the kdp system of *Escherichia coli. Biochim Biophys Acta* **1143:**62-66.

Koostra WI, Smith PI (1969) D- and L-alanylphosphosophatidyl glycerols from *Mycoplasma laidlairii* strain B. *Biochemistry* **8:**4794-4806.

Kosaric N, Carroll KK (1971) Phospholipids of *Listeria monocytogenes. Biochim Biophys Acta* **239:**428-442.

Kroll RG, Booth IR (1981) The role of potassium transport in the generation of a pH gradient in *Escherichia coli. Biochem J* **198:**691-698.

Kroll RG, Booth IR (1983) The relationship between K+ transport, pH and pHi in *Escherichia coli. Biochem J* **216:**709-716.

Kroll RG, Patchett RA (1992) Induced acid tolerance in *Listeria monocytogenes*. *Lett Appl Microbiol* **14:**224-227.

Krulwich TA, Agus R, Schneier M, Guffanti AA (1985) Buffering capacity of bacilli that grow at different pH ranges. *J Bacteriology* **162:**768-772.

Krulwich TA, Ito M, Gilmour R, Guffanti AA (1997) Mechanisms of cytoplasmic pH regulation in alkaliphilic strains of *Bacillus*. *Extremophiles* **1:**163-169.

Kubalski A (1995) Generation of giant protoplasts of *Escherichia coli* and an inner-membrane anion selective conductance. *BBA* **1238:**177-182.

Kuhtreiber WM, Jaffe LF (1990) Detection of extracellular calcium gradients with a calcium-specific vibrating electrode. *J Cell Biol* **110:**1565-1573.

La Spada G, Biundo T, Nardella R, Meli S (1999) Regulatory volume decrease in nematocytes isolated from acontia of *Aiptasia diaphana*. *Cell Mol Biol* **45:**249-258.

Lang F, Busch GL, Ritter M, Volkl H, Waldegger S, Gulbins E, Haussinger D (1998) Functional significance of cell volume regulatory mechanisms. *Physiol Rev* **78:**247-306.

Lebrun M, Audurier A, Cossart P (1994) Plasmid-borne cadmium resistance genes in *Listeria monocytogenes* are similar to cadA and cadC of *Staphylococcus aureus* and are induced by cadmium. *J Bacteriol* **176:**3040-3048.

Leder I (1972) Interrelated effects of cold shock and osmotic pressure on the permeability of the *Escherichia coli* membrane to permease accumulated substrates. *J Bacteriol* **111:**211-219.

Leistner L (1987) Shelf-stable products and intermediate moisture foods based on meat. In: LB Rockland and LR Beuchat (eds.) *Water Activity: Theory and Applications to Food.* Marcel Dekker Inc., NY, pp. 295-327.

Lens P, DeBeer D, Cronenberg C, Ottengraf S, Verstraete W (1995) The use of microsensors to determine population distributions in UASB aggregates. *Water Sci Techn* **31**:273-280.

LePage C, Fayolle F, Hermann M, Vandecasteele J-P (1987) Changes in the lipid composition of *Clostridium acetobutylicum* during acetone-butanol fermentation: effects of solvents, growth temperature and pH. *J Gen Microbiol* **133:**103-110.

Lepock JR, Frey HE, Inniss WE (1990) Thermal analysis of bacteria by differential scanning calorimetry: relationship of protein denaturation in situ to maximum growth temperature. *Biochim Biophys Acta* **1055:**19-26.

Leriche V, Chassaing D, Carpentier B (1999) Behaviour of *L. monocytogenes* in an artificially made biofilm of a nisin-producing strain of *Lactococcus lactis. Int J Food Microbiol* **51:**169-182.

Letellier L, Bonhivers M (1996) Intrinsic and extrinsic channels in bacteria. In: WN Konings, HR Kaback, JS Lolkema (eds.) *Transport Processes in Eukaryotic and Prokaryotic Organisms.* Elsevier, Amsterdam, pp. 615-636.

Levina NN, Lew RR, Hyde GJ, Heath IB (1995) The roles of Ca^{2+} and plasma membrane ion channels in hyphal tip growth of *Neurospora crassa. J Cell Sci* **108:**3405-3417.

Levina N, Totemeyer S, Stokes NR, Louis P, Jones MA, Booth IR (1999) Protection of *Escherichia coli* cells against extreme turgor by activation of MscS and MscL mechanosensitive channels: identification of genes required for MscS activity. *EMBO J* **18:**1730-1737.

Lew RR (1996) Pressure regulation of the electrical properties of growing *Arabidopsis thaliana L.* root hairs. *Plant Physiol* **112:**1089-1100.

Lew RR (1998) Comparative analysis of Ca^{2+} and H^{+} flux magnitude and location along growing hyphae of *Saprolegnia ferax* and *Neurospora crassa. Eur J Cell Biol* **78:**892-902.

Lew RR (1999) Comparative analysis of Ca^{2+} and H^{+} flux magnitude and location along growing hyphae of *Saprolegnia ferax* and *Neurospora crassa. Eur J Cell Biol* **78:**892-902.

Lew RR (2000) Electrobiology of root hairs. Root hairs: cell and molecular biology. pp. 115-139.

Lewis BD, Karlin-Neumann G, Davis RW, Spalding EP (1997) Ca^{2+}-activated anion channels and membrane depolarizations induced by blue light and cold in *Arabidopsis* seedlings. *Plant Physiol* **114:**1327-1334.

Lewis TE (2001) Characterisation and application of Australian thraustochytrids. PhD thesis, University of Tasmania.

Lewis TE, Nichols PD, McMeekin TA (1999) The biotechnological potential of Thraustochytrids. *Marine Biotechnol* **1:**580-587.

Li Z-S, Delrot S (1987) Osmotic dependence of the transmembrane potential difference of broadbean mesocarp cells. *Plant Physiology* **84:**895-899.

Li ZY, Ward OP (1994) Production of docosahexaenoic acid by *Thraustochytrium roseum*. *J Ind Microbiol* **13:**238-241.

Lichko LP, Okorokov LA, Kulaev IS (1980) Role of vacuolar ion pool in *Saccharomyces carlsbergensis*: potassium efflux from vacuoles is coupled with manganese or magnesium influx. *J Bacteriol* **144:**666-671.

Lin J, Smith MP, Chapin KC, Baik HS, Bennett GN, Foster JW (1996) Mechanisms of acid resistance in enterohemorrhagic *Escherichia coli*. *Appl Environ Microbiol* **62:**3094-3100.

Lloyd D, Stupfel M (1991) The occurrence and functions of ultradian rhythms. *Biol Rev* **66:**275-299.

Lloyd D, Rossi EL (1992) Ultradian Rhythms in Living Systems. London: Springer-Verlag.

Lloyd D, Kippert F (1993) Intracellular coordination by the ultradian clock. *Cell Biology Int* **17:**1047-1052.

Lolkema JS, Poolman B, Konings WN (1996) Secondary transporters and metabolic energy generation in bacteria. In: WN Konings, HR Kaback, JS Lolkema (eds.) *Transport Processes in Eukaryotic and Prokaryotic Organisms*. Elsevier, Amsterdam, pp. 229-260.

Lowen PC, Hengge-Aronis R (1994) The role of sigma factor s^s (KatF) in bacterial global regulation. *Annu Rev Microbiol* **48:**53-80.

Luard EJ (1982) Growth and accumulation of solutes by *Phytophthora cinnamoni* and other fungi in response to changes in external osmotic potential. *J Gen Microbiol* **128:**2583-2590.

Lucas WJ, Kochian LV (1986) Ion transport processes in corn roots: An approach utilizing microelectrode techniques. In: *Advanced Agricultural Instrumentation: Design and Use.* (Gensler WG, ed.). pp. 402-425. Dordrecht: Matinus Nijhoff.

Luli GW, Strohl WR (1990) Comparison of growth, acetate production, and acetate inhibition of *Escherichia coli* strains in batch and fed-batch fermentations. *Appl Environ Microbiol* **56:**1004-1011.

Lyons JM (1973) Chilling injury in plants. *Ann Rev Plant Physiol* **24:**445-466.

Mackey BM (1999) Injured bacteria. In: *The microbiological Safety and Quality of Food.* Aspen Publishers Inc., Gaithersburg, MD, V.1, pp. 315-341.

Maftah A, Renault D, Vignoles C, Hechard Y, Bressollier P, Ratinaud MH, Cenatiempo Y, Julien R (1993) Membrane permeabilization of *Listeria monocytogenes* and mitochondria by the bacteriocin mesentericin Y105. *J Bacteriol* **175:**3232-3235.

Maloney PC (1990) Microbes and membrane biology. *FEMS Microbiol Rev* **87:**91-102.

Maloney PC, Wilson TH (1996) Ion-coupled transport and transporters. In: *Escherichia coli and Salmonella. Cellular and Molecular Biology.* P Neidhardt (ed.) ASM Press, Washington, DC, V. 1, pp. 1130-1148.

Marr AG, Ingraham JL (1962) Effects of temperature on the composition of fatty acids in *Escherichia coli*. *J Bacteriol* **84:**1260-1267.

Martin I, Ruysschaert JM, Sanders D, Giffrd CJ (1996) Interaction of the lantibiotic nisin with membranes revealed by fluorescence quenching of an introduced tryptophan. *Eur J Biochem* **239:**156-164.

Martin RB (1984) Bioinorganic chemistry of calcium. In: *Metal ions in biological systems*. Siegel H (ed.) New York: Marcel Dekker. **17:**1-49.

Martinac B, Buecher M, Delcour AH, Adler J, Kung C (1987) Pressure-sensitive ion channel in Escherichia coli. *Proc Natl Acad Sci USA* **84:**2297-2301.

Mason DJ, Allman R, Lloyd D (1993) Uses of membrane potential dyes with bacteria. In: *Flow Cytometry in Microbiology* (Lloyd D, ed). London: Springer. pp. 67-81.

Masson F, Lacroix C, Paquin C (1994) Direct measurement of pH profiles in gel beads immobilizing *Lactobacillus helveticus* using a pH sensitive microelectrode. *Biotechnol Techniq* **8:**551-556.

Mastronicolis SK, German JB, Smith GM (1996) Diversity of the polar lipids of the food-borne pathogen *Listeria monocytogenes*. *Lipids* **31:**635-640.

Mastronicolis SK, German JB, Megoulas N, Petrou E, Foka P, Smith GM (1998) Influence of cold shock on the fatty-acid composition of different lipid classes of the food-borne pathogen *Listeria monocytogenes*. *Food Microbiol* **15:**299-306.

Mata MT, Baquero F, Perez-Diaz JC (2000) A multidrug efflux transporter in *Listeria monocytogenes*. *FEMS Microbiol Lett* **187:**185-188.

Mazia D, Schatten G, Sale W (1975) Adhesion of cells to surfaces coated with polylysine. *J Cell Biol* **66:**198-200.

McAinsh MR, Hetherington AM (1998) Encoding specificity in Ca^{2+} signalling systems. *Trend Plant Sci* **3:**32-36.

McAinsh MR, Webb AAR, Taylor JE, Hetherington AM (1995) Stimulus-induced oscillations in guard cell cytosolic free calcium. *Plant Cell* **7:**1207-1219.

McDonald LC, Fleming HP, Hassan HM (1990) Acid tolerance of *Leconostoc mesenteroides* and *Lactobacillus plantarum. Appl Environ Microbiol* **56:**2120-2124.

McFeters GA, Yu FP, Pyle BH, Stewart PS (1995) Physiological methods to study biofilm disinfection. *J Indust Microbiol* **15:**333-338.

McLaggan D, Naprstek J, Buurman ET, Epstein W (1994) Interdependence of K^+ and glutamate accumulation during osmotic adaptation of *Escherichia coli. J Biol Chem* **269:**1911-1917.

Meng S, Bennett GN (1992) Regulation of the *Escherichia coli* cad operon: a system for neutralization of flow extracellular pH. *J Bacteriol* **174:**2569-2669.

Miller AL (1989) Ion currents and growth regulators in plant root development. *Biol Bulletin* **176:**65-70.

Miller JD, Jones EBG (1983) Observations on the association of thraustochytrid marine fungi with decaying seaweed. *Bot Marina* **26:**345-351.

Miller ES, Bates RA, Koebel DA, Fuchs BB, Sonnenfeld G (1998) 2-deoxy-D-glucose-induced metabolic stress enhances resistance to *Listeria monocytogenes* infection in mice. *Physiol Behav* **65:**535-543.

Mitchell P (1961) Coupling of phosphorylation to electron and hydrogen transfer by a chemiosmotic type of mechanism. *Nature* **191:**144-148.

Mitchell P (1973) Perfomance and conservation of osmotic work by proton coupled solute porter systems. *J Bioenergetics* **4:**63-91.

Miwa, T, Esaki, H, Umemori, J, Hino, T (1997) Activity of H^+-ATPase in ruminal bacteria with special reference to acid tolerance. *Appl Environ Microbiol* **63:**2155-2158.

Miyagi A, Ohta H, Kodama T, Fukui K,. Kato K, Shimono T (1994) Metabolic and energetics aspects of the growth response of *Streptococcus rattus* to environmental acidification in anaerobic continuous culture. *Microbiol* **140:**1945-1952.

Moll GN, Konings WN, Driessen AJM (1998) The lantibiotic nisin induces transmembrane movement of a fluorescent phospholipid. *J Bacteriol* **180:**6565-6570.

Moll GN, Clark J, Chan WC, Bycroft BW, Roberts GC, Konings WN, Driessen AJ (1997) Role of transmembrane pH gradient and membrane binding in nisin pore formation. *J Bacteriol* **179:**135-140.

Mongin AA, Aksentsev SL, Orlov SN, Konev SV (1997) Hypoosmotic shock activates Ca^{2+} channels in isolated nerve terminals. *Neurochem Int* **31:** 835-843.

Montville TJ, Bruno MEC (1994) Evidence that dissipation of proton motive force is a common mechanism of action for bacteriocins and other antimicrobial proteins. *Int J Food Microbiol* **24:**53-74.

Montville TJ, Chen Y (1998) Mechanistic action of pediocin and nisin: recent progress and unresolved questions. *Appl Microbiol Biotechnol* **50:**511-519.

Montville TJ, Winkowski K (1997) Biologically Based Preservation Systems and Probiotic Bacteria. In: *Food Microbiology. Fundamentals and Frontiers* Doyle MP, Beuchat LR, Montville TJ (eds.). Washington: ASM Press. pp. 557-558.

Montville TJ, Winkowski K, Ludescher RD (1995) Models and mechanisms for bacteriocin action and application. *Int Dairy J* **5:**797-814.

Morgunov NS, Hirsch DJ (1991) Sodium transport in salamander proximal tubule at 5.5 degrees C. *Am J Physiol* **260:**F323-330.

Moss ST (1985) An ultrastructural study of taxonomically significant characters of the *Thraustochytriales* and the *Labyrinthuales*. *Bot J Linnean Soc* **91:**329-357.

Mukherjee KD (1999) Production and use of microbial oils. *INFORM* **10:**308-313.

Mundt LJO (1986) Lactic acid streptococci. In: *Bergey's manual of systematic bacteriology* PHA Sneath, NS Mair, Sharpe ME, Holt JG (eds.), Williams and Wilkins, Baltimore, Md., V. 2, pp. 1065-1066.

Murata N, Wada H (1995) Acyl-lipid desaturases and their importance in the tolerance and acclimatization to cold of cyanobacteria. *Biochem J* **308:**1-8.

Murata N, Los DA (1997) Membrane fluidity and temperature perception. *Plant Physiol* **115:**875-879.

Mustafa SMD, Pilcher CWT, Williams KI (1999) Cooling-induced bronchoconstriction: the role of ion-pumps and ion-carrier systems. *Pharm Res* **39:**125-136.

Nagata S (1995) Lethal effect of carbonyl cyanide m-chlorophenilhydrazone on *Escherichia coli* and a halotolerant *Brevibacterium* species. *Microbios* **81:**73-83.

Nakayama H, Mitsui T, Nishihara M, Kito M (1980) Relation between growth temperature of *E. coli* and phase transition temperatures of its cytoplasmic and outer membranes. *Biochim Biophys Acta* **601:**1-10.

Nannen NL, Hutkins RW (1991) Proton-translocating adenosine triphosphate activity in lactic acid bacteria. *J Dairy Sci* **74:**747-751.

Neidelman SL (1987) Effect of temperature on lipid unsaturation. *Biotechnol Genet Eng Rev* **5:**245-268.

Neijssel OM, Teixeira de Matos MJ, Tempest DM (1996) Growth yield and energy distribution. In: *Escherichia coli* and *Salmonella. Cellular and Molecular Biology* Neidhardt FC (ed.). Washington: ASM Press. **V.2**: pp.1683-1692.

Newman IA (2001). Ion transport in roots: measurement of fluxes using ion-selective microelectrodes to characterize transporter function. *Plant Cell Environ* **24:**1-14.

Nicholls DG, Ferguson SJ (1992) Bioenergetics 2. Academic Press, London, 255 p.

Nichols DS, McMeekin TA, Nichols PD (1994) Manipulation of polyunsaturated, branched-chain and *trans*-fatty acid production in *Shewanella putrefaciens* strain ACAM 342. *Microbiol* **140:**577-584.

Nichols DS, Nichols PD, McMeekin TA (1995) Ecology and physiology of psychrophilic bacteria from Antarctic saline lakes and sea ice. *Sci Prog* **78:**311-347.

Nichols DS, Brown JL, Nichols PD, McMeekin TA (1997) Production of eicosapentaenoic and arachidonic acids by an antarctic bacterium: response to growth temperature. *FEMS Microbiol Lett* **152:**349-354.

Nishida I, Murata N (1996) Chilling sensitivity in plants and cyanobacteria: the crucial contribution of membrane lipids. *Annu Rev Plant Physiol Plant Mol Biol* **47:**541-568.

Nobel PS (1974) Introduction to Biophysical Plant Physiology. WH Freeman and Co., San Francisco.

Norris V, Grant S, Freestone P, Canvin J, Sheikh FN, Toth I, Trinei M, Modha K, Norman RI (1996) Calcium signalling in bacteria. *J Bacteriol* **178:**3677-3682.

Nurnberger T, Nennsteil D, Jabs T, Sacks WR, Hahlbrock K, Scheel D (1994) High affinity binding of a fungal oligopeptide elicitor to parsley plasma membranes triggers multiple defense responses. *Cell* **78:**449-460.

O'Driscoll B, Gahan CG, Hill C (1996) Adaptive acid tolerance response in *Listeria monocytogenes*: isolation of an acid-tolerant mutant which demonstrates increased virulence. *Appl Environ Microbiol* **62:**1693-1698.

O'Sullivan E, Condon S (1999) Relationship between acid tolerance, cytoplasmic pH, and ATP and H^+-ATPase levels in chemostat cultures of *Lactococcus lactis*. *Appl Environ Microbiol* **65:**2287-2293.

Okazaki Y, Tazawa M (1990) Calcium ion and turgor regulation in plant cells. *J Membr Biol* **114:**189-194.

Onoda T, Oshima A (1988) Effects of Ca^{2+} and protonophore on growth of an *Escherichia coli* L-form. *J Gen Microbiol* **134:**3071-3077.

Orlov SN, Kolosova IA, Cragoe EJ, Gurlo TG, Mongin AA, Aksentsev SL, Konev SV (1993) Kinetics and peculiarities of thermal inactivation of volume-induced Na^+/H^+ exchange, $Na^+,K^+,2Cl^-$ cotransport and K^+,Cl^- cotransport in rat erythrocytes. *Biochim Biophys Acta* **1151:**186-192.

Orlowski J, Kandasamy R, Shull GE (1992) Molecular cloning of putative members of the Na/H exchanger gene family. cDNA cloning, deduced amino acid sequence, and mRNA tissue expression of the rat Na/H exchanger NHE-1 and two structurally related proteins. *J Biol Chem* **267:**9331-9339.

Orskov F (1986) Facultative anaerobic Gram-negative rods. In: *Bergey's Manual of Systematic Bacteriology.* NL Krieg (ed.) Williams and Wilkins, Baltimore, MD, V. 1, pp. 408-600.

Padan E, Schuldiner S (1987) Intracellular pH and membrane potential as regulators in the prokaryotic cell. *J Membr Biol* **95:**189-198.

Padan E, Schuldiner S (1994) Molecular physiology of Na^+/H^+ antiporters, key transporters in circultion of Na^+ and H^+ in cells. *Biochim Biophys Acta* **1185:**129-151.

Padan E, Schuldiner S (1996) Bacterial Na^+/H^+ antiporters – molecular biology, biochemistry and physiology. In: *Transport Processes in Eukaryotic and Prokaryotic Organisms*. WN Konings, HR Kaback, JS Lolkema (eds.) Elsevier, Amsterdam. pp. 501-532.

Panaretou B, Piper PW (1992) The plasma membrane of yeast acquires a novel heat-shock protein (hsp30) and displays a decline in proton-pumping ATPase levels in response to both heat shock and the entry to stationary phase. *Eur J Biochem* **206:**635-640.

Panoff J-M, Corroler D, Thammavongs B, Boutibonnes P (1997) Differentiation between cold shock proteins and cold acclimation proteins in a mesophilic gram-positive bacterium, *Enteroccocus faecalis* JH2-2. *J Bacteriol* **179:**4451-4454.

Parker C, Hutkins RW (1997) *Listeria monocytogenes* Scott A transports glucose by high-affinity and low-affinity glucose transport systems. *Appl Environ Microbiol* **63:**543-546.

Pearl M, Arav A (2000) Chilling sensitivity in zebrafish (*Brachydanio rerio*) oocytes is related to lipid phase transition. *Cryo-Letters* **21:**171-178.

Peberdy JF, Toomer DK (1975) Effect of nutrient starvation on the utilization of storage lipids in *Nortierella ramanniana*. *Microbios* **13:**123-131.

Petersen OH (1992) Ion channels. Ten years of patch-clamp studies. *Biochem Pharmacol* **43:**1-2.

Pettersson S (1995) Low root zone temperature effects on net mineral nutrient uptake and distribution in barley (*Hordeum vulgare*). *J Plant Physiol* **145:**459-464.

Phan-Thanh L, Montagne A (1998) Physiological and biochemical aspects of the acid survival of *Listeria monocytogenes*. *J Gen Appl Microbiol* **44:**183-191.

Phan-Thanh L, Mahouin F, Alige S (2000) Acid responses of *Listeria monocytogenes*. *Inter J Food Microbiol* **55:**121-126.

Pharmawati M, Shabala SN, Newman IA, Gehring CA (1999) Natriuretic peptides and cGMP modulate K^+, Na^+, and H^+ fluxes in *Zea mays* roots. *Mol Cell Biol Res Comm* **2:**53-57.

Phillips Scientific (1988). Atomic Absorption Spectroscopy Data Book. Phillips Scientific Ltd, Cambridge, UK.

Pine L, Weaver GB, Malcolm JB, Brooks JB, Daneshvar MI (1989) Physiological studies on the growth and utilization of sugars by *Listeria* species. *Can J Microbiol* **35:**245-254.

Piotrowska G, Filek M, Kacperska A (2000) The effects of freezing on membrane electric potential in winter oilseed rape leaves. *Acta Physiol Plant* **22:**69-75.

Porter D, Lingle WL (1992) Endolithic thraustochytrid marine fungi from planted shell fragments. *Mycologia* **84:**289-299.

Prasad TK, Anderson MD, Stewart CR (1994) Acclimation, hydrogen peroxidase, and abscisic acid protect mitochondria against irreversible chilling injury in maize seedlings. *Plant Physiology* **105:**619-627.

Premaratne RJ, Lin W-J, Johnson EA (1991) Development of an improved chemically defined minimal medium for Listeria monocytogenes. *Appl Environ Microbiol* **57:**3046-3048.

Radwan SS, Soliman AH (1988) Arachidonic acid from fungi utilizing fatty acids with shorter chains as sole sources of carbon and energy. *J Gen Microbiol* **134:**387-393.

Raghukumar S (1992) Bacteriovary: a novel dual role for thraustochytrids in the sea. *Marine Biol* **113:**165-169.

Raghukumar S, Sharma S, Raghukumar C, Sathe-Pathak V, Chandramohan D (1994) Thraustochytrid and fungal component of marine detritus. 4. Laboratory studies on decomposition of leaves of the mangrove *Rhizophora apiculata* Blume. *J Exp Marine Biol Ecology* **183:** 113-131.

Raison JK (1979) Membrane lipids: structure and function. In: *Encyclopedia of Plant Physiology* (ed. P.K. Stumpf), pp. 57-83. Academic Press, New York.

Ramos A, Poolman B, Santos H, Lolkema JS, Konings WN (1994) Uniport of anionic citrate and proton consumption in citrate metabolism generates a proton motive force in *Leuconostoc oenos*. *J Bacteriol* **176:**4899-4905.

Rapp PE (1987) Why are so many biological systems periodic? *Progr Neurobiol* **29:** 261-273.

Rapp PE, Mees AI, Sparrow CT (1981) Frequency encoded biochemical regulation is more accurate than amplitude dependent control. *J Theor Biol* **90:**531-544.

Rasmussen K, Lewandowski Z (1998) The accuracy of oxygen flux measurements using microelectrodes. *Water Res* **32:**3747-3755.

Rauferova L, Metlicka R, Benes I, Kotyk A, Janacek K (1997) Cell volume regulation in *Claviceps fusiformis*. An animal-type Na, K-ATPase operating in a fungus? *Biochem Mol Biol Int* **41:**153-160.

Raven PH, Evert RF, Eichhorn SE (1999) Biology of plants. 6th edition. WH Freeman and Co, New York

Reay DS, Nedwell DB, Priddle J, Ellis-Evans JC (1999) Temperature dependence of inorganic nitrogen uptake: reduced affinity for nitrate at suboptimal temperatures in both algae and bacteria. *Appl Environ Microbiol* **65:**2577-2584.

Reich J, Sel'kov EE (1981) Energy Metabolism of the Cell: A Theoretical Treatise. San Diego: Academic Press.

Reifarth FW, Clauss W, Weber WM (1999) Stretch-independent activation of the mechanosensitive cation channel in oocytes of *Xenopus laevis*. *Biochim Biophys Acta* **1417:**63-76.

Reinhold L, Seiden A, Volokita M (1984) Is modulation of the rate of proton pumping a key event in osmoregulation? *Plant Physiol.* **75:**846-849.

Riemann F, Schaumann K (1993) Thraustochytrid protists in Antarctic fast ice? *Antarctic Sci* **5:**279-280.

Rep M, Albertyn J, Thevelein JM, Prior BA, Hohmann S (1999) Different signalling pathways contribute to the control of GPD1 gene expression by osmotic stress in *Saccharomyces cerevisiae Microbiol* **145:** 715-727.

Rowbury RJ (1995) An assessment of environmental factors influencing acid tolerance and sensitivity in *Escherichia coli, Salmonella* spp. and other enterobacteria. *Lett Appl Microbiol* **20:**333-337.

Rubinstein B (1982) Regulation of H^+ excretion. Effects of osmotic shock. *Plant Physiol* **69:**939-944.

Ruhr E, Sahl HG (1985) Mode of action of the peptide antibiotic nisin and influence on the membrane potential of whole cells and on cytoplasmic and artificial membrane vesicles. *Antimicrob Agents Chemother* **27:**841-845.

Russell JB, Diez-Gonzalez F (1998) The effects of fermentation acids on bacterial growth. *Adv Microb Physiol* **39:**205-234.

Russell LM, Rosenberg H (1979) Linked transport of phosphate, potassium ions and protons in *Escherichia coli. Biochem J* **184:**13-21.

Russell NJ (1989) Adaptive modifications in membranes of halotolerant and halophilic microorganisms. *J Bioenerg Biomembr* **21:**93-113.

Russell NJ (1990) Cold adaptation in microorganisms. *Phil Trans R Soc Lond* **B326:** 595-611.

Russell NJ, Evans RI, ter Steeg PF, Hellemons J, Verheul A, Abee T (1995) Membranes as a target for stress adaptation. *Int J Food Microbiol* 1995 **28:**255-261.

Sahl HG (1985) Bactericidal cationic peptides involved in bacterial antagonism and host defence. *Microbiol Sci* **2:**212-217.

Sahl HG (1991) Pore formation in bacterial membranes by cationic lantibiotics. In: *Nisin and novel lantibiotics*. G Jung and HG Sahl (eds), ESCOM science Publishers, Leiden, The Netherlands.

Saimi Y, Martinac B, Delcour AH, Minorsky PV, Gustin MC, Culbertson MR, Adler J, Kung C (1992) Patch clamp studies of microbial ion channels. *Method Enzymology* **207:**681-691.

Salema M, Poolman B, Lolkema JS, Loureiro-Dias MC, Konings WN (1994) Uniport of monoanionic L-malate in membrane vesicles from *Leuconostoc oenos*. *Eur J Biochem* **225:**289-295.

Salhany JM, Yamane T, Shulman RG, Ogawa S (1975) High resolution ^{31}P nuclear magnetic resonance studies of intact yeast cells. *Proc Natl Acad Sci USA* **72:**4966-4970.

Sanders D (1988) Fungi. In: SoluteTransport in Plant Cells and Tissues. Backer DA and Hall JL (eds.). Harlow: Longman. p. 106.

Sanders D, Bethke P (2000) Membrane transport. In: *Biochemistry and Molecular Biology of Plants.* Buchanan BB, Gruissem W, and Jones RL (eds). Rockville: American Society of Plant Physiologists. pp.110-158.

Sarkadi B, Attisano L, Grinstein S, Buchwald M, Rothstein A (1984) Volume regulation of *Chinese hamster* ovary cells in anisoosmotic media. *Biochim Biophys Acta* **774:**159-168.

Schleyer M, Schmid R, Bakker EP (1993) Transient, specific and extremely rapid release of osmolytes from growing cells of *Escherichia coli* K-12 exposed to hypoosmotic shock. *Arch Microbiol* **160:**424-431.

Seeliger HPR, Jones D (1986) Listeria. In: *Bergey's manual of systematic bacteriology* PHA Sneath, NS Mair, Sharpe ME, Holt JG (eds.), Williams and Wilkins, Baltimore, Md., V. 2, pp. 1235-1245.

Shabala SN (2000) Ionic and osmotic components of salt stress specifically modulate net ion fluxes from bean leaf mesophyll. *Plant Cell Environ* **23:**825-837.

Shabala SN, Newman IA (1997a) H+ flux kinetics around plant roots after short-term exposure to low temperature: identifying critical temperatures for plant chilling tolerance. *Plant Cell Environ* **20:**1401-1410.

Shabala SN, Newman IA (1997b) Proton and calcium flux oscillations in the elongation region correlate with root nutation. *Physiol Plant* **100:**917-926.

Shabala SN, Newman IA (1998) Osmotic sensitivity of Ca^{2+} and H^{+} transporters in corn roots: effect on fluxes and their oscillations in the elongation region. *J Membr Biol* **161:**45-54.

Shabala S, Newman I (1999) Light-induced changes in hydrogen, calcium, potassium, and chloride ion fluxes and concentrations from the mesophyll and epidermal tissues of bean leaves. Understanding the ionic basis of light-induced bioelectrogenesis. *Plant Physiol* **119:**1115-1124.

Shabala S, Shabala L (2001) Kinetics of net H^{+}, Ca^{2+}, K^{+}, Na^{+}, NH_4^{+}, and Cl^{-} fluxes associated with post-chilling recovery of plasma membrane transporters in *Zea mays L.* leaf and root tissues. *Physiol Plant* (In press).

Shabala S, Babourina O, Newman I (2000) Ion-specific mechanisms of osmoregulation in bean mesophyll cells. *J Exp Bot* **51:**1243-1253.

Shabala SN, Newman IA, Morris J (1997) Oscillations in H^{+} and Ca^{2+} ion fluxes around the elongation region of corn roots and effects of external pH. *Plant Physiol* **113:**111-118.

Shabala L, Shabala S, Ross T, McMeekin T (2001a) Membrane transport activity and ultradian ion flux oscillations associated with cell cycle of *Thraustochytrium* sp. *Aust J Plant Physiol* **28:**87-99.

Shabala L, Ross T, Newman I, McMeekin T, Shabala S (2001b) Measurements of net fluxes and extracellular changes of H^+, Ca^{2+}, K^+, and NH_4^+ in *Escherichia coli* using ion-selective microelectrodes. *J Microbiol Methods* **46:**119-129.

Shadbolt C, Ross T, McMeekin TA (2001) Differentiation of the effects of lethal pH and water activity: food safety implications. *Lett Appl Microbiol* **32:**99-102.

Sharom M, Willemot C, Thompson JE (1994) Chilling injury induces lipid phase changes in membranes of tomato fruit. *Plant Physiol* **105:**305-308.

Shaw M, Ingraham JL (1965) Fatty acid composition of *Escherichia coli* as a possible controlling factor of the minimal growth temperature. *J Bacteriol* **90:**141-146.

Shepherd VA, Beilby MJ (1999) The effect of an extracellular mucilage on the response to osmotic shock in the charophyte alga *Lamprothamnium papulosum*. *J Membr Biol* **170:**229-242.

Shepherd VA, Beilby MJ, Heslop DJ (1999) Ecophysiology of the hypotonic response in the salt-tolerant charophyte alga *Lamprothamnium papulosum*. *Plant, Cell Environ* **22:**333-346.

Siegenthaler PA, Belsky MM, Goldstein S (1967a) Phosphate uptake in an obligately marine fungus: a specific requirements for sodium. *Science* **155:**93-94.

Siegenthaler PA, Belsky MM, Goldstein S, Menna M (1967b) Phosphate uptake in an obligately marine fungus. II. Role of culture conditions, energy sources, and inhibitors. *J Bacteriol* **93:**1281-1288.

Siegumfeldt H, Rechinger KB, Jakobsen M (1999) Use of fluorescence ratio imaging for intracellular pH determination of individual bacterial cells in mixed cultures. *Microbiol* **145:**1703-1709.

Silver S (1996) Transport of inorganic cations. In: *Escherichia coli and Salmonella. Cellular and Molecular Biology*. F Neidhardt (ed.) ASM Press, Washington, DC, V. 1, pp. 1091-1102.

Singh A, Ward OP (1996) Production of high yields of docosahexaenoic acid by *Thraustochytrium roseum* ATCC 28210. *J Indust Microbiol* **16:**370-373.

Slayman CL (1977) Energetics and control of transport in *Neurospora*. In: *Water Relations in Membrane Transport in Plants and Animals*. Jungreis AM, Hodges TK, Kleinzeller A, and Schultz SG (eds.). New York: Academic Press. p.69.

Slayman CL (1992) Molecular correlates of physiological regulation in a P-type H^+-ATPase. *Acta Physiol Scand* **607:**137-140.

Slayman CL, Long WS, Gradmann D (1976) "Action potentials" in *Neurospora crassa*, a mycelial fungus. *Biochim Biophys Acta* **426:**732-744.

Sleator RD, Gahan CG, Abee T, Hill C (1999) Identification and disruption of BetL, a secondary glycine betaine transport system linked to the salt tolerance of *Listeria monocytogenes* LO28. *Appl Environ Microbiol* **65:**2078-2083.

Smith DA, Saldana R (1992) Model of the Ca^{2+} oscillator for shuttle streaming in *Physarum polycephalum. Biophys J* **61:**368-380.

Smith PJS (1995) Non-invasive ion probes – tools for measuring transmembrane ion flux. *Nature* **378:**645-646.

Smith PJ, Hammar K, Porterfield DM, Sanger RH, Trimarchi JR (1999) Self-referencing, non-invasive, ion selective electrode for single cell detection of trans-plasma membrane calcium flux. *Microsc Res Tech* **46:**398-417.

Smoot LM, Pierson MD (1998a) Influence of environmental stress on the kinetics and strength of attachment of *Listeria monocytogenes* Scott A to Buna-N rubber and stainless steel. *J Food Prot* **61:**1286-1292.

Smoot LM, Pierson MD (1998b) Effect of environmental stress on the ability of *Listeria monocytogenes* Scott A to attach to food contact surfaces. *J Food Prot* **61:**1293-1298.

Soupene E, He L, Yan D, Kustu S (1998) Ammonia acquisition in enteric bacteria: physiological role of the ammonium/methylammonium transport B (AmtB) protein. *Proc Natl Acad Sci USA* **95:**7030-7034.

Sparrow FK (1943) The aquatic Phycomycetes exclusive of the Saprolegniaceae and Pythium. Ann Arbor: Univ. of Michigan Press.

Spudich JL (1998) Variations on a molecular switch: transport and sensory signalling by archaeal rhodopsins. *Mol Microbiol* **28:** 1051-1058.

Standard Methods (1985) For the examination of water and wastewater. MAH Franson (ed.) American Public Health Association, Washington, DC, 16th edition. 1268 p.

Stein WD (1986) Transport and Diffusion across Cell Membranes. San Diego: Academic Press.

Stein WD (1990) Channels, Carriers, and Pumps – An Introduction to Membrane Transport. San Diego: Academic Press.

Stento NA, Ryba NG, Kiegle EA, Bisson MA (2000) Turgor regulation in the salt-tolerant alga *Chara logifolia. Plant, Cell Environ* **23:**629-637.

Steudle E, Lelkes PI, Zimmermann U (1977) Turgor regulation in *Valonia.* In: *Transmembrane Ionic Exchanges in Plants.* M Thellier, A Monnier, J Dainty (eds.) Cebtre Natl Res Sci: Paris.

Stevenson R, Silver S (1977) Methylammonium uptake by *Escherichia coli*: evidence for a bacterial NH_4^+ transport system. *Biochem Biophys Res Commun* **75:**1133-1139.

Stewart E, Gow NAR, Bowen DV (1988) Cytoplasmic alkalinisation during germ tube formation in *Candida albicans. J Gen Microbiol* **134:**1079-1087.

Stim KP, Bennett GN (1993) Nucleotide sequence of the *adi* gene, which encodes the biodegradative acid-induced arginine decarboxylase of *Escherichia coli. J Bacteriol* **175:**1221-1234.

Stinner JN, Hartzler LK (2000) Effect of temperature on pH and electrolyte concentration in air-breathing ectotherms. *J Exp Biol* **203:**2065-2074.

Stokes DL, Nakamoto RK (1994) Structures of P-type and F-type ion pumps. *Curr Opin Sruct Biol* **4:**197-203.

Storey KB, Storey JM (1988) Freeze tolerance in animals. *Physiol Rev* **68:** 27-84.

Stumpe S, Schlosser A, Schleyer M, Bakker EP (1996) K^+ circulation across the prokaryotic cell membrane: K^+-uptake systems. pp. 473-499.

Sukharev S, Martinac B, Arshavsky VY, Kung C (1993) Two types of mechanosensitive channels in the *Escherichia coli* cell envelope: solubilization and functional reconstitution. *Biophysical J* **65:**177-183.

Suller MT, Lloyd D (1999) Fluorescence monitoring of antibiotic-induced bacterial damage using flow cytometry. *Cytom* **35:**235-241.

Sumner JL, Ross T, McMeekin TA (2000) Food poisoning rates in Australia: an alternative view. *Food Australia* **52:**274-276.

Svobodova J, Konopasek I, Kapralek F, Svoboda P (1995) Effect of benzyl alcohol and ethanol on cold-shock response of *Bacillus subtilis*. *Folia Microbiol* **40:**633-638.

Szwergold BS (1992) NMR spectroscopy of cells. *Annu Rev Physiol* **54:**775-798.

Takahashi K, Isobe M, Muto S (1997a) An increase in cytosolic calcium ion concentration precedes hypoosmotic shock-induced activation of protein kinases in tobacco suspention culture cells. *FEBS Let* **401:**202-206.

Takahashi K, Isobe M, Knight MR, Trewavas AJ, Muto S (1997b) Hypoosmotic shock induces increases in cytosolic Ca^{2+} in tobacco suspention-culture cells. *Plant Physiol* **113:**587-594.

Takahashi N, Yamada T (1999) Acid-induced acid tolerance and acidogenicity of non-mutans streptococci. *Oral Microbiol Immunol* **14:**43-48.

Takahata K, Monobe K, Tada M, Weber PC (1998) The benefits and risks of n-3 polyunsaturated fatty acids. *Biosci Biotechnol Biochem* **62:**2079-2085.

Termonia Y, Ross J (1982) Entrainment and resonance in glycolysis. *Proc Natl Acad Sci USA* **79:**2878-2881.

Thieringer HA, Jones PG, Inouye M (1998) Cold shock adaptation. *BioAssays* **20:**49-57.

Thome-Ortiz PE, Pena A, Ramirez J (1998) Monovalent cation fluxes and physiological changes of *Debaryomyces hansenii* grown at high concentrations of KCl and NaCl. *Yeast* **14:**1355-1371.

Tsien RY (1989) Fluorescent indicators of ion concentrations. In: *Fluorescence Microscopy of Living Cells in Culture.* YL Wang, DL Taylor (eds.) Academic Press, London, pp. 127-156.

Tsuchido T, Nishino T, Kato Y, Takano M (1995) Involvement of membrane lipids in cold shock-induced autolysis of *Bacillus subtilis* cells *Bioscience Biotechnol Biochem* **59:**1636-1640.

Tyerman SD, Beilby M, Whittington J, Juswono U, Newman I, Shabala S (2001) Oscillations in proton transport revealed from simultaneous measurements of net current and net proton fluxes from isolated root protoplasts: MIFE meets patch-clamp. *Aust J Plant Physiol* **28:**591-604.

Van Brunt J, Harold FM (1980) Ionic control of germination of *Blastocladiella emersonii* zoospores. *J Bacteriol* **141:**735-744.

Van de Vossenberg JLCM, Ubbink-Kok T, Elferink MG, Driessen AJ, Konings WN (1995) Ion permeability of the cytoplasmic membrane limits the maximum growth temperature of bacteria and archaea. *Mol Microbiol* **18:**925-932.

Van de Vossenberg, JLCM, Driessen ALM, da Costa MS, Konings WN (1999) Homeostasis of the membrane proton permeability in *Bacillus subtilis* grown at different temperatures. *Biochim Biophys Acta* **1419:**97-104.

Veld G, Driessen AJM, Konings WN (1993) Bacterial solute transport proteins in their lipid environment. *FEMS Microbiol Rev* **12:**293-314.

Verheul A, Rombouts FM, Abee T (1998) Utilization of oligopeptides by *Listeria monocytogenes* Scott A. *Appl Environ Microbiol* **64:**1059-1065.

Verheul A, Rombouts FM, Beumer RR, Abee T (1995a) An ATP-dependent L-carnitine transporter in *Listeria monocytogenes* Scott A is involved in osmoprotection. *J Bacteriol* **177:**3205-3212.

Verheul A, Hagting A, Amezaga MR, Booth IR, Rombouts FM, Abee T (1995b) A di- and tripeptide transport system can supply *Listeria monocytogenes* Scott A with amino acids essential for growth. *Appl Environ Microbiol* **61:**226-233.

Verheul A, Glaasker E, Poolman B, Abee T (1997a) Betaine and L-carnitine transport by *Listeria monocytogenes* Scott A in response to osmotic signals. *J Bacteriol* **179:**6979-6985.

Verheul A, Russell NJ, Van't Hof R, Rombouts FM, Abee T (1997b) Modifications of membrane phospholipid composition in nisin-resistant *Listeria monocytogenes* Scott A. *Appl Environ Microbiol* **63:**3453-3457.

Waite BL, Hutkins RW (1998) Bacteriocins inhibit glucose PEP-PTS activity in *Listeria monocytogenes* by induced efflux of intracellular metabolites. *J Appl Microbiol* **85:**287-292.

Waite BL, Siragusa GR, Hutkins RW (1998) Bacteriocin inhibition of two glucose transport systems in *Listeria monocytogenes. J Appl Microbiol* **85:**287-292.

Wang J, Mitsui K, Tsurugi K (1998) The GTS1 gene product influences the ultradian oscillations of glycolysis in cell suspension of the yeast *Saccharomyces cerevisae. Biochem Biophys Res Com* **244:**239-242.

Wang MY, Siddiqi MY, Ruth TJ, Glass ADM (1993) Ammonium uptake by rice roots. II. Kinetics of $^{13}NH_4^+$ influx across the plasmalemma. *Plant Physiol* **103:**1259-1267.

Ward JM (1997) Patch-clamping and other molecular approaches for the study of plasma membrane transporters demystified. *Plant Physiol* **114:**1151-1159.

Ward OP (1980) Microbial production of long-chain PUFAs. *INFORM* **6:**683-688.

Wasserman AJ, McClellan G, Somlyo AP (1986) Calcium-sensitive cellular and subcellular transport of sodium, potassium, magnesium, and calcium in sodium-loaded vascular smooth muscle. Electron probe analysis. *Circ Res* **58:**790-802.

Watson N, Dunyak DS, Rosey EL, Slonczewsi JL, Olsen ER (1992) Identification of elements involved in transcriptional regulation of the *Escherichia coli cad* operon by external pH. *J Bacteriol* **174:**530-540.

Weete JD, Kim H, Gandhi SR, Wang Y, Dute R (1997) Lipid and ultrastructure of *Thraustochytrium* sp. ATCC 26185. *Lipids* **32:**839-845.

Wells JG, Shipman LD, Greene KD, Sowers EG (1991) Isolation of *Escherichia coli* serotype O157:H7 and other shiga-like-toxin-producing *Escherichia coli* from dairy cattle. *J Clin Microbiol* **29:**985-989.

Wethered JM, Jennings DH (1985) Major solutes contributing to solute potential of *Thraustochytrium auerum* and *T. roseum* after growth in media of different salinities. *Trans British Mycol Soc* **85:**439-446.

White C, Gadd GM (1995) Determination of metals and metal fluxes in algae and fungi. *Science Total Environ* **176:**107-115.

White PJ, Clarkson DT, Earnshaw MJ (1987) Acclimation of potassium influx in rye (*Secale cereale*) to low root temperatures. *Planta* **171:**377-385.

WHO/FAO (2001) Exposure assessment of *Listeria monocytogenes* in ready-to-eat foods. http://www.fao.org/es/esn/pagerisk/techdocs.htm (12.02.2001)

Wiedmann M, Arvik TJ, Hurley RJ, Boor KJ (1998) General stress transcription factor sigmaB and its role in acid tolerance and virulence of *Listeria monocytogenes*. *J Bacteriol* **180:**3650-3656.

Willis JS, Anderson GL (1998) Activation of K-Cl cotransport by mild warming in guinea pig red cells. *J Membr Biol* **163:**193-203.

Willshaw GA, Thirlwell J, Jones AP, Parry RL, Hickey M (1994) Vero cytotoxin producing *Escherichia coli* O157 in beefburgers linked to an outbreak of diarrhea, haemorrhagic colitis and haemolytic uraemic syndrome in Britain. *Lett Appl Microbiol* **19:**304-307.

Winkowski K, Bruno MEC, Montville TJ (1994) Correlation of bioenergetic parameters with cell death in *Listeria monocytogenes* cells exposed to nisin. *Appl Environ Microbiol* **60:**4186-4188.

Wong PC, Hau KP, Fong WF (1995) Membrane Ca^{2+} fluxes in rat hepatoma cells exposed to a supraphysiological concentration of asparagines. *Biochem Mol Biol Int* **35:**1161-1167.

Wood JM (1999) Osmosensing in bacteria: signals and membrane-based sensors. *Microbiol Mol Biol Rev* **63:**230-262.

Wouters PC, Glaasker E, and Smelt JPPM (1998) Effects of high pressure on inactivation kinetics and events related to proton efflux in *Lactobacillus plantarum. Appl Environ Microbiol* **64:**509-514.

Xu KD, Stewart PS, Chen X (1996) Transport limitation of chlorine disinfection of *Pseudomonas aeruginosa* entrapped in alginate beads. *Biotechnol Bioengin* **49:**93-100.

Xu KD, Stewart PS, Xia F, Huang CT, McFeters GA (1998) Spatial physiological heterogeneity in *Pseudomonas aeruginosa* biofilm is determined by oxygen availability. *Appl Environ Microbiol* **64:**4035-4039.

Yeagle PL (1989) Lipid regulation of cell membrane structure and function. *FASEB J* **3:**1833-1842.

Yokota A, Amachi S, Ishii S, Tomita F (1995) Acid activity of a mutant of *Lactococcus lactis* subsp, *lactis* C2 with reduced membrane-bound ATPase activity. *Biosci Biotechnol Biochem* **59:**2002-2007.

Yoshida S (1991) Chilling-induced inactivation and its recovery of tonoplast H^+-ATPase in mung bean cell suspension cultures. *Plant Physiol* **95:**456-460.

Yoshida S (1994) Low temperature-induced cytoplasmic acidosis in cultured mung bean (*Vigna radiata* [L.] Wilczek) cells. *Plant Physiol* **104:**1131-1138.

Yoshida S, Hotsubo K, Kawamura Y, Murai M, Arakawa K, Takezawa D (1999) Alterations of intracellular pH in response to low temperature stresses. *J Plant Res* **112:**225-236.

Young KM, Foegeding PM (1993) Acetic, lactic and citric acids and pH inhibition of *Listeria monocytogenes* Scott A and the effect on intracellular pH. *J Appl Bacteriol* **74:**515-520.

Yu FP, McFeters GA (1994a) Physiological responses of bacteria in biofilms to disinfection. *Appl Environ Microbiol* **60:**2462-2466.

Zheng T, Driessen AJM, Konnings WN (1988) Effect of cholesterol on the branched-chain amino acid transport system of *Streptococcus cremonis*. *J Bacteriol* **170:**3149-3198.

Zimmermann S, Ehrhardt T, Plesch G, Muller-Rober B (1999) Ion channels in plant signalling. *Cell Mol Life Sci* **55:**183-203.

Appendix A

EXPERIMENTAL SOLUTIONS

1. Experimental solution used in experiments with thraustochytrid ACEM C

Experimental solution contained:

$CaCl_2$	0.1 mM
KCl	0.2 mM
NaCl	1.0 mM
glucose	in a range from 0 to 5%

Experimental solution was adjusted to pH 5.5 with 5 M HCl.

Low concentrations of Na^+ and K^+ in the measuring solution were due to requirements to maximize the signal to noise ratio for measurements of the net fluxes of these ions (Newman, 2001).

2. Experimental solutions used in experiments with bacteria

Experimental solution N1

Experiments with *E. coli* SB1 were performed using modified minimal media (MMM). Unless otherwise noted, the composition of the MMM used throughout the experiments was:

K_2HPO_4	8.6 mM
NaCl	8.6 mM
$MgSO_4$	0.83 mM
$(NH_4)_2SO_4$	4.5 mM
$CaCl_2$	0.1 mM.

The concentration of glucose varied from 0.1% (w/v) to 0.05% (w/v), and 0.01% (w/v) depending on design of the experiment.

This modification of Minimal Broth Davis was required to reduce the buffering capacity and to increase the signal to noise ratio of the flux measurements.

Experimental solution N2

Experimental solution contained:

$(NH_4)_2HPO_4$	0.5 mM
KCl	0.2 mM
NaCl	0.1 mM
$MgSO_4$	0.2 mM
glucose	varied (0 mM; 1 mM; 10 mM)

Experimental solution was adjusted to pH 6.0 using 5M HCl if not indicated otherwise.

Appendix B

PREPARATION OF NISIN SOLUTION

Stock solution

A stock solution of 10, 000 IU/g activity was prepared from the stock powder (1, 000, 000 IU/g activity) by the following procedure:

- 0.75% NaCl solution was adjusted to pH 2.0 with HCl;
- 0.01 g/ml of the stock powder was dissolved in 200 mL of the above solution;
- nisin stock solution was filter sterilised and kept in the dark at 4 °C.

The nisin stock solution was added to the Experimental solution N2 (Appendix A) to give the desired nisin concentration. For control experiments, an equivalent volume of HCl in solution at pH 2.0 was added to the Experimental solution N2.

Appendix C

PREPARATION OF INHIBITORS

All the stock solutions were prepared in an appropriate experimental solution used for an experiment if not stated otherwise.

1. CCCP (carbonyl cyanide *m*-chlorophenyl-hydrazon) preparation

Stock solution (10 mM):

Sigma Chemical Co., St. Louis, USA

Catalog No. C-2759

CCCP	0.041 g
Experimental solution	20 mL

CCCP was dissolved in 1-2 drops of 4 M NaOH followed by dilution in the experimental solution. pH was adjusted using 4 M HCl until the first precipitation occurred. Final pH of solution was within the range of pH 8.2-8.5.

Application:

CCCP was applied to an experimental chamber together with the appropriate amount of HCl to compensate for the pH change. The necessary HCl amount was determined experimentally in each case before the experiments commencing.

2. Sodium orthovanadate (Na_3VO_4)

Sigma Chemical Co., St. Louis, USA

Catalog No. S-6508

Stock solution (50 mM):

Na_3VO_4	0.184 g
Experimental solution	20 mL

Sodium orthovanadate was dissolved in 1-2 drops of 4 M NaOH and the following procedures of stock preparation and the inhibitor application were similar to those for CCCP.

3. DCCD (1,3-dicyclohexylcarbodiimide).

Aldrich Chemical Co., Inc., WI, USA

Catalog No. D 8,000-2

Stock solution (10 mM):

DCCD	0.0412 g
Ethanol 96%	10 mL
Experimental solution	10 mL

DCCD was dissolved in ethanol followed by addition of the Experimental solution N2.

4. Lantanum chloride ($LaCl_3$) .

Sigma Chemical Co., Steinheim, Germany

Catalog No. L-41319

Stock solution (10 mM):

$LaCl_3 \cdot 7\ H_2O$	0.0743 g
Experimental solution	20 mL

Lantanum chloride was directly dissolved in the experimental solution used.